Thermal influences on sex determination and differentiation in two Australian dragon lizards (*Pogona vitticeps* and *Amphibolurus muricatus*)

by

Sarah Louise Whiteley
BA BSc (Hons)

A thesis submitted to the University of Canberra
to fulfil the requirements for the degree of
Doctor of Philosophy

Institute for Applied Ecology
University of Canberra
Australia
3rd March 2022

Abstract

How does temperature determine sex? Ever since the discovery of temperature dependent sex determination (TSD) in the 1960s, this seemingly simple question has ultimately remained unanswered. Since this discovery, many vertebrate species have been shown to possess TSD, or other types of environmentally sensitive sex determination systems (ESD). This ranges from the incubation temperature influencing sex in reptile embryos (a classic TSD system), to changes in social hierarchies initiating sex change in adult fish through stress hormone signalling pathways. The question then becomes not only how does temperature determine sex, but how does any environmental cue influence sex? In the face of this overwhelming variety and evolutionary diversity, progress towards reaching an answer to this question has been difficult. A practical guide to discovering new species with sex determination systems characterised by gene-environment interactions is presented in Chapter 2 (published in Sexual Development). In answering how the environment can determine sex, researchers are ultimately seeking to uncover a mechanism that can both sense an environmental cue and translate that to cellular changes which can determine sex. In recent years, due in large part to advances in genetic sequencing technologies, commonalities in the genes and pathways involved in sensing and transducing environmental cues have begun to emerge. Bringing together this understanding in a new synthesis is the foundation of this thesis presented in Chapter 3: the CaRe model. Published in Biological Reviews, this model proposes the proximal mechanisms sensing and transducing an environmental cue in sex determination is cellular calcium and redox regulation. The predictions made from this model serve as the basis for the subsequent chapters presented in this thesis.

The subsequent body of work I present provides new advances in understanding how temperature determines sex in two emerging model reptile species (*Amphibolurus muricatus* and *Pogona vitticeps*), which has significant implications for understanding thermosensitive sex determination systems in vertebrates more broadly. By combining classical developmental biology techniques with next generation sequencing technology, this thesis provides new insights into the genetic mechanisms underlying sex determination in these two species. In Chapter 4 (published in Proceedings B) I present the first characterisations of embryonic development in *A. muricatus* and provide evidence that this species has sex reversal. The work on *P. vitticeps*, a better understood model species with temperature induced male to female sex reversal, presented in Chapter

5 (published in PLoS Genetics) reveals the genetic underpinnings of the sex reversal process for the first time. Importantly, this research provides new experimental support for predictions made by the CaRe model. In Chapter 6 (under review at Science Advances) new isoforms characterising sex reversal are revealed, as are the dynamics of gene and morphological responses to temperature switches in Chapter 7 (under review at BMC Genomics). Finally, as an important final step in further establishing *P. vitticeps* as a model species, mammalian antibodies were established as cross reacting in the species (Chapter 8, published in Biology of Reproduction).

Ultimately, how temperature, or indeed any other environmental cue, determines sex remains an incomplete puzzle. It seems unlikely that these complex and diverse sex determination systems will fit cleanly into a specific definition. Rather an intricate patchwork of genetic mechanisms will likely make up the sex determination systems of environmentally sensitive species, where in some cases there may be overlap, but in many others there will not be. Taken together, the work presented in this thesis brings new understanding to the sex determination systems of two Australian dragon lizards, but also highlights the complexities of these systems, and how much more there is left to discover about the intricate mechanisms governing environmentally sensitive sex determination systems.

Author's Declaration

Except where clearly acknowledged in footnotes, quotations and the bibliography, I certify that I am the sole author of the thesis submitted today entitled "Thermal influences on sex determination and differentiation in two Australian dragon lizards (*Pogona vitticeps* and *Amphibolurus muricatus*)."

I further certify that to the best of my knowledge the thesis contains no material previously published or written by another person except where due reference is made in the text of the thesis.

The material in the thesis has not been the basis of an award of any other degree or diploma except where due reference is made in the text of the thesis.

24/9/21

Sarah Louise Whiteley

24/9/21

Arthur Georges

Publications

The following chapters have been peer reviewed and published in scientific journals. All papers are presented as they have been published, with alterations made only to formatting to adhere to thesis guidelines.

Chapter 2: Temperature induced sex reversal in reptiles: Prevalence, discovery, and evolutionary implications.

Whiteley, S. L., Castelli, M. A., Dissanayake, D. S. B., Holleley, C. E., & Georges, A. (2021). Temperature induced sex reversal in reptiles: Prevalence, discovery, and evolutionary implications. Sexual Development, https://doi.org/10.1159/000515687

Chapter 3: Cellular calcium and redox regulation: The mediator of vertebrate environmental sex determination?

Castelli, M. A., Whiteley, S. L., Georges, A., & Holleley, C. E. (2020). Cellular calcium and redox regulation: the mediator of vertebrate environmental sex determination? Biological Reviews, 95(3), 680–695. https://doi.org/10.1111/brv.12582

Chapter 4: Ovotestes suggest cryptic genetic influence in a reptile model for temperature dependent sex determination.

Whiteley, S. L., Georges, A., Weisbecker, V., Schwanz, L. E., Holleley, C. E. (2021). Ovotestes suggest cryptic genetic influence in a reptile model for temperature dependent sex determination. Proceedings of the Royal Society B, 288(20202819). https://doi.org/10.1098/rspb.2020.2819

Chapter 5: Two transcriptionally distinct pathways drive female development in a reptile with both genetic and temperature dependent sex determination.

Whiteley, S.L., Holleley, C.E., Wagner, S., Blackburn, J., Deveson, I.W., Marshall Graves, J.A., Georges, A. (2021). Two transcriptionally distinct pathways drive female development in a reptile with both genetic and temperature dependent sex determination. PLoS Genetics, 17(4): e1009465. https://doi.org/10.1371/journal.pgen.1009465

The following chapters are currently under peer review with the listed journals:

Chapter 6: Truncated *jarid2* and *kdm6b* transcripts are associated with temperature-induced sex reversal during development in a dragon lizard.

Whiteley, S. L., Wagner, S., Holleley, C. E., Deveson, I. W., Marshall Graves, J. A., Georges, A. In review at *Science Advances.*

Chapter 7: Developmental dynamics of sex reprogramming by high incubation temperatures in a dragon lizard.

Whiteley, S. L., Holleley, C. E., Georges, A. In review at *BMC Biology.*

Chapter 8: Dynamics of epigenetic modifiers and environmentally sensitive proteins in a reptile with temperature induced sex reversal.

Whiteley, S. L., McCuaig, R. D., Holleley, C. E., Rao, S., Georges, A. In review at *Biology of Reproduction.*

Acknowledgements

An undertaking as large as a PhD thesis cannot be done alone. I have so many people to thank for helping me during my PhD, without whom I never would have finished.

My supervisors, Arthur and Clare, deserve the highest praise, and I cannot express how thankful I am to have completed my PhD with their guidance. Without their unwavering support and encouragement, I don't think I would have lasted even one year. They have taught me what it means to be a scientist, and for that I will be forever grateful.

The members of Team Pogona have been a constant source of support during my PhD. I want to thank Jenny Marshall Graves, Paul Waters, Hardip Patel, fellow PhD students Kris Wild, Phil Pearson, and Duminda Dissanayake, for always having the time to answer questions and talk about ideas. I would also like to thank my external advisors Craig Smith and Vera Weisbecker for their contribution to manuscripts.

Meghan Castelli and Sarah Bates deserve special thanks for being with me during the hardest times of my PhD and seeing me through to the better moments that were ahead. Thank you both so much, I couldn't have done it without you cheering me on.

None of the work I completed during my PhD would have been possible without the Animal House facility. I particularly want to thank Jacqui Richardson and Wendy Ruscoe for all their hard work caring for the dragons and making sure we always had enough eggs during the breeding season. I also want to acknowledge the many lives sacrificed by my two study species, *Pogona vitticeps* and *Amphibolurus muricatus*, to advance my research, and our understanding of sex determination systems in reptiles.

Many aspects of my PhD relied on the technical expertise of others. I would particularly like to thank Ira Deveson and James Blackburn at the Garvan Institute of Medical Research. Without their incredible abilities to sequence from microscopic tissues, my PhD would look very different. I also owe many of my results to the team at the University of Queensland's histology facility lead by Darryl Whitehead. Erica Mu, Heather Middleton, and Arnault Gauthier always produced the most beautiful slides, which were integral to the success of my PhD. I would also like to thank Jin Dai for his assistance in the lab and patience with many tedious protocols. Craig Smith and members of his lab deserve my thanks for introducing me to organ culture for the first time.

I would like to thank Sudha Rao and Robert McCuaig for their expertise in immunohistochemistry which was essential in producing the data presented in Chapter 7. Amanda Bain also deserves thanks for providing logistical support.

A large part of my PhD was done during the COVID-19 pandemic, the silver lining of which was that I could work from home. Many long hours were spent working at my desk with my bearded dragon, Whizz, on my lap before he unfortunately passed away. I always found it so amusing that while I was working, he would be there with me totally oblivious to my many frustrations with the strange data his species could always be relied upon to produce. But my lap didn't stay empty for long, and soon the role was then taken up by my cat, Hermes, who spent much of the day keeping me company with his purring.

Although my family didn't really understand why I wanted to study dragons, they always urged me to pursue a career in science. It is thanks to them that, as my Pop always likes to say, the world is my oyster. And last, but certainly not least, I want to give special thanks to my partner, David, who came with me to Canberra, and has supported me without question through many gruelling years of study. Quite simply, I wouldn't be where I am now without him.

Table of Contents

List of Figures

List of Tables

Chapter 1 Introduction

Phenotypic sex is one of the most fundamental traits of any organism as its influence extends from embryonic development to sexual maturity, and eventual reproductive success. Phenotypic sex underlies many critical life history traits and has profound consequences for an individual's fitness. Nearly all eukaryotic life has two distinct sexes (males and females) that allows for sexual reproduction, a key evolutionary innovation that enhances genetic diversity through recombination [1].

Sex determination is the process by which the fate of the bipotential gonad is decided, causing it to develop as either ovaries or testes. Despite this conserved outcome, sex determining modes are highly variable between different lineages. In some vertebrate groups, like mammals and birds, sex is determined by genes on sex chromosomes, which is known as genetic sex determination (GSD). Other groups, particularly fish and reptiles, sex is often determined by environmental factors, such as temperature dependent sex determination (TSD). The evolutionary histories of many reptile taxa are characterised by numerous transitions between GSD and TSD [2], and in some species, sex can be determined by interactions between genes and the environment [3,4]. So while GSD and TSD were long presumed to exist as a mutually exclusive dichotomy, current evidence indicates that instead exist along a continuum [5].

Since the discovery of TSD in *Agama agama* in 1966 [6] precisely how temperature, or indeed any other environmental factor, determines sex has become a central question at the crossroads of genetics, evolutionary, and developmental biology. Approaching an answer to this question is the central aim of this thesis. In order to do this, I present in this thesis a series of publications that together bring new insights into how temperature determines sex, and the ways in which temperature can influence the differentiation of sexual phenotypes. In Chapter 2 (published in *Sexual Development*) I provide an overview of what is currently known about sex reversal in reptiles and give practical approaches to identifying sex reversal in new species. One such approach was used in Chapter 4 (published in *Proceedings of the Royal Society B*) to identify *Amphibolurus muricatus* as potentially displaying sex reversal. Chapter 3 follows by providing a theoretical basis I jointly developed with Meghan Castelli, which informs my subsequent experimental work. This paper presents a novel model for the biochemical processes by which an environmental cue, such as temperature, is sensed by the cell and transduced to determine sex. Termed the CaRe hypothesis, this model proposes highly conserved

cellular mechanisms (calcium signalling and redox status) allow the cell to receive and respond to environmental cues. This model provides a critical foundation for understanding the results presented in the subsequent data chapters. In these chapters, I present experimental work conducted on two agamid lizards with thermosensitive sex determination systems: the Jacky dragon (*Amphibolurus muricatus*) and the central bearded dragon (*Pogona vitticeps*). The work conducted on *A. muricatus* is presented in Chapter 4 (published in *Proceedings of the Royal Society B*). In this paper I present the first characterisations of embryonic development, including sex differentiation, in this species, which is a popular model for the evolution of TSD. The developmental characteristics uncovered by this work suggest that *A. muricatus* has previously unknown cryptic genetic influence on sex determination. This work brings new insights into the complex nature of gene-environment interactions in thermosensitive sex determination systems and highlights the need to study these influences across the vertebrate phylogeny.

In my subsequent chapters, I use the emerging model species, *P. vitticeps*, which has a GSD system (ZZ/ZW female heterogamety) with thermal override, causing the development of sex reversed females (male ZZ genotype and female phenotype, denoted as ZZf) [3]. As the embryonic development of sexual phenotypes for this species have already been characterised [7,8], I continue to build on this foundation by conducting a large incubation experiment to sequence isolated gonadal tissues at key developmental stages at different incubation temperatures. This extensive dataset was used in both 4.6.3 (published in *PLoS Genetics*) and 5.6.8 (in review at *Science Advances*). These two publications for the first time reveal the gene expression patterns (4.6.3) and splicing characteristics (5.6.8) of *P. vitticeps* embryos undergoing temperature induced sex reversal. The gene expression patterns of sex reversal provide support for the predictions made by the theoretical model presented in Chapter 3, and implicate numerous genes associated with TSD in other species. In 5.6.8, the splicing of key genes identified in 4.6.3, show patterns unique to sex reversed *P. vitticeps* that are not shared with other TSD species. This highlights that although the same genes may be commonly implicated in thermosensitive sex determination pathways across evolutionary disparate lineages, how they are regulated and the chromatin remodelling actions they perform are not necessarily conserved.

To further understand the influence of temperature on both gonadal morphology and gene expression changes, I present a temperature switch experiment in Chapter 7. The data from this chapter provides additional experimental support for genes and pathways

implicated in the CaRe model (Chapter 3) and in both 4.6.3 and 5.6.8. Importantly, it also provides support for a hypothesis that sex reversal relies on the male sex determining signal being overridden by the feminising influence of high incubation temperatures [8].

Finally, an important element of this thesis is to generate molecular resources that not only improve current understanding of the influence of temperature on sex determination and differentiation, but to also pave the way for future research. The data presented in Chapter 8 presents the first immunohistochemical staining on *P. vitticeps*, validating that antibodies raised in mammals for mammalian targets can cross-react in adult reptile gonads. The antibodies used target proteins implicated in sex reversal in previous chapters, and now exists as an essential resource for further study on protein dynamics in embryonic gonads under the influence of temperature.

Together, the data I present in this thesis provides a new understanding of the genetic mechanisms underlying sex reversal and yields new insights into the evolutionary complexities of thermosensitive sex determination in diverse vertebrate lineages.

1.1 Vertebrate sex determination: Fundamental processes across the phylogeny

Millions of years of evolution separating vertebrate groups create a diverse patchwork of sex determination mechanisms across the phylogeny [9,10]. Mammals and birds posses stable GSD systems. In mammals (XX/XY male heterogametic system), sex is determined by a gene on the Y chromosome, *SRY*, which is the master regulator of male development. Without the action of *SRY* female development progresses, and the male pathway fails to initiate [11]. In birds (ZZ/ZW female heterogametic system), sex is determined by dosage of *DMRT1*, which lies on the Z chromosome. Male development is driven by a double dose of this gene, while a single copy of *DMRT1* allows female development to progress [12]. The downstream genetic pathways initiated to drive ovarian or testes development are very well characterised in mammals and birds, in large part due to the ability to readily manipulate gene function in model organisms like mouse and chicken [13]. As a highly diverse taxa, identifying master sex genes in fish has proven challenging, and so far few have been identified (reviewed by [13]). While sex chromosome systems have been identified in many reptiles, thus far no master sex determining genes have been identified in any reptile species [15].

Regardless of how sex is determined, the pathways that are initiated to drive ovarian or testes development are remarkably similar between vertebrates. The development of the gonad is a fascinating process, as it is the only organ in the embryo that can differentiate along two opposing trajectories (ovaries or testes). While their position in the pathway, or the way they are regulated might change, the same suite of genes are consistently implicated in gonad differentiation. Male development is typically characterised by expression of genes such as *DMRT1* and *SOX9* while female development usually involves upregulation of *FOXL2* and *CYP19A1* [16]. The morphological structures of the differentiated gonads are also highly similar between different vertebrates, particularly during embryonic development. In mammals, birds, and reptiles, the bipotential gonad develops in close association with the kidney, forming the urogenital system. The cellular structure of the bipotential gonad is largely indistinguishable between these groups, as are the structures of the differentiated ovaries and testes [17]. Ovaries are characterised by the proliferation of the cortex layer and degradation of the medulla, while testes are characterised by the proliferation of the medulla and the degradation of the cortex. The cell types and structures, such as Sertoli cells and seminiferous tubules in testes, and oogonia in the granulosa layer of ovaries, are shared between the major vertebrate groups [18]. Given this level of conservation in gonad structure, why the upstream modes for determining sex are so diverse is an enduring mystery.

1.2 A unified model for environmentally sensitive sex determination

Environmental sex determination (ESD) is a broad term encompassing a variety of sex determining modes, such as temperature dependent sex determination (TSD), and systems where other environmental cues and genes interact to determine sex. The ESD systems of many fish and reptile species are poorly understood compared to GSD systems, particularly those in mammals. TSD is the best studied, though precisely how temperature, or any other environmental factor, determines sex remains unknown.

Understanding ESD has seemed an intractable problem due to the complexities of these systems, which has hindered research on many fronts. From this complexity arose a need to succinctly review the current understanding of sex reversal in reptiles, and most importantly, provide practical steps towards understanding known sex reversal systems

and identifying new species with sex reversal. This critical gap is addressed in Chapter 2, which is published as part of a special issue in *Sexual Development*.

In fish, the interactions between sex and the environment are hugely diverse, and a wide variety of cues can determine sex, or initiate sex change in adulthood. The same cue may cause the opposite outcome in different species, and different cues can cause the same outcome in a single species (reviewed by [14,19,20]). In reptiles with TSD there are three major patterns that have been characterised; females can be produced at high temperatures and males at low (Type Ia), males are produced at high temperatures an females at low (Type Ib), and females are produced at both high and low temperatures and balanced sex ratios are produced at intermediate temperatures (Type II, Figure 1.1). In other species, the influence of genes on sex chromosomes can be overridden by temperature to cause sex reversal [21]. Given this staggering diversity, it is not surprising that the complexities of ESD systems have remained poorly understood.

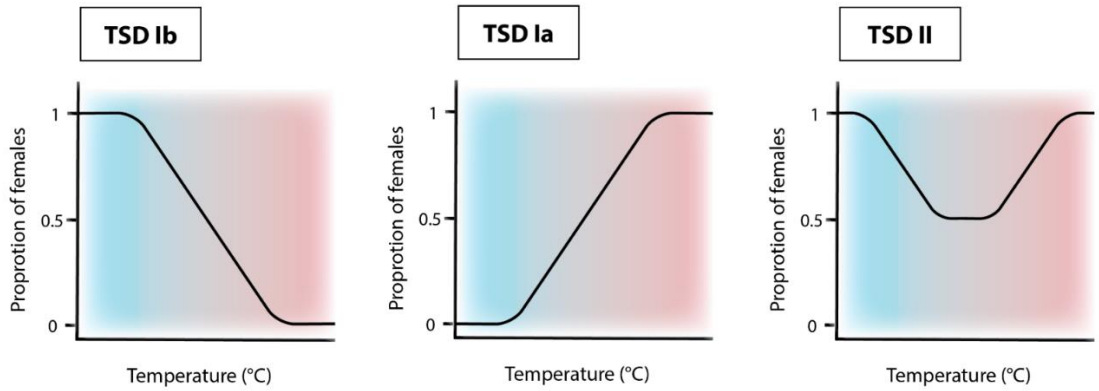

Figure 1.0.1: Patterns of temperature dependent sex determination (TSD) characterised in vertebrates. TSD pattern Ib is characterised by females being produced at low temperatures and males at high temperatures, while TSD pattern Ia is the opposite. Species with TSD II produce females at high and low temperatures, and approximately 50:50 sex ratios at intermediate temperatures. Blue denotes low temperatures and red denotes high temperatures increasing along the X-axis. Figure adapted from [577].

The fundamental question in ESD research is by what mechanism is the environmental cue sensed to determine sex. For many years, research on TSD in particular has focused on identifying genes that display sensitivity to the environment, an approach based on the assumption that a single gene is the master regulator of TSD. However, given the huge diversity of TSD systems, and the evolutionary flexibility of sex determination modes, it is highly unlikely that this would be the case. The control of TSD by a single gene further begs the question as to how the expression of this gene is regulated by temperature. The

sensing of temperature necessarily relies on biochemical processes innate to the cell that have the ability to modulate signalling pathways and alter gene expression. It is this biochemical mechanism that is proposed in Chapter 3. Termed the CaRe model, it proposes that temperature, or any other environmental cue, is sensed in the cell by calcium and reactive oxygen species (hence the abbreviation CaRe), molecules that occur in the cells of all eukaryotes and that are inherently environmentally sensitive. Outlined in this chapter is support for this model, and importantly additional experimental work has since been published in a TSD turtle, *Trachemys scripta*, to further support it [22].

T. scripta currently has the best studied TSD system of any reptile. In this species, males are produced at low incubation temperatures (26°C) and females at high (31°C). Functional experiments have demonstrated at the high female producing temperatures (FPT), calcium influx occurs in the cell, as was proposed in the CaRe model. This calcium influx triggers phosphorylation of STAT3, a protein which then blocks the action of KDM6B, a chromatin remodelling gene that would otherwise activate the male pathway through demethylation of the *DMRT1* promoter [22–24]. While functional experimentation is lacking, there is now support for CaRe mechanisms in *Pogona vitticeps* as well, outlined in Chapter 5 and Chapter 7.

1.3 Understanding the effects of temperature in *Amphibolurus muricatus*

The CaRe model also posits that pathways downstream from calcium and reactive oxygen species may not be conserved between even closely related species. Indeed, even between species in the same genus, the temperature sensitive channels in the cell membrane that allows intracellular calcium influx are not shared [25,26]. This highlights the importance of maintaining a phylogenetic perspective on research in ESD systems. To this end, the research undertaken in Chapter 4 (published in *Proceedings B*) on *Amphibolurus muricatus* sought to create resources and an improved understanding of the influence of temperature on sex in a new species in a genus where these processes were undescribed. *A. muricatus* has a Type II pattern of TSD and has been commonly used as a model in evolutionary studies due to its short generation time. In 2011, a paper was published questioning whether species with this pattern of TSD may in fact have an underlying genetic influence. How indeed can such a range of temperatures produce the same phenotypic outcome? An alternative explanation was proposed; Type II pattern species may have sex reversal at both extreme temperatures [27]. My investigation of this

in *A. muricatus* revealed that this may in fact be true. In close relative *Pogona vitticeps*, sex reversal was shown to be characterised by the presence of ovotestes, a gonadal phenotype with both male and female traits. It was hypothesised that ovotestes develop during sex reversal due to competing signals between genes on sex chromosomes and temperature [8]. It then follows that if ovotestes are an indicator of sex reversal, species with Type II TSD like *A. muricatus* would be expected to have ovotestes at a frequency of approximately 50% at extreme temperatures.

Analysis of gonad differentiation at three incubation temperatures revealed ovotestes occur close to the expected frequencies at high and low female producing temperatures in *A. muricatus*. This suggests that it indeed may have sex reversal as proposed by Quinn et al. [27], and provides the impetus for ongoing research on the sex determination system in this species, and indeed in other reptile species with a Type II TSD pattern.

1.4 Genetic regulation underlying sex reversal in *P. vitticeps*

Several epigenetic processes and cellular pathways have been implicated in TSD suggesting they play a conserved role in the regulation of sex determination and differentiation in environmentally sensitive species. As outlined by the CaRe model (Chapter 3), the environmental cue is initially sensed by the cell via calcium and redox mechanisms, which initiate a range of changes in the cell leading to alterations in gene expression. It is expected that many of the same processes would be involved in temperature induced sex reversal, but the genetic changes associated with sex reversal had never been described. The research presented in Chapter 5, Chapter 6, and Chapter 7 describe these processes for the first time using transcriptomic data from isolated embryonic gonads at different developmental stages. In 4.6.3 (published in *PLoS Genetics*) gene expression profiles were compared between normal ZW female embryos incubated at 28°C with sex reversing ZZf embryos incubated at 36°C. This reveals developmental gene expression changes during sex reversal in *P. vitticeps*, and implicates all genes previously associated with TSD. Two of these genes are particularly critical (*JARID2* and *KDM6B*), and their splicing patterns were investigated in 5.6.8 (in review at *Science Advances*). The final experiment involved switching temperatures at different developmental stages and provided additional support for a central role of these genes in the sex reversal pathway in *P. vitticeps* (Chapter 7).

Given the importance of these genes in sex reversal, Chapter 8 presents the first immunohistochemical staining in adult gonads for *P. vitticeps*. This provides a critical resource for ongoing research on the role of *JARID2, KDM6B, CIRBP* during sex reversal.

1.5 Towards a new understanding of sex reversal in reptiles

The overarching aim of this thesis is to gain new insight into the ways that temperature can influence thermosensitive sex determination and differentiation in two reptile species, the Jacky dragon (*Amphibolurus muricatus*) and the central bearded dragon (*Pogona vitticeps*). To address this aim, I present this thesis as a series of seven chapters (two published reviews and five data chapters) that together give novel insights into the thermosensitive sex determination systems of these two species, and the environmentally sensitive systems in vertebrates more broadly.

The central question in ESD research is by what mechanisms are environmental signals sensed by the cell and transduced to determine sex. The publications presented in this thesis brings improved understanding of the complexities that underlie environmentally sensitive sex determination systems and provides new directions for ongoing research.

Chapter 2 Temperature induced sex reversal in reptiles: Prevalence, discovery, and evolutionary implications

Published: Sexual Development, 2021

Whiteley, S. L., Castelli, M. A., Dissanayake, D. S. B., Holleley, C. E., & Georges, A. (2021). Temperature induced sex reversal in reptiles: Prevalence, discovery, and evolutionary implications. Sexual Development, https://doi.org/10.1159/000515687

2.1 Abstract

Sex reversal is the process by which an individual develops a phenotypic sex that is discordant with its chromosomal or genotypic sex. Sex reversal occurs in many lineages of ectothermic vertebrates, such as fish, amphibians, and at least one agamid and one scincid reptile species. Sex reversal is usually triggered by an environmental cue that alters the genetically determined process of sexual differentiation but can also be caused by exposure to exogenous chemicals, hormones, or pollutants. Despite the occurrence of both temperature sex determination (TSD) and genetic sex determination (GSD) broadly among reptiles, only two species of squamate have thus far been demonstrated to possess sex reversal in nature (GSD with overriding thermal influence). The lack of species with unambiguously identified sex reversal is not necessarily a reflection of a low incidence of this trait among reptiles. Indeed, sex reversal may be relatively common in reptiles, but little is known of its prevalence, the mechanisms by which it occurs, or the consequences of sex reversal for species in the wild under a changing climate. In this review, we present a roadmap to the discovery of sex reversal in reptiles, outlining the various techniques that allow new occurrences of sex reversal to be identified, the molecular mechanisms that may be involved in sex reversal and how to identify them, and approaches for assessing the impacts of sex reversal in wild populations. We discuss the evolutionary implications of sex reversal and use the central bearded dragon (Pogona vitticeps) and the eastern three-lined skink (Bassiana duperreyi) as examples of how species with opposing patterns of sex reversal may be impacted differently by our rapidly changing climate.

Ultimately, this review serves to highlight the importance of understanding sex reversal both in the laboratory and in wild populations and proposes practical solutions to foster future research.

Key words: temperature-dependent sex determination, TSD, genotypic sex determination, GSD, sex chromosome

2.2 Introduction

The sex of an animal is one of its most fundamental traits as it shapes sex-specific morphology, physiology, and behaviour. In vertebrates, sex can be determined either genetically or by the environment. For species with genetic sex determination (GSD), the sexual phenotype is concordant with its chromosomal complement. For species with temperature-dependent sex determination (TSD), the sexual phenotype is determined the environmental conditions that embryos experience in the absence of sex chromosomes [28]. In some species with GSD, however, environmental factors (e.g., temperature) can override the genetic determinant and cause sex reversal during embryonic development, resulting in an individual with a sexual phenotype that is discordant with its genotype [21,28,29]. For species with male heterogamety (XX/XY), this usually results in reversal of the female genotype and generation of XX males, and for species with female heterogamety (ZZ/ZW) this results in reversal of the male genotype and generation of ZZ females. One fish and one amphibian species display reversal of the heterogametic sex (generation of ZW males in response to temperature), but this has not been observed in any amniote, presumably because of the reduced fitness or viability arising from the production of YY or WW individuals [30–32]. In reptiles, temperature is the only factor definitively demonstrated to influence sex (temperature sex determination; TSD), though some evidence exists for water restriction [30].

Sex reversal occurs commonly in fish [31,33] and in some amphibians [34–36], but has been confirmed in only two reptiles, the Australian central bearded dragon (*Pogona vitticeps*) and the eastern three-lined skink (*Bassiana duperreyi*) [3,37,38]. Sex reversal may also occur in the yellow-bellied water skink (*Eulamprus heatwolei*), the common collared lizard (*Crotaphytus collaris*), the multi-ocellated racerunner (*Eremias multiocellata*), the Japanese gecko (*Gekko japonicus*), the spotted snow skink (*Niveoscincus ocellatus*), and the Jacky dragon (*Amphibolurus muricatus*), though this has not yet been definitively confirmed [39–44]. As a result, little is known about the mechanisms or consequences of sex reversal. The paucity

of reptile species with confirmed sex reversal systems is not necessarily a reflection of low incidence of this trait. Identifying and confirming genotypic sex in reptiles can be challenging, requiring considerable time and resources to develop reliable assays. Homomorphic sex chromosomes are common in reptiles, necessitating the use of advanced cytological techniques [45] or sequencing technologies to identify sex-specific sequences [42,46–50]. There is also limited understanding as to the individual and population-level consequences of sex reversal in the wild, particularly under changing climatic regimes [51,52]. The occurrence of sex reversal in a species has considerable implications for conservation management, particularly given the climatic perturbations caused by global warming.

In this review, we outline the various techniques that allow new examples of sex reversal to be identified, candidate molecular mechanisms for sex reversal, and approaches for assessing the impacts of sex reversal in wild populations, with particular attention to the difficulties of confirming both genotypic and phenotypic sex in reptiles. We discuss the evolutionary implications of sex reversal using *P. vitticeps* and *B. duperreyi* as case studies to assess how different species with sex reversal may be impacted by a rapidly changing climate.

2.3 Molecular mechanisms driving sex reversal

How sex reversal occurs at a molecular level is not currently known, though may involve temperature sensing through calcium and reactive oxygen species signalling in *P. vitticeps* [29,53,54]. While these ancient and ubiquitous environmental sensing mechanisms are very promising candidates for the transduction of an environmental signal to a sex determining signal, experimental demonstration is lacking [53].

Calcium and redox signalling pathways are conserved between phylogenetically disparate species, and thus further insight about sex reversal mechanisms may be gleaned from well-studied TSD models, such as the red-eared slider turtle, *Trachemys scripta*. In this species, calcium signalling at high temperatures was causally demonstrated to be required for female development [22]. In *T. scripta, P. vitticeps,* and the American alligator, *Alligator mississippiensis,* the epigenetic modifier KDM6B and potentially its splicing variants play an important role in the temperature driven regulation of sex determination [55]. In *T. scripta,* KDM6B initiates the male developmental cascade *via* demethylation of the promoter region of the male pathway-initiating gene *DMRT1* [23,24]. Despite little being currently understood

about sex reversal, it is clear that there are similarities between *P. vitticeps* and distantly related alligator and turtle species with TSD. Ongoing research effort is required to better understand what genes and pathways are conserved between these evolutionarily disparate lineages.

The reptile phylogeny is marked by numerous transitions between TSD and GSD systems even between closely related lineages [reviewed by 8]. This, coupled with the broad phylogenetic distribution of developmental processes associated with thermolabile sex (asynchronous gonadal and genital development), lay the groundwork for future investigations of the occurrence of sex reversal [8,54]. Ultimately sex reversal must occur by repression of the sex signals originating from the sex chromosomes, and amplification of signals for the development of the opposite sex driven by incubation temperature. The epigenetic mechanisms by which this occurs remain unknown and is a compelling area of ongoing research.

2.4 Detection of sex reversal

Sex-reversed individuals can be either generated in the laboratory or found in the wild. However, many reptiles possess poorly differentiated sex micro-chromosomes, and many more have homomorphic sex macrochromosomes, so instances of sex reversal do not easily come to attention. This can complicate both the detection of sex reversal and the identification of the mechanisms driving it, because both genetic and environmental factors may contribute to sex determination even in the absence of discernible sex chromosomes [56].

The first indications of sex reversal in a species may be gleaned from incubation experiments where eggs are incubated across a range of temperatures and the offspring sex ratios are obtained. Many TSD species exhibit sex ratio patterns where females are produced at high and low temperatures, and balanced sex ratios are produced at intermediate temperatures [Nagahama et al., 2020]. Modelling has lead to the hypothesis that species with this pattern may possess an underlying ZZ/ZW system [27]. Indeed, there is evidence to suggest this may be the case for the Jacky dragon, *Amphibolurus muricatus* [39].

Cytogenetic techniques present opportunities to detect new examples of sex reversal by identification of sex chromosomes, and a mismatch between the chromosome complement and sexual phenotype. Early researched involved using approaches like AFLPs, CGH, and BAC-

mapping [see 13–15 for examples. Reviewed by Deakin et al., 2019]. Now, a variety of sequencing based approaches are possible, particularly since the advent of next generation sequencing, which allows for techniques like assaying the sex-biased expression of candidate genes with RNA-seq [60], or mapping read depth in whole genome sequencing to identify regions on sex chromosomes [47,61]. Reduced representation sequencing approaches such as RAD-seq, ddRAD-seq, and DArT-seq [36,41,62–64] can also be useful, however these techniques target only a subset of the genome and may fail to identify markers in species with limited genetic differentiation between the sexes [65]. It is also becoming increasingly important to incorporate both cytogenetic and sequencing based approaches to obtain the most complete picture of sex chromosomes in a species [reviewed by 25]. For example, in *B. duperreyi,* heteromorphic sex chromosomes were first detected using cytogenetic approaches [37] and then sex reversal was first demonstrated using polymerase chain reaction (PCR) targeting a sequence unique to the Y chromosome [4], which was later refined using similar methods [67]. New markers for this species have also been identified using an in silico whole genome subtraction approach [50].

Laboratory experimentation is necessary to quantitatively characterise temperature-sex relationships, typically through examining sexual outcomes resulting from controlled crosses and incubation experiments. However, it is equally important to demonstrate the occurrence of sex reversal in wild populations, and whether the trigger of sex reversal established in the laboratory also affects natural populations. Evidence is growing in some fish species that multiple cues may trigger sex reversal, but these cues may not always be biologically relevant in natural populations [34,68,69]. Some studies in TSD reptiles show evidence of interactions between different environmental variables, as well as maternal effects like egg size and yolk hormones [30,70,71]. So, while laboratory based experiments will always be essential, appropriate field studies will be required to avoid mis-interpretation of what could be a laboratory artefact, caused by conditions that do not occur in the wild.

The identification of species with sex reversal can be difficult, and a lack of clear direction for how to definitively demonstrate sex reversal in a species has likely contributed to a lack of identification. We present a workflow to provide guidance for the process of identifying sex reversal and propose numerous avenues for research in both field and laboratory settings (Figure 2.1). Ultimately, reliable identification of both genotypic and phenotypic sex is required to definitively demonstrate the occurrence of sex reversal in a species (Figure 2.1).

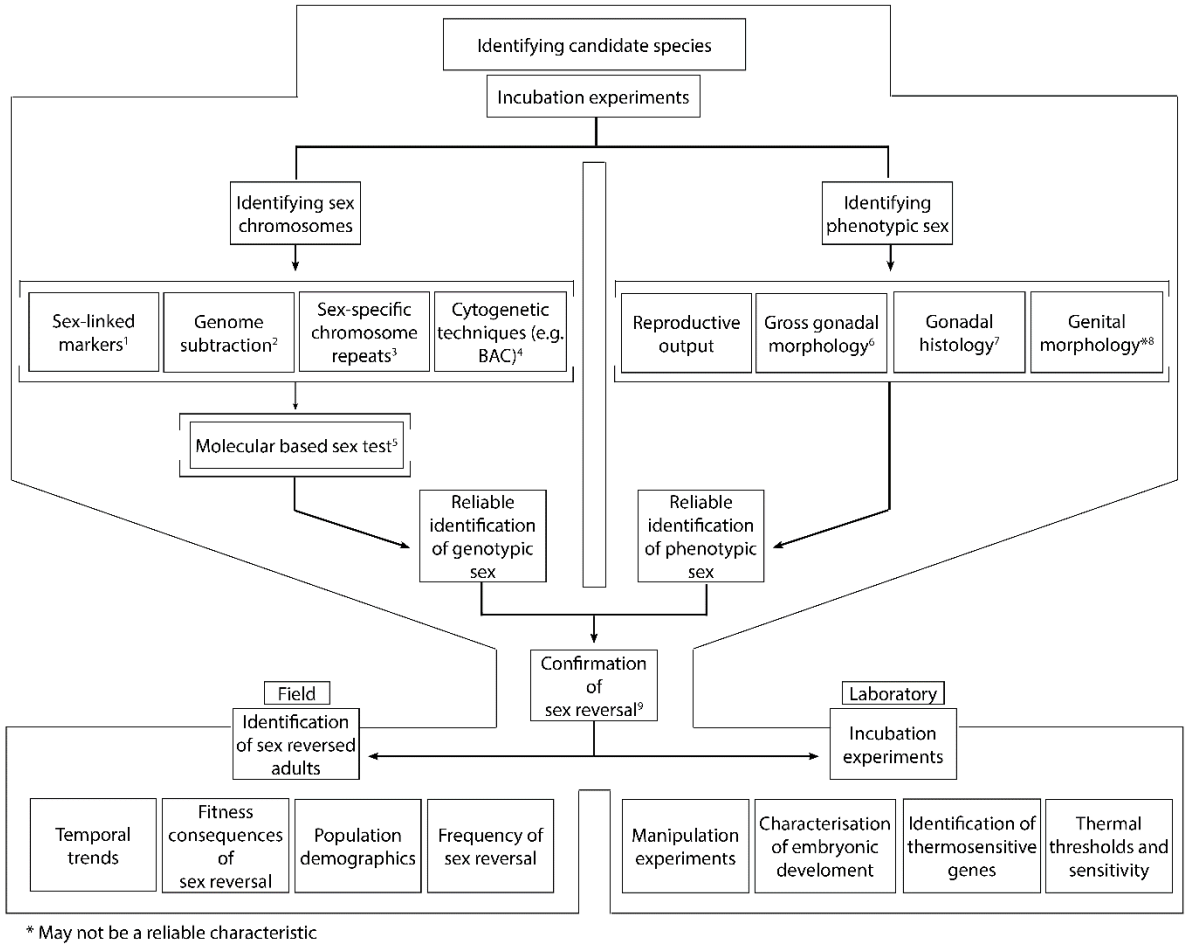

Figure 2.1: Workflow proposing strategies for identifying new examples of sex reversal. Reliable confirmation of both genotypic (A) and phenotypic (B) sex is ultimately required to identify sex reversal in a new species, which is defined as an individual being discordant between its genotypic and phenotypic sex. Potential research applications in both field and laboratory studies are also suggested following the identification of sex reversal. See references for further details of how these approaches and techniques have been used; [1][72], [2][50], [3][73], [4][66], [5][41], [6,7][74], [8][75], [9][38].

2.5 Examples of Reptile Sex Reversal

Pogona vitticeps has a ZZ/ZW GSD system, but high incubation temperatures (>32°C) result in reversal of males (ZZ genotype) to phenotypic females in the laboratory and in the wild [3,38,45]. *Bassiana duperreyi* has an XX/XY system of GSD in which low incubation temperatures (<20°C) result in reversal of the female XX genotype to phenotypic male [4]. The directionality of sex reversal in these two cases may not be coincidental, for it avoids the production of WW and YY individuals and the associated fitness consequences in both cases. The contrasting GSD systems and sex reversal conditions of these species make them ideal to

compare the effects of sex reversal in wild populations (Figure 2.2). We focus our attention on these two species as the only definitive and well-studied cases of reptile sex reversal in both the laboratory and the wild.

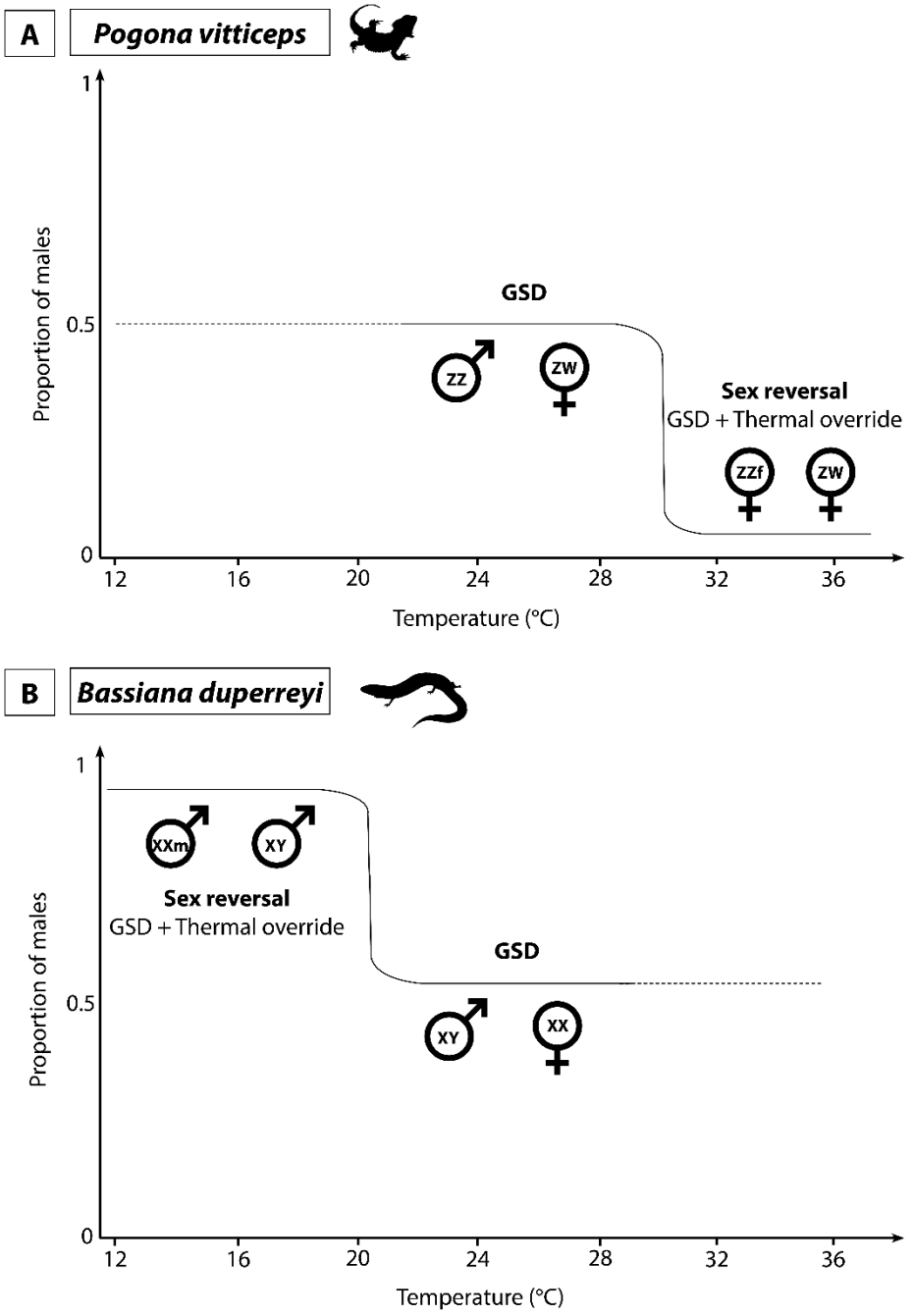

Figure 2.2: Schematic representation of sex reversal characteristics in *Pogona vitticeps* and *Bassiana duperreyi*. In *P. vitticeps* (A) sex reversal occurs when an individual with a male genotype (ZZ) is incubated at temperatures above 32°C, causing it to develop as a phenotypic female. In *B. duperreyi* (B) an individual with a female phenotype (XX) incubated at low temperatures will reverse its sex and develop as a phenotypic male.

In both *P. vitticeps* and *B. duperreyi* sex-reversed individuals occur in the wild, albeit at a lower proportion than either of their concordant counterparts. In *P. vitticeps*, sex-reversed ZZ females are fertile, with greater fecundity than concordant ZW females [3], and there are other attributes with implications for their fitness, like increased levels of activity and boldness [76,77]. The offspring of sex reversed females have a greater propensity to reverse, which may influence sex ratios across populations. There is conflicting evidence for this in wild populations. The occurrence of sex reversal was reported to increase in a wild population between 2003 to 2011 [3] but a second long-term, range-wide study did not find evidence of an increase in the rate of sex reversal over a 38-year period [78]. Specifically, sex reversal occurred in 12 of the 38 years, at rates ranging from 6-27% of phenotypically female individuals [78]. In *B. duperreyi*, 28% sex-reversed XX males arise in nests [21] and survive to adulthood [79], but whether the sex reversed males are fertile remains to be determined. Unlike *P. vitticeps*, gravid females and viable eggs are not evidence of fertility of sex reversed individuals, because the father of the clutch is typically unknown. Controlled mating and incubation experiments will be required to confirm that sex reversed XX males are in fact capable of producing viable sperm and fertilizing eggs. Alternatively, parentage studies of exhaustively sampled wild populations may be able to detect sex reversed fathers of clutches, but this approach is complicated in the case of *B. duperreyi* by communal nesting. Behaviour and survivorship of sex-reversed *B. duperreyi* has not yet been studied, so the fitness consequences of reversal are unclear. Ultimately, if these phenotypic effects result in altered survivability or reproductive success then sex reversal can affect population demographic processes and transitions from GSD to TSD.

2.6 Population processes and transitions between sex determining systems

The mechanisms of sex determination are rapidly evolving in many vertebrate species [1]. However, it is not understood whether this rapid evolution of sex determination mechanisms in reptiles is enough to accommodate current climatic change, or indeed if species are exhibiting sex reversal under pressure from changing environmental conditions. Modelling shows that as the frequency of sex reversal increases in a population, a likely response is a reduction in frequency and possible losses of the W or Y chromosome under Fisher's frequency-dependent selection [80,81]. Alternatively, an evolutionary response that alters the temperature at which sex reversal occurs could happen, however effective heritability in temperature thresholds is

low so the former scenario is more likely [82]. As a result, evolution of thermal thresholds is slow, whereas decline in frequency and ultimately loss of the Y or W chromosome is driven by the much stronger frequency-dependent selection [80]. Such loss of the W chromosome is predicted to happen in *P. vitticeps* under a warming climate in small isolated populations [52]. We also predict the complete loss of the Y chromosome from the wild population of *B. duperreyi* at higher elevational sites should the climate ever cool [79]. Indeed, Fisher's frequency-dependent selection alone is sufficient to drive transitions between GSD and TSD under changing climate scenarios [3]. However, conventional selection under a range of proposed scenarios (see Schwanz and Georges, this volume) may still be required to maintain TSD once it has been achieved.

Latitude and altitude, as landscape correlates of average temperature conditions, are useful for generating expectations about the frequency and spatial distribution of sex reversal. Indeed, cooler alpine areas have the highest rates of sex reversal in *B. duperreyi*, which decrease with decreasing elevation and associated increases in mean air temperature [79]. The field observations agree well with controlled laboratory experiments, incubating eggs at different temperatures [4,37]. Increasing global temperatures are likely to alleviate the demographic impact of sex ratio skew in *B. duperreyi* because temperatures consistently higher than 23°C result in a genetic influence only, producing a 50:50 sex ratio. However, even short term decreases in temperature (<20°C) during the natural incubation period, likely to persist during global warming, will be sufficient to cause sex reversal in high elevation populations [79]. So far, we know little about the sex reversal frequency in natural nests compared to the adults in higher elevational sites where nest temperatures are below 20°C. Our proposed models for *B. duperreyi* show that the frequency of the XY genotype is predicted to decline with decreasing incubation temperature as the system maintains a 1:1 sex ratio equilibrium. In fact, under current climate regimes within the species range, some with averages below 18°C, we expect the complete loss of the Y chromosome at some elevational sites [79].

The case of *P. vitticeps* appears more complex under warming climatic conditions. The overproduction of females by the reversal of the ZZ genotype to a female phenotype will deliver a disadvantage to the ZW females under Fisher's frequency dependent selection. This will potentially drive the frequency of the ZW genotype down as the system comes to local equilibrium. We expect to see (a) an increase in the frequency of ZZ reversal and (b) a decrease in the frequency of the ZW genotype with increasing latitude across the widespread range of

Pogona vitticeps. However, widespread sex reversal and overabundance of females will result in selection for the rarer sex (see Schwanz and Georges, this volume), which under warming conditions would be ZZ males, resulting in evolution of the sex reversal threshold. Although the frequency of sex reversal is spatially clustered in *P. vitticeps*, no trend in the frequency of sex reversal was observed with latitude and sex reversal was absent in the hottest parts of the species range [78]. Thus, local adaptation in the propensity to reverse sex may provide a better explanation for the distribution of reversal in this species [78]. Individuals that do not sex-reverse at sex-reversing temperatures (possessing a higher individual threshold for sex reversal) have a reproductive advantage, and their offspring may inherit this higher sex reversal threshold [52]. In this way, a transition to a TSD system and loss of the W chromosome may not occur under climate change, if local adaptation in the pivotal temperature for sex reversal occurs fast enough to avoid the action of frequency dependent selection in bringing the sex ratio to equilibrium. The fact that *P. vitticeps* has accommodated different climatic regimes across the landscape through local adaptation in the propensity to sex reverse over evolutionary time does not necessarily translate to an adequate capacity to respond in the same way under rapid climate change. Climate change may threaten numerous species with environmentally sensitive sex determination, largely by skewing population sex ratios [51,83–87]. The complex ways that climate change may interact with sex reversal in different species remains to be investigated fully.

2.7 Conclusion

As little is currently understood about sex reversal in reptiles, this understudied area warrants far greater attention. So long as sex reversal is confirmed only in two species it will remain unclear as to whether sex reversal is widespread throughout the reptile phylogeny, or if it occurs only rarely. We suggest there is likely an unappreciated diversity in sex reversal cues and mechanisms in reptiles, which may impact wild populations, particularly in the face of a rapidly changing climate. Future research will greatly benefit from marrying field and lab-based research to better understand all aspects of sex reversal. There is much to be gained from identifying sex reversal in additional species and establishing new sex reversal model systems. This will inform on the commonalities and differences in molecular mechanisms underlying sex reversal, and its fitness consequences. Ultimately by understanding sex reversal, we can understand the complex ways in which the environment can interact with sex to drive the evolution of sex determination systems in reptiles, and vertebrates more broadly.

Chapter 3 Cellular calcium and redox regulation: The mediator of vertebrate environmental sex determination?

Published: Biological Reviews, 2020

Castelli, M. A.*, **Whiteley, S. L.***, Georges, A., & Holleley, C. E. (2020). Cellular calcium and redox regulation: the mediator of vertebrate environmental sex determination? Biological Reviews, 95(3), 680–695. https://doi.org/10.1111/brv.12582

** Authors contributed equally*

3.1 Abstract

Many reptiles and some fish determine offspring sex by environmental cues such as incubation temperature. The mechanism by which environmental signals are captured and transduced into specific sexual phenotypes has remained unexplained for over 50 years. Indeed, environmental sex determination (ESD) has been viewed as an intractable problem because sex determination is influenced by myriad genes that may be subject to environmental influence. Recent demonstrations of ancient, conserved epigenetic processes in the regulatory response to environmental cues suggest that the mechanisms of ESD have a previously unsuspected level of commonality, but the proximal sensor of temperature that ultimately gives rise to one sexual phenotype or the other remains unidentified. Here, we propose that in ESD species, environmental cues are sensed by the cell through highly conserved ancestral elements of regulation of calcium and redox (CaRe) status, then transduced to activate ubiquitous signal transduction pathways, or influence epigenetic processes, ultimately to drive the differential expression of sex genes. The early evolutionary origins of CaRe regulation, and its essential role in eukaryotic cell function, gives CaRe a propensity to be independently recruited for diverse roles as a 'cellular sensor' of environmental conditions. Our synthesis provides the first

cohesive mechanistic model connecting environmental signals and sex determination pathways in vertebrates, providing direction and a framework for developing targeted experimentation.

Key words: oxidative stress, reactive oxygen species, calcium signalling, temperature dependent sex determination, epigenetics.

3.2 Introduction

The mechanisms by which sex is determined and the processes by which sexual phenotypes subsequently differentiate (sexual differentiation) have been a focus of enquiry for many centuries [88,89]. The structures of the testes and ovaries are highly conserved across vertebrates [17,90], so it is not surprising that the genes and regulatory processes governing gonad formation and differentiation share a high degree of commonality [5,16,91]. Despite the conservation of gonadal morphology, sex in vertebrates is influenced by a wide variety of mechanisms, broadly divided into genetic sex determination (GSD) and environmental sex determination (ESD), as well as mixed systems in which genes and environment interact to determine sex [1]. ESD systems occur in species from 15% of vertebrate orders. They use several different environmental cues including light regime, social stress, pH and temperature [1].

Decades of research on model and non-model organisms have documented the extraordinary variety of sex-determining environmental signals, and characterised different downstream elements of sex differentiation pathways in ESD systems. However, recent work implicating ancient, conserved epigenetic mechanisms in the regulatory response to environmental cues suggests that the mechanisms of ESD have a previously unsuspected level of commonality [24,55,92]. This poses the fundamental question: what is the mechanism by which such a wide variety of environmental cues are transduced to determine sex by a common molecular sensor?

The conservation of epigenetic elements in ESD suggests the action of a biochemical sensor common to all ESD species. Such a sensor must be (*i*) inherently environmentally sensitive, (*ii*) capable of interacting with components of known sex differentiation pathways, and (*iii*) conserved in function yet plastic enough to be recruited to capture and transduce different environmental signals for different phenotypic outcomes.

Here, we propose a general model in which sex determination is mediated by cellular calcium (Ca^{2+}) and redox (reactive oxygen species; ROS) status, which are subject to environmental influence. Elements of this hypothesis have been discussed in six recent papers that explicitly posited the involvement of either ROS production or Ca^{2+} flux in directing the outcomes of ESD [25,26,93–96]. We suggest that these two interrelated signalling systems [97] work together to initiate sex determination.

Here, we refer to calcium and redox status collectively as CaRe status, and propose a model for its biological action in ESD. We review evidence that CaRe status (and its subsequent effects on CaRe-sensitive regulatory pathways) is an environmentally sensitive mediator of complex biochemical cascades, and therefore a promising candidate for the capture and transduction of environmental signals into a sexual outcome. We propose that these CaRe-sensitive regulatory pathways have been co-opted independently and repeatedly to determine sex in different vertebrate lineages, acting as the crucial missing link between sex and the environment.

3.3 Calcium and redox regulation in the cell

3.3.1 Roles of ROS and Ca^{2+}

ROS and Ca^{2+} constitute some of the most important signalling molecules in the cell, and are both involved in a staggering variety of essential cellular processes [98–100]. The subtle ways in which these interactions can be modulated allows cellular responses to be fine-tuned according to the cellular context [101,102].

ROS are highly reactive by-products of cellular respiration, and can cause cellular damage when production exceeds that of the cell's antioxidant capacities [103,104]. ROS are produced mainly in the electron transport chain in the mitochondria, but can be generated elsewhere in the cell. They are typically rapidly dismuted through a series of antioxidant reactions [99,101,105]. If ROS production outweighs the antioxidant capacity of the cell, the redox environment can be altered to an oxidizing state [106]. However, at physiologically moderate levels (eustress), ROS possess vital cellular signalling roles in growth, homeostasis, reproduction, and programmed apoptosis [107–109]. When acting in their capacity as signalling molecules, ROS can influence protein conformation and function through the oxidative modification of accessible cysteine residues and reversible changes to disulphide bonds

[107,110–112]. Even subtle subcellular alterations in redox state can drive differential gene expression [113,114] through physiological or epigenetic mechanisms [115,116], and ultimately influence cell and tissue-specific environmental responses.

In close concert with redox signals, Ca^{2+} flux co-regulates many cellular signalling and environmental sensing functions [100,117–119], and displays considerable evolutionary flexibility in recruitment to these different functions [120]. Ca^{2+} concentrations inside the cell are tightly controlled by numerous calcium pumps and channels on the plasma membrane [121], and are mediated by Ca^{2+} release from internal stores in the mitochondria and endoplasmic and sarcoplasmic reticula [122–124]. Ca^{2+}-mediated signalling is crucial for orchestrating cell signalling cascades, which are highly sensitive to and modulated by the amplitude, duration, and subcellular localisation of Ca^{2+} [122,125]. Such finely tuned signal transduction cascades, which primarily involve protein phosphorylation or dephosphorylation, allow Ca^{2+} to control a wide variety of highly specific responses to environmental variables [124,126].

3.3.2 Environmental sensitivity of Ca^{2+} and ROS

We propose that CaRe status is the most promising candidate for encoding extrinsic environmental signals in the cell, and provide a framework in which CaRe status determines sex in environmentally sensitive species. On a biochemical level, ROS and Ca^{2+} levels in the cell are affected by many environmental factors, such as temperature [127], ultraviolet (UV) light [128,129], and hypoxia [130]. CaRe status can therefore indicate the presence and magnitude of an environmental signal and initiate a cellular response.

Ca^{2+} signalling has been implicated in temperature-dependent sex determination (TSD) through the temperature-sensitive regulation of transient receptor potential (TRP) cation channel expression in two TSD alligator species (American alligator, *Alligator mississippiensis* and Chinese alligator, *Alligator sinensis* [25,26] and a freshwater turtle *Mauremys reevesii* [131]. These plasma membrane channels control the flow of Ca^{2+} ions into the cell, and are thermosensitive at least in mammals [120], although TRP channel function is unknown for other vertebrates [25,120]. Within the TRP family, *TRPV4* exhibits temperature-specific differential expression in *A. mississippiensis* [25], and three other TRP family genes (*TRPV2, TRPC6,* and *TRPM6*) displayed temperature- and sex-biased expression in *A. sinensis* [26]. It was suggested that these channels act as the initial temperature sensor mechanism in alligators that regulates the expression of downstream sexual development genes through Ca^{2+} signalling

[26]. The application of TRPV4 antagonist drugs in *A. mississippiensis* partially interfered with male development, producing testes-like gonads with incomplete Mullerian ducts [25]. This suggests that TRPV4 operates alongside other, as yet unidentified, thermosensitive mechanisms acting in concert with Ca^{2+}, such as those involving ROS. In the turtle *M. reevesii*, the application of a TRPV1 and TRPM8 inhibitor altered sex ratios under certain incubation conditions, and although the authors accredited this to inhibited thermoregulatory behaviour rather than altered sex gene expression, the result could be due to inference with Ca^{2+} signalling [131].

TRP channels also respond to different wavelengths of visible light [132], and other research has proposed the effect of light on intracellular calcium concentrations to be mediated by ROS production [133]. Additionally, the oxidation of cysteine residues can sensitize and activate TRPA1 [134] and TRPV1 [135,136], further substantiating the link between the two messenger systems in response to various stimuli. TRP channels are also sensitive to and can be modulated by steroid hormones, particularly in sperm cells [137].

ROS production is directly influenced by the environment, primarily through the metabolism-enhancing effects of temperature [138,139], although pH (Maurer et al., 2005; Wang et al., 2009), UV light [142] and photoperiod-influenced circadian rhythms [143] can also alter oxidative state. Developmental rate in some reptiles accelerates with temperature, as does mitochondrial respiration [144], so it is feasible that that ROS could accumulate more quickly at a higher temperature, activating responses to oxidative stress. Further, antioxidant capacity in embryos varies in response to incubation temperature in a TSD turtle (red-eared slider, *Trachemys scripta elegans*), indicating that metabolic rate and ROS accumulation vary with temperature [106]. Additionally, yolk deposition of antioxidants is greater in birds with shorter developmental periods [145], suggesting that even in a homeothermic taxon, faster development results in greater oxidative stress. In some fish species, water temperature affects redox status and oxidative damage, although the effects have not been investigated in the context of sex determination [146].

Environmental cues do not necessarily need to be abiotic, as many species of fish display forms of socially cued sex change, commonly through the reorganisation of dominance hierarchies [20]. Oxidative stress has been shown to correlate with social status in species of fish [147] and primates [148], probably through the increased behavioural costs of defending and maintaining dominance. Signals of differential calcium regulation and responses to

oxidative stress were both observed in dominant male bluehead wrasse (*Thalassoma bifasciatum*), further indicating differential regulation of these messenger systems during sex change [149].

Combined with evidence on the environmental sensitivity of calcium channels, these studies show that a wide range of environmental conditions, including temperature, during development can alter both redox state and calcium flux. This raises the possibility that CaRe status could have a role as a cellular sensor for a broad range of environmental cues responsible in developmental programming and variation in different species.

3.4 Connections between CaRe status and sex determination

3.4.1 Signal transduction pathways

As discussed above, CaRe status is clearly a strong candidate for the capture of environmental signals by the cell. We propose here that the signal captured by CaRe status is then transduced *via* ubiquitous signalling pathways that influence epigenetic processes to govern sex differentiation.

The interactions between CaRe status and cellular organisation and function are complex, and so can interact with a variety of pathways involved in sex determination. Here we discuss CaRe-sensitive candidates likely to transduce an environmental signal; the nuclear factor kappa-light-chain-enhancer of activated B cells (NF-κB), heat shock response and antioxidant response pathways, and explore the potential interactions between CaRe status and another candidate pathway for ESD, the vertebrate stress axis (Table 3.1)

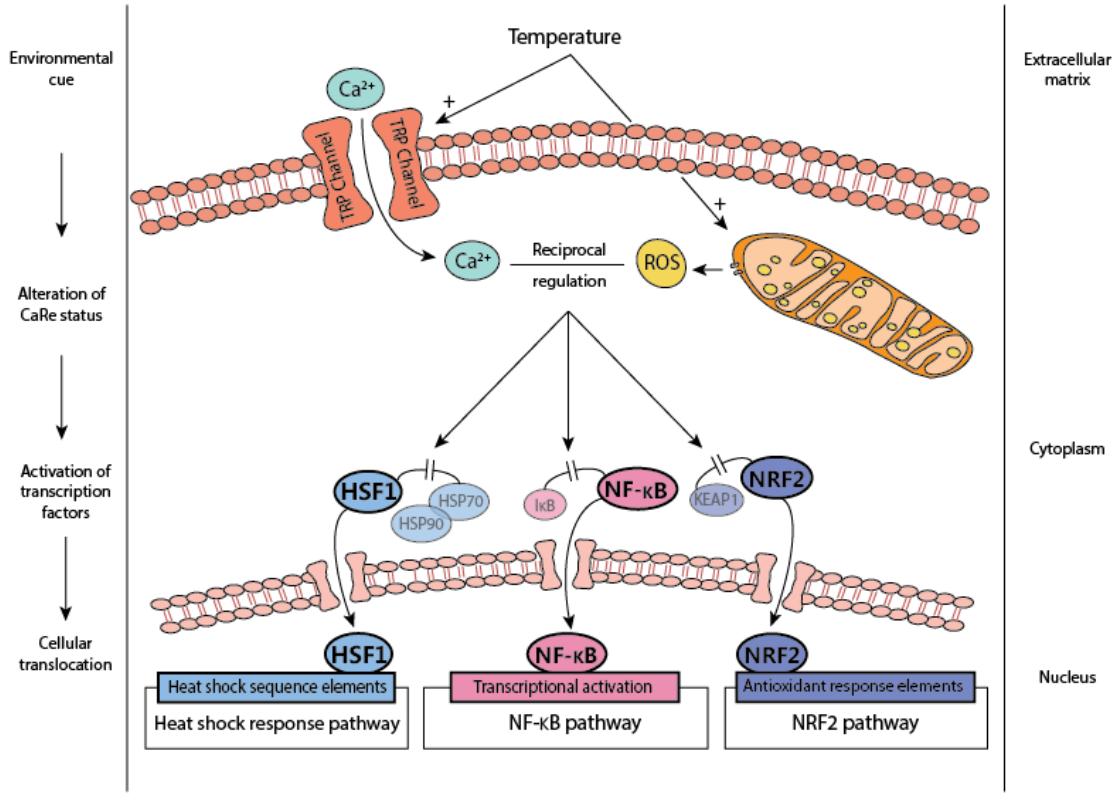

Figure 3.1. A subset of environmental response pathways hypothesised to be involved in environmental sex determination, activated by external signals integrated into the cell as calcium and redox (CaRe) status. This simplified model outlines how an environmental cue, in this case temperature, can alter CaRe status by causing an influx of Ca^{2+} ions through innately thermosensitive transient receptor potential (TRP) channels, and an increase in reactive oxygen species (ROS) production by mitochondria through increased metabolic rate. With their reciprocal co-regulation, both Ca^{2+} and ROS can act in concert to activate transcription factors [heat shock factor 1 (HSF1); nuclear factor erythroid-related factor 2 (NRF2)] and pathways [nuclear factor kappa-light-chain-enhancer of activated B cells (NF-κB)], which then translocate from the cytoplasm to the nucleus to alter the transcription of target genes involved in sex determination. HSP, heat shock protein; KEAP1, Kelch-like ECH-associated protein 1.

3.4.1.1 The NF-κB pathway

The NF-κB pathway is involved in a wide variety of cellular processes and can be activated by Ca2+ influx, ROS, and ROS-induced glutathione production [110,111,122,150] (Figure 3.1).

The NF-κB pathway has well-established associations with numerous sex determination genes in mammalian development. However, its role has been less well studied in ESD taxa [151–153] (Table 3.1). Analysis of the transcriptome during development in two TSD species (the alligator *A. sinensis* and painted turtle, *Chrysemys picta*) showed that differential

expression of various genes in the NF-κB pathway is associated with temperature at key developmental stages, but this has not been backed up by functional studies [26,154].

A single study directly demonstrated a role for NF-κB in vertebrate sex determination using the zebrafish (*Danio rerio*) [155]. While the genetics of sex determination in laboratory strains of *D. rerio* lacking a W chromosome [156] are not yet well understood, it appears to have a polygenic basis that is sensitive to environmental factors such as temperature and hypoxia [157,158]. Danio rerio is unusual in that a juvenile ovary initially forms, and either continues to mature as an ovary, or transitions into testes through the promotion of selective apoptosis [159,160]. Manipulating the induction or inhibition of the NF-κB pathway prior to gonadal commitment led to a female or male bias, respectively, demonstrating its role in suppressing the apoptotic pathways that trigger the transition to testis development [155]. Sex cell-specific apoptosis is a well-established mechanism in sex determination in *D. rerio* [161], as well as in other teleosts [162–164] and other model organisms such as *Drosophila melanogaster* [165] and *Caenorhabditis elegans* [166–168]. Manipulating the NF-κB pathway thus presents opportunities for exploring the link between CaRe regulation and ESD (Figure 3.2).

Table 3.1: Calcium and redox (CaRe)-sensitive elements, their functions relating to epigenetic modulation, cellular localisation and their roles in environmental sex determination (ESD) or temperature sex determination (TSD).

Candidate element	Cellular functions and known roles in environmental sex determination		References
Nuclear to cytoplasmic translocation			
CIRBP Cold-inducible RNA-binding protein	**Functions**	• Translocation to cytoplasm induced by numerous environmental stressors including temperature and oxidative state • Typically associates with cytoplasmic stress granules where it acts as a mRNA chaperone	[90,92,154,169,170]
	ESD roles	• Candidate gene for TSD in *Chelydra serpentina* • Thermosensitive expression in *Chrysemys picta* and *Apalone spinifera*	
hnRNPs Heterogeneous ribonucleoprotein particle family	**Functions**	• Involved in numerous cellular processes including splicing regulation, pre-mRNA processing, nuclear export of mRNA, chromatin remodelling • Interacted with *p38 MAPK* stress induced signalling pathway, and the EED subunit of the PRC2 complex	[171–174]
	ESD roles	• Thermosensitive expression in *Caretta* • Posited as candidates for the regulation of TSD	
Cytoplasmic to nuclear translocation			
NRF2 Nuclear factor (erythroid-derived 2)-like 2	**Functions**	• Regulates expression of antioxidant genes under oxidative stress through transactivation of antioxidant response elements	[107,175]
HSF1 Heat shock factor 1	**Functions**	• Transcriptional regulator of all heat shock proteins • Redox and temperature regulated • Induced by *p38 MAPK* phosphorylation	[26,171,176–179]
	ESD roles	• Role of heat shock response established for majority of TSD species • Involved in female sexual development in *Oryzias latipes*	
HSPs Heat shock protein family	**Functions**	• Molecular chaperone for steroids and hormones, participates in cell signalling • Roles in maintaining protein stability, folding, and transmembrane transport	(Harry et al., 1990; Brostrom & Brostrom, 2003; He et al., 2009; Kohno et al., 2010; Tedeschi et al., 2016, 2015; Casas et al., 2016; Czerwinski et al., 2016; Bentley et al., 2017; Lin et al.,
	ESD roles	• Thermosensitive expression in *Alligator mississippiensis* and *Alligator sinensis* • Markers of thermal stress, and thermosensitive expression in *Caretta* • Downregulation of *HSP10*-associated apoptosis during sex reversal in *Monopterus albus* • Various HSPs associated with social sex change in *Amphiprion bicinctus*	

		• *HSP90* upregulated in *Oreochromis niloticus* undergoing temperature-induced sex reversal	2018; Tao et al., 2018; Wang et al., 2019)
Protein kinases Family includes mitogen-activated, cAMP-dependent, calcium/calmodulin-dependent	**Functions**	• Multitude of cellular roles centring on ability to catalyse protein phosphorylation, so playing an integral role in numerous signal transduction cascades	[26,154,184]
	ESD roles	• Temperature-dependent expression in *Alligator sinensis* and *Chrysemys picta* • Male-biased expression in *Pagellus erythrinus* and *Pagrus pagrus*	
JAK-STAT pathway Janus kinase/signal transducers and activators of transcription	**Functions**	• Redox-regulated signalling cascade for stress response	[149,154,185]
	ESD roles	• Components of pathway show thermosensitive expression in *Chrysemys picta* • Progressive upregulation during sex change in *Thalassoma bifasciatum*	
NF-κB pathway Nuclear factor kappa light-chain-enhancer of activated B cells	**Functions**	• Redox-regulated signalling cascade for environmental stress response • Activation has anti-apoptotic effects	[26,154,155,186]
	ESD roles	• Components of pathway show thermosensitive expression in *Chrysemys picta* and *Alligator sinensis* • Crucial for sexual differentiation in *Danio rerio* • Male-biased expression in *Lates calcarifer*	
No subcellular translocation known/not applicable			
JARID2 & JMJD3 Jumonji and AT-rich interaction domain-containing 2 (*JARID2*) and lysine demethylase 6B (*JMJD3/KDM6B*)	**Functions**	• Members of the Jumonji chromatin remodelling gene family • *JARID2* mediates Polycomb repressive complex (PRC2) deposition of silencing H3K27me3 marks • *JMJD3* catalyses demethylation of H3K27me3	[24,55,149,154,187,188]
	ESD roles	• Retained intron associated with sex reversal in *Pogona vitticeps*, *Alligator mississippiensis* and *Trachemys scripta elegans* • TSD in *Trachemys scripta elegans*, *Chrysemys picta*, and *Apalone spinifera* • Thermal adaptation in *Anolis* lizards (*A. allogus*, *A. homolechis*, *A. sagrei*) • Associated transition to masculine phenotype during sex change in *Thalassoma bifasciatum* • Upregulated in response to temperature in *Dicentrarchus labrax*	
AP1 Transcription factor, activator protein-1	**Functions**	• Acts as a point of integration of many signalling pathways involved in responses to environmental signals (e.g. MAPKs, NF-κB, HSPs) • Redox controlled switch determines ability to bind DNA	[189]

TRPs Transient receptor potential cation channels	**Functions**	• Innately thermosensitive channels that allow the passive transfer of Ca^{2+} across the plasma membrane	[25,26,149,190]
	ESD roles	• Known thermosensitivity, temperature-dependent expression in *Alligator sinensis* and *Alligator mississippiensis* • Calcium signalling enrichment during sex change in *Thalassoma bifasciatum*	
TET enzymes Ten-eleven translocation methylcytosine dioxygenases	**Functions**	• Redox-dependent DNA methylation	[149]
	ESD roles	• Expression strongly associated with sex change in *Thalassoma bifasciatum*	
DNMTs DNA methyltransferases	**Functions**	• Sensitive to redox state and calcium concentration • Action influenced by the redox microenvironment of chromatin	[149,184,191]
	ESD roles	• Associated with sex change in *Thalassoma bifasciatum* • Sex-biased expression in *Pagellus erythrinus* and *Pagrus*	

Abbreviations: MAPK, mitogen-activated protein kinase; mRNA, messenger ribonucleic acid; PRC2, polycomb repressive complex 2

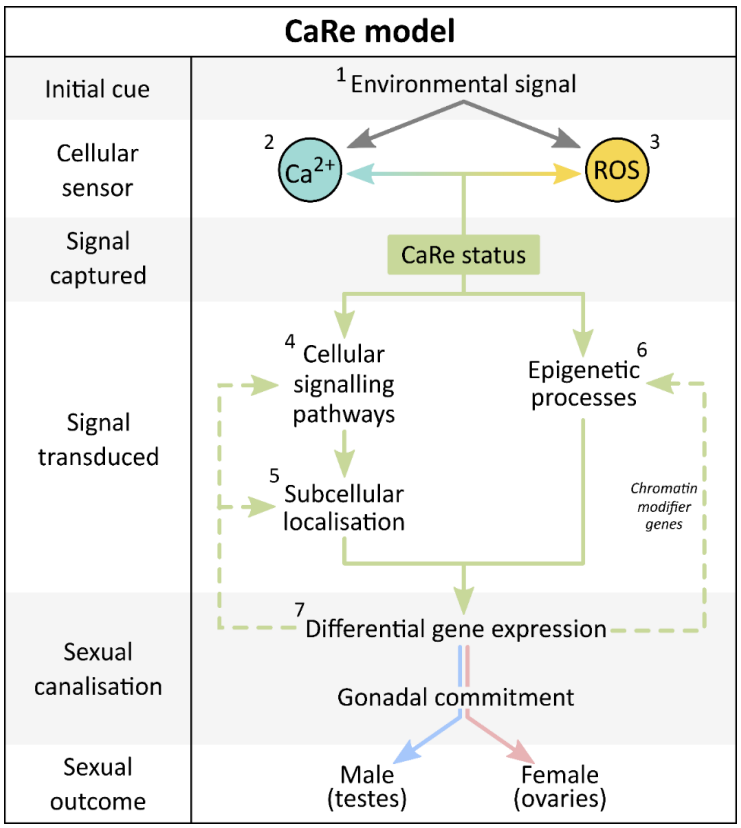

Figure 3.2. Generalised model for the influence of environment on sexual fate in vertebrates, identifying target stages for manipulation techniques that facilitate rigorous testing of the model. Solid lines indicate the top-down influence from environmental cue to sexual outcome, while dashed lines indicate areas where there is potential for feedback loops to occur. Incubation/rearing conditions during the environmentally sensitive period can be expanded to include not just the environmental stimulus the species is known to respond to, but other calcium and redox (CaRe)-altering stimuli, such as ultraviolet (UV) light, green light, or pH (1). Ca2+ flux can be manipulated either through the addition of calcium (typically accompanied by the calcium transporter ionomycin) or through altering the function of transient receptor potential (TRP) channels, either through RNA interference or the administration of TRP channel agonist and antagonist drugs (2). Reactive oxygen species (ROS) production can be manipulated by the direct addition of oxidants (e.g. H2O2) or antioxidants, or by application of ROS-inducing drugs (e.g. doxorubicin) (3). A range of approaches could be taken to interfere with cellular signal transduction pathways, which would vary depending on the pathway of interest (4). Subcellular localisation is similarly pathway specific, but for example small peptides can be used to inhibit nuclear factor kappa-light-chain-enhancer of activated B cells (NF-κB) nuclear translocation [192] (5). The role of epigenetic regulators can be investigated using agents for histone demethylation (e.g. 5-azacytidine), or through agents that inhibit the epigenetic regulatory machinery, for example polycomb repressive complex 2 (PRC2) inhibitors [193] (6). Genes suspected to be involved in the determination of sexual fate can be downregulated

through gene knock-down, RNA interference, or the addition of downstream products including hormones or hormone disruptors (e.g. oestrogen, testosterone, corticosterone, or fadrozole) (7).

3.4.1.2 Heat shock proteins and the heat shock response

Several authors have proposed a role in TSD for heat shock proteins (HSPs) [171,176,178] (Table 3.1). These proteins are chaperones and regulators of transcription factor binding, functions which are essential for maintaining cell function at extreme incubation temperatures [194,195].

Heat shock causes Ca^{2+} concentration to rise according to time and temperature, and concurrently increases levels of the oxidising agent hydrogen peroxide [127,196]. This change in CaRe status can activate heat shock factor 1 (HSF1), which in turn regulates expression of heat shock protein genes (notably *HSP70*), whose actions are required for protection against heat-induced cell damage [127,177,182,196] (Figure 3.1). Incubation temperature affects the expression of many HSPs in reptiles (Table 3.1), however, no consistent patterns have emerged even between closely related species, suggesting that HSPs exhibit considerable evolutionary flexibility [94,171,176,178,194]. Inconsistent patterns of expression of HSPs across species, and their role as molecular chaperones across a wide range of temperatures, might explain the variety of ESD responses to temperature across species [120,182].

Particularly interesting is that environmental triggers of HSPs extend beyond temperature. Some members of the HSP family show differential expression during socially induced sex change in the two-banded anemonefish (*Amphiprion bicinctus*) [183], and HSP10 is associated with female to male sex reversal (the trigger of sex reversal is not yet known) in the rice field eel (*Monopterus albus*), where it plays a role in inhibiting apoptosis in male germ cells [162]. Given HSPs demonstrated roles in sex determination across ESD taxa, and responsiveness to diverse environmental stimuli, they are promising candidates for further study (Figure 3.2).

3.4.1.3 Oxidative stress and the antioxidant response

Cellular responses to oxidative stress commonly involve induction of the cell's inbuilt antioxidant defence system [197]. The response is generally initiated by nuclear factor erythroid-related factor 2 (NRF2), whose action is critical for the oxidative stress response and cytoprotection [175,198]. Ordinarily NRF2 persists in the cytoplasm at low levels bound in an inactive state with KEAP1 (Kelch-like ECH-associated protein 1). However,

in a state of oxidative stress the bond with KEAP1 is broken, allowing NRF2 to translocate to the nucleus where it binds to antioxidant responsive elements. This initiates expression of genes such as thioredoxins, peroxiredoxins, and glutaredoxins that are critical to launching an antioxidant response to oxidative stress [199] (Figure 3.1).

These antioxidants quench ROS and cross-talk with proteins involved in the NF-κB pathway [111]. Glutathione is particularly crucial in the oxidative stress response, as the ratio of its oxidised and reduced states (GSH:GSSG ratio) is responsible for sensing the redox status of the cell [110,115,200,201]. Glutathione directly modifies chromatin structure *via* histone glutathionylation, increasing the binding of transcription factors and upregulating gene expression [202]. This has been demonstrated in mammals, in which glutathione enhances decondensation of the paternal genome in a newly fertilised egg [203–205].

Broadly, the response of antioxidant genes to environmental changes may be able to affect chromatin structure, essentially 'priming' key regions for binding by transcription factors, such as components of the NF-κB pathway [110], and the polycomb repressive complex PRC2, which is likely to be involved in reptile sex reversal [55,206]. The antioxidant response can therefore induce changes in gene expression and protein function which may contribute to the broader processes taking place during sex determination and differentiation in environmentally sensitive species (Table 3.1).

3.4.1.4 Synergism between hormonal and oxidative stress

The hypothalamic–pituitary–adrenal (HPA) axis in reptiles, birds and mammals or inter-renal (HPI) axis in fish and amphibians has a role in sex determination in a range of taxa (see reviews in [207,208]). Among gonochoristic (single-sex) fish, cortisol-mediated sex determination in response to temperature is well supported by experimental application of cortisol [32,209–211]. Cortisol has not yet been experimentally demonstrated to be a mediator of sex change in sequentially hermaphroditic teleost fish, but transcriptomic evidence suggests cortisol upregulation, supporting a role for the HPI axis in the repression of aromatase and the regulation of downstream epigenetic effectors of gene regulation [149,207,212,213].

Even in these fish species in which the stress axis has been co-opted as the environmental sensory mechanism, CaRe pathways may play a synergistic role in initiating, maintaining or mediating sex determination or sex change. Hormonal stress

results in oxidative stress *via* an increase in metabolic rate [214], and Ca^{2+} has a very strong association with sexual reproduction in fish [215–217]. For example, a social cue such as the removal of a dominant male induces HPI activation and glucocorticoid production in the dominant female of some species [207]. Elevated hormonal stress then results in aromatase repression and elevated androgen production through glucocorticoid receptor (GR) nuclear localisation and glucocorticoid receptor element (GRE) occupation in key genomic regions [149,218]. Concurrently, hormonal stress leads to oxidative stress through elevated metabolism and energy production [214], and alteration in CaRe status through one or more of the mechanisms described herein. There is extensive cross-talk between the hormonal stress axis and CaRe-sensitive pathways, creating opportunities for the two to synergise. CaRe-sensitive HSPs chaperone GRs, and GRs further interact extensively with the NF-κB pathway in a stimulus-, time-, and cell-specific manner to control responses to stimuli [219]. Whether CaRe pathways play a causative or synergistic role with stress hormones in species that have co-opted the HPI axis for sex determination (as many teleost fish clearly have) is not yet known, but there is evidence to suggest that these interactions exist.

Among crocodilians, turtles, and squamates there is little, and contradictory, evidence for the involvement of stress hormones in ESD. Temperature sex-reversed adult bearded dragons (*Pogona vitticeps*) display greatly upregulated pro-opiomelanocortin (*POMC*) gene expression in the brain, suggesting stress axis upregulation [55]. However, in other reptiles, manipulating incubation temperature and yolk corticosteroids during the embryonic period of sex determination has not demonstrated a causal link between temperature and glucocorticoid production [70,220–222]. Additionally, gonads of TSD reptiles cultured in isolation from the brain were still found to respond to temperature, suggesting that the effect of temperature on the HPA axis is not the temperature-sensitive mechanism in reptiles [223–225]. Thus, there is substantial evidence that the stress axis plays a role in ESD in teleost fish, but evidence for stress axis activation as a cause or consequence of sex reversal among reptiles remains equivocal. It is therefore unlikely that the stress axis is central to the temperature-sensitive mechanism in all vertebrates, but a common role for CaRe mechanisms is plausible in both teleost fish and reptiles with ESD.

3.4.2 Subcellular localisation

A commonality among many of the candidate pathways and proteins discussed herein is that their mode of action requires cellular translocation in response to changes in CaRe status [226,227] (Figure 3.1, Table 3.1). A change in localisation of transcription factors is necessarily upstream of any changes in nuclear organisation and gene expression. For example, in mammals the testis-inducing transcription factor (SOX9) must be translocated from the cytoplasm to the nucleus for normal testes development to occur. Otherwise, the developing gonads retain ovary-like characteristics even when expression levels of *SOX9* are maintained [228]. This process in mammals is regulated by the CaRe-sensitive catabolite activator protein cyclic AMP (cAMP) and protein kinase A phosphorylation [229,230], and by Ca^{2+}-calmodulin nuclear entry pathways [231]. It is plausible that a similar process, linked more directly to environmental conditions, occurs in vertebrates with ESD. While numerous candidates whose function relies on changes in cellular localisation have been associated with ESD, functional studies in this context are currently lacking, so future experimentation would benefit from considering these processes (Figure 3.2).

3.4.3 Alternative splicing and epigenetic remodelling

As well as the signal transduction pathways discussed above, there are other mechanisms that can also modulate gene expression in response to environmentally driven changes in CaRe status (Table 3.1). While these are as yet poorly understood, evidence is building that post-transcriptional processes including alternative splicing and epigenetic remodelling are involved in ESD.

In the 1990s, differential splicing was proposed to control TSD after differential expression of heterogeneous ribonucleoprotein particles (hnRNPs) was discovered in two TSD turtles (diamondback terrapin, *Malaclemys terrapin* and loggerhead turtle, *Caretta caretta*) [171,172,232] (Table 3.1). Splicing factors in the hnRNP family were suggested to regulate expression of key genes in a temperature-dependent manner at crucial stages in development, although the mechanism by which thermosensitivity is conferred on hnRNPs was (and remains) unidentified [172,173,233,234].

Subsequently, sex-specific associations with a single nucleotide polymorphism, embryonic expression profiles, and protein localisation in the TSD snapping turtle (*Chelydra serpentina*) suggested that *CIRBP* (cold-inducible RNA-binding protein;

CIRP, A18 hNRNP) was critical for determining sex [90]. This gene has thermosensitive expression in the pond slider turtle (*Trachemys scripta*) [235] and Chinese alligator (*A. sinensis*) [26], so this gene may be involved in TSD more broadly. CaRe status may be involved in the regulation of *CIRBP*, as it can be activated by a variety of environmental stressors that cause changes in CaRe, including osmotic shock, hypoxia, heat, and oxidative stress [170]. *CIRBP* may also be involved in mediating CaRe-regulated feedback loops, as upon activation it can function as an RNA chaperone or post-transcriptional regulator of many CaRe-sensitive genes [169,170,236,237].

Recent work supports the early evidence for a role of alternative splicing of key chromatin remodelling genes in TSD in reptiles. A sex-associated retained intron event in two members of the Jumonji gene family *JARID2* and *JMJD3* (also called *KDM6B*) occurs in three thermally sensitive reptile species (*Pogona vitticeps*, *Alligator mississippiensis*, and *Trachemys scripta*; [55]). In *P. vitticeps*, intron retention (IR) occurs only in sex-reversed females produced at high incubation temperatures. There is variation among these species in the pattern of sex-associated IR, perhaps arising from different ancestral genetic sex determination systems [55]. In a fish that undergoes socially cued sex change, the bluehead wrasse *Thalassoma bifasciatum*, *JARID2* and other cofactors within the PRC2 (*EZH2, SUZ12, EED, RNF2*) are transiently downregulated during female to male transition [149]. Both *JARID2* and *JMJD3* also exhibit thermosensitive expression in the brains of sex-reversed (neomale) Nile tilapia (*Oreochromis niloticus*) [238]. The PRC2 complex is also involved in orchestrating the commitment of sexual fate in GSD species, primarily through chromatin remodelling on the sex chromosomes [239].

JARID2 and JMJD3 regulate the tri-methylation of histone H3, lysine 27 (H3K27), and are involved in orchestrating embryonic development and sexual differentiation [240,241] (

Figure 3.3). Knockdown of *JMJD3* in a TSD turtle (*T. scripta elegans*) at male-producing temperatures triggers female development in 80% of embryos that survive [24]. JMJD3 mediates transcription of the male-determining gene *DMRT1* [23] by demethylating the repressive H3K27me3 near its promoter [24]. Downregulation of *JMJD3* by upstream mechanisms responding to high temperature results in persistent tri-methylation of H3K27, which suppresses *DMRT1* and promotes the female developmental pathway (

Figure 3.3). Upregulation of *JMJD3* in response to lower temperature results in de-methylation of H3K27me3 near the *DMRT1* promoter, activating *DMRT1* expression and promoting the male developmental pathway (

Figure 3.3). In alligators, switching embryos from a low female-producing temperature to a high male-producing temperature results in downregulation of *JARID2* and *JMJD3*, further demonstrating the commonality of these chromatin remodelling pathways in reptiles [93]. The interplay between thermo-responsive intron retention and activity of *JMJD3* [24,55] is not well understood [206]. However, these recent findings have dramatically shifted the focus of inquiry from direct thermosensitivity of candidate sex-determining genes to higher-order thermosensitive epigenetic processes that differentially downregulate or upregulate influential sex genes [206].

CaRe status may be directly linked to the epigenetic processes discussed above. ROS release from mitochondria [242] and hydrogen peroxide exposure [243] can alter histone methylation, and the oxidative status of a *JMJD3*-regulating transcription factor (STAT6) directly alters *JMJD3* [244]. JARID2 and the associated epigenetic remodelling complex PRC2, and JMJD3, exhibit a wide range of responses to oxidative and other cellular stressors, triggered by environmental signals such as heat shock [245]. The actions of hnRNPs also change depending on their oxidation status. For example, the activity of hnRNPk (a chaperone and inhibitor of HSF1 binding to heat shock elements) alters depending on the oxidation status of a single redox-sensitive cysteine residue, affecting the activation of heat shock response genes [174]. Alternatively, epigenetic processes may be mediated by the CaRe-responsive signalling pathways detailed above. The NF-κB pathway is known to control some histone methylation marks, perhaps *via* the transcriptional regulation of *KDM2B*, another lysine demethylase [246], and HSF1 has been demonstrated to open chromatin structure to assist the recruitment of other transcription factors [247]. These examples point to a promising area of future research, directed at the CaRe-sensitive epigenetic processes driving ESD.

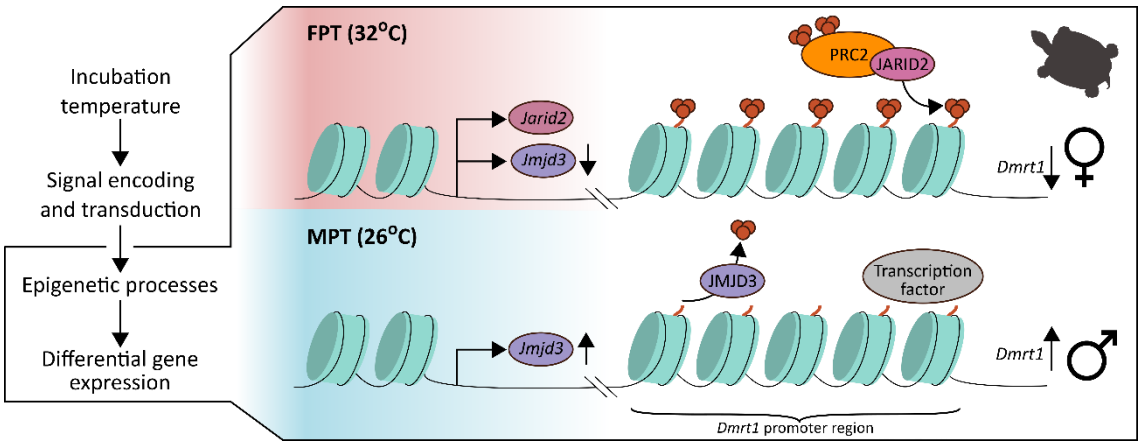

Figure 3.3. A schematic diagram showing the action of Jumonji family genes in altering the expression of a key sex gene in the red-eared slider turtle (Trachemys scripta elegans) based on the work of Ge et al., (2017, 2018). At female-producing temperatures (FPT), the chromatin modifier JMJD3, a histone demethylase, is downregulated, presumably under the influence of calcium and redox (CaRe)-mediated upstream signal transduction pathways. This allows the polycomb repressive complex 2 (PRC2) complex to deposit heritable methylation marks on histone 3 lysine 27 (H3K27me3), in part due to the action of JARID2. The methylation marks deposited in the DMRT1 promoter give permanence to the trimethylation and repression through cell division, ultimately leading to ovary development. At male-producing temperatures (MPT), JMJD3 is upregulated, likely under the influence of upstream CaRe-mediated signal transduction pathways. JMJD3 removes the H3K27me3 marks deposited by the PRC2 complex on the DMRT1 promoter, which then opens this region for transcription by as yet unidentified transcription factors, so altering the developmental trajectory toward a male fate. [After Georges & Holleley (2018)]. Image credit (turtle silhouette) Roberto Díaz Sibaja under PhyloPic Creative Commons attribution unported license 3.0.

3.5 Evolutionary significance of CaRe regulation

Tightly controlled regulation of intracellular levels of Ca^{2+} and ROS is essential for life, and has been since the emergence of the earliest eukaryotes [248]. The regulatory mechanisms by which Ca^{2+} and ROS are sensed, and the genetic pathways involved in responding to these signalling molecules, are therefore highly conserved [249]. The evolution of sexual reproduction itself has been proposed as an adaptive response to mitigate the subcellular damage caused by increased production of ROS in an oxygen-rich environment [250]. An alternative view is that ROS production by bacterial endosymbionts may have driven the evolution of sexual reproduction as a mechanism to allow for DNA repair through recombination [251].

In a facultatively sexual multicellular alga (*Volvox carteri*), temperature-induced ROS production triggered sexual reproduction [252], and treatment with antioxidants completely inhibited temperature-induced sexual reproduction [250]. There is a fundamental association between ROS and the regulation of sexual reproduction in all

three eukaryotic domains [253]. ROS are known to control sexual/asexual reproductive modes in fungi [254], affect germination and gametogenesis in plants [255,256], and influence reproductive phenotypes in multicellular animals [257].

Canalisation of the downstream regulatory pathways of gonad development, indicated by the relative commonality of gonadal structure, releases upstream elements of the regulation from selection. Provided functional ovaries or testes result, diversity in the upstream regulatory processes will be tolerated by selection [16,258]. The resultant evolutionary flexibility might account for the phylogenetic variability of ESD systems, which has been difficult to explain [1,5,259]. In particular, the independent re-emergence of TSD from GSD can be seen as a gain of sensitivity to the environment without the disruption of underlying CaRe mechanisms, which are essential for life [258,260,261]. Sensitivity to CaRe status can therefore be rapidly regained if there is selective pressure to do so. This may require only small-scale biochemical changes, allowing rapid responses in shorter evolutionary time scales compared with larger scale genetic or physiological changes.

3.6 Applying the CaRe model in theory and practice

3.6.1 Summary of the model

We have provided a simplified and generalised framework that proposes a critical role for CaRe regulation in environmentally sensitive sex determination systems. The CaRe model we present posits that an environmental influence, for example temperature, acts as a cue to stimulate a regulatory cascade that ultimately delivers a sexual outcome (testes or ovaries) (Figure 3.2). Such temperature cues act upon thermosensitive ion channels to regulate Ca^{2+} flux, interacting with ROS production driven by metabolic rate, resulting in a CaRe status that captures the environmental signal. CaRe status is decoded and transmitted to the nucleus *via* signal transduction pathways, such as the NF-κB and heat shock response pathways, potentially moderated by antioxidant activity (Figure 3.1). Each of these signal transduction pathways is likely to involve changes in subcellar localisation of key transcription factors such as HSF1, which can influence expression of genes responsible for developmental outcomes [262] (Figure 3.1). CaRe status can also be transmitted *via* epigenetic or post-translational modifications, so that a diverse array of CaRe-sensitive cellular pathways can ultimately drive differential gene expression and direct sexual outcomes.

3.6.2 Testing hypotheses derived from the model

While our model is necessarily speculative, it forms a basis for the generation of testable hypotheses and the re-examination of existing data. Models such as this have proven immensely successful in setting priorities and giving direction to research on the genes and gene products responsible for sexual differentiation [12,17].

Functional analysis will be critical for determining the role of CaRe in ESD systems and elucidating the species-specific pathways involved. Our model identifies target stages at different levels of the pathway for manipulation techniques, which can be applied to a wide range of study species (Figure 3.2). Manipulation of such ubiquitous signal transduction pathways is likely to present practical barriers (e.g. lethality), so we suggest that functional manipulation should exploit the wide variety of targeted inhibitor drugs and enhancers in both *in vitro* and *in vivo* experiments. We might borrow approaches from the biomedical and cancer research fields, in which these regulatory pathways are becoming well characterised and techniques for their manipulation are becoming more accessible. Gene editing techniques such as the clustered regularly interspaced short palindromic repeats (CRISPR-Cas9) system [263], combined with drug manipulation and transcriptomic approaches, will increase understanding of the role of these ubiquitous signal transduction pathways in both model and non-model species with ESD.

Understanding the mechanisms by which environmental signals are transduced to determine sex will have broader implications beyond the evolution of ESD systems. Practical applications could include manipulation of sex ratios in aquaculture systems, which frequently rear ESD species. Precise control of sex ratios in farmed species could increase efficiency of food production for a growing human population [19]. More broadly, a better understanding of ESD is increasingly important for assessing the biological impacts of climate change on environmentally sensitive species [264–268]. Already populations of ESD species are experiencing skewed sex ratios caused by rising global temperatures [51,84,85,211,269]. By understanding how an environmental signal is transduced to a sexual outcome, novel conservation management strategies could be devised to avoid or mitigate these impacts of climate change.

3.7 Conclusions

(1) A universal cellular sensor in ESD systems must be (*i*) inherently environmentally sensitive, (*ii*) capable of interacting with components of known sex determination pathways, and (*iii*) highly conserved in function yet plastic enough to be recruited for the transduction of different environmental signals for different phenotypic outcomes.

(2) CaRe status meets these requirements for a cellular sensor, and associated CaRe-sensitive pathways are promising candidates for the transduction of the environmental cue to orchestrate sex determination and differentiation in ESD species. Several lines of evidence support our model that CaRe-sensitive pathways have been independently and repeatedly co-opted as the mechanism by which an environmental signal is transduced to a sexual outcome in ESD species.

(3) The CaRe model is so far the only unifying model that has been proposed for ESD in vertebrates. Continued investigation of the role of CaRe regulation in ESD through explicit testing of CaRe mechanisms proposed in this review will not only advance understanding of evolutionary developmental biology and genetics, but may also at last identify the cellular sensing mechanism of ESD.

(4) We posit that what has been viewed as an intractable problem of identifying the environmentally sensitive element(s) among myriad possible candidates with putative influences on sexual differentiation, instead involves the more tractable challenge of identifying highly conserved ancestral elements of cellular machinery under the influence of equally highly conserved signalling pathways.

(5) We present this model as a basis for future experimentation that goes beyond simply examining gene expression. Our model incorporates signal reception, capture of the signal by the cell, receipt of the signal by established cellular signal transduction pathways, and the transduction of signals to the epigenome to direct gene expression leading to discrete sexual outcomes.

Chapter 4 Ovotestes suggest cryptic genetic influence in a reptile model for temperature dependent sex determination

Published: Proceedings of the Royal Society B, 2021

Whiteley, S. L., Georges, A., Weisbecker, V., Schwanz, L. E., Holleley, C. E. (2021). Ovotestes suggest cryptic genetic influence in a reptile model for temperature dependent sex determination. Proceedings of the Royal Society B, 288(20202819). https://doi.org/10.1098/rspb.2020.2819

4.1 Abstract

Sex determination and differentiation in reptiles is complex. Temperature dependent sex determination (TSD), genetic sex determination (GSD) and the interaction of both environmental and genetic cues (sex reversal) can drive the development of sexual phenotypes. The Jacky dragon (*Amphibolurus muricatus*) is an attractive model species for the study of gene-environment interactions because it displays a form of Type II TSD, where female-biased sex ratios are observed at extreme incubation temperatures and approximately 50:50 sex ratios occur at intermediate temperatures. This response to temperature has been proposed to occur due to underlying sex determining loci, the influence of which is overridden at extreme temperatures. Thus, sex reversal at extreme temperatures is predicted to produce the female biased sex ratios observed in *A. muricatus*. The occurrence of ovotestes during development is a cellular marker of temperature sex reversal in a closely related species *Pogona vitticeps*. Here we present the first developmental data for *A. muricatus*, and show that ovotestes occur at frequencies consistent with a mode of sex determination that is intermediate between GSD and TSD. This is the first evidence suggestive of underlying unidentified sex determining loci in a species that has long been used as a model for temperature dependent sex determination.

Keywords: *Amphibolurus muricatus*, gonad development, genital development, temperature reaction norms

4.2 Background

The determination and differentiation of a sexual phenotype is a major event in vertebrate development, shaping the form and behaviour of individuals, and influencing the ecological properties of species [270]. Among terrestrial vertebrates, the evolution of sexual development in squamates (lizards and snakes) is particularly labile, unlike the stable genetic sex determination mechanism of mammals. Squamates are therefore increasingly viewed as important models for understanding the molecular and developmental basis for sexual development in vertebrates [53,206,270].

Temperature-dependent sex determination (TSD), whereby incubation temperature determines sex in the absence of sex chromosomes, is a sex determination mode occurring in at least 10% of squamate species [270,271]. It is also possible for squamates to have genotypic sex determination, and for temperature to have a sex determining influence in the presence of sex chromosomes [3,38]. In such cases, extreme temperatures can override the influence of sex chromosomes, causing a discordance between an individuals sex chromosome complement and its phenotypic sex (sex reversal) [21,29]. There are only two known naturally occurring examples of such sex reversal: the Australian central bearded dragon *Pogona vitticeps*, and the three-lined skink *Bassiana duperreyi* [3,4]. In these two species, it is clear that genetic factors and temperature can interact, so blurring the dichotomy between GSD and TSD [272]. These two species are unlikely to represent the only instances of sex reversal in squamates, and its occurrence is likely more widespread than currently appreciated in reptiles, as well as other vertebrate groups [21,40].

Through its influence on sex determination, temperature also plays an important role in the differentiation of gonads and genitalia. In many female squamates, male genitalia often develop concurrently with differentiated ovaries, and the hemipenes do not regress until late in development, or post-hatching. This asynchrony between gonadal and genital phenotypes in female squamates is termed temporary pseudohermaphroditism (TPH) [8] and requires a combination of concurrent histology and hemipenal morphology to establish. TPH arises possibly because male genitalia may be a developmental default for some squamates (likely those with ZZ/ZW systems), that is overridden by other cues

causing genital feminisation [7,8]. In *P. vitticeps*, temperature-induced sex reversal causes the development of ovotestes, a rare gonadal phenotype with characteristics of both testes and ovaries [8]. Ovotestes were observed at a highly specific developmental period (stage 9) exclusively at sex reversing temperatures [8]. It was hypothesized that ovotestes developing during sex reversal occurs due to antagonism between opposing cues from environmental stimuli and sex chromosomes, and therefore can be used as cellular marker of sex reversal [8]. In TSD species, ovotestes can also occur due to incubation at the pivotal temperature (produces 50:50 sex ratios), drug manipulations, or developmental abnormalities, though they are ultimately a rarely observed phenotype, particularly under natural conditions [273–277]. Importantly, ovotestes are not observed at the more extreme incubation temperatures that produce a single sex in TSD species.

The Jacky dragon (*Amphibolurus muricatus*), an Australian agamid lizard, is a model for studies on the evolution and adaptative significance of TSD [278–282]. In this species, female-biased sex ratios are obtained at high (30-32°C) and low (23-25°C) temperatures, whereas approximately 50:50 sex ratios are produced at intermediate temperatures (27-30°C) [283]. Though considered a classic TSD species, this sex ratio pattern has been hypothesised to occur by temperature overriding an underlying GSD system [27]. Under this hypothesis, sex chromosomes are the primary sex determining influence at intermediate temperatures and thus produce 50:50 sex ratios, while extreme temperatures induce sex reversal in half of the individuals (assuming half of the individuals are genetically male) [27]. Therefore, if ovotestes indeed indicate sex reversal [8], *A. muricatus* developing at temperatures outside of the pivotal range should develop otherwise rarely observed ovotestes at a frequency of approximately 50%.

In this study, we investigate Quinn et. al.'s [2011] hypothesis that *A. muricatus* has a cryptic genetic sex determination mechanism with thermal override by assessing the frequencies of ovotestes at extreme incubation temperatures. For this purpose, we provide the first simultaneous characterisation of gonadal and genital development for *A. muricatus.* We also consolidate important baseline information on the development of this species, by assembling the first quantitatively rigorous confirmation of the thermal reaction norms of sex ratios in this species and also providing the first staging descriptions for this emerging model organism. Our data suggests that *A. muricatus* may indeed have an unidentified genetic influence on sex determination that is overridden by extreme temperatures, highlighting the need for further study on the sex determination mode of this species.

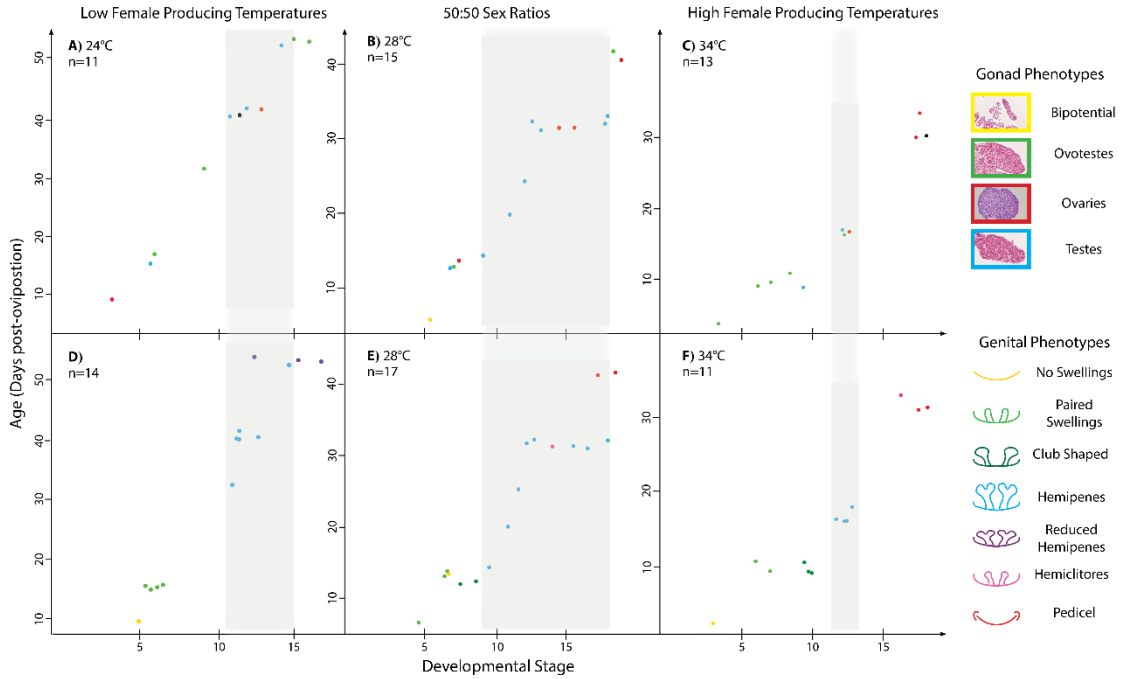

Figure 4.1: Development of gonad (panels A-C) and genital (panels D-F) phenotypes in *Amphibolurus muricatus* at three different incubation temperatures (24°C, 28°C and 34°C). Data for gonad and genital phenotypes is matched between individuals (supplementary file S1).

4.3 Results

For the developmental data presented in this study, eggs from *A. muricatus* were incubated at 24°C, 28°C, and 34°C, temperatures that have been established to produce female biased sex ratios at the extremes, and approximately even sex ratios at the intermediate temperature. Eggs were sampled throughout embryonic development (Figure 4.1, supplementary file S1) and staged according to the system development for close relative, *Pogona vitticeps* [7].

4.3.1 Temperature reaction norms of sex ratios

Our combined dataset (n = 806 individuals, supplementary file S3) confirms that *A. muricatus* does exhibit Type II TSD (Figure 4.2). However, the proportion of female individuals is not 100% at extreme temperatures, as has been reported by incubation experiments with smaller sample sizes [278,280]. This is the most comprehensive profile

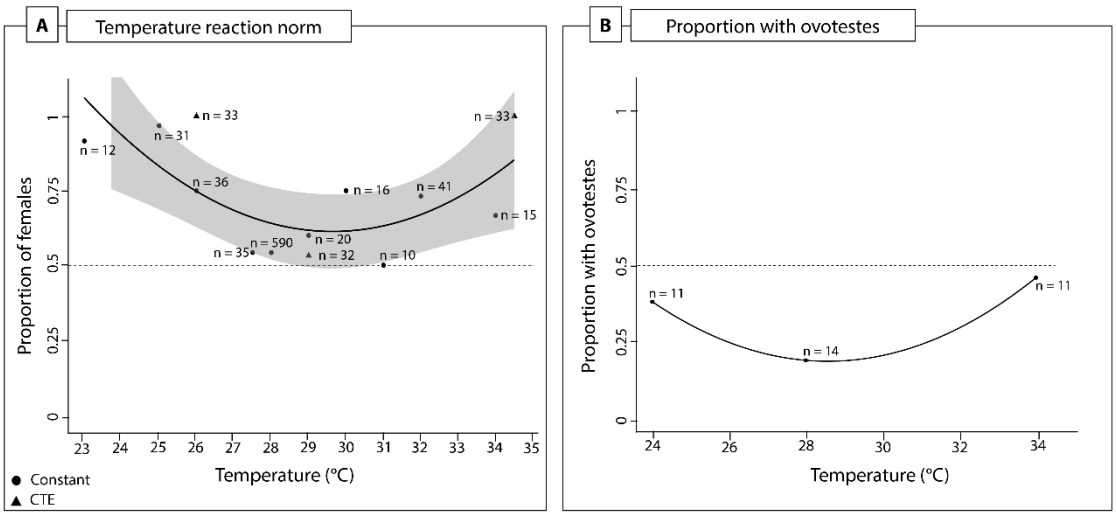

Figure 4.2: Temperature reaction norms (A) and proportion of ovotestes (B) for *Amphibolurus muricatus*. The reaction norms were calculated by fitting a polynomial logistic regression model to the dataset, which was obtained by compiling incubation data from this study and pre-existing datasets (supplementary file S1). Grey shading indicated 95% confidence intervals. The proportion of ovotestes was obtained from developmental data produced for this study, and fitted with a polynomial regression model (supplementary file S2).

of the temperature reaction norms for sex ratios in this species to date, and reveals that more variation in sex ratios exists than previously reported (supplementary file S2). Pearson's Chi-squared test showed that sex ratios differed significantly from 50:50 ratios at every temperature except for 27.5°C (P = 2.2e-16, supplementary file S3).

4.3.2 Frequency of ovotestes

Consistent with our hypothesis, assuming a GSD system with a thermal override, the proportion of ovotestes is highest at extreme temperatures and occurs at frequencies approaching 50% (Table 4.1, Figure 4.2).

Of the samples with characterised gonadal phenotypes (the gonads of some samples were unable to be characterised, supplementary file S1), ovotestes were observed more frequently at 24°C (n = 4 of 11, 36%) and 34°C (n = 5 of 11, 45%) compared to the moderate incubation temperature at 28°C (n = 2 of 14, 14%; Figure 4.2). In total, across all samples with a characterized gonadal phenotype in all incubation temperatures, 31% had ovotestes (n = 11 of 36) (Table 4.1, supplementary file S1).

There was considerable morphological variation observed in the ovotestes. Some samples exhibited rudimentary seminiferous tubules and a cortex layer, while others

exhibited well defined tubules and a cortex layer (Figure 4.3). Unlike what is seen in *P. vitticeps*, where ovotestes were observed during a narrow developmental range (stage 9-9.5) [8], ovotestes were observed at disparate developmental stages in *A. muricatus*, spanning stages 3 – 16 (a range equivalent to approximately 72% of embryonic development; , supplementary file S1). Given the wide range of developmental stages at which ovotestes were observed, they were concurrent with every genital phenotype observed during development (Figure 4.3, supplementary file S1).

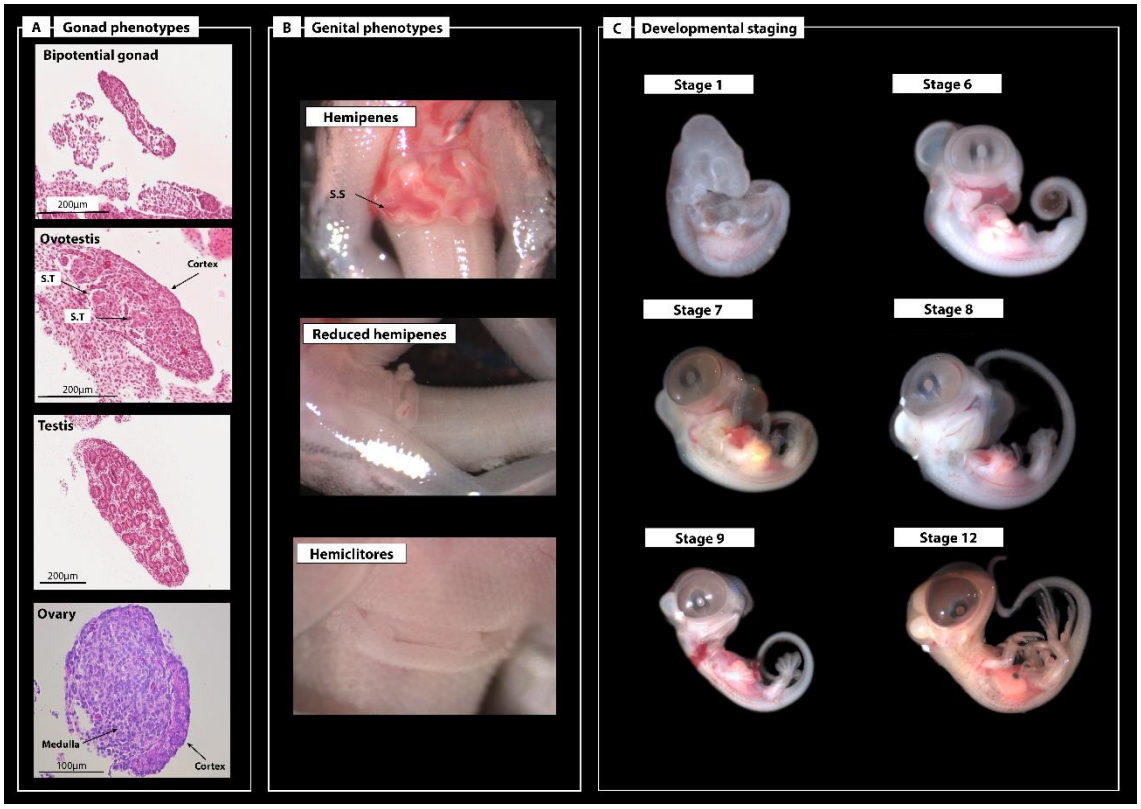

Figure 4.3: Development of gonad (panels A-C) and genital (panels D-F) phenotypes in *Amphibolurus muricatus* at three different incubation temperatures (24°C, 28°C and 34°C). Data for gonad and genital phenotypes is matched between individuals (supplementary file S1).

4.3.3 Timing of gonad differentiation and sex ratios

The gonadal morphologies observed in *A. muricatus* are similar to those previously described for other reptile species (Figure 4.3). The gonad initially forms as a long ridge of undifferentiated tissue along the mesonephros, before differentiating into ovaries or testes. Ovaries exhibit a distinct cortex and degenerating medulla (Figure 4.3). In testes the cortex degenerates and the medulla proliferates with seminiferous tubules (Figure 4.3). However, there are key differences in the timing of gonadal differentiation between

individuals. Differentiated ovaries were observed as early as stage 4 at 24°C, which is considerably earlier than has been observed in other reptile species (Table 4.2). By contrast, bipotential gonads were observed in a stage 5 specimen at 28°C (Figure 4.1).

Of the specimens that had differentiated gonads (not including ovotestes), 67% had testes at 24°C and 40% had testes at 34°C. At 28°C, which produces 50:50 sex ratios, we observed a male bias (75% of samples with differentiated gonads had testes; supplementary file S1).

Table 4.1: Embryos with ovotestes characterized in this study, including incubation temperature, developmental stage (based on staging system for close relative, *Pogona vitticeps* [7]), and corresponding genital phenotype. Ovotestes were observed at all incubation temperatures (though only two were observed at 28°C), and occurred alongside all possible genital phenotypes. They were also observed across a wide range of developmental stages. This data is also represented in , and supplementary file S1. Age is days post-oviposition (dpo).

Egg ID	Incubation temperature	Age (dpo)	Stage	Gonadal phenotype	Genital phenotype
9144:01:03	24	16	6	Ovotestes	Paired swellings
81826:01:01	24	32	10	Ovotestes	Bilobed hemipenes
9171:01:06	24	53	16	Ovotestes	Reduced hemipenes
9131:01:04	24	53	16	Ovotestes	Reduced hemipenes
9165:01:01	28	13	7	Ovotestes	Club shaped
9130:01:01	28	41	18	Ovotestes	Pedicel
82431:01:03	34	3	3	Ovotestes	Developing cloaca
9130:01:07	34	10	6	Ovotestes	Paired swellings
9130:01:04	34	10	6	Ovotestes	Paired swellings
9165:01:02	34	10	9	Ovotestes	Club shaped
9138:01:01	34	17	12	Ovotestes	Bilobed hemipenes

4.3.4 Genital development

Gross genital development follows the same processes as has been previously described for *P. vitticeps* [7]. The cloacal area forms early in development, followed by the growth of paired swellings. These swellings continue to grow and eventually become bilobed hemipenes (Figure 4.3). In females, hemipenes eventually regress to hemiclitores, then a pedicel. In presumptive female specimens (those with differentiated ovaries), hemipenes occurred at all three incubation temperatures (Figure 4.1).

At 24°C, hemipenes had not regressed completely by the latest stage assessed (stage 16). However, these specimens also possessed ovotestes suggesting that the lack of total hemipenis regression may have occurred because of insufficient hormone signalling from the gonad (assuming development was ultimately on a female trajectory). One stage 12 specimen exhibited temporary pseudohermaphroditism (TPH), which is characterized with the concurrent appearance of differentiated ovaries and bilobed hemipenes [8]. At 28°C hemipenes are observed between stages 9 and 17, with one stage 16 specimen exhibiting TPH. Two stage 18 specimens exhibited a pedicel, with one having ovaries and the other ovotestes, suggesting that hemipenis regression can still occur without fully differentiated gonads. At 34°C one stage 13 specimen exhibited TPH. Hemipenis regression was observed in three specimens, with two developing a pedicel at stage 18 (, supplementary file S1).

While the gross genital morphologies are similar between *A. muricatus* and *P. vitticeps*, the timing of development differs. In *P. vitticeps* bilobed hemipenes have developed in both sexes by approximately stage 11. In females hemipenis regression leading to hemiclitores occurring by approximately stage 16.5 [7]. In *A. muricatus* hemipenes develop earlier and persist for longer during development; the first specimens observed with hemipenes were at stage 9 and the oldest possessed hemipenes at stage 17. In *P. vitticeps*, the TPH phase in females persists from approximately stage 8 to 15. In *A. muricatus*, the timing of the TPH phase is less well established due to having fewer samples, however we estimate the TPH phase in *A. muricatus* as occurring between approximately stage 9 to 17, so although it might begin slightly later it probably lasts slightly longer in *A. muricatus* compared to *P. vitticeps* (Figure 4.4).

Table 4.2: Timing of gonadal differentiation in species with temperature dependent sex determination in which gonadal development has been characterised. The stage and staging system used in the original publication is provided, which has been calibrated to the staging system used for *Pogona vitticeps* and *Amphibolurus muricatus* to compare the timing of differentiation. Where only the thermosensitive period (TSP) is given, stages of the lower and upper bounds of the period or the average to the *P. vitticeps* staging system is provided.

Species	**Gonad differentiation/ TSP period**	**Staging system**	***P. vitticeps/A. muricatus* equivalent**	**Original reference**
Alligator mississippiensis	Stage 23	[284]	Stage 13	[285]
Apalone spinifera	Stage 18-20	[286]	Stage 9	[287]
Calotes versicolor	Stage 34	[288]	Stage 9	[289]
Chelydra serpentina	Stages 14-16 (TSP period)	[286]	Stage 14 = Stage 5 Stage 16 = Stage 6	[290]
Crocodylus palustris	Stages 21-25 (TSP period)	[284]	Stage 13 (average)	[291]
Emys orbicularis	Male differentiation at stage 17, female differentiation at stage 19	[286]	Stage 17 = Stage 8 Stage 19 = Stage 9	[292]
Eublepharis macularius	Stages 33-37 (TSP period)	Dufaure and Hubert 1961	Stage 33 = Stage 6 Stage 37 = Stage 14	[293]
Malayemys macrocephala	Stage 17	[286]	Stage 8	[294]
Pogona vitticeps	Stage 8	[7]	NA	[7]
Trachemys scripta	Stages 14-20 (TSP period)	[295]	Stage 14 = Stage 5 Stage 20 = Stage 9	[296]

4.4 Discussion

Our results confirm our prediction that approximately half of *A. muricatus* specimens incubated at extreme temperatures display ovotestes. This provides support for Quinn et al.'s (2011) suggestion that *A. muricatus* possess a cryptic genetic component to sex determination whilst simultaneously exhibiting a thermal override. We expect that ovotestes in *A. muricatus* are occurring due to antagonism between genetic and thermal influences on sex, as proposed for *P. vitticeps* [8]. A GSD system with thermal override in *A. muricatus* would also explain why extreme incubation temperatures do not produce 100% females, because sex reversal generally occurs at slightly lower than absolute frequencies (approximately 96%) in *P. vitticeps* [3].

In *P. vitticeps*, ovotestes were observed exclusively in association with sex reversal, and occurred during a very limited developmental period [8]. In *A. muricatus*, ovotestes

occurrence was far less stable. Ovotestes were observed at all three incubation temperatures (though at a low frequency at 28°C), and across a wide range of developmental stages. We also observed male biased sex ratios (67% at 24°C, 75% at 28°C, and 40% at 34°C). Understanding that sex determination modes can exist on a continuum between GSD and TSD can clarify such observations in *A. muricatus*. Even in TSD species, heritable genetic variation in thermal thresholds can influence sex ratios, particularly at the pivotal temperature [297]. These differences in thresholds can subsequently shift an individual embryo's propensity for developing as one sex or the other at a given temperature, which can create sex ratio biases, such as those we observed in *A. muricatus* [225,298–300]. We argue that such genetic variation in thermal thresholds likely exists alongside other genotypic determinants of sex in *A. muricatus*, so explaining the variation observed in both sex ratios and ovotestes frequency at different incubation temperatures [78]. This is akin to observations in close relative, *P. vitticeps*, where rates of sex reversal increase as temperature increases, though some individuals do not reverse sex [3]. Maternal genotype also influences rates of sex reversal; offspring of sex reversed mothers reverse at lower temperatures compared to offspring of concordant mothers [3]. We propose that differences observed between the two species may be due to the genetic determinant of sex being less fixed in *A. muricatus* compared with *P. vitticeps*, which possess differentiated sex microchromosomes [45]. A particularly intriguing scenario might be that *A. muricatus* represents an early stage of sex chromosome evolution, where a small number of sex-linked genes produce the unusual timing of ovotestes that we observed.

The development of the European pond turtle, *Emys orbicularis*, offers support for an interaction between a genetic and thermal sex determination mechanism we propose for *A. muricatus. E. orbicularis* was presumed to have TSD based on incubation experiments and hatchling sex ratios in the laboratory, until additional research revealed that temperature can override a weak genetic mechanism of sex determination identified by differential expression of H-Y antigens in gonadal tissues [56,301]. H-Y antigens are widely associated with XX/XY and ZZ/ZW systems in a variety of reptiles (reviewed in [302]). The joint action of H-Y expression and thermal sensitivity in *E. orbicularis* thus implies that some genetic factors likely influence thermally-sensitive sex determination in many reptiles, and a similar process may be occurring in *A. muricatus* (reviewed in [5]). However, it is important to note that the functional roles of H-Y antigens are not well elucidated, particularly how they may influence sex determination [21].

As with *A. muricatus*, the embryonic development of *E. orbicularis* is often characterised by the presence of ovotestes. In the turtle, they may persist post-hatching but ultimately resolve as testes [303]. It appears that ovotestes occur readily in this species due to a high sensitivity to small fluctuations in estrogens, which can rapidly drive the development of an ovarian cortex but fails to fully repress the seminiferous tubule proliferation in the medulla [304,305]. It is possible that estrogen sensitivity may also drive ovotestes development (and its lability) in *A. muricatus*, though it is unknown how estrogen levels may be influenced by varied incubation temperatures in *A. muricatus*. Testosterone, or the balance between testosterone and estrogen, may also influence ovotestes development, however further study is required. It is currently unknown if ovotestes persist post-hatching in *A. muricatus*, or if they resolve by hatching, as has been reported for *P. vitticeps*. The timing in ovotestes occurrence greatly differs to that of *P. vitticeps*, and may be more similar to *E. orbicularis*, however this remains to be investigated fully.

Understanding the genetic underpinnings of ovotestes development in reptiles would also be of great benefit. To date, no ovotestes in reptiles have been sequenced to reveal the gene expression profiles of this unusual phenotype. In many fish species, ovotestes occur comparatively often, and sequencing has revealed novel insights into the genetic machinery responsible for ovotestis development, for example in the rice field eel and black porgy [306–308]. In mammals, ovotestes are typically only associated with disorders of sexual development, however the Iberian mole possess ovotestes and RNA sequencing has shown how they develop [309]. Interestingly, despite the wide phylogenetic divide between these groups, many of the same genes (e.g., aromatase and DMRT1) have been implicated, so it would be particularly intriguing for future research to assess this in reptiles.

We present the first comprehensive thermal reaction norms for sex ratios in *A. muricatus* by combining our data with previously published sex ratio data. We show that contrary to previous reports, the only incubation temperature that did not exhibit significant deviation from 50:50 sex ratios was 27.5°C. This suggests that the intermediate temperature range of this species may be far narrower than previously reported [280,283,310], and that small sample sizes limit the accuracy of earlier reported sex ratios. This may also go some way to explaining the male biased sex ratios we observed in our study. Further, our observation of two samples with ovotestes at 28°C

can also be explained by this trend, as 50:50 sex ratios are not actually expected at this temperature.

Lastly, we also show *A. muricatus* is the fourth squamate discovered to exhibit temporary pseudohermaphroditism (TPH; male genitalia occurs alongside differentiated ovaries), another condition previously considered unusual. This supports suggestions that TPH may occur in female squamates and is associated with thermolabile sex determination (Figure 4.4; [8]). Histological studies on squamate gonads are rare, but we expect that further investigation of genital and gonadal development will reveal TPH to be a common occurrence among squamates, particularly among those with retained hemipenes in the female juveniles [311–314].

4.5 Conclusions

Our results indicate strong potential for extensive and unappreciated diversity in genetic, temperature, and possibly other cues in the differentiation of sex in squamates. Our understanding of the interaction between genes and the environment in reptile sex determination remains poorly characterized, so this area provides many compelling avenues for future research. *A. muricatus* emerges as a particularly important study species to identify the nature of genetic mechanisms influencing sex, such as evidence of cryptic sex chromosomes. It will also be imperative to identify loci that have sex associated alleles in adults from intermediate temperatures. Definitive demonstration of the genetic mechanisms underlying sex, combined with identification of phenotype, will be required confirm our suggestion that sex reversal occurs in this species. *A. muricatus* would then represent the third squamate with sex reversal, and would the first with sex reversal at both extremes of temperature. We hope that our suggestion of sex reversal in *A. muricatus* provides the impetus to examine the sex determination modes of TSD squamates more closely, and highlights novel approaches that can be taken to uncover previously unidentified complexities in reptile sexual development.

4.6 Materials and Methods

4.6.1 Egg incubations and sampling

During the 2018-19 breeding season, eggs were obtained from both wild caught (n = 4) and captive bred females (n = 4) for the developmental data. Females were provided with nesting substrate and allowed to lay naturally. If the female retained eggs for a prolonged

period of time, they were induced to lay with an intraperitoneal injection of 10-30 IU of oxytocin followed by a 10 IU dose of calcium carbonate solution. Eggs were weighed and randomly allocated to one of three incubation temperatures (24°C, 28°C, 34°C). Eggs were placed individually in glass jars filled damp vermiculite (four parts vermiculite to five parts water by weight) and covered with Glad Wrap® known to allow the diffusion of oxygen. Eggs were subsequently randomly allocated to a target developmental stage (6, 12 and 15), the sampling day estimated based on incubation data from *Pogona vitticeps* and adjusted for differing incubation durations [7]. Six eggs were sampled at day of lay to establish stage at lay (two eggs from three clutches). This showed that eggs were consistently at stage 2 based on the staging system developed for *P. vitticeps* [7]. Every embryo was staged and photographed fresh, and the urogenital system (UGS) was dissected. In total, 44 embryos were obtained. All procedures were carried out in accordance with animal ethics procedures from the University of Canberra (Project 270). Additional incubations were carried out at the University of Canberra and the University of New South Wales, and this data was used to generate the temperature reaction norms (Supplementary File S1).

4.6.2 Histology and phenotype characterisation

All UGS samples for histology were prepared at the University of Queensland's School of Biomedical Science's Histology Facility. Samples were processed for haematoxylin and eosin staining following standard histological procedures described in [8]. The gonadal phenotypes for each sample were characterised following established morphological characteristics, with the operator blind to incubation temperature [8].

4.6.3 Supplementary Figures

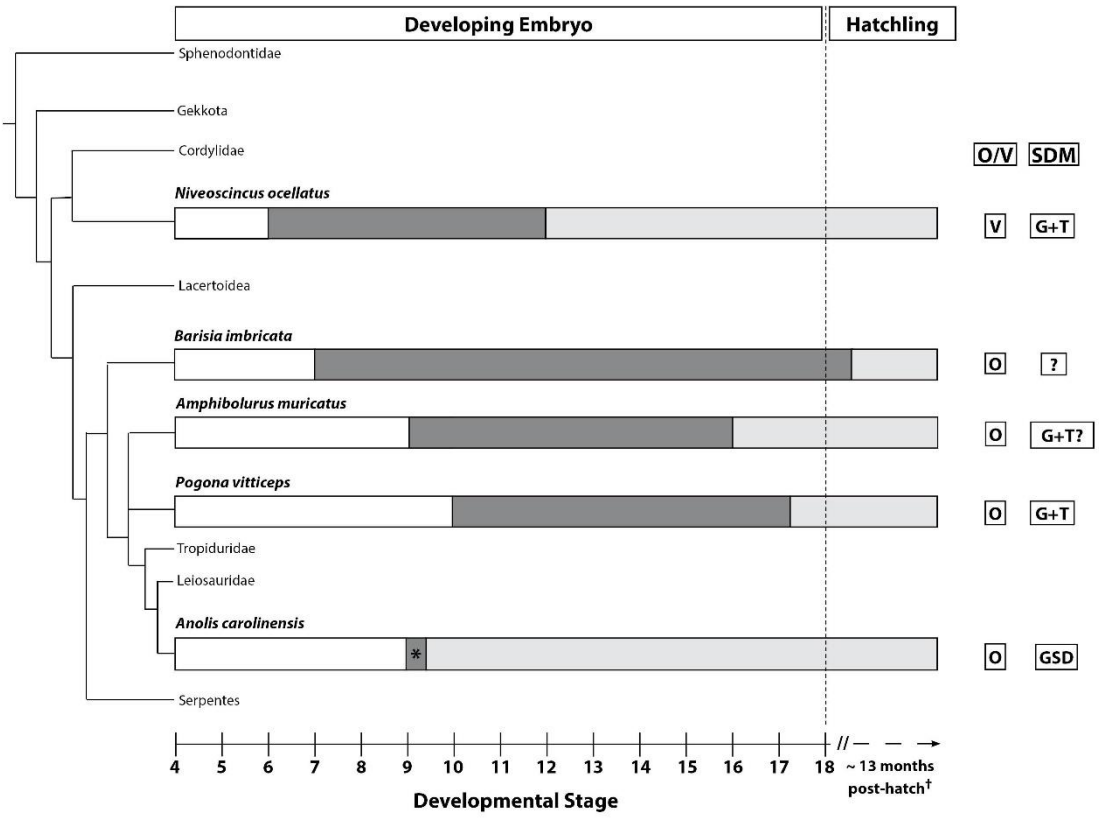

Figure 4.4: Illustrative squamate phylogeny adapted from [8] with the addition of *Amphibolurus muricatus* as the fourth species to exhibit temporary pseudohermaphroditism (TPH) during female development. The duration of the TPH phase is an approximation based on incubation data at the three temperatures used in this study (24°C, 28°C, and 34°C) O/V = oviparity/viviparity, SDM = sex determination mode, GSD = genetic sex determination, G+T = GSD with thermal interaction.

4.6.4 Supplementary Files

All supplementary files are available online at https://doi.org/10.6084/m9.figshare.c.5268964.

Supplementary File S1: Developmental data at three incubation temperatures (24°C, 28°C, and 34°C) in *Amphibolurus muricatus*. NA denotes samples whose gonads were unable to be characterized histologically.

Supplementary File S2: Incubation data used for the generation of the temperature response norms in *Amphibolurus muricatus*. Any data obtained from previously published studies includes the reference in the "source" column [283,315].

Supplementary File S3: Complete output from row-wise Chi-square test in R (v. 1.2.5). Columns B and C (Male and Female) respectively are the proportions of each sex observed at each incubation temperature. These numbers were obtained from the data collated in supplementary file S3.

Supplementary File S4: Temperature fluctuation program data from [282] used to calculate the constant temperature equivalent (CTE) [316].

Chapter 5 Two transcriptionally distinct pathways drive female development in a reptile with both genetic and temperature dependent sex determination

Published: PLoS Genetics, 2021

Whiteley, S. L., Holleley, C. E., Wagner, S., Blackburn, J., Deveson, I.W., Marshall Graves, J.A., Georges, A., (2021). Two transcriptionally distinct pathways drive female development in a reptile with both genetic and temperature dependent sex determination. PLoS Genetics. doi.org/10.1371/journal.pgen.1009465

5.1 Abstract

How temperature determines sex remains unknown. A recent hypothesis proposes that conserved cellular mechanisms (calcium and redox; 'CaRe' status) sense temperature, and identify genes and regulatory pathways likely to be involved in driving sexual development. We take advantage of the unique sex determining system of the model organism, *Pogona vitticeps*, to assess predictions of this hypothesis. *P. vitticeps* has ZZ male: ZW female sex chromosomes whose influence can be overridden in genetic males by high temperatures, causing male-to-female sex reversal. We compare a developmental transcriptome series of ZWf females and temperature sex reversed ZZf females. We demonstrate that early developmental cascades differ dramatically between genetically driven and thermally driven females, later converging to produce a common outcome (ovaries). We show that genes proposed as regulators of thermosensitive sex determination play a role in temperature sex reversal. Our study greatly advances the search for the mechanisms by which temperature determines sex.

5.2 Introduction

Sex determination in vertebrates may be genetic or environmental. In genetic sex determination (GSD), offspring sex is determined by sex chromosomes inherited from each parent, which bear either a dominant gene on the heteromorphic sex chromosome (as with *SRY* in humans) [317,318], or a dosage sensitive gene on the homomorphic sex chromosome (as with *DMRT1* in birds) [319]. However, some fish and many reptile species exhibit environmental sex determination (ESD), whereby a variety of external stimuli can determine sex, most commonly involving temperature (temperature dependent sex determination, TSD) [16,320]. While GSD and ESD are commonly viewed as a dichotomy, the reality is far more complex. Sex determination in vertebrates exists as a continuum of genetic and environmental influences [5] whereby genes and environment can interact to determine sex [3,4,21].

The genetic mechanisms that act in highly conserved pathways that ultimately yield testes or ovaries are quite well characterised [1,16,321]. Yet, despite decades of research on ESD systems, and TSD in particular, the upstream mechanisms by which an external signal is transduced to determine sex remains unknown [270]. Recent research led to the hypothesis that the cellular sensor initiating ESD is controlled by the balance of redox regulation and calcium (Ca^{2+}) signalling (CaRe) [53]. The CaRe hypothesis proposes a link between CaRe sensitive cellular signalling and the highly conserved epigenetic processes that have been implicated in thermolabile sex (TSD and temperature sex reversal) [22,24,55,206,270]. The CaRe hypothesis posits that in ESD systems a change in intracellular Ca^{2+} (probably mediated by thermosensitive transient receptor potential TRP channels) and increased reactive oxygen species (ROS) levels caused by high temperatures, alter the CaRe status of the cell, triggering cellular signalling cascades that drive differential sex-specific expression of genes to determine sex. The CaRe hypothesis makes several testable predictions for how an environmental signal is captured and transduced by the gonadal cells to deliver a male or a female phenotype.

Species in which genes and environment both influence sex determination provide unique opportunities to directly compare the regulatory and developmental processes involved in sex determination. By early gonad differentiation directed by genotype and temperature, it is possible to assess predictions of the CaRe hypothesis. In our model species, the central bearded dragon (*Pogona vitticeps*), we can compare female development via thermal and genetic cues because extreme temperatures (>32˚C)

override the male sex-determining signal from the ZZ sex micro-chromosomes to feminise embryos [3,38]. This makes it possible to distinguish between the previously confounded effects of thermal stress and phenotypic sex by comparing gene expression throughout embryonic development in sex reversed ZZf females with genetic ZWf females.

We can explore the predictions of the CaRe model, namely that under sex-reversing conditions, we will see differential regulation of: 1) genes involved in responding to Ca^{2+} influx and signalling; 2) genes involved in antioxidant and/or oxidative stress responses; 3) genes with known thermosensitivity, such as heat shock proteins; 4) candidate TSD genes, such as *CIRBP* and Jumonji family genes; 5) signal transduction pathways such as the JAK-STAT and NF-κB pathways.

We compared gene expression profiles in *P. vitticeps* embryonic gonads at three developmental stages (6, 12, and 15; [7,8] for ZWf and ZZf eggs incubated at 28°C and 36°C respectively; Figure 5.1). This allowed us to compare drivers of sex determination and differentiation under genetic or thermal influence. We found that very different regulatory processes are involved in temperature-driven regulation compared to gene-driven regulation, although both lead to a conserved outcome (ovaries, Figure 5.2). We discovered dramatic changes in cellular calcium homeostasis in the gonads of ZZf individuals incubated at high sex reversing temperatures, which fulfill predictions of the CaRe hypothesis that this is the key driver of temperature induced feminization. We argue that differential expression of calcium channels, and subsequent alterations of the intracellular environment combined with increased ROS production encode, then transduce, the thermal signal into altered gene expression, ultimately triggering male to female sex reversal in *P. vitticeps*.

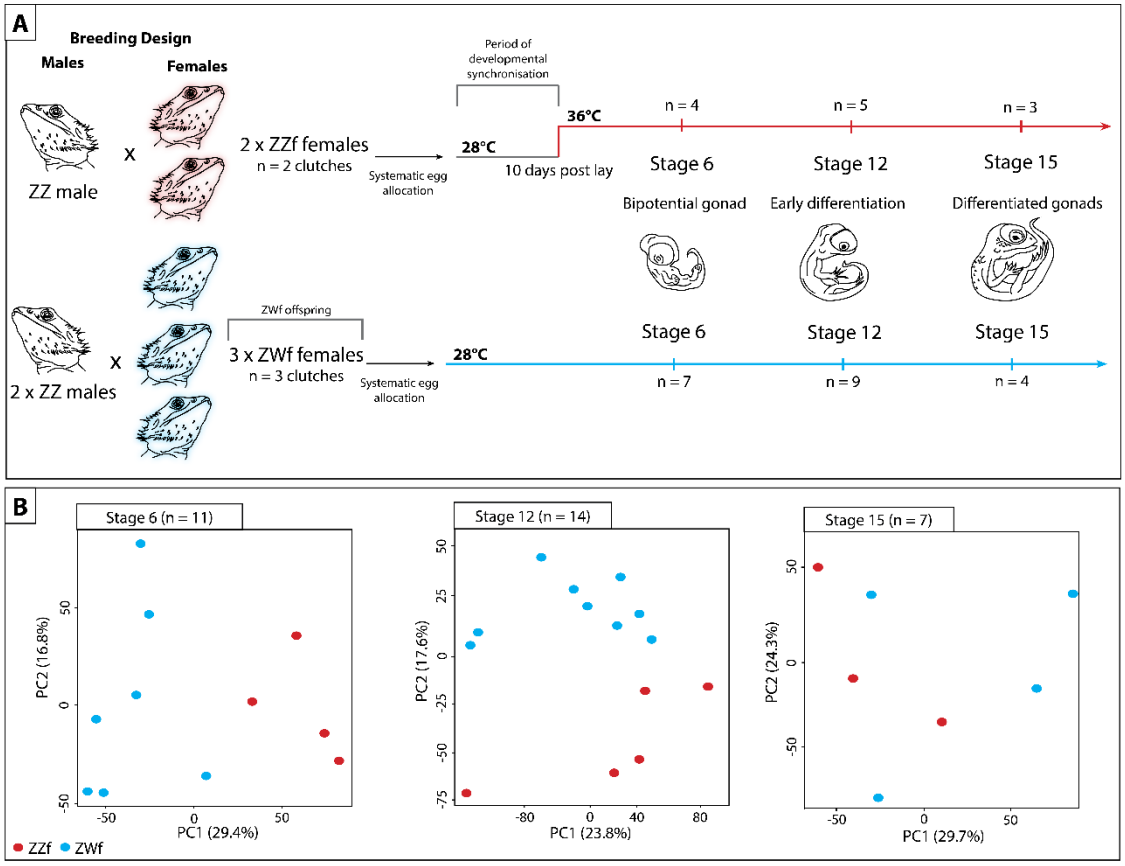

Figure 5.1: Schematic representation of experimental design used in this study to compare the differences between genetic sex determination and temperature dependent sex determination. (A) Summary of experiment showing how the parental crosses were designed, and how eggs were allocated and incubated. Eggs from sex reversed females (ZZf) were initially incubated at 28°C for 10 days, then were switched to 36°C. Eggs were sampled at the same three developmental stages (6, 12, and 15) based on [7,8]. At stage 6 the gonad is bipotential, at stage 12 the gonad is in the early stages of differentiation, and it completely differentiated by stage 15. Eggs from concordant females (ZWf) were incubated at 28°C and sampled at the same three developmental stages as the ZZf eggs. (B) PCA plots showing the first and second principal components of read count per gene between ZZf (red) and ZWf (blue) at each stage of development.

5.3 Results

5.3.1 Gene-drive female determination in ZWf embryos

Comparisons between stages in ZWf embryos (Figure 5.1, Figure 5.11, Additional file S1) showed that many genes were differentially expressed between stages 6 and 12 (210 genes downregulated and 627 genes upregulated at stage 12), but few genes were differentially expressed between stages 12 and 15 (2 genes upregulated at stage 15).

SOX9 and *GADD45G*, genes strongly associated with male development in mammals, were downregulated from stage 6 to stage 12, whereas various female related genes were upregulated, such as *PGR*, *ESR2*, *CYP19A1*, and *CYP17A1*. *BMP7*, a regulator of germ cell proliferation was upregulated at stage 12 [322], as were components of the NOTCH signalling pathway (*JAG2*, *DLL3*, *DLL4*), which are required for the suppression of Leydig cell differentiation [323,324]. *SRD5A2*, whose product catalyses the 5-α reduction of steroid hormones such as testosterone and progesterone, was also upregulated [325,326].

Notably, there was little differential expression between stages 12 and 15, suggesting that genetically driven ovarian development is complete by stage 12 (Additional file S1).

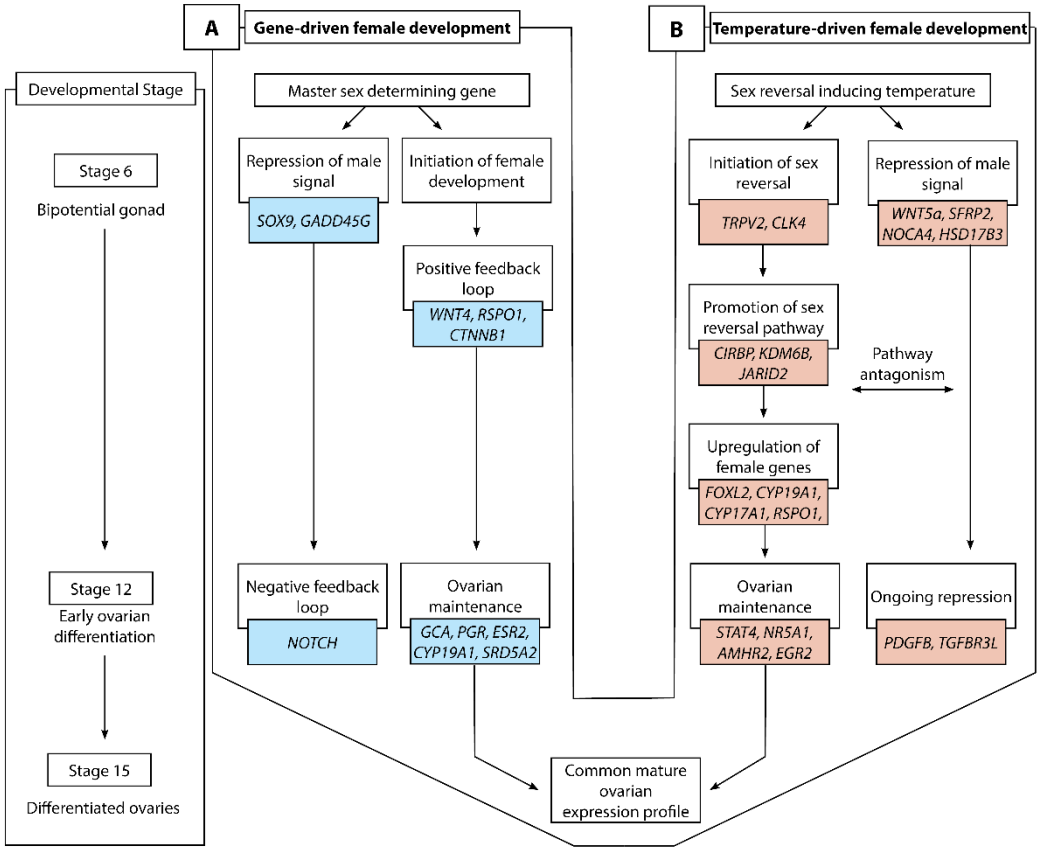

Figure 5.2: Schematic overview of gene-driven (blue) and temperature-driven (red) female developmental pathways in *Pogona vitticeps*. The pathways are initially different (from stages 6 to 12), but they ultimately converge on highly similar expression profiles when ovarian differentiation has occurred by stage 15. Both pathways are characterised by repression of a male signal, however this signal is stronger in temperature-driven females and appears to require ongoing repression when compared with the gene-driven females.

5.3.2 Temperature-driven female determination in ZZf embryos

Differential expression analysis of temperature-driven female development in ZZf embryos revealed many genes are differentially expressed between stages 6 and 12 (297 downregulated and 511 upregulated at stage 12) and no genes are differentially expressed between stage 12 and 15 (Figure 5.3, Figure 5.11, Additional file S1), suggesting completion of the ovarian development by stage 12 also in ZZf females.

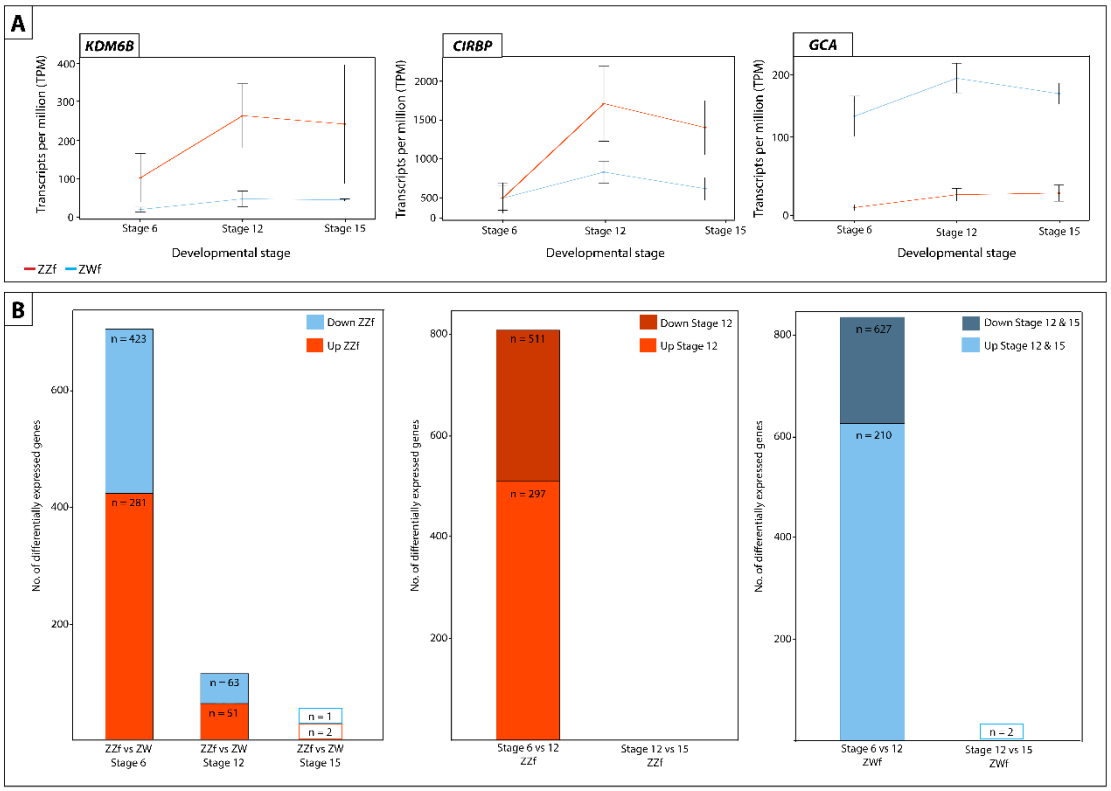

Figure 5.3: (A) Expression (transcripts per million, TPM) ± SE of three genes differentially expressed at all three developmental stages between ZZf and ZWf, with *KDM6B* and *CIRPB* (outlined in red) having consistently higher expression in ZZf embryos, and *GCA* having higher expression in ZWf. (B) Bar graphs representing the number of differentially expressed genes in all comparisons between ZZf and ZWf, and between developmental stages. MA plots of this data are available in fig. S1. Differentially expressed genes were determined as having *P* values ≤ 0.01 and $\log_2$-fold changes of 1, -1.

Upregulation of *FZD1*, a receptor for *Wnt* family proteins required for female development, suggests the activity of female pathways in ZZf embryos [327]. As was seen for ZWf females, canonical NOTCH ligands *DLL3* and *DLL4* were upregulated from stage 6 to stage 12 in ZZf females. However, this did not coincide with upregulation of JAG ligands or NOTCH genes, and the GO term "negative regulation of NOTCH

signalling" was enriched within the group of genes upregulated from stage 6 to 12 in ZZf females (Additional file S2). Further, *PDGFB*, which is required for Leydig cell differentiation, was upregulated [328]. Together, this suggests that the NOTCH signalling pathway may not be activated, and Leydig cell recruitment is not strongly repressed at stage 12 in ZZf. Alternatively, the absence of NOTCH signalling may indicate an important transition from progenitor cells to differentiated gonadal cell types in the early stages of the developing ovary [329]. These apparent differences in NOTCH signalling between ZZf and ZWf embryos suggests that ovarian development has progressed further in ZWf females.

Interestingly, genes typically associated with male development show diverse regulation in ZZf embryos, with some being downregulated and some being upregulated from stage 6 to 12. These included *WNT5a* and *SFRP2,* which are both involved in testicular development in mice [330,331], *NCOA4,* which enhances activity of various hormone receptors, and exhibits high expression in testes in mice during development [332], and *HSD17B3,* which catalyses androstenedione to testosterone [333]. Unlike what as observed in ZWf embryos, *SOX9* and *GADD45G* were not differentially expressed between stages 6 and 12 in ZZf embryos. *TGFBR3L*, which is required for Leydig cell function in mouse testis [334], and *NR5A1*, *SOX4*, and *AMHR2* [335–338] were also differentially expressed between stages 6 and 12 (Additional file S1).

A suite of genes typically associated with female development were upregulated from stage 6 to 12 [92], for example, *FOXL2*, *CYP17A1, RSPO1,* and *ESRRG*. As was also observed in stage 12 ZWfs, *ESR2, BMP7, CYP19A1,* and *PGR,* were more highly expressed at stage 12 in ZZfs. Notably, *CYP19A1* was much more strongly upregulated in stage 12 ZZfs compared with stage 12 ZWfs (Additional file S1). The increase in sex specific genes was also reflected in enriched GO terms at stage 12, which included "hormone binding", "steroid hormone receptor activity", and "female sex determination" (Additional file S2).

5.3.3 Ovarian maintenance in sex reversed ZZf females

The maintenance of female gene expression and ovarian development in stage 12 ZZf females may be centrally mediated by *STAT4* (Figure 5.4). As a member of the *JAK-STAT* pathway, *STAT4* is transduced by various signals, including reactive oxygen species, to

undergo phosphorylation and translocate from the cytoplasm to nucleus [185,339,340]. At stage 12, *STAT4* is upregulated, alongside *PDGFB* compared to stage 6 in ZZf females. *PDGFB* is known to activate *STAT4* [339]. Various *STAT4* target genes, notably *AMHR2*, *NR5A1*, *EGR1,* and *KDM6B* [339] are also upregulated at stage 12 (Additional file S1). Consistent with this link is the observation that a member of the same gene family, *STAT3,* is implicated in TSD in *Trachemys scripta* [22].

Several targets of *STAT4* are upregulated at stage 12, including *AMHR2* and *NR5A1*. Though typically associated with male development, *AMHR2* and *NR5A1* may also have roles in ovarian development. Although it is the primary receptor for *AMH*, *AMHR2* exhibits considerable evolutionary flexibility is sometimes associated with ovarian development (reviewed by [337]). *NR5A1* is also often associated with male development, as it positively regulates expression of *AMH* and *SOX9* in mammals [11]. However, *NR5A1* can also interact with *FOXL2* and bind to *CYP19A1* promoter to promote female development [341,342]. The upregulation of *FOXL2* and *CYP19A1,* but not *AMH* or *SOX9,* suggests that *NR5A1* is involved in the establishment of the ovarian pathway in ZZf females.

EGR1 positively regulates *DMRT1* expression through promoter binding in Sertoli cells, but knock-out of this gene can also cause female infertility in mice [343–345]. EGR1 is also associated with female development in birds, likely controlling the production of steroid hormones [335]. As was observed for *NR5A1*, *DMRT1* was also lowly expressed, suggesting it is not activated by *EGR1* in ZZf females.

One explanation for these expression trends is that male-associated genes are not strongly repressed at this stage during the sex reversal process, and that more prolonged exposure to the sex reversing temperature is required to firmly establish the female phenotype. However, we argue that the results more strongly suggest ROS-induced activation of *STAT4*, and subsequent phosphorylation and translocation, probably mediated by *PDGFB*, allows for the transcriptional activation of *NR5A1*, *AMHR2*, and *EGR1*, which in the temperature driven process of sex reversal in the ZZf embryos serve to maintain the ovarian phenotype.

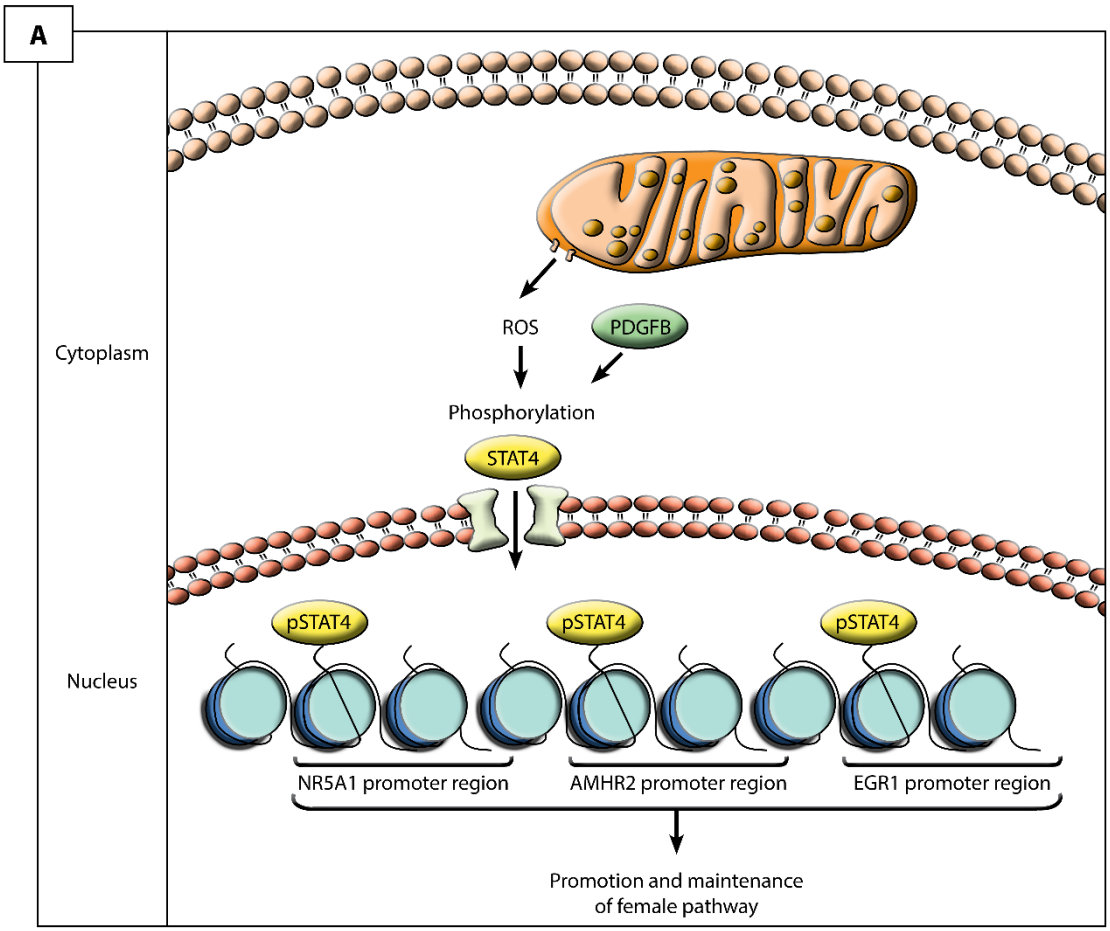

B

Gene ID	Gene Name	Log FC	Log CPM	F	P-value	FDR
AMHR2	Anti-Müllerian hormone receptor type 2	-1.96	7.85	23.49	3.17E-5	1.56E-3
EGR1	Early growth response 1	-2.58	5.74	30.80	4.14E-6	4.05E-4
NR5A1	Nuclear receptor subfamily 5 group A member 1	-1.30	7.87	15.21	4.69E-4	9.66E-3
PDGFB	Platelet derived growth factor subunit B	-2.83	4.58	72.33	1.10E-9	2.35E-6
STAT4	Signal transducer and activator of transcription 4	-1.36	3.57	16.94	2.56E-4	6.47E-3

Figure 5.4: Hypothesized pathway for the maintenance of the ovarian phenotype in stage 12 sex reversed ZZf *Pogona vitticeps*. Given the upregulation of these genes, it is likely that reactive oxygen species induce the phosphorylation, and subsequent activation and nuclear translocation of STAT4, likely mediated by PDGFB. Once in the nucleus, STAT4 is able to bind to promoter regions of known target genes, *NR5A1*, *AMHR2* and *EGR2* to regulate their expression and promote ovarian development.

5.3.4 Differential regulation of female developmental pathways

To better understand differences in ovarian developmental pathways, we compared gene expression of ZZf with ZWf embryos at each developmental stage. There are large gene expression differences between normal ZWf females and ZZf sex reversed females early

in development, before the bipotential gonad differentiates into an ovary. These differences are most pronounced early in development and diminish as development progresses. Stage 6 had the largest number of differentially expressed genes (DEGs) (281 genes higher expressed in ZWf embryos, 423 genes higher expressed in ZZf), with fewer DEGs at stage 12 (51 genes upregulated in ZWf, 63 genes upregulated in ZZf), and fewest at stage 15 (1 gene upregulated in ZWf, 2 genes upregulated in ZZf) (Figure 5.3, Additional file S3, Figure 5.10). This suggests that the sex reversed embryos start out on a male developmental trajectory, which they pursue beyond the thermal cue (3 days when the eggs were switched to high incubation temperatures, Figure 5.1), but by stage 12 development has been taken over by female genes.

Gene ontology (GO) enrichment analysis showed important differences between ZZf and ZWf at stage 6, and provides independent support for the role of calcium and redox regulation in ZZf females as proposed by the CaRe model (Figure 5.5, Additional file S4). GO processes enriched in the gene set higher expressed in ZZf at stage 6 included "oxidation-reduction processes", "cytosolic calcium ion transport", and "cellular homeostasis" (Figure 5.5, Additional file S4). GO function enrichment also included several terms related to oxidoreductase activities, as well as "active transmembrane transporter activity" (Figure 5.5, Additional file S4). No such GO terms were enriched in the gene set higher expressed in ZWf. Instead, enriched GO terms included "anatomical structure development", and "positive regulation of developmental growth" (Figure 5.5, Additional file S4).

Genes involved in female sex differentiation were higher expressed at stage 6 in normal ZWf embryos compared to sex reversed ZZf embryos (Additional file S3). These included *FOXL2*, *ESR2*, *PGR*, and *GATA6* [91,346]. Higher expression of *LHX9*, a gene with a role in bipotential gonad formation in mammals and birds, was more highly expressed in ZWf embryos [11,347–349]. Two genes with well described roles in male development, *SOX4* and *ALDH1A2* [350–352], were also higher expressed in ZWf embryos, suggesting they have an as yet unknown function in the early establishment of the ovarian trajectory in *P. vitticeps*.

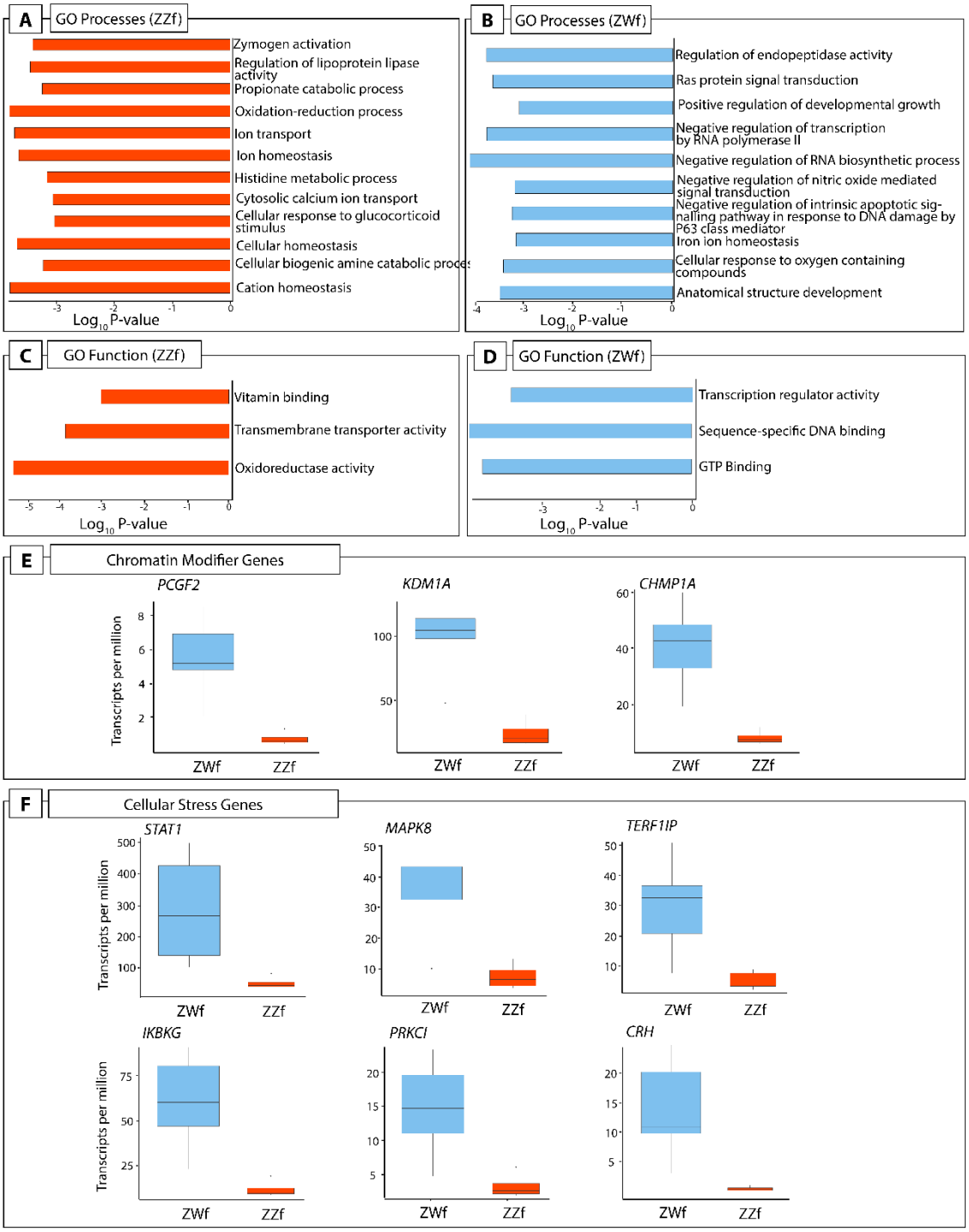

Figure 5.5: (A) A subset of GO processes and (C) GO functions enriched in stage 6 ZZf embryos compared with ZWf. (B) A subset of GO processes and (D) GO functions enriched in stage 6 ZWf embryos compared with ZZf. Complete results of GO analysis for all developmental stages in ZZf and ZWf for enriched GO processes and functions is provided in Additional file S2. Differentially expressed chromatin modifier (E) and cellular stress (F) genes in *Pogona vitticeps* at stage 6 comparing ZWf and ZZf females.

Taken together, these results further suggest that ZWf females are committed to the female pathway earlier than ZZf females. This is not surprising, since ZWf females possess sex chromosomes from fertilisation, whereas ZZf individuals have had only 3 days of exposure to a sex reversal inducing incubation temperature (Figure 5.1**).** This data is the first to demonstrate a difference in timing of genetic signals between gene and temperature driven development in the same species.

Three genes were constantly differentially expressed between ZWf and ZZf embryos at all three developmental stages (Figure 5.3). *GCA* (grancalcin) was upregulated in ZWf embryos, and *KDM6B* and *CIRBP* were upregulated in ZZf embryos at all developmental stages. *GCA* is a calcium binding protein commonly found in neutrophils and is associated with the Nf-κB pathway [353,354]. It has no known roles in sex determination, but its consistent upregulation in ZWf embryos compared to ZZf embryos suggests *GCA* is associated with gene driven ovarian development, at least in *P. vitticeps*.

Further analysis of gene expression trends using K-means clustering analysis [355] was used to investigate genes associated with female development, and to determine to what extent these genes are shared between ZZf and ZWf embryos (Figure 5.6, Additional file S5). Clusters with upward trends reflect genes likely to be associated with female development, so clusters 1 and 4 in ZWf (ZWC1 and ZWC4), and clusters 1 and 2 in ZZf (ZZC1 and ZZC2), were explored in greater detail (Figure 5.6, Additional file S5).

ZWC4 and ZZC2 shared 374 genes. Enriched GO terms included "germ cell development" and "reproductive processes" (Additional file S6), consistent with a link with female development. Genes identified included *FIGLA*, a gene known to regulate oocyte-specific genes in the female mammalian sex determination pathway [356], and *STRA8* which controls entry of oocytes into meiosis. Intriguingly, the GO term "spermatid development" was also enriched, encompassing many genes with known roles in testes function, including *ADAD1* and *UBE2J1* [357,358]. This suggests that genes involved in male sex determination in mammals may have been co-opted for use in the ovarian pathway in reptiles, so their roles require further investigation in other vertebrate groups, particularly given the complex nature of gene expression in sperm cell types.

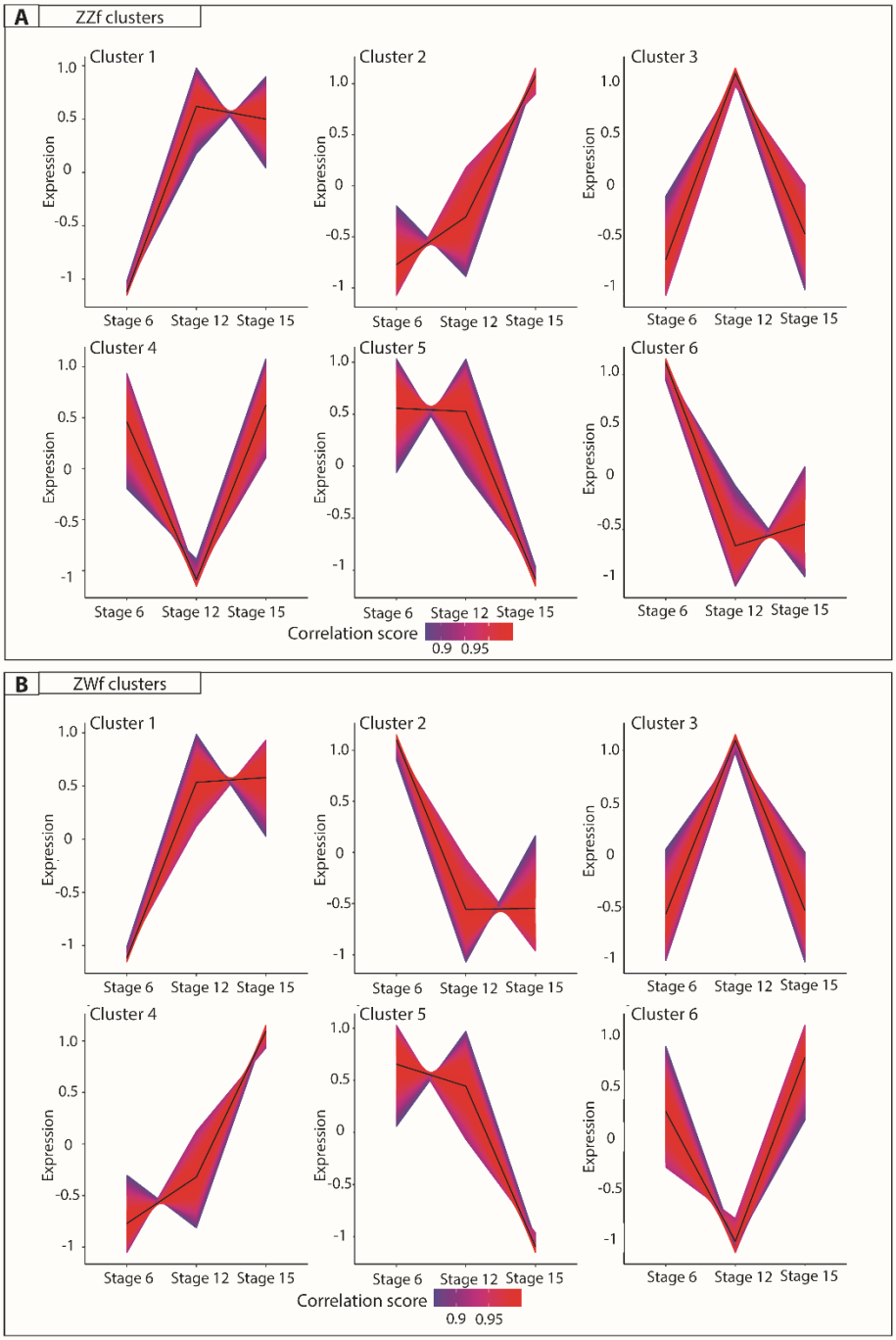

Figure 5.6: K-means clustering analysis on normalized counts per million for ZZf (A) and ZWf (B) across all developmental stages. The colour depicts the correlation score of each gene in the cluster, where numbers approaching one (red) have the strongest correlation. All gene lists produced for each cluster are provided in Additional file S5.

ZWC1 and ZZC1 shared 998 genes. ZZC1 has about 700 unique genes and ZWC1 about 500. GO analysis on shared genes between these clusters (n = 998) revealed enrichment terms such as “kinase binding” and “intracellular signal transduction” (Additional file S5). Genes unique to ZZC1 included members of heat shock protein

families (*HSPB11, HSPA4, HSP90AB1, HSPH1, HSPB1, HSPD1*), heterogenous ribonucleoprotein particles (*HNRNPUL1*), mitogen activated proteins (including *MAPK1, MAPK9, MAP3K8*), and chromatin remodelling genes (*KDM2B, KDM1A, KDM5B, KDM3B*). GO enrichment for genes unique to ZZC1 included "mitochondrion organisation", "cellular localisation", and "ion binding", while GO enrichment for genes unique to ZWC1 included "regulation of hormone levels" and numerous signalling related functions (Additional file S6).

Taken together, our results show that although the same ovarian phenotype is produced in genetic and temperature induced females, this end is achieved via different gene expression networks. This is most pronounced at stage 6, after which the extent of the differences decreases through development. This reflects canalisation of the gonadal fate to a shared outcome (ovaries, Figure 5.2).

5.3.4.1 Signature of hormonal and cellular stress in ZWf females

Previous work on *P. vitticeps* has shown a more than 50-fold upregulation of a hormonal stress response gene, *POMC,* in sex reversed adult females, leading to the suggestion that induction of sex reversal is in response to temperature stress, or that it is an inherently stressful event, the effects of which persist into adult life [55]. We therefore investigated the expression of stress related genes in ZZf and ZWf embryos.

We found considerable evidence that ZZf embryos experience oxidative stress, likely resulting from increased ROS production (discussed in detail below). However, contrary to our expectations, we found that ZWf embryos showed higher expression than ZZf of hormonal stress genes and pathways that have been hypothesized to be involved in sex reversal (Figure 5.5, Additional file S3). Genes upregulated in ZWf embryos compared to ZZf embryos included *STAT1*, a component of the JAK-STAT pathway, with several roles in stress responses [359], and *MAP3K1* and *MAPK8*, which are typically involved in mediating stress-related signal transduction cascades [360–362]. *TERF2IP* is also upregulated; this gene is involved in telomere length maintenance and transcription regulation [363]. When cytoplasmic, *TERF2IP* associates with the l-kappa-B-kinase (IKK) complex and promotes IKK-mediated phosphorylation of RELA/p65, activating the NF-κB pathway and increasing expression of its target genes [364]. Notably two members of the IKK complex, *IKBKG* (also known as *NEMO*) and *PRKCI*, which

are involved in NF-κB induction, were also upregulated in ZWf embryos compared to ZZf embryos (Figure 5.4), implying activation of the NF-κB pathway [365]. This pathway is typically associated with transducing external environmental signals to a cellular response [111,366], but also has diverse roles in sex determination in mammals, fish, and invertebrate models (reviewed by [53]).

CRH, another gene upregulated at stage 6 in ZWf females compared with ZZf females (Figure 5.5, supplementary file S3), is best known for its role as a neuropeptide synthesised in the brain in response to stresses that trigger the hypothalamic-pituitary-adrenal (HPA) axis [367,368]. The role of *CRH* production in the gonads, particularly in ovaries is currently poorly understood [20,31,33,369]. High *CRH* expression in ZWf gonads is the first observation of this in reptiles. The role of the hormonal stress response during embryonic development, and its apparent discordance with results observed in adults in *P. vitticeps* requires further investigation [55].

5.3.5 Cellular signalling cascades driving sex reversal

Results of this study provide considerable corroborative support for the CaRe model, which proposes a central role for calcium and redox in sensing and transducing environmental signals to determine sex. Many of the genes and pathways predicted by the CaRe model to be involved in sex reversal were shown to be upregulated in ZZf embryos at stage 6 compared to ZWf embryos. We use the CaRe model as a framework to understand the roles of each signalling participant in their cellular context during the initiation of sex reversal (Figure 5.7). This interpretation is also independently supported by GO analysis, showing enrichment of expected terms, such as "cytosolic calcium ion transport" (Additional file S4), as well as k-means clustering analysis (Additional files S4, S5).

Cluster 6 in ZZf (Figure 5.6) shows genes whose expression decreases after stage 6, so is likely to include genes responsible for the initial response to temperature and initiation of sex reversal, whose continuing action is not required once the ovarian trajectory has been established. Consistent with this assumption, as well as with predictions from the CaRe model, the 4050 genes in this cluster were enriched for GO terms that included "oxidation-reduction process" and various oxidoreductase activities (Additional files S5, S6).

A

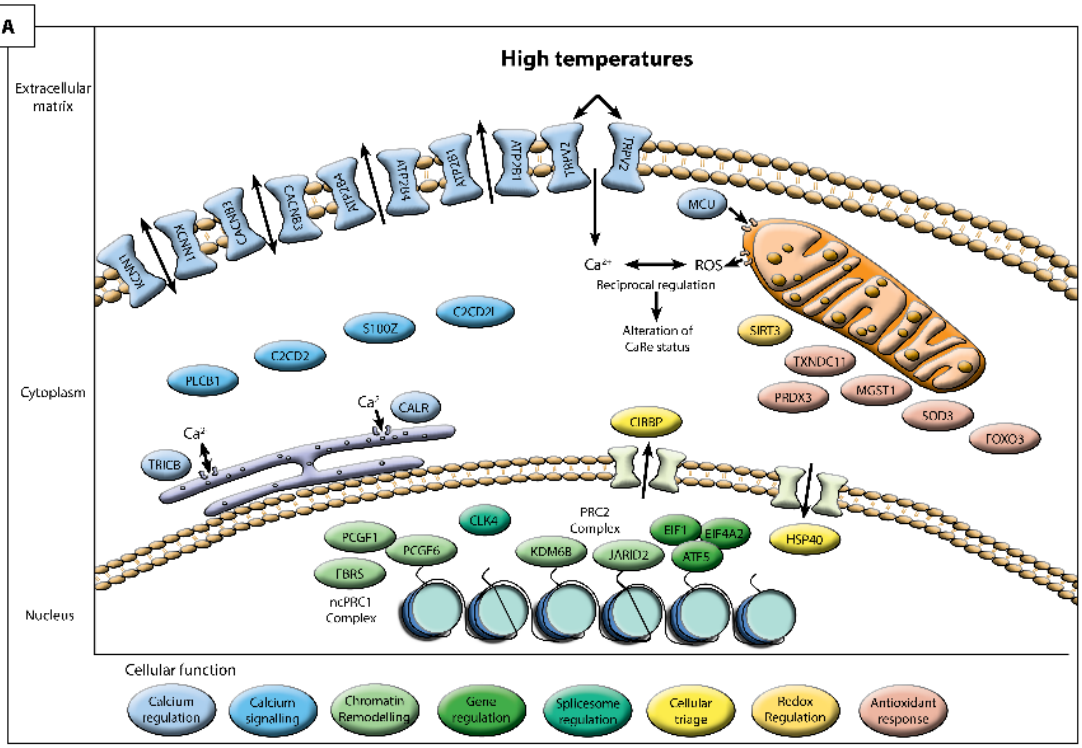

B

Gene ID	Gene Name	logFC	logCPM	F	P-Value	FDR
ATF5	Activating transcription factor 5	2.075	6.445	20.868	8.20E-5	3.42E-3
ATP2B1	ATPase plasma membrane Ca^{2+} transporting 1	1.162	5.455	24.183	3.09E-5	2.13E-3
ATP2B4	ATPase plasma membrane Ca^{2+} transporting 4	1.561	6.369	35.685	1.63E-6	4.31E-4
C2CD2	C2 calcium dependent domain containing 2	1.320	4.706	26.474	1.64E-5	1.60E-3
C2CD2L	C2CD2 like	1.330	3.288	17.857	2.12E-4	5.71E-3
CACNB3	Calcium voltage-gated channel auxiliary subunit beta 3	1.541	7.079	44.339	2.50E-7	1.69E-4
CALR	Calreticulin	1.397	9.378	23.407	3.86E-5	2.37E-3
CIRBP	Cold inducible RNA binding protein	1.166	9.763	41.691	4.32E-7	2.29E-4
CLK4	CDC like kinase 4	1.330	5.681	19.118	1.41E-4	4.47E-3
DNAJC28	DnaJ heat shock protein family (Hsp40) member C28	1.252	3.039	15.643	4.44E-4	8.72E-3
EIF1	Eukaryotic translation initiation factor 1	1.176	8.435	17.443	2.43E-4	6.11E-3
EIF4A2	Eukaryotic translation initiation factor 4A2	1.168	8.158	59.491	1.53E 8	2.87E 5
FBRS	Fibrosin	1.153	8.243	30.247	6.08E-6	8.95E-4
FOXO3	Forkhead box O3	1.129	5.798	18.598	1.67E-4	4.88E-3
JARID2	Jumonji and AT-rich interaction domain containing 2	2.296	8.620	40.274	5.85E-7	2.57E-4
KCNN1	Potassium calcium-activated channel subfamily N member 1	1.164	5.594	15.939	4.01E-4	8.21E-3
KDM6B	Lysine demethylase 6B	3.503	9.291	120.703	6.40E-12	1.08E-7
MCU	Mitochondrial calcium uniporter	1.018	5.466	26.624	1.57E 5	1.56E 3
MGST1	Microsomal glutathione S-transferase 1	1.351	7.830	29.858	6.71E-6	9.47E-4
PCGF1	Polycomb group ring finger 1	1.408	5.170	19.275	1.34E-4	4.42E-3
PCGF6	Polycomb group ring finger 6	1.072	4.330	19.318	1.33E-4	4.39E-3
PLCB1	Phospholipase C beta 1	1.763	3.649	24.040	3.22E-5	2.17E-3
PRDX3	Peroxiredoxin 3	1.336	7.212	29.894	6.65E 6	9.46E 4
S100Z	S100 calcium binding protein Z	4.202	3.813	23.471	3.79E-5	2.37E-3
SIRT3	Sirtuin 3	1.264	2.359	18.039	2.00E-4	5.52E-3
SOD3	Superoxide dismutase 3	2.317	1.806	17.239	2.59E-4	6.33E-3
TMEM38B	Transmembrane protein 38B	1.437	3.311	26.252	1.74E-5	1.62E-3
TRPV2	Transient receptor potential cation channel subfamily V member 2	3.239	3.951	45.162	2.12E-7	1.49E-4
TXNDC11	Thioredoxin domain containing 11	1.024	6.160	23.816	3.43E-5	2.26E-3

Figure 5.7: Hypothesised cellular environment (*A*) of a ZZf gonad at stage 6 in *Pogona vitticeps* based on differential expression analysis (*B*) using the CaRe model as a framework [53]. We used this approach to understand the cellular context responsible for driving sex reversal in ZZf samples. This reveals that calcium signalling likely plays a very important role in mediating the temperature signal to determine sex. Influx of intracellular calcium is likely mediated primarily by TRPV2, and may also be influenced by KCNN1 and CACNB3. This influx appears to trigger significant changes in the cell to maintain calcium homeostasis. MCU, ATP2B1, CALR and

TRICB all play a role in this process by sequestering calcium and pumping it back out of the cell, in which KCNN1 and CACNB3 may have a role. Calcium signalling molecules C2CD2, C2CDL2, and S100Z are likely responsible for encoding and translating the calcium signal leading to changes in gene transcription. Changes in gene expression are likely mediated primarily by the two major Polycomb Repressive Complexes, PRC1 and PRC2. Members of these two complexes (PCGF1, PCGF6, KDM6B, and JARID2) transcriptionally regulate genes by controlling methylation dynamics of their targets, the latter two of which have been previously implicated in sex reversal [24,55]. ATF5 may also play a role in gene regulation, and alternative splicing, which has been implicated in sex reversal [55] may be mediated by CLK4. High temperatures necessarily increase cellular metabolism, which in turn increases the amount of reactive oxygen species (ROS) produced by the mitochondria. ROS can cause cellular damage at high levels, so trigger an antioxidant response, which is observed here in the upregulation of MGST1, PRDX3, TXNDC11 and FOXO3. Also of note is the upregulation of CIRBP, which has numerous functions in response to diverse cellular stresses, and has been implicated in TSD.

5.3.5.1 Calcium transport, signalling, and homeostasis

Our data suggest that exposure to high temperatures may cause a rapid increase in cytosolic Ca^{2+} concentrations, as calcium influx is probably mediated by the thermosensitive calcium channel, *TRPV2* [120,370]. *TRPV2* was upregulated in stage 6 ZZf embryos compared to ZWf embryos (Figure 5.7). Transient receptor potential (TRP) ion channels, including *TRPV2,* have previously been implicated in TSD in *Alligator sinensis* and *A. mississippiensis*, as well as the turtle *Trachemys scripta* [25,26,93,94].

TRPV2 mediated Ca^{2+} influx may trigger a cascade of changes within the gonadal cells of ZZf females, which restore calcium homeostasis, critical to avoid apoptosis [248,371]. We observed evidence of such a homeostatic response, with the upregulation of seven genes involved in Ca^{2+} transport and sequestration in ZZf females compared to ZWf females at stage 6 (Figure 5.6). Specifically, *MCU*, *ATP2B1*, *ATP2B4*, together regulate calcium homeostasis through active transport of calcium into the mitochondria and into the extracellular space [372–374]. *KCNN1* and *CACNB3* encode proteins required for the formation of plasma membrane channels controlling the passage of Ca^{2+} [375–377]. *CACNB3* and *KCNN1* have well characterised roles in the nervous system, and excitable cell types in muscle, but their association with TSD in embryonic gonads is novel [375,376]. Evidence is also building for a broader role for voltage-gated calcium channels, including *CACNB3*, in orchestrating Ca^{2+} signalling and gene regulation [378]. We suggest that *KCNN1* and *CACNB3* in gonads of TSD species play roles in mediating

the homeostatic response to elevated cytosolic Ca^{2+} concentrations, and are involved in the subsequent modulation of Ca^{2+} signalling pathways.

TRPC4, another TRP family gene was, upregulated in stage 12 compared to stage 6 in both ZZf and ZWf embryos. *TRPC4* is expressed in mouse sperm and inhibited by progesterone [137,379] but has no known association with sex determination. *TRPC4* belongs to the TRPC superfamily, which all conduct calcium ions into the cell, typically through phospholipase C and calmodulin signalling pathways, G-protein-coupled receptors, and receptor tyrosine kinases [380,381]. Notably, *PLCL2* a phospholipase gene, together with calmodulin genes *CALM1* and *CAMKK1,* were upregulated alongside *TRPC4* from stage 6 to stage 12 in ZZf embryos but not in ZWf embryos (Additional file S3). Given *TRPC4* is upregulated from stage 6 to 12 in both ZZf and ZWf females, it may play a more conserved role in ovarian development in *P. vitticeps*.

Several genes with functions in calcium metabolism were upregulated in stage 6 ZZf embryos compared to stage 6 ZWf embryos. *CALR* encodes a multifunctional protein that acts as a calcium binding storage protein in the lumen of the endoplasmic reticulum, so is also important for regulating Ca^{2+} homeostasis [124,371,382]. *CALR* is also present in the nucleus, where it may play a role in regulation of transcription factors, notably by interacting with DNA-binding domains of glucocorticoid and hormone receptors, inhibiting the action of androgens and retinoic acid [382–386]. *TMEM38B* (commonly known as *TRICB*) is also found on the endoplasmic and sarcoplasmic reticula, where it is responsible for regulating the release of Ca^{2+} stores in response to changes in intracellular conditions [387].

MCU, ATP2B1, ATP2B4, KCNN1, CACNB3, CALR, and *TMEM38B* have no known roles in vertebrate sex determination, so their association with sex reversal in *P. vitticeps* is new. This upregulation during the early stage of sex reversal suggests that they are upstream modulators involved in the transduction of environmental cues that trigger sex determination cascades, which is consistent with predictions made by the CaRe hypothesis.

We hypothesize that intracellular Ca^{2+} increases in stage 6 ZZf gonads, and further observe that Ca^{2+} signalling related genes are also upregulated in ZZf females compared to stage 6 ZWf females (Figure 5.7). *C2CD2* and *C2CD2L* are both thought to be involved

in Ca^{2+} signalling, although there is no functional information about these genes. Of note is the significant upregulation of *S100Z,* which is a member of a large group of EF-hand Ca^{2+} binding proteins that play a role in mediating Ca^{2+} signalling [388]. The EF-hand domain is responsible for binding Ca^{2+}, allowing proteins like that encoded by *S100Z* to 'decode' the Ca^{2+} biochemical signal and translate this to various targets involved in many cellular functions including Ca^{2+} buffering, transport, and enzyme activation [389,390]. *PLCB1* also contains an EF-hand binding domain and behaves similarly, being activated by many extracellular stimuli and effecting numerous signalling cascades. It can translocate to the plasma membrane and nucleus, and release Ca^{2+} from intracellular stores [391]. Some Ca^{2+} related genes (*GCA* and *CALM1*) are also upregulated in ZWf embryos, but make only a small proportion of the overall response in differential gene expression (Additional file S3).

5.3.5.2 Oxidative stress in response to high temperatures

The upregulation of antioxidant genes in ZZf compared to ZWf embryos suggests that the gonadal cells in the ZZf embryos are in a state of oxidative stress (Figure 5.7). As was proposed by the CaRe model, we see results consistent with the prediction that high incubation temperatures increase metabolism, which increases the production of reactive oxygen species (ROS) by the mitochondria, resulting in oxidative stress [53]. ROS are required for proper cellular function, but above an optimal threshold, they can cause cellular damage [104,392]. Crossing this threshold launches the antioxidant response, which causes the upregulation of antioxidant genes to produce protein products capable of neutralising ROS [393,394]. We observed upregulation of redox related genes, specifically of *TXNDC11*, *PRDX3*, *MGST1* in ZZf embryos compared to ZWf embryos at stage 6. Also upregulated was *FOXO3*, which plays a role in oxidative stress responses, typically by mediating pro-apoptotic cascades [395,396]. Importantly, antioxidants play other cellular roles besides neutralisation of ROS. One of these is the alteration of cysteine resides through a process known as S-glutathionylation [397].

Various redox related genes were downregulated from stage 6 to 12 in ZZf embryos but not in ZW embryos, including *GLRX* and *PRDX3* [398], as well as numerous genes involved in ROS induced DNA damage repair; *LIG4, ENDOD1,* and *HERC2* [399]. This indicates a need for expression of these genes specifically in ZZf embryos in early stages that ceases in transition to stage 12. *STAT4*, a member of the ROS-induced JAK-STAT

pathway (Simon et al. 1998), and *DDIT4*, which is involved stress responses to DNA damage [400], were both upregulated from stage 6 to stage 12 in ZZf embryos.

The vertebrate antioxidant response is typically initiated by *NRF2*, but we observed no differential expression of *NRF2*, only upregulation of some of its known targets in ZZf embryos [401]. This may mean that the action of *NRF2* is depends more on its translocation from the cytoplasm to the nucleus to modulate transcription of target genes, a process that does not necessarily rely on increased expression of *NRF2* [401]. Alternatively, NRF2 upregulation may have occurred prior to sampling.

Oxidative stress has previously been proposed to have a role in TSD, based on the upregulation of genes involved in oxidative stress response. One of these genes, *UCP2*, was upregulated at high male producing temperatures in *A. mississippiensis* [93]. *UCP2*, and others genes involved in oxidative stress responses, were also implicated in UV induced masculinisation in larvae of a thermosensitive fish species (*Chirostoma estor*) [95]. Notably, we found that *UCP2* was upregulated between stages 6 to 12 in ZZf *P. vitticeps* embryos, suggesting a sustained response to thermal stress in the mitochondria (Additional file S3).

5.3.5.3 Temperature response and cellular triage

We also observed upregulation of genes involved in response to more generalised environmental stress in ZZf compared to ZWf embryos, as expected since the embryos exposed to high temperature were experiencing a state of thermal stress (Figure 5.7). Notably, *CIRBP* a promising candidate for regulation of sex determination under thermal influence, is approximately 10-fold upregulated in ZZf compared to ZWf (Additional file S3). *CIRBP* has a highly conserved role in generalised stress responses [170]. It has been suggested to be a putative sex determining gene in the TSD turtle *Chelydra serpentina* [90], and is differentially expressed at different incubation temperatures in *Alligator sinensis* [26]. We also observed the upregulation of *CLK4* in ZZf compared to ZWf embryos, a gene that has been recently shown to be inherently thermosensitive, and to regulate splicing of temperature specific *CIRBP* isoforms [402].

We found that *ATF5* is upregulated in ZZf embryos compared to ZWf embryos (Figure 5.7). *ATF5* has diverse roles in stimulating gene expression or repression through

binding of DNA regulatory elements. It is broadly involved in cell specific regulation of proliferation and differentiation, and may also be critical for activating the mitochondrial unfolded protein response [403]. This gene is induced in response to various external stressors, and is activated via phosphorylation by eukaryotic translation initiation factors, two of which (*EIF1* and *EIF4A2;* [404]) are also upregulated in ZZf embryos compared to ZWf embryos.

Though not well studied in the context of sex determination, heat shock factors and proteins have been implicated in female sex determination in mammals and fish, and may also play a conserved role in the ovarian pathway in *P. vitticeps* [94,154,176,179,405]. Surprisingly, only one gene associated with canonical heat shock response (*HSP40*, also known as *DNAJC28*) was differentially expressed following exposure to high temperature in stage 6 ZZf females compared to ZWf embryos (Additional file S3). This could mean either that a heat shock response occurs prior to sampling, or that *P. vitticeps* uses different mechanisms to cope with heat shock.

5.3.5.4 Chromatin remodelling

We observed upregulation of several components of two major chromatin remodelling complexes, polycomb repressive complexes PRC1 and PRC2, in both the genotype-directed ZWf and the temperature-directed ZZf female pathways in *P. vitticeps* (Figure 5.7). Chromatin modifier genes *KDM6B* and *JARID2* are involved in regulation of gene expression during embryonic development and epigenetic modifications in response to environmental stimulus [245,406]. *JARID2* and *KDM6B* were both upregulated in ZZf embryos compared to ZWf embryos in stages 6 and 12, and *KDM6B* was also upregulated at stage 15. These genes have recently been implicated in two TSD species (*Alligator mississippiensis*, and *Trachemys scripta*) and temperature sex reversed adult *Pogona vitticeps* [24,55,93,94].

We also found that two other members of the PRC1 complex, *PCGF6* and *PCGF1*, were upregulated in ZZf embryos at stage 6 compared to ZWf embryos (Figure 5.7). *PCGF6* is part of the non-canonical PRC1 complex (ncPRC1) that mediates histone H2A mono-ubiquitination at K119 (H2AK119ub) [407,408]. *PCGF6* acts a master regulator for maintaining stem cell identity during embryonic development [409], and is known to bind to promoters of germ cell genes in developing mice [407]. *PCFF1* exhibits similar

functions by ensuring the proper differentiation of embryonic stem cells [410]. The ncPRC1 complex also promotes downstream recruitment of PRC2 and H3K27me3, so that complex synergistic interactions between PRC1 (both canonical and non-canonical) and PRC2 can occur [411,412].

We found that other components of both PRC1 and PRC2 complexes were also upregulated in ZWf embryos compared to ZZf embryos (Figure 5.5, supplementary file S3). A member of the canonical PRC1 complex, *PCGF2* (also known as *MEL18*), was upregulated in ZWf embryos compared to ZZf embryos [411]. This gene has previously been implicated in temperature induced male development in *Dicentrachus labrax* [187], and is required for coordinating the timing of sexual differential in female primordial germ cells in mammals [413]. *KDM1A*, a histone demethylase that is required for balancing cell differentiation and self-renewal [414], was upregulated in ZWf embryos compared to ZZf embryos. *CHMP1A* was upregulated in ZWf, and is likely to be involved in chromosome condensation, as well as targeting PcG proteins to regions with condensed chromatin [415].

Thus, we conclude that the initiation of sex reversal in ZZf *P. vitticeps* involves a complex cascade of cellular changes initiated by temperature. Our data are consistent with the predictions of the CaRe hypothesis that high temperatures are sensed by the cell via TRP channels, which causes an increase in intracellular increase of Ca^{2+}. Coincident with this is an increase of ROS production in the mitochondria that causes a state of oxidative stress. Together, Ca^{2+} and ROS alter the CaRe status of the cell, trigger a suite of alternations in gene expression including chromatin remodelling, which drives sex reversal (Figure 5.7).

5.4 Discussion

We used the unique sex characteristics of our model reptile species, *Pogona vitticeps*, which determines sex genetically but sex reverses at high temperature, to assess predictions of the CaRe hypothesis [53]. By sequencing isolated embryonic gonads, we provide the first data to represent a suite of key developmental stages with comparable tissue types, and will be a valuable resource for this reptilian model system. There are few transcriptomes of GSD reptiles during embryonic development; the only dataset available prior to this study was a preliminary study of the spiny softshell turtle, *Apalone*

spinifera [154], which was inadequate for the inter-stage comparisons required to explore genetic drivers of gonad differentiation.

Our analysis of expression data during embryogenesis of normal ZWf females and temperature sex reversed ZZf females revealed for the first time differences in gene-driven and temperature-driven female development in a single species. Early in development, prior to gonad differentiation, the initiation of the sex reversal trajectory differs from the genetic female pathway both in the timing and genes involved. As development proceeds, differences in expression patterns become less until the pathways converge on a conserved developmental outcome (ovaries). Our ability to compare two female types in *P. vitticeps* allowed us to avoid previously intractable confounding factors such as sex or species-specific differences, which provided unprecedented insight into parallel female pathways. We have identified a suite of candidate genes for further functional study, and provided new insight into the conserved evolutionary origins of the labile networks governing environmentally sensitive sex determination pathways.

The maintenance of ovarian differentiation seems to require the operation of different pathways in gene and temperature driven female development. This may involve a pathway centrally mediated by *STAT4* in sex reversed *P. vitticeps*, which has not been previously described, so requires additional confirmation with functional experiments. It will be interesting to determine if a role for these genes occurs in other species. Another STAT family gene, *STAT3*, has recently been demonstrated to play a critical role in the phosphorylation of *KDM6B* and subsequent demethylation of the *DMRT1* promoter required for male development in *T. scripta* [22]. The involvement of different genes in the same family is intriguing in its implications; while different genes may be co-opted, natural selection may favour gene families with conserved functions even between evolutionarily disparate lineages.

Our data provided insight into the molecular landscape of the cell required to initiate temperature induced sex reversal. This is the first dataset to capture temperature-induced sex reversal in a reptile, and remarkably we have simultaneously implicated all functional candidates that have previously been identified to be involved in TSD across a range of other species (Table 5.1). Our results also identified novel genes involved with thermosensitive sex determination, and provide corroborative evidence for the CaRe hypothesis [53]. Importantly, our work highlights avenues for future studies to conduct

functional experiments to definitively identify the genes and pathways implicated here in sex reversal. Observation and manipulation of intracellular calcium concentrations, as has been conducted in *T. scripta* [22], will also be crucial for fully understanding the role of calcium signalling in sex reversal.

Our results highlight the complexity of initiating thermolabile systems. Indeed, it has been suggested that thermolabile sex determination involves system-wide displacement of gene regulation with multiple genes and gene products responding to temperature leading to the production of one sex or the other – a parliamentary system of sex determination (151). We take an intermediate position, arguing for a central role for Calcium-Redox balance as the proximal cellular sensor for temperature, but interacting with other required thermosensitive genes or gene products (e.g. CLK4) to influence ubiquitous signalling pathways and downstream splicing regulation, epigenetic modification and sex gene expression. The level of interaction between each thermosensitive element remains to be explored. For example, if temperature can be sensed by both *TRPV2* and *CLK4,* are both required to initiate sex reversal, or is the signal from only one sufficient? This raises the possibility that no single proximal sensor of the environmental exists, but that several thermosensitive elements early in development must come together to orchestrate alterations in gene expression.

It has been suggested that the products of TRP family genes act as mediators between the temperature signal and a cellular response through Ca^{2+} signalling and subsequent modulation of downstream gene targets [25,26,93]. Notably, different TRP channels are implicated in two alligator species; *TRVP4* in *A. mississippiensis,* but *TRPV2, TRPC6,* and *TRPM6* in *A. sinsensis*. In *T. scripta, TRPC3* and *TRPV6* are upregulated at male producing temperatures (26°C), while *TRPM4* and *TRPV2* are upregulated at female producing temperatures (31°C), as is the case for *TRPV2* in *P. vitticeps* [94]. The diversity of TRP channels recruited for roles in environmental sex determination hints at considerable evolutionary flexibility, perhaps the result of repeated and independent co-option of these channels in TSD species. As may be the case for STAT family genes, the evolution of environmentally sensitive sex determination pathways may involve the use of different genes within gene families that have conserved functions.

Our data also highlights the importance of chromatin remodelling genes in sex reversal in *P. vitticeps*. *KDM6B* and *JARID2* have been previously implicated sex differentiation in adult *P. vitticeps* [55], embryonic *T. scripta* [22,24] and embryonic *A. mississippiensis* [55]. Sex-specific intron retention was observed in TSD alligators and turtle, and was exclusively associated with sex reversal in adult *P. vitticeps* [55]. Subsequently, knockdown of *KDM6B* in *T. scripta* caused male to female sex reversal by removing methylation marks on the promoter of *DMRT1*, a gene critical in the male sex determination pathway [24]. *KDM6B* and *JARID2* have also been associated with TSD in another turtle species (*Chrysemys picta*) [154], female to male sex change in the bluehead wrasse, *Thalassoma bifasciatum* [416], and thermal responses in the European bass, *Dicentrarchus labrax* [417].

It is currently unknown if the unique splicing events in *KDM6B* and *JARID2* in adult sex reversed *P. vitticeps* that cause intron retention and presumed gene inactivation, also occur in embryos. Given the high expression of these genes during embryonic development at sex reversing temperatures, it would be surprising if this pattern was observed. We also show a significant role for *CIRBP* as the only other gene, alongside *KDM6B*, to be consistently upregulated during sex reversal in all developmental stages assessed. *CIRBP* is a mRNA chaperone, which could be required to stabilise transcripts of crucial sex specific genes during oxidative, cellular and/or thermal stress. It has been proposed as a novel TSD candidate gene in the turtle, *Chelydra serpentina* [90] This gene remains a promising candidate for mediating thermosensitive responses in TSD more broadly, and its role needs to be explored in more detail.

5.5 Conclusions

The alternative female pathways in *P. vitticeps* demonstrates that there is inherent flexibility in sex determination cascades even within the same species. This is consistent with the idea that, provided a functional gonad is produced, considerable variation in sex determining and differentiation processes at the early stages of development is tolerated under natural selection (151). Perhaps this makes the astonishing variability in sex determination between diverse species less surprising. Our findings provide novel insights, and are a critical foundation for future studies of the mechanisms by which temperature determines sex.

Table 5.1: All genes, full gene names, functional categories and associations with either gene (ZWf) or temperature driven (ZZf) female development mentioned in the paper. NA denotes a gene that was mentioned, but was not differentially expressed. Genes with an asterisk are those that have previously been implicated in thermosensitive sex determination cascades, either in *Pogona vitticeps*, or in another reptile species.

Gene ID	Gene Name	Functional Category	Association
ADAD1	Adenosine deaminase domain containing 1 [testis-specific]	Sex determination and differentiation (Male-specific)	ZWf/ ZZf
ALDH1A2	Retinal dehydrogenase 2	Sex determination and differentiation (Male-specific)	ZWf
AMH	Anti-Müllerian hormone	Sex determination and differentiation	NA
AMHR2	Anti-Müllerian hormone receptor 2	Sex determination and differentiation	ZZf
ATF5	Activating transcription factor 5	Stress response	ZZf
ATP2B1	ATPase plasma membrane Ca^{2+} transporting 1	Calcium signalling	ZZf
ATP2B4	ATPase plasma membrane Ca^{2+} transporting 4	Calcium signalling	ZZf
BMP7	Bone morphogenetic protein 7	Sex determination and differentiation	ZZf
C2CD2	C2 calcium-dependent domain containing 2	Calcium signalling	ZZf
C2CD2L	C2 calcium-dependent domain containing 2 like	Calcium signalling	ZZf
CACNB3	Calcium voltage-gated channel auxiliary subunit beta 3	Calcium signalling	ZZf
CALM1	Calmodulin 1	Calcium signalling	ZWf/ ZZf
CALR	Calreticulin	Calcium signalling	ZZf
CAMKK1	Calcium/calmodulin dependent protein kinase kinase 1	Calcium signalling	ZZf
CHMP1A	Chromatin modifying protein 1A	Chromatin remodelling	ZWf
CIRBP*	Cold-inducible binding protein	Temperature-sensing	ZZf
CLK4*	CDC like kinase 4	Temperature-sensing	ZZf
CRH	Corticotropin releasing hormone/factor	Stress response	ZWf
CYP17A1	Cytochrome P450 17A1	Sex determination and differentiation (Female-Specific)	ZWf/ ZZf
CYP19A1	Aromatase	Sex determination and differentiation (Female-Specific)	ZWf/ ZZf
DDIT4	DNA damage inducible transcript 4	DNA damage repair	ZZf
DLL3	Delta like canonical Notch ligand 3	Sex determination and differentiation (Male-specific)	ZWf/ ZZf
DLL4	Delta like canonical Notch ligand 4	Sex determination and differentiation (Male-specific)	ZWf/ ZZf
DMRT1	Doublesex and mab-3 related transcription factor 1	Sex determination and differentiation (Male-specific)	NA
EGR1	Early growth response 1	Sex determination and differentiation	ZZf
EIF1	Eukaryotic translation initiation factor 1	Translation initiation	ZZf
EIF4A2	Eukaryotic translation initiation factor 4A2	Translation initiation	ZZf
ENDOD1	Endonuclease domain containing 1	DNA damage repair	ZZf

ESR2	Estrogen receptor 2	Sex determination and differentiation (Female-Specific)	ZWf
ESRRG	Estrogen related receptor gamma	Sex determination and differentiation (Female-Specific)	ZZf
FIGLA	Folliculogeneisis specific basic helix-loop-helix	Sex determination and differentiation (Female-Specific)	ZWf/ ZZf
FOXL2	Forkhead box L2	Sex determination and differentiation (Female-Specific)	ZWf/ ZZf
FOXO3	Forkhead box O3	Redox regulation	ZZf
FZD1	Frizzled class receptor 1	Sex determination and differentiation	ZZf
GADD45G	Growth arrest and DNA damage inducible gamma	Sex determination and differentiation	ZWf
GATA6	GATA binding factor 6	Sex determination and differentiation	ZWf
GCA	Grancalcin	Calcium signalling	ZWf
GLRX	Glutaredoxin	Redox regulation	ZZf
GPX1	Glutathione peroxidase	Redox regulation	ZZf
HERC2	HECT and RLD domain containing E3 ubiquitin protein ligase 2	DNA damage repair	ZZf
HNRNPUL1	Heterogeneous nuclear ribonucleoprotein U like 1	Splicing	ZWf/ ZZf
HSD17B3	Hydroxysteroid 17-beta dehydrogenase 3	Sex determination and differentiation	ZZf
HSP40	DNAJ heat shock protein family (hsp40) member B1	Temperature-sensing	ZZf
HSP90AB1	Heat shock protein 90 alpha family class B member 1	Temperature-sensing	ZWf/ ZZf
HSPA4	Heat shock protein family A (Hsp70) member 4	Temperature-sensing	ZWf/ ZZf
HSPB1	Heat shock protein family B (Small) member 1	Temperature-sensing	ZWf/ ZZf
HSPB11	Heat shock protein family B (Small) member 11	Temperature-sensing	ZWf/ ZZf
HSPD1	Heat shock protein family D (Hsp60) member 1	Temperature-sensing	ZWf/ ZZf
HSPH1	Heat shock protein family H (Hsp110) member 1	Temperature-sensing	ZWf/ ZZf
IKBKG/NEMO	NF-κB essential modulator	NF-kB pathway	ZWf
JAG2	Jagged 2	Sex determination and differentiation	ZWf
JARID2*	Jumonji and AT-rich interaction domain containing 2	Chromatin remodelling	ZZf
KCNN1	Small conductance calcium-activated potassium channel protein 1	Calcium signalling	ZZf
KCTD1	Potassium channel tetramerization domain containing 1	Sex determination and differentiation (Male-specific)	ZZf
KDM1A	Lysine demethylase 1A	Chromatin remodelling	ZWf/ ZZf
KDM2B	Lysine demethylase 2B	Chromatin remodelling	ZWf/ ZZf
KDM3B	Lysine demethylase 3B	Chromatin remodelling	ZWf/ ZZf
KDM5B	Lysine demethylase 5B	Chromatin remodelling	ZWf/ ZZf

KDM6B*	Lysine demethylase 6B	Chromatin remodelling	ZZf
LHX9	LIM homeobox 9	DNA damage repair	ZWf
LIG4	DNA ligase 4	DNA damage repair	ZZf
MAP3K8	Mitogen-activated protein kinase kinase kinase 8	Stress response	ZWf/ ZZf
MAPK1	Mitogen-activated protein kinase 1	Stress response	ZWf/ ZZf
MAPK9	Mitogen-activated protein kinase 9	Stress response	ZWf/ ZZf
MCU	Mitochondrial calcium uniporter	Calcium signalling	ZZf
MGST1	Microsomal glutathione S-transferase 1	Redox regulation	ZZf
NANOS1	Nanos C2HC-type zinc finger 1	Sex determination and differentiation (Female-Specific)	ZWf
NCOA4	Nuclear receptor coactivator 4	Sex determination and differentiation	ZZf
NEIL3	Nei like DNA glycosylase 3	DNA damage repair	ZZf
NR5A1	Nuclear receptor subfamily 5 group A member 1	Sex determination and differentiation	ZZf
NRF2	Nuclear factor, erythroid 2 like 2	Redox regulation	NA
PCGF1	Polycomb group ring finger 1	Chromatin remodelling	ZZf
PCGF2/Mel18	Polycomb group ring finger 2	Chromatin remodelling	ZWf
PCGF6	Polycomb group ring finger 6	Chromatin remodelling	ZZf
PCYOX1L	Prenylcysteine oxidate 1 like	Redox regulation	ZZf
PDGFB	Platelet derived growth factor subunit B, paralog of mammalian *PDGFA*	Sex determination and differentiation	ZZf
PGR	Progesterone receptor	Sex determination and differentiation (Female-Specific)	ZWf
PLCB1	Phospholipase C Beta 1	Calcium signalling	ZZf
PLCL2	Phospholipase C like 2	Calcium signalling	ZZf
POMC	Proopiomelanocortin	Stress response	NA
PRDX3	Peroiredoxin 3	Redox regulation	ZZf
PRKCI	Protein kinase C iota	NF-kB pathway	ZWf
RSPO1	R-spondin 1	Sex determination and differentiation (Female-Specific)	ZWf/ ZZf
S100Z	S100 calcium binding protein Z	Calcium signalling	ZZf
SFRP2	Secreted frizzled related protein 2	Sex determination and differentiation (Male-specific)	ZZf
SOX4	SRY-box transcription factor 4	Sex determination and differentiation (Male-specific)	ZWf
SOX9	Sry-box 9	Sex determination and differentiation (Male-specific)	NA
SQOR	Sulfide quinone oxidoreductase	Redox regulation	ZZf
SRD5A2	Steroid 5 alpha reductase 2	Sex determination and differentiation	ZWf
STAT1	Signal transducer and activator of transcription 1	Stress response	ZWf
STAT4	Signal transducer and activator of transcription 4	Stress response	ZZf
STRA8	Stimulated by retinoic acid 8	Sex determination and differentiation	ZWf/ ZZf

TERF2IP	Telomeric repeat-binding factor 2-interacting protein 1	NF-kB pathway	ZWf
TGFBR3L	Transforming growth factor beta receptor 3-like, paralog of mammalian *TGFBR3*	Sex determination and differentiation	ZZf
TMEM38B/TRICB	Trimeric intracellular cation channel type B	Calcium signalling	ZZf
TRPC4	Transient receptor potential cation channel subfamily C member 4	Temperature-sensing	ZZf
TRPV2*	Transient receptor potential cation channel subfamily V member 2	Temperature-sensing	ZZf
TXNDC11	Thioredoxin domain containing 11	Redox regulation	ZZf
UBE2J1	Ubiquitin-conjugating enzyme E2 J1	Sex determination and differentiation	ZWf/ ZZf
UCP2	Oxidative stress responsive-gene uncoupling protein-2	Redox regulation	ZZf
WNT5a	Wnt family member 5a	Sex determination and differentiation	ZZf

5.6 Materials and Methods

5.6.1 Animal breeding and egg incubations

Eggs were obtained during the 2017-18 breeding season from the research breeding colony at the University of Canberra. Breeding groups comprised three sex reversed females (ZZf) to one male (ZZ), and three concordant females (ZWf) to two males (Figure 5.1). Paternity was confirmed by SNP genotyping (Figure 5.8). Females were allowed to lay naturally, and eggs were collected at lay or within two hours of lay. Eggs were inspected for viability as indicated by presence of vasculature in the egg, and viable eggs were incubated in temperature-controlled incubators (±1°C) on damp vermiculite (4 parts water to 5 parts vermiculate by weight). Clutches from sex reversed females (that is, ZZf x ZZm crosses) comprised eggs with only ZZ genotypes. These were initially incubated at 28°C (male producing temperature, MPT) to entrain and synchronise development. After 10 d of incubation, half of the eggs selected at random from each clutch was shifted to 36°C (female producing temperature, FPT). Clutches from ZWf x ZZm crosses were incubated at 28°C throughout the incubation period (Figure 5.1). Sample sizes are given in Figure 5.1 and Additional file S7.

5.6.2 Embryo sampling and genotyping

Eggs from both temperatures were sampled at times corresponding to three developmental stages (6, 12 and 15 [7], taking into account the differing developmental rates between 28°C and 36°C. These stages equate to the bipotential gonad, recently differentiated gonad, and differentiated gonad respectively [8]. Embryos were euthanized

by intracranial injection of 0.1 ml sodium pentobarbitone (60mg/ml in isotonic saline). Individual gonads were dissected from the mesonephros under a dissection microscope and snap frozen in liquid nitrogen. Isolation of the gonad from the surrounding mesonephros was considered essential for studying transcriptional profiles within the gonad. Embryos from three different ZZf x ZZm clutches from each treatment class (temperature x stage) were selected for sequencing, and randomized across sequence runs to avoid batch effects. Embryos from concordant ZWf x ZZm crosses potentially yield both ZW and ZZ eggs, so these were genotyped using previously established protocols [3,7]. Briefly, this involved obtaining a blood sample from the vasculature on the inside of the eggshell on a FTA® Elute micro card (Whatman). DNA was extracted from the card following the manufacturer protocols, and PCR was used to amplify a W specific region [3] so allowing the identification of ZW and ZZ samples.

5.6.3 RNA extraction and sequencing

RNA from isolated gonad samples was extracted in randomized batches using the Qiagen RNeasy Micro Kit (Cat. No. 74004) according to the manufacturer protocols. RNA was eluted in 14 µl of RNAase free water and frozen at -80°C prior to sequencing. Sequencing libraries were prepared in randomized batches using 50 ng RNA input and the Roche NimbleGen KAPA Stranded mRNA-Seq Kit (Cat. No. KK8420). Nine randomly selected samples were sequenced per lane using the Illumina HiSeq 2500 system, and 25 million read-pairs per sample were obtained on average. Read lengths of 2 x 150bp were used. All samples were sequenced at the Kinghorn Centre for Clinical Genomics (Garvan Institute of Medical Research, Sydney). All sample RNA and library DNA was quantified using a Qubit Instrument (ThermoFisher Scientific, Scoresby, Australia), with fragment size and quality assessed using a Bioanalyzer (Agilent Technologies, Mulgrave, Australia).

5.6.4 Gene expression profiling

Paired-end RNA-seq libraries (.fastq format) were trimmed using trim_galore with default parameters (v0.4.1; https://www.bioinformatics.babraham.ac.uk/projects/trim_galore/, last access 21-Apr-2020). Trimmed reads were aligned to the *Pogona vitticeps* NCBI reference genome (pvi1.1, GenBank GCA_900067755.1; [418]) using STAR (v2.5.3; [419]), with splice-aware alignment guided by the accompanying NCBI gene (*Pvi1.1*) annotation (.gtf format). Likely PCR duplicates and non-unique alignments were removed using

samtools (v1.5 ; [420]). Gene expression counts and normalised expression values (reported in TPM) were determined using RSEM (rsem-calculate-expression; v1.3.1; [421]).

5.6.5 Identification of non-sex reversed specimens

Normalised transcripts per million (TPM) for a panel of sex-specific genes (*SOX9, AMH, DMRT1, FOXL2, CYP19A1, CYP17A1*) were inspected across the three stages to identify if any samples showed aberrant expression patterns. This approach was also used to determine if any of the stage 12 and 15 samples from the 36°C treatment had not undergone sex reversal by comparing expression levels between ZWf and ZZf embryos; the rate of sex reversal is 96% at 36°C [3] (12
, Additional file S8). The five samples from clutch 9 exhibited significantly higher expression values for *SOX9, AMH*, and *DMRT1* and represented clear outliers. This was also supported by multidimensional scaling (MDS) plots, so the decision was made to regard the five samples from clutch 9 as aberrant and exclude them from subsequent analyses (Figure 5.10, Figure 5.11, Additional file S9). Any ZZf samples with male-like gene expression patterns (high expression for male-specific genes, and low expression for female-specific genes) were considered to have not been reversed (sex reversal is not 100% at 36°C) and were removed (two stage 15 samples).

5.6.6 Differential expression analysis

Differential expression analysis of ZZf and ZWf transcripts was conducted on raw counts using the EdgeR package (Bioconductor v 3.9 [422]) in R (v 1.2.1335, [423]), following standard procedures outlined in the EdgeR users guide [422,424]. Lowly expressed genes, which was applied to genes with fewer than ten counts across three samples, were removed from the raw counts (19,285 genes) so that the total number of genes retained was 17,075. Following conversion to a DGElist object in EdgeR, raw counts were normalised using the upper-quartile method (calcNormFactors function) [425]. Estimates for common negative binomial dispersion parameters were generated (estimateGLMCommonDisp function) [424], followed by generation of empirical Bayes dispersion estimates for each gene (estimateGLMTagwiseDisp function) [424,426]. A quasi-likelihood binomial generalised log-linear model was fitted (glmQLFit function) and the glmQFTest function was used to compare contrasts within the design matrix [427–431]. A P-value cut-off of 0.01 and a $\log_2$-fold change threshold of 1 or -1 was applied to all contrasts (topTags function) [427]. Contrasts were used to assess differential

expression between ZZf and ZWf samples across each developmental stage. Raw count (Additional file S10) and expression files (Additional file S11) from this analysis are supplied. Gene ontology (GO) analysis was conducted for each set of differentially expressed genes using GOrilla [432,433]. The filtered count data file (17,075 genes) was used for the background gene set at a P-value threshold of 10^{-3}.

5.6.7 K-means clustering analysis

K-means clustering analysis was performed on normalised counts per million extracted from the DGElist object produced by the initial process of the DGE analysis using edgeR (see above). Counts for each gene were averaged for each treatment group, and the number of clusters was selected using the sum of squared error approach, which was further validated by checking that each cluster centroid was poorly correlated with all other cluster centroids (maximum correlation 0.703 in ZWf clusters, and 0.65 in ZZf clusters). A total of 6 clusters was chosen, and clustering analysis was conducted using the kmeans function in R package stats v3.6.2. Resultant gene lists were sorted by unique and shared genes between clusters with similar trends between ZWf and ZZf (cluster 1 in ZWf, cluster 3 in ZZf, and cluster 3 in ZWf and cluster 5 in ZZf). Both unique and shared genes from each cluster and pairs of clusters (cluster 1 and 3, and clusters 3 and 5) were then analysed for gene ontology (GO) enrichment using GOrilla [432,433]. The filtered count data file (17,075 genes) was used for the background gene set at a P-value threshold of 10^{-3}.

5.6.8 Supplementary Figures

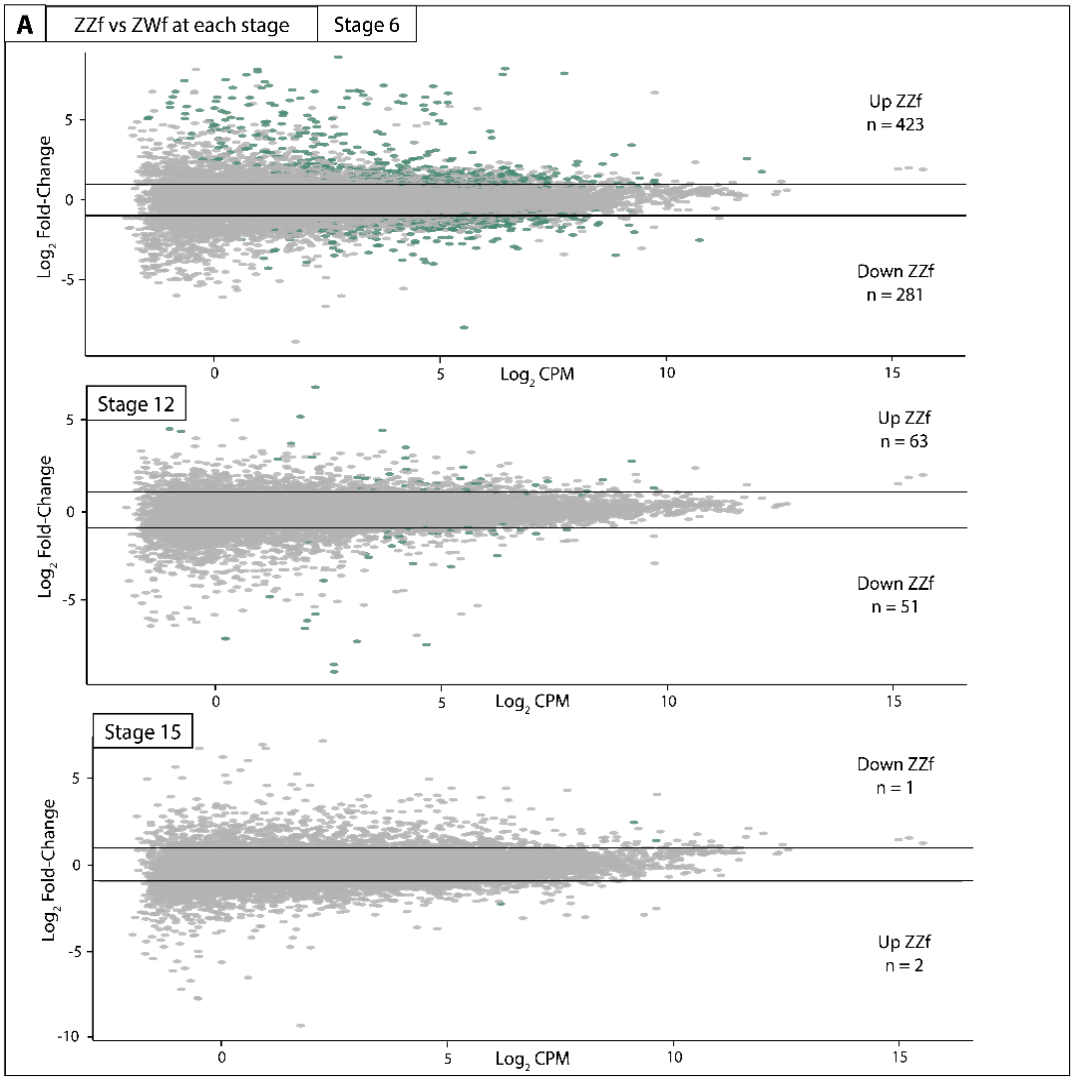

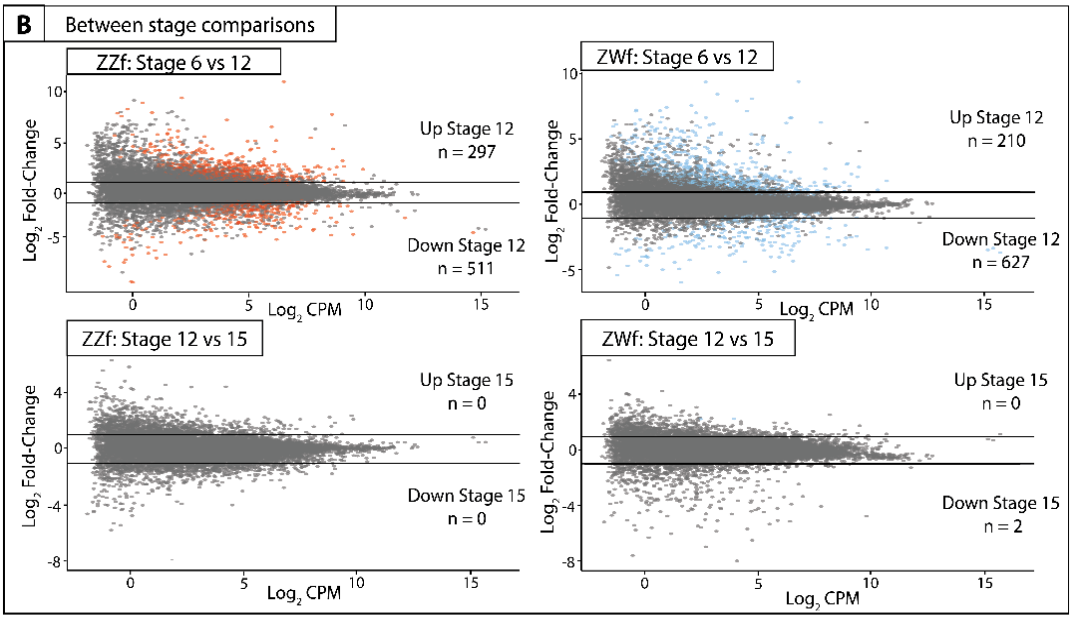

Figure 5.9: MA plots of read counts per gene from differential expression analysis conducted between ZZf and ZWf (A) and comparisons between stages for both ZZf and ZW (B). Differentially expressed genes (*P* values ≤ 0.01, $\log_2$-fold change of 1, -1) are coloured (colour indicative of significant fold change), and the total number of genes are indicated in each plot. Grey indicates no differential expression, horizontal lines indicate $\log_2$-fold changes of 1, -1. CPM: normalised counts per million

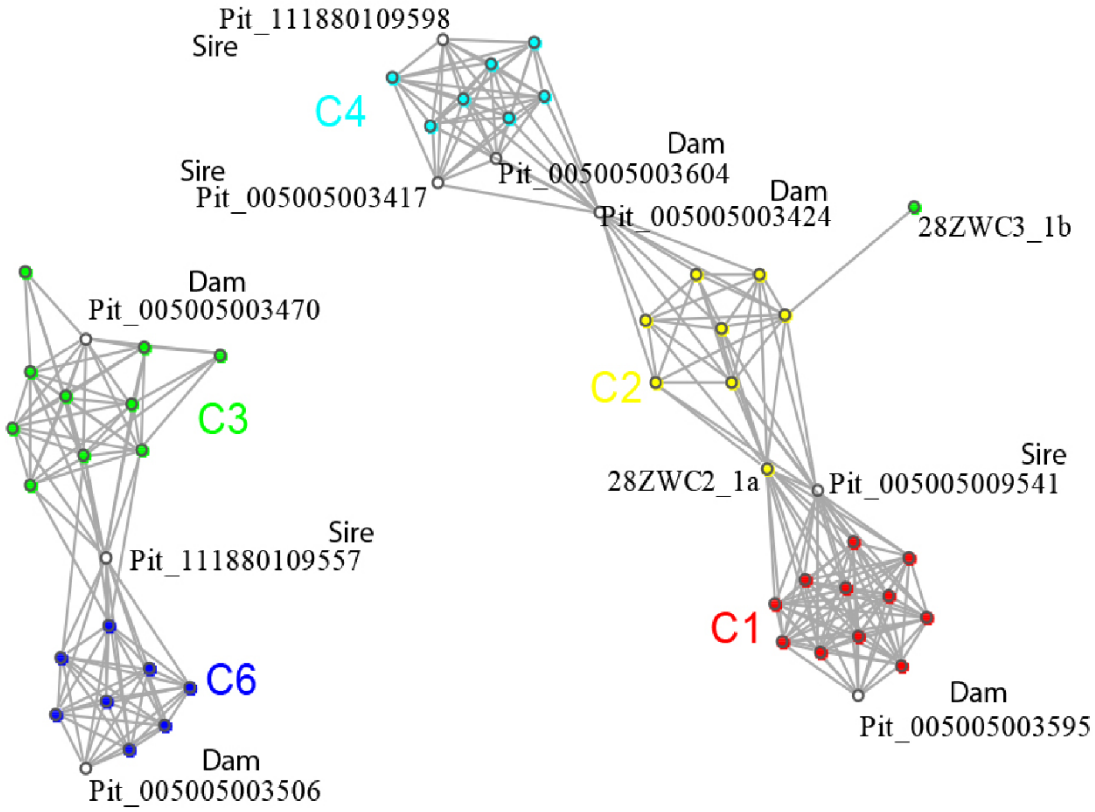

Figure 5.8: Network analysis of parental and offspring SNPs to confirm paternity of clutches used in this experiment. SNP data was generated by Dart sequencing, a reduced genome representation sequencing method at Diversity Arrays Technology, University of Canberra.

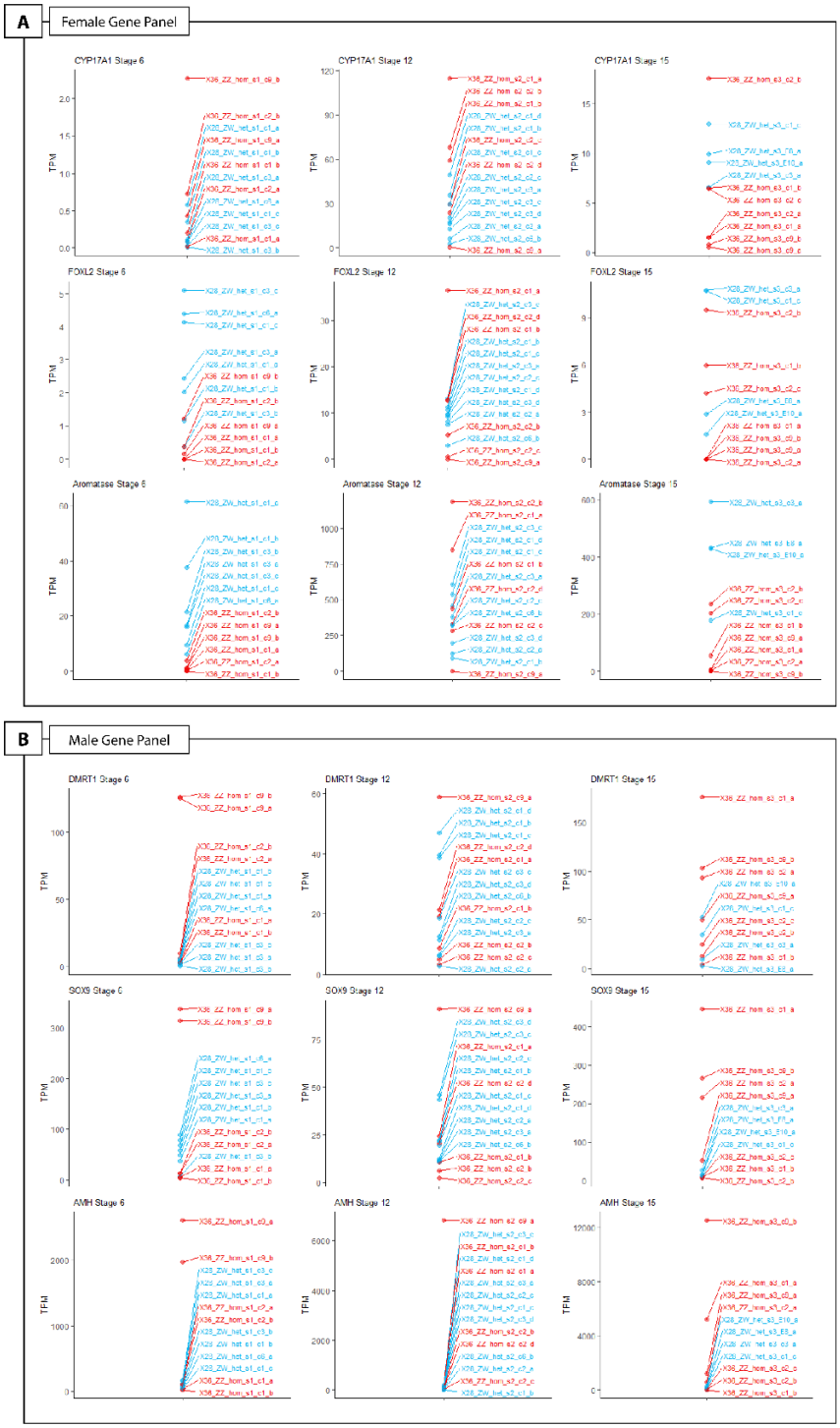

Figure 5.10: Expression (TPM, transcripts per million) of female-specific genes (*CYP17A1*, *FOXL2*, *CYP19A1*; panel (A) and male-specific genes (*DMRT1*, *SOX9*, *AMH*; panel (B) across three developmental stages (6, 12, 15) [7,8] for all samples to aid in the identification of samples with aberrant expression patterns. Samples from later developmental stages that exhibit low expression of female-specific genes are likely to have not undergone sex reversal. Sample ID labels correspond to incubation temperature (36°C or 28°C in red or blue respectively), maternal genotype/maternal homozygosity/maternal heterozygosity (ZZf or ZWf), sample stage (s1 = stage 6, s2 = stage 12, s3 = stage 15), clutch number (c1, c2, etc.), and replicate ID (e.g., "a" denotes the sample was the first replicate for that sampling point).

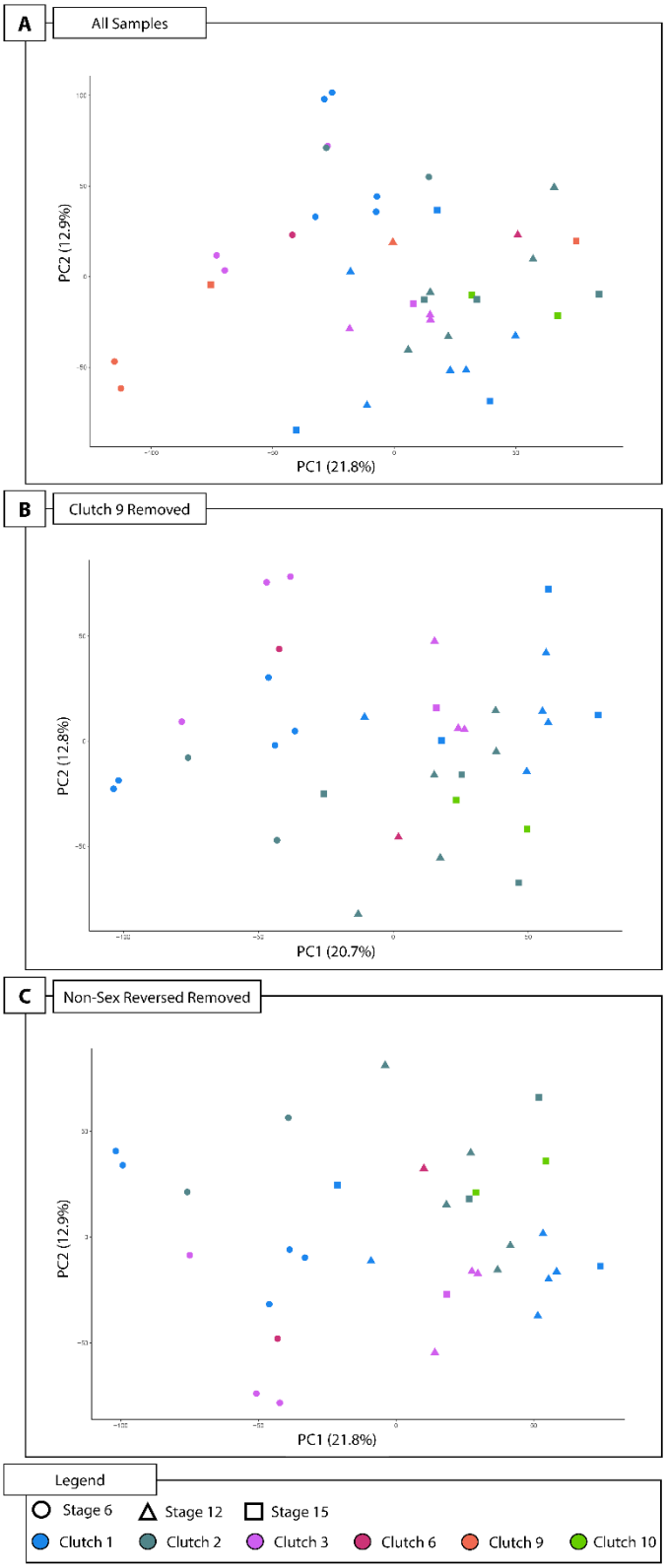

Figure 5.11: Principal components analysis (PCA) plots performed on normalised counts per million for filtered genes following the EdgeR pipeline described in the materials and methods section. (A) PCA of all samples (n = 39) (B) PCA of samples with clutch 9 removed (n = 32). (C) PCA of samples with clutch 9 samples removed and two samples that had not undergone sex reversal. This is the final dataset upon which all analysis was performed (n = 30).

5.6.9 Supplementary Files

S1 Data: Differentially expressed genes between developmental stages 6 and 12, and 12 and 15 for ZZf and ZWf females generated from EdgeR's "topTags" function. Results are sorted by log-fold change, with a cut-off of 1 or -1 applied, and a P-value threshold of 0.01. For the stage 6 and 12 comparison, genes with positive log-fold changes are upregulated at stage 12, while for the stage 12 and 15 comparison, genes with a positive log-fold change are upregulated at stage 15. No genes were differentially expressed between stages 12 and 15 in ZZf females.
https://doi.org/10.1371/journal.pgen.1009465.s001

S2 Data: Gene ontology (GO) enrichment for process and function for the stage 6 and 12 comparison for ZZf and ZWf (S1 Data). GO enrichment was not possible for the stage 12 and 15 comparison because differentially expressed genes were lacking. GO enrichment was generated from GOrilla at a significance threshold of $P \leq 0.05$. https://doi.org/10.1371/journal.pgen.1009465.s002

S3 Data: Differentially expressed genes between ZZf and ZWf for each developmental stage generated from EdgeR's "topTags" function. Results are sorted by log-fold change, with a cut-off of 1 or -1 applied, and a P-value threshold of 0.01 Genes with positive log-fold changes are upregulated in ZZf embryos, genes with negative log-fold changes are upregulated in ZWf. https://doi.org/10.1371/journal.pgen.1009465.s003

S4 Data: Gene ontology (GO) enrichment for process and function generated from GOrilla at a significance threshold of $P \leq 0.05$ for differentially expressed genes at stages 6 and 12 for ZZf and ZWf samples (S3 Data). https://doi.org/10.1371/journal.pgen.1009465.s004

S5 Data: Gene list outputs for K-means clustering analysis (n = 6), and comparative information for matched clusters between ZZf and ZWf (ZZC1 and ZWC1, and ZZC2 and ZWC4) including genes that are unique and shared between each cluster. https://doi.org/10.1371/journal.pgen.1009465.s005

S6 Data: Gene ontology (GO) process and function enrichment for genes in ZZf C1, and genes shared between ZZC5 and ZWC3 generated from GOrilla at a significance threshold of $P \leq 0.05$. https://doi.org/10.1371/journal.pgen.1009465.s006

S7 Data: Summary of all embryonic gonad samples sequenced for this study, including incubation temperature, genotype, parental cross, developmental stage, and clutch for each sample. Unique sample identifiers are matched to those used in raw data inputs (S10 and S11 Data). https://doi.org/10.1371/journal.pgen.1009465.s007

S8 Data: Outputs from pairwise T-tests conducted between stage 15 (n = 7) and stage 15 ZZf samples suspected not to have undergone sex reversal (n = 2). The normalised transcripts per million (TPM) for six genes, three male (*AMH*, *DMRT1*, *SOX9*) and three female genes (*FOXL2*, *CYP19A1*, *CYP17A1*) were used. The two samples suspected of not undergoing sex reversal show significantly different expression levels for four of these genes, and differences just above the significance threshold of ≤0.05 for the other two genes. On this basis, these two samples were removed from further analysis. https://doi.org/10.1371/journal.pgen.1009465.s008

S9 Data: Outputs from one way analysis of variance (ANOVAs) between all clutches (clutch 1, 2, 3, 6, and 9) across each developmental stage (6, 12 and 15) for a panel of sex specific genes (*AMH*, *SOX9* and *DMRT1*) to determine whether clutch 9 exhibits aberrant expression levels. The normalised transcripts per million (TPM) generates from the EdgeR pipeline described in the materials and methods was used. Based on the results from this analysis, five samples from clutch 9 were excluded from further analysis. https://doi.org/10.1371/journal.pgen.1009465.s009

S10 Data: Raw counts for all samples (n = 39) for all genes (n = 19,284) prior to any filtering or sample removal. Sample ID labels correspond to incubation temperature (36 or 28), maternal genotype/maternal homozygosity/maternal heterozygosity (ZZf or ZWf), sample stage (s1 = stage 6, s2 = stage 12, s3 = stage 15), clutch number (c1, c2, etc.), and replicate ID (e.g., "a" denotes the sample was the first replicate for that sampling point). Sample data is also available in S7 Data.
https://doi.org/10.1371/journal.pgen.1009465.s010

S11 Data: Raw expression values (TPM, transcripts per million) all samples (n = 39) for all genes (n = 19,284) prior to any filtering or sample removal.

Sample ID labels correspond to incubation temperature (36 or 28), maternal genotype/maternal homozygosity/maternal heterozygosity (ZZf or ZWf), sample stage (s1 = stage 6, s2 = stage 12, s3 = stage 15), clutch number (c1, c2, etc.), and replicate ID

(e.g., “a” denotes the sample was the first replicate for that sampling point). Sample data is also available in S7 Data. https://doi.org/10.1371/journal.pgen.1009465.s011

Chapter 6 Truncated *jarid2* and *kdm6b* transcripts are associated with temperature-induced sex reversal during development in a dragon lizard

In Review: Science Advances

Whiteley, S. L., Wagner, S., Holleley, C. E., Deveson, I.W., Marshall Graves, J.A., Georges, A. (*in review*). Truncated *jarid2* and *kdm6b* transcripts are associated with temperature-induced sex reversal during development in a dragon lizard.

6.1 Abstract

Sex determination and differentiation in reptiles is complex. In the model species, *Pogona vitticeps*, high incubation temperature can cause male to female sex reversal. To elucidate the epigenetic mechanisms of thermolabile sex, we used an unbiased genome-wide assessment of intron retention during sex reversal. The previously implicated chromatin modifiers (*jarid2* and *kdm6b*) were two of three genes to display sex reversal specific intron retention. In these species, embryonic intron retention resulting in C-terminally truncated *jarid2* and *kdm6b* isoforms consistently occurs at low temperatures. Sex reversal is uniquely characterised by a high prevalence of N-terminally truncated isoforms of *jarid2* and *kdm6b*, which are not present at low temperatures, or in two other reptiles with temperature dependent sex determination. This work verifies that chromatin modifying genes are involved in highly conserved temperature responses, but can also be transcribed into isoforms with novel sex-determining roles.

6.2 Introduction

Sex in vertebrates is determined by various factors, ranging from genes on sex chromosomes (genetic sex determination, GSD), environmental factors such as temperature (temperature dependent sex determination, TSD), and interactions between genes and the environment [3,16,270,272]. While the GSD pathways of mammals are well understood, the more complex systems involving both genes and environmental cues of other vertebrate lineages are still poorly characterised. Since the discovery of TSD in the lizard, *Agama agama*, over 50 years ago [6], some 15% of vertebrate species, particularly fish and reptiles, have been shown to have TSD or other forms of environmental sex determination (ESD) [271]. Although many hypotheses have been proposed, precisely how an environmental cue is received and transmitted to the regulatory and epigenetic processes that determine sex remains a mystery. Nor is it clear how, once the environmental signal is captured by the cell, the signal is transduced to influence the regulatory processes that determine sexual fate.

The dragon lizard *Pogona vitticeps* is a model organism well placed to explore these questions. It has a ZZ/ZW system of chromosomal sex determination [45], but this system is subject to sex reversal of the ZZ genotype to a female phenotype by high temperatures (above 32°C) both in the laboratory [434] and in the wild [3,78]. Sex reversed ZZf females are viable and fertile. Two chromatin modifiers have repeatedly been shown to be associated with thermal response in sex determination in reptiles including *P. vitticeps*: KDM6B and JARID2. Lysine demethylase KDM6B acts on histone H3K27me3 [435]. A second gene product JARID2 (encoded by Jumonji and AT-rich interaction domain containing 2, *jarid2*) is a component of PRC2 (Polycomb Repressive complex 2), a complex responsible for the methylation of histone H3 to yield H3K27me3 marks [240,435] and so is thought to act in opposition to KDM6B, though this action has not yet been demonstrated in reptiles. The chromatin dynamics that genes *kdm6b* and *jarid2* are involved in chromatin remodelling and regulate are essential for proper embryonic development through the determination of cell fate and ensuring the transmission of the chromatin state through cell divisions [240,241,245,435–440].

Evidence is emerging of a role for alternative splicing as an important regulatory process during embryonic development, producing different transcript isoforms which can encode divergent protein variants in embryos and adults, and at different stages of embryonic development [441–445]. Temperature-dependent alternative splicing is

commonly observed in TSD reptiles, and has been suggested to be an essential process in both TSD [171,172,291,446–448] and sex reversal [54,55]. For example, genes *kdm6b* and *jarid2* and their differential splicing patterns have been implicated in the regulation of TSD in two species, the American alligator (*Alligator mississippiensis*) and the red eared slider turtle (*Trachemys scripta*) [23,24,93,449]. Functional work in *T. scripta* has shown KDM6B demethylates the promotor of a key sex gene *dmrt1* [23] to determine the trajectory of the sex differentiation pathway [22,24]. Intron retention in *kdm6b* and *jarid2 also* occurs in gonads of adult central bearded dragons (*Pogona vitticeps*) that were sex reversed by high incubation temperature [55]. Homology of the *kdm6b* and *jarid2* elements which display intron retention, indicates an attribute that has remained conserved over approximately 200 million years of divergence [9].

Our previous research suggested that intron retention in *kdm6b* and *jarid2* during sex reversal alters histone demethylation actions, an modifies the dosage of unknown sex determining genes, thus re-directing developmental canalisation that otherwise would have followed the homogametic sex (ZZ, male) [55]. Analysis of embryonic transcriptomes in *P. vitticeps* showed significant upregulation of *kdm6b* and *jarid2* in sex reversing embryos when compared with embryos at a normal incubation temperature [54]. The next step is to examine splicing patterns during embryonic development, and specifically during sex reversal, in *P. vitticeps*.

Here we present the first global analysis of RNA splicing during sex reversal in gonadal tissues of embryonic *P. vitticeps*. We show that novel splicing events occur exclusively during sex reversal, suggesting a role for alternative splicing in responding to high temperatures by initiating and maintaining the sex reversal cascade in *P. vitticeps*. Contrary to the expression patterns we previously observed in adult *P. vitticeps* [24], intron retention in *jarid2* and *kdm6b* occurs at normal incubation temperatures during embryogenesis, whereas perfect splicing of these genes occurs only at sex reversing temperatures. We also show that two novel N-terminally truncated isoform variants of *jarid2* and *kdm6b* transcripts are present uniquely in sex reversed embryos. The splicing profile of sex reversing *P. vitticeps* embryos also differs from that of two TSD species, *A. mississippiensis* and *T. scripta*, suggesting splicing regulation of *jarid2* and *kdm6b* during sex reversal is distinct from typical TSD pathways. This research highlights an important role for specific splicing events during sex reversal that may occur in species with thermolabile sex more broadly, and suggests that whereas ancient epigenetic

modifier genes may be commonly implicated in thermosensitive sex determination pathways, the means by which they are regulated may not be conserved.

6.3 Results

6.3.1 Global analysis of intron retention during embryonic development

An unbiased analysis of intron retention events across the whole gonadal transcriptome using IRFinder [450] identified only a few genes with differentially retained introns in *P. vitticeps* (Supplementary Data 6.1). Aside from *kdm6b* and *ja*rid2 (discussed in detail below), only one gene, *fbrs* (fibrosin), exhibited differentially retained introns between sex reversed ZZf females and embryos of both sexes (ZWf and ZZm) incubated at 28°C at every developmental stage. Transcripts *fbrs*, retain introns 16 and 17 more frequently in ZZf females, while intron 13 was retained more frequently in both ZWf and ZZm embryos at 28°C compared with 36°C sex reversed ZZf (Figure 6.6). All retained introns contain numerous stop codons in every phase, so intron-retaining transcripts are expected to be non-functional. *Fbrs* was upregulated during sex reversal [54], and its association with the non-canonical PRC1 complex may indicate it has a role in chromatin remodelling in the sex reversal cascade [451]. Intron retention may therefore fine tune the availability of this regulator. Beyond this link, *fbrs* has no known function in sex determination or differentiation, so the role of these isoforms in *P. vitticeps* development remains unknown and is not explored further here.

The generality of intron retention in reptile sex determination was examined by comparing transcripts in alligator and turtle to those in *P. vitticeps*, and particular note was taken of genes that showed differential intron retention across reptile clades. IRFinder analysis of a published RNA-sequencing dataset of an embryonic time series of *A. mississippiensis* [93] and *T. scripta* [94] showed that *jarid2* and *kdm6b* were the only genes with differentially retained introns that were shared between all three species, consistent with our previous results [55].

One other gene, *mov10*, showed an IR event in both *P. vitticeps* and *T. scripta* but not alligator. This gene (Mov10 RISC complex RNA helicase) encodes an RNA helicase with diverse roles in mRNA export and nonsense-mediated decay, and has no known roles in sex determination [452]. Two other genes show intron retention events in both *A. mississippiensis* and *T. scripta* but not *P. vitticeps*; *sra1* (steroid receptor RNA activator

1) and *rsrp1* (arginine and serine rich protein 1). *Sra1* functions as a RNA binding protein and transcriptional regulator, particularly of hormone related genes, but has not previously been implicated in sex determination [453]. *Rsrp1* (paralogue of *srsf6*) encodes a splicing factor, the phosphorylation of which is controlled by CLK4 [402]. In *T. scripta*, six other genes displayed intron retention events that were not observed in the other species (Supplementary Data 6.1).

We then focussed on the two chromatin remodelling genes *jarid2* and *kdm6b*, as they were the only genes that showed differential intron retention in all three species.

6.3.2 Splicing of chromatin remodelling gene jarid2

In *P. vitticeps* retention of intron 15 in *jarid2* (Figure 6.1a) and intron 18 in *kdm6b* (Figure 6.2a) occurred only in normal ZWf and ZZm embryos incubated at 28°C. This is the opposite pattern to the one previously described for adult *P. vitticeps*, in which intron retention occurred in sex reversed ZZf females, while retention was rare in ZWf females and ZZm males [55].

For *jarid2*, premature stop codons in intron 15 would lead to premature termination of translation, so producing truncated protein isoforms lacking the C-terminal zinc finger domain (ΔC-JARID2. Thus intron retention occurs in normal ZZm males and ZWf females in the embryos, but in sex reversed ZZf female adults in *P. vitticeps*.

We investigated this surprising finding by studying *jarid2* intron retention in detail during embryogenesis in *P. vitticeps*. At 28°C, approximately 40% of *jarid2* transcripts retained intron 15 in both ZWf females and ZZm males (Figure 6.1b), compared with nearly zero intron retention at 36˚C across all developmental stages assessed (Figure 6.1b).

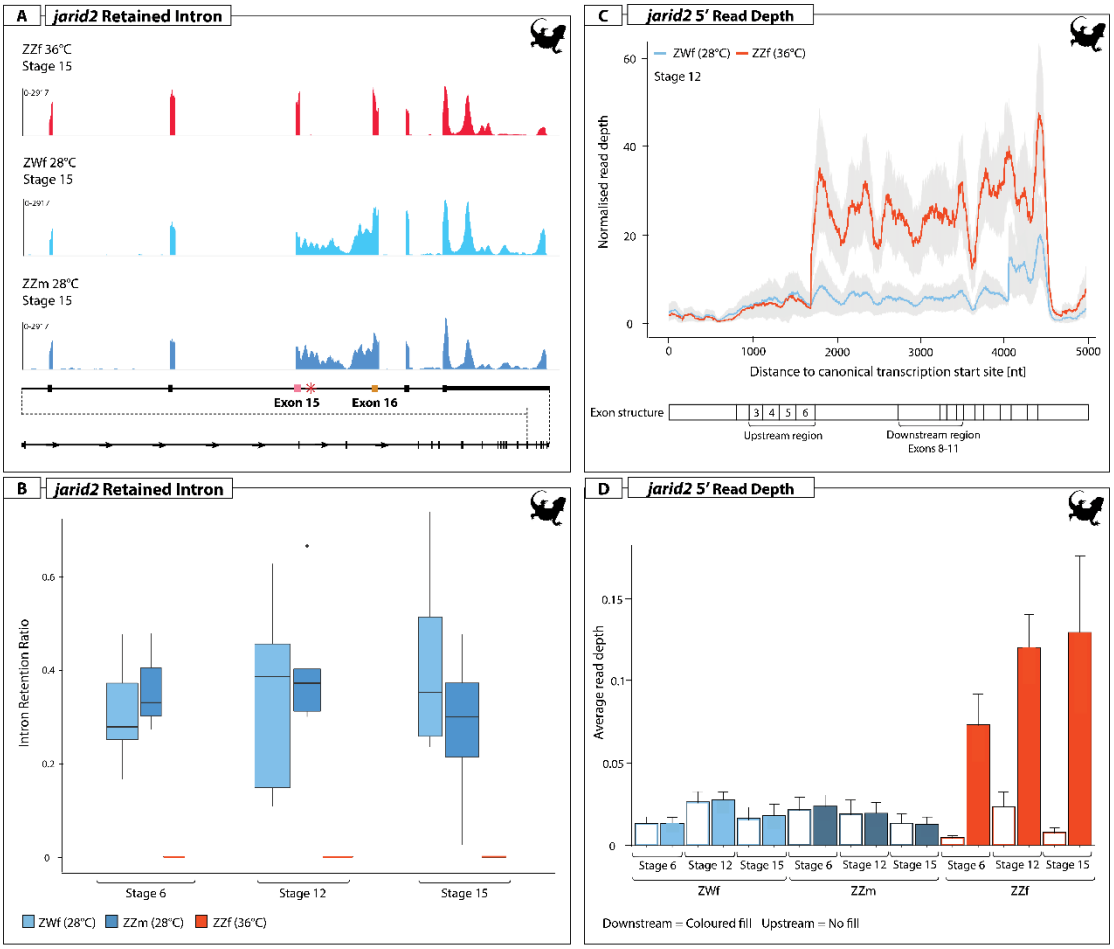

Figure 6.1: Isoforms of *jarid2* present during embryonic development in *Pogona vitticeps* at normal (28°C) and sex reversal inducing (36°C) temperatures. A) Read depth of stage 15 sex reversed female (red), concordant female (light blue), and male (dark blue) depicting the intron retention event in intron 15 in *jarid2*. B) The rate of intron 15 retention across the three developmental stages assessed for the three sex classes (note that it is zero for all ZZf at 36˚C). C) Normalised read depth for *jarid2* depicting the dramatic increase in read depth in sex reversed females (red) likely indicating a 5’ truncated isoform. D) Average read depth of upstream (coloured fill) and downstream (no fill) regions of *jarid2* showing a significant increase in read depth in sex reversed females (red).

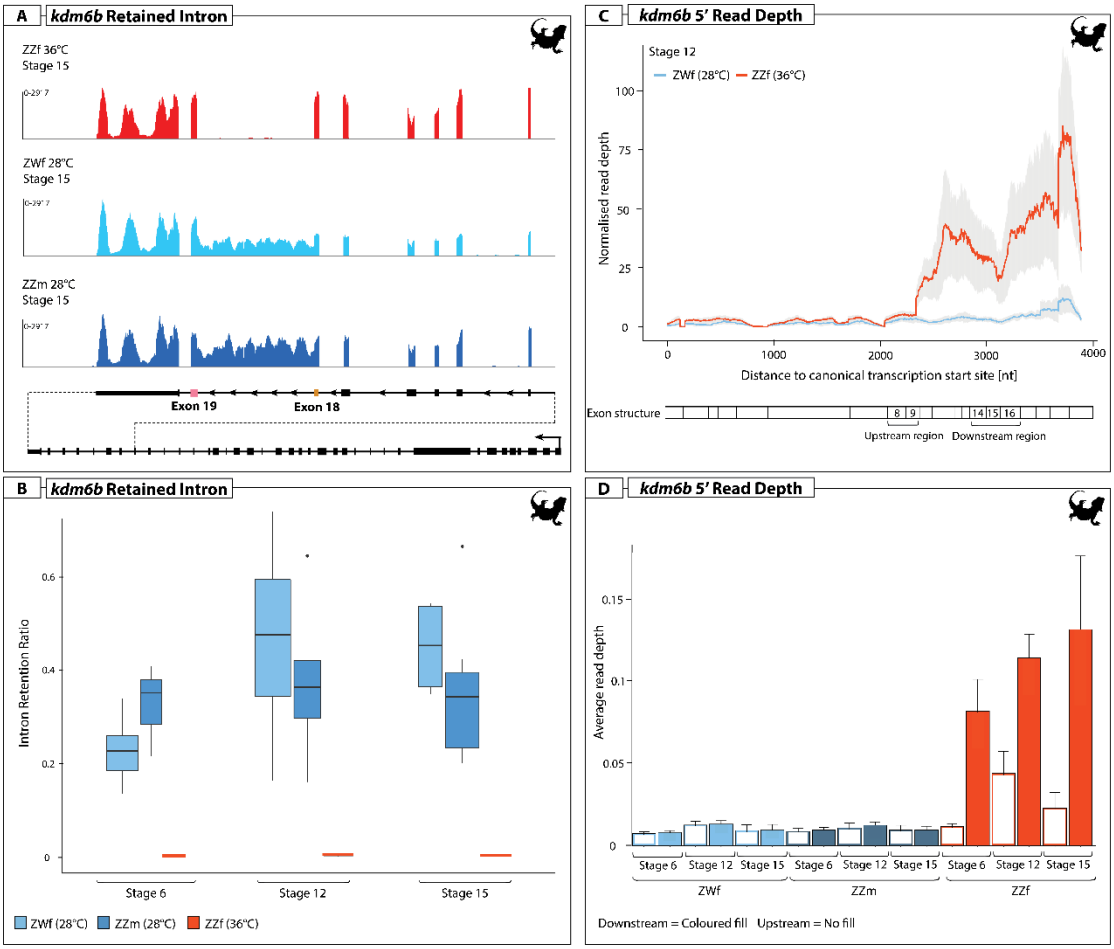

Figure 6.2: Isoforms of *kdm6b* present during embryonic development in *Pogona vitticeps* at normal (28°C) and sex reversal inducing (36°C) temperatures. A) Read depth of stage 15 sex reversed female (red), concordant female (light blue), and male (dark blue) depicting the intron retention event in intron 18 in *kdm6b*. B) The rate of intron 18 retention across the three developmental stages assessed for the three sex classes (note that it is zero for all ZZf at 36˚C). C) Normalised read depth for *kdm6b* depicting the dramatic increase in read depth in sex reversed females (red) that corresponds with the ΔN-KDM6B isoform. D) Average read depth of upstream (coloured fill) and downstream (no fill) regions of *kdm6b* showing a significant increase in read depth in sex reversed females (red).

We also discovered another *jarid2* isoform by examining read depth throughout the gene. We found that read depth of *jarid2* in sex reversed ZZf embryos dramatically increased from slightly downstream from the start of exon 7 to the end of the transcript (Figure 6.1c).

This strongly indicated the presence of a *jarid2* transcript isoform lacking the 5' region in ZZf embryos, which was absent in both normal ZWf females and ZZm males incubated at 28°C. IRfinder analysis detected partial retention of intron 6, the intron preceding exon 7, in ZZf embryos (Supplementary Data 6.1). Indeed, more than 90% of isoforms lacked the 5' part of the transcript in ZZf embryos (Figure 6.1d). The read coverage over intron 6 in ZZf embryos is unlikely to result from an intron retention event,

so an alternative transcription start site within intron 6 or at the beginning of exon 7 is a more likely explanation (Figure 6.3a). This interpretation is supported by uneven read depth over intron 6, which increases from 5' towards 3', as well as the higher number of reads spanning the intron 6 – exon 7 boundary compared to the exon 6 – intron 6 boundary (Figure 6.1). The most significant read depth increase occurred at the beginning of exon 7, suggesting that most transcripts start at the beginning of exon 7. The first two potential AUG start codons after the strongest incline in read depth are in frame with the canonical protein and display strong protein translation initiation sites (Kozak sequence AAGAUGAGA and AAAAUGGA).

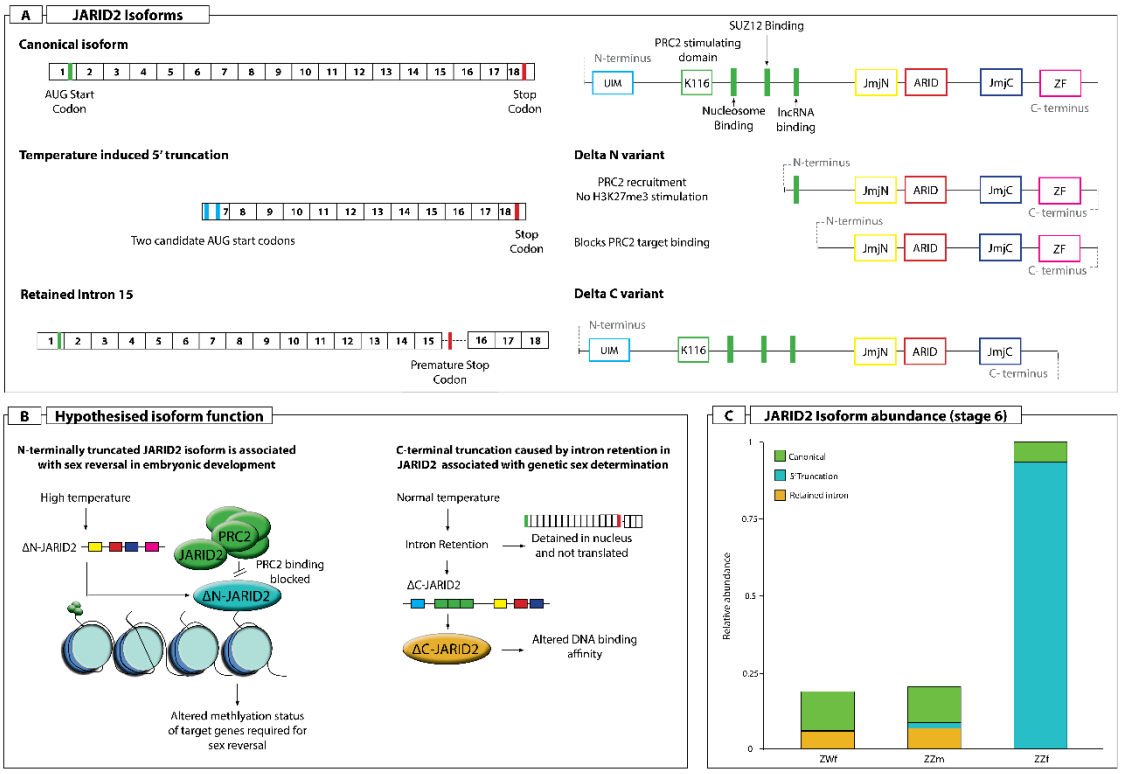

Figure 6.3: Isoforms of *jarid2* present during embryonic development in *Pogona vitticeps*. A) Transcript structure of the three observed *jarid2* isoforms and the potential resulting protein variants with important functional domains indicated. B) Hypothesised function of JARID2 isoforms during sex determination in *P. vitticeps*. Owing to truncation of a PRC2 binding and stimulating domain, the ability of ΔN-JARID2 to bind PRC2 and stimulate might be negatively affected. It is likely still able to bind typical target regions, and blocks PRC2 from methylating these sites. The C-terminally truncated isoform produced from the retention of intron 15 may be detained in the nucleus [578], or it may still be translated into a protein (ΔC-JARID2), but with reduced DNA binding affinity or altered target specificity owing to the missing C-terminal zinc finger domain. C) Relative abundance of the three *jarid2* isoforms observed at stage 6 in the three sex classes. UIM = Ubiquitin interaction motif, ZF = Zinc finger.

Translation of the 5' truncated transcript is likely to be initiated at one of those two initiation codons. Intriguingly, the resulting N-terminal truncated protein (ΔN-JARID2) lacks the PRC2 stimulating domain and the domain responsible for binding to SUZ12, a core subunit of the PRC2 complex (Figure 6.3c). A similar variant has been recently described in human epidermal keratinocytes [454].

6.3.3 Splicing of chromatin remodelling gene kdm6b

In sex reversed *P. vitticeps* ZZf embryos, approximately half of the *kdm6b* transcripts retain intron 18 (Figure 6.3b). This would be translated into a truncated protein that retains the demethylating functions of the JmjC domain (ΔC-KDM6B) but lacks the C-terminus containing zinc finger and C-helix domains (Figure 6.4a). The role of the ΔC-KDM6B variant and its potentially altered target specificity during sex reversal requires further investigation.

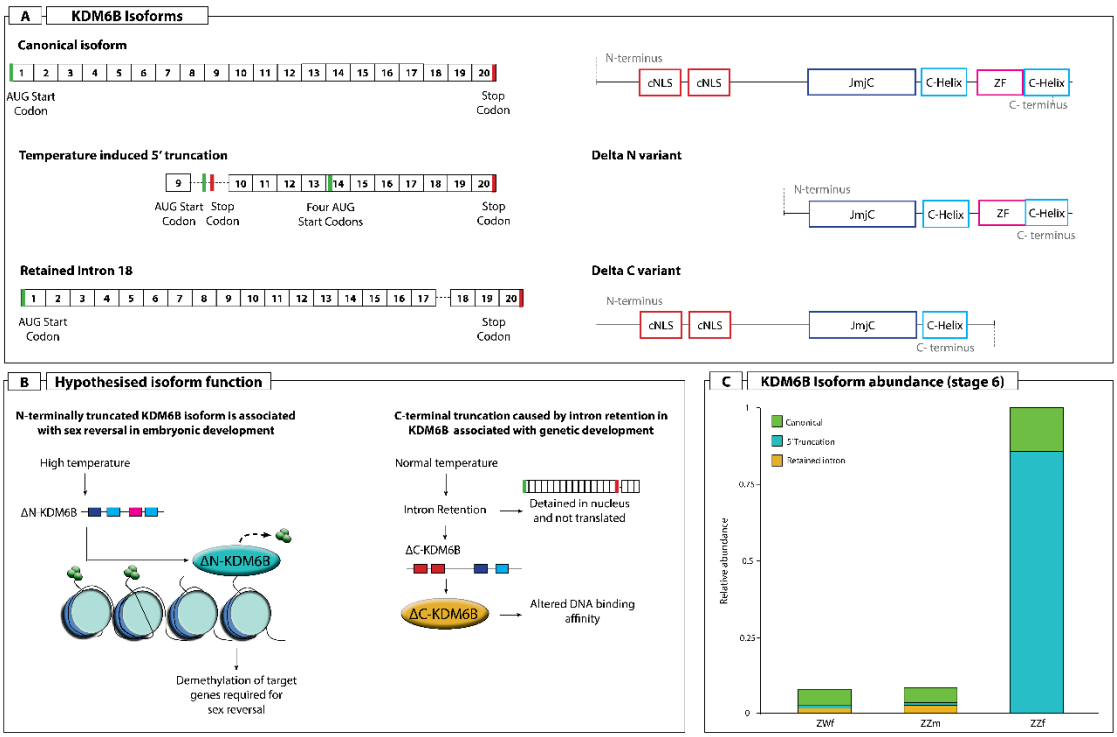

Figure 6.4: Isoforms of *kdm6b* present during embryonic development in *Pogona vitticeps*. A) Transcript structure of the three observed *kdm6b* isoforms and the potential corresponding protein variants with functional domains indicated. B) Hypothesised function of KDM6B isoforms during sex determination in *P. vitticeps*. The N-terminal region is poorly described for KDM6B, so we hypothesise that although the annotated canonical nuclear localisation domains (cNLS) are truncated, given the high expression of *kdm6b* is it likely that ΔN-KDM6B is still translated. We also suggest that it retains its demethylation function owing to retention of the JmjC domain, allowing it to demethylate target genes required for the initiation of sex reversal. The C-terminally truncated isoform produced by retention of intron 18 may be detained in the nucleus and not translated [578], or it may still be translated (ΔC-KDM6B) but have reduced DNA binding affinity or altered target specificity owing to the missing zinc finger and C-helix C-terminal domains. C) Relative abundance of the three *kdm6b* isoforms observed at stage 6 in the three sex classes.

We found that, as for *jarid2*, read depth for ZZf embryos in *kdm6b* increased considerably from exon 10 to the end of the transcript, indicating presence of an isoform lacking the 5' end (Figure 6.2d). Intron 9, preceding exon 10, was also detected in the IRfinder analysis as partially retained in ZZf embryos (Supplementary Data 6.1). An alternative transcription start site within intron 9 of *kdm6b* seems a likely explanation. In such a 5' truncated transcript the first AUG triplet occurs in exon 14, which contains four AUG triplets in frame with the canonical KDM6B protein. The N-terminal truncated protein translated from any of the four AUG codons would start just before the demethylating JmjC domain. Previous research characterising KDM6B protein function in mammalian cell lines revealed the presence of classical nuclear localisation signals (cNLSs) in the N-terminal region that are required for nuclear localisation, and subsequent demethylation actions, of KDM6B [455]. Most *kdm6b* transcripts in sex

reversed ZZf embryos lack the 5' end, so the putative ΔN-KDM6B protein is likely to have altered localisation dynamics, but this remains to be tested (Figure 6.4a).

Thus both chromatin remodelling genes, *jarid2* and *kdm6b*, show differential intron retention and alternative transcription start sites in *P. vitticeps*. Truncation of the 5' region of the transcripts leads to proteins lacking the functional domains in these regions. In ΔN-JARID loss of the PRC2 interacting domains could lead to competitive inhibition of the canonical JARID, whereas in ΔN-KDM6B, the JmjC domain is retained, so it probably still exhibits lysine demethylase activity but loses localisation signals.

6.4 Discussion

In this study, we demonstrate temperature-specific alternative splicing events and alternative initiation sites in *jarid2* and *kdm6b*, which all are likely to play key regulatory roles in sex reversal in *Pogona vitticeps*. We show that intron retention in *kdm6b* and *jarid2* occurs only at low incubation temperatures during embryogenesis, and changes to the opposite pattern in adults [55].

As previously reported, the same intron retention event causing C-terminally truncated *kdm6b* and *jarid2* isoforms occurs exclusively during low temperature incubation and not high temperature incubation of *A. mississippiensis*, *T. scripta*, and *P. vitticeps* [55]. Thus our present observations on *P. vitticeps* embryos now demonstrates that the pattern of intron retention in embryos is the same in all three species, and occurs at low temperatures in the three widely divergent reptiles. These low temperature intron retention events are distinct from the novel 5' truncated *kdm6b* and *jarid2* isoforms which occur only during high temperature sex reversal in *P. vitticeps* embryos, and are absent in *T. scripta* and *A. mississippiensis* embryos under the incubation temperatures investigated here.

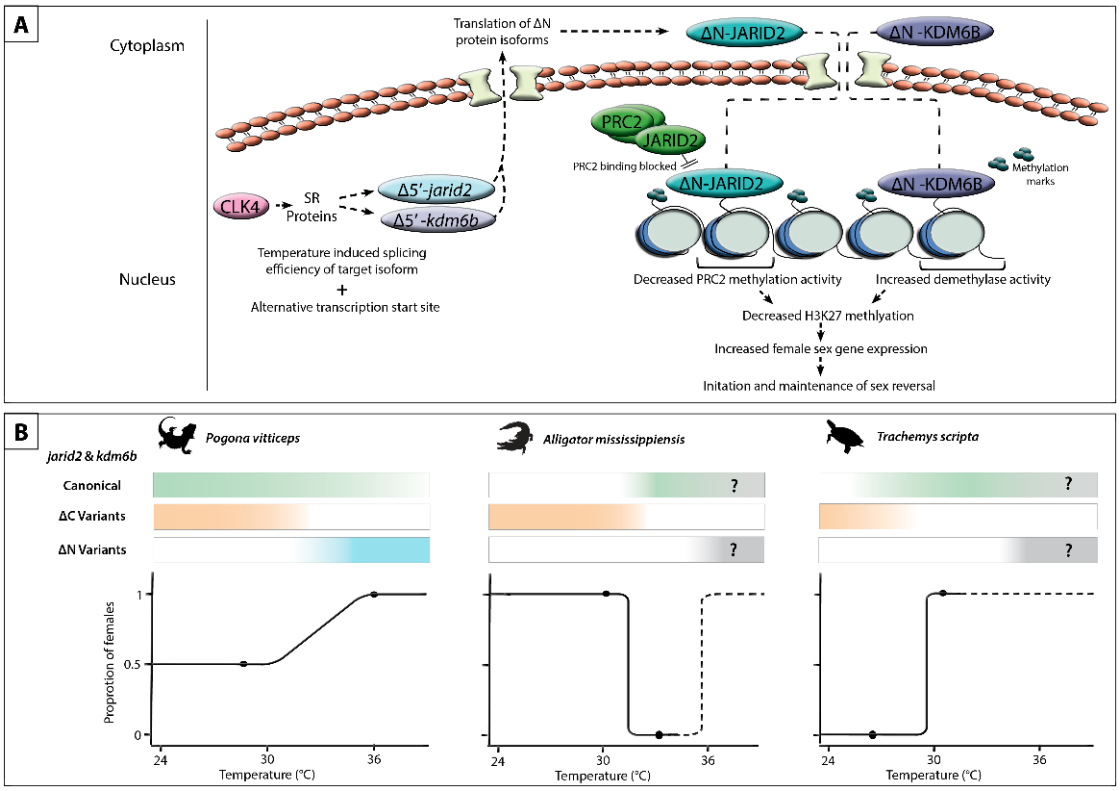

Figure 6.5: Hypothesised pathway for the role of the ΔN *jarid2* and *kdm6b* transcript and protein isoforms during temperature induced sex reversal in *Pogona vitticeps* embryos, and presence of isoforms at different incubation temperatures in *P. vitticeps*, *Alligator mississippiensis*, and *Trachemys scripta*. (A) We hypothesise that under high incubation temperatures, splicing of *jarid2* and *kdm6b* is altered, potentially by CLK4 modulating SR proteins, to create the ΔN variants. If translated to a protein, the ΔN-JARID2 isoform lacking the PR2 interacting domains, can compete with the canonical JARID2 protein and the PRC2 complex by binding at the same target sites. The ΔN-KDM6B isoform likely retains its demethylating functions at the JmjC is intact. Together the ΔN variants may decrease levels of H3K27 methylation (a repressive chromatin mark) so causing an increase in female sex gene expression required for the initiation and maintenance of male to female sex reversal. This hypothesised pathway can be followed from left to right in the diagram (B) Schematic representation of the presence of ΔN and ΔC *jarid2* and *kdm6b* isoforms in the three species at the incubation temperatures that have been assessed. For *A. mississippiensis* and *T. scripta*, the dotted lines at high incubation temperatures denotes the possibility that that the ΔN variants may be present under these conditions, but has not been assessed. The colour gradients denote where the variants have been demonstrated at a given incubation temperature, and the question marks in *A. mississippiensis* and *T. scripta* denote high incubation temperatures where the ΔN variants may occur but have not been assessed.

These new findings have important implications for our understanding of the thermolabile sex determination systems in these three species. For *P. vitticeps*, we now know that the patterns of isoform expression are not consistent between embryos and adults, as was previously assumed [55]. Importantly, it seems unlikely that the ΔC JARID2 and KDM6B variants have a role in sex determination, as they were observed in the GSD pathways of both ZZm males and ZWf females at 28°C (Figure 6.5b). The

dynamics of protein translation and function of both the ΔC and ΔN variants present exciting direction for ongoing research.

It would be interesting to discover if more extreme incubation temperatures in *T. scripta* and *A. mississippiensis* induces expression of the ΔN JARID2 and KDM6B isoforms (Figure 6.5b). In *T. scripta* it has been conclusively demonstrated that at the male producing temperature (MPT) *kdm6b* is highly expressed and is required to demethylate the *dmrt1* promoter and initiate male development [24]. We also know that the ΔC KDM6B variant is expressed at the MPT in this species, but the functional implications of this for the induction of the male sex determination cascade remains unknown, as does the role of the ΔC JARID2 isoform.

Much less is known about the sex determination pathways in *A. mississippiensis.* Of particular interest is that in this species, females can be produced at high as well as low incubation temperatures (approximately 35°C) [456]. But no transcriptomic work has yet been conducted at such a high incubation temperature. It is possible that this more extreme female-producing temperature may generate a similar cellular effect as is seen during sex reversal in *P. vitticeps,* and the ΔN JARID2 and KDM6B variants may be expressed (Figure 6.5b). If this is the case, it would have important implications for the evolution of the ΔN variants in thermosensitive sex determination systems. Based on previous research [402], we propose a crucial role for the splicing regulator CLK4 in the *P. vitticeps* sex reversal cascade (Figure 6.5a). This research assessed the activity profiles of CLK4 in different species found that it functioned at temperatures relevant to each species [402]. The activity of CLK4, and the SR proteins that it regulates, in *P. vitticeps* during sex reversal remains unknown.

In *P. vitticeps* the alternative *jarid2* transcript is expected to translate into ΔN-JARID2 protein in ZZf females. This is a novel variant of JARID2 (ΔN-JARID2) present in gonadal cells from stage 6. A similar truncated ΔN-JARID2 transcript was characterised recently in human epidermal keratinocytes [454], and was suggested to display competitive inhibition of PRC2 on target sites. Whereas full-length JARID2 recruits PRC2 to its target sites by binding both nucleosome and PRC2 domains and stimulates the H3K27 methylating activity of PRC2, ΔN-JARID2 was suggested to still bind to its target sites but to block PRC2 binding and/or activity at those sites because it lacks the PRC2 binding and stimulating domains (Figure 6.3b) [454]. Thus – in mammalian cells at least – the function of ΔN-JARID2 appears to be antagonistic to the

canonical JARID2 isoform. We suggest that this mode of action may be critical during sex reversal to alter the expression of sex specific genes through modulation of H3K27 methylation, so initiating male to female sex reversal from stage 6 of development (Figure 6.5a).

Another interesting parallel between human and dragon ΔN-JARID2 variants is their association with cellular calcium concentration. In human cell lines, ΔN-JARID2 is observed when cellular calcium concentrations are increased [454]. The same may be true in dragons, as we know from previous work that activation of the calcium channel (*trpv2*) and a suite of genes associated with calcium signalling are upregulated during high temperature sex reversal [54]. Whether the ΔN-JARID2 isoform is present in other species, or if it can be generated under heat stress conditions, and what its role may be, is currently unknown. It has been proposed that calcium signalling plays an important role in sensing and transducing external cues in environmentally sensitive sex determination systems [53]. If, as in humans, dragon ΔN-JARID2 is influence by calcium this would provide important support for the role of calcium in mediating temperature responses and triggering changes in the cell.

Human and dragon ΔN-JARID2 forms appear to be similar and their function may be analogous, but the variants are generated via different mechanisms, constituting an unusual form of convergent evolution. Human ΔN-JARID2 is generated via post-translational cleavage of the protein, whereas dragon ΔN-JARID2 is generated via the activation of an alternative transcription start site.

We also identified a novel 5' truncated *kdm6b* transcript isoform, which could be translated into a truncated ΔN-KDM6B protein. Newly identified in this study, the function of the ΔN-KDM6B variant is unknown. We hypothesise that, as has been shown for ΔN-JARID2, it has an antagonistic function to the canonical JARID2, maintaining the active de-methylated state of key genes necessary to initiate and promote the sex reversal pathway, diverting development away from the normal male development of the homogametic sex (Figure 6.5). In mammalian cell lines, classical nuclear localisation signals (cNLSs) in the N-terminal region regulate the nuclear localisation of KDM6B [455]. As balanced KDM6B localisation between the nucleus and cytoplasm is a mechanism by which H3K27me3 methylation levels can be

regulated, we propose that modification of this histone is involved in *P. vitticeps* sex reversal, providing a compelling avenue for future research.

Comparisons of transcript isoforms in *P. vitticeps, A. mississippiensis* and *T. scripta* show that JARID2 and KDM6B are consistently implicated in thermosensitive sex determination cascades across evolutionarily disparate lineages. However, there are critical differences between the three species. The 5' truncated transcript isoforms that encode the truncated ΔN-JARID2 and ΔN-KDM6B proteins appear only in sex reversed embryonic *P. vitticeps*, suggesting a unique pathway for the evolution of these genes. Investigation of isoform variants in other species with thermosensitive sex determination is needed to determine whether these variants are specific to *P. vitticeps*, or are associated with sex reversal more broadly.

Our observations of these transcript variants in *P. vitticeps* raises important questions. What regulates splicing and transcription start site choice for these genes, and how to they related to thermosensitivity and sexual development? There are likely to be many other genes involved in thermal sensitivity of sex reversal in *P. vitticeps*. CLK4, a protein kinase that regulates the activation of serine and arginine rich (SR) proteins that control mRNA splicing [457], is a very promising candidate. CLK4 activity controls *jarid2* intron retention in two turtle species, so may play a role in regulating the splicing patterns we observed during sex reversal in *P. vitticeps* (Figure 6.5a). The findings from this research open up many new avenues for future research, including determining the range of temperatures at which the ΔN variants may be functioning in *P. vitticeps*, and demonstrating their function in regulating sex determination cascades. The effect temperature fluctuations during incubation in natural nests on splicing modulation also needed to be investigated [449].

While much remains to be understood about thermosensitive sex determination systems, our demonstration of novel splicing events during reversal in *P. vitticeps* represents an important advance. We reveal complex and evolutionary dynamic roles for *jarid2* and *kdm6b* across divergent lineages, bringing new insight into the elusive molecular mechanisms by which temperature determines sex. More broadly, our work adds to the body of evidence demonstrating that *jarid2* exists in different forms that can have completely opposing functions. Fully understanding the complexities of splicing in

such chromatin modifying genes may redefine our understanding of the dynamics of transcriptional activation and repression during vertebrate development.

6.5 Materials and Methods

6.5.1 Egg incubations, sampling, and sequencing for Pogona vitticeps

The dataset used in this study has been described in full in [54]. Briefly, eggs from ZZf and ZWf mothers were collected at or soon after lay, and incubated at 28°C. Following a period of developmental entrainment (10 day), eggs from ZZf females were switched to 36°C. Eggs at each temperature were sampled at stages 6, 12, and 15 according to the staging criteria established for *P. vitticeps* [7] in order to capture the bipotential gonads, and early and late stages of gonad differentiation [8]. The isolated embryonic gonads were dissected, and total RNA was extracted using the Qiagen RNeasy Micro kit (Cat. No. 74004) according to the manufacturer protocols. Sequencing libraries were prepared in randomised batches using the Roche NimbleGen KAPA Stranded mRNA-seq kit (Cat. No. KK8420), and samples were sequenced on the Illumina HiSeq 2500 system at the Kinghorn Centre for Clinical Genomics (Garvan Institute of Medical Research, Sydney). On average, 25 million read-pairs per sample were obtained.

6.5.2 Data analysis

The paired-end RNA-seq libraries for *P. vitticeps* were trimmed using cutadapt [458] with -q 20 -m 20 -max-n 4 -trim-n. Trimmed reads were aligned to the *Pogona vitticeps* genome assembly pvi1.1 (GCA_900067755.1; http://ftp.ensembl.org/pub/release-100/fasta/pogona_vitticeps/dna/Pogona_vitticeps.pvi1.1.dna.toplevel.fa.gz) [418] using STAR (v2.7.0f) [419] with splice-aware alignment guided by the accompanying Ensembl gene annotation (pvi1.1.100). Parameters were chosen to output only unique alignments and to assure compatibility with IRFinder (--outFilterMultimapNmax 1 --outSAMstrandField intronMotif --outFileNamePrefix --outSAMtype BAM Unsorted).. To reduce the amount of scaffolds in the genome assembly those with no genes annotated were excluded. Paired-end sequencing libraries for *Alligator mississippiensis* were obtained from [93] data accessioned on the DNA Databank of Japan Sequence Read Archive accession number DRA004128-41. Paired-end sequencing libraries for

Trachemys scripta were obtained from [94] data accessioned on NCBI's SRA database (Bioproject PRJNA331105). Owing to insufficient replicates for robust analysis, *A. mississippiensis* samples DDR048634-DDR04636 and *T. scripta* stage 26 samples were excluded. The libraries were trimmed and aligned as described above for *P. vitticeps.* For *A. mississippiensis* the genome assembly ASM28112v4 (RefSeq GCF_000281125.3) was used with accompanying NCBI gene annotation (GCF_000281125.3_ASM28112v4_genomic.gtf). For *T. scripta* the genome assembly CAS_Tse_1.0 (RefSeq GCF_013100865.1) was used with accompanying NCBI gene annotation (GCF_013100865.1_CAS_Tse_1.0_genomic.gtf).
Approximations of the developmental stages for *A. mississippiensis* and *T. scripta* with the staging system from *P. vitticeps* are provided in Table 6.1.

Table 6.1: Developmental stages of *Alligator mississippiensis* and *Trachemys scripta* from previously published datasets [93,94] used in this study and the approximately equivalent stages to *Pogona vitticeps* [7], including timing of gonadal development. The stage equivalency was based on described characteristics for each developmental stage from the systems for *A. mississippiensis* and *T. scripta* respectively in order to standardise the timing of gonadal development between the three species.

Species	**Staging System**	**Original developmental stage**	***P. vitticeps* equivalent**	**Timing of gonad development**
Alligator mississippiensis	[284]	19	10	Bipotential gonad
		20	12	Early gonad differentiation
		21	13	Sex differentiation
		22	14	Sex differentiation
		23	14	Sex differentiation
***Trachemys* scripta**	[295]	15	6	Bipotential gonad
		17	7	Sex differentiation
		19	9	Sex differentiation
		21	11	Gonad commitment

To conduct an unbiased analysis of splicing patterns across whole transcriptomes obtained for the three species, IRFinder [450] was used to detect differentially retained introns between ZZf and ZWf embryos across development in *P. vitticeps*, and between

male and female producing temperatures across development in *A. mississippiensis* and *T. scripta*. For *T. scripta* two *jarid2* transcript isoforms were removed from the annotation gtf file (XM_034762362.1 and XM_034762363.1). They were not expressed in any sample but interfered with correct recognition of intron retention events in the major transcript isoform. Before differential intron retention analysis, introns were excluded with an intron depth (intronDepth) or a maximum of spliced reads (maxSplice) of >= 5 in less than two samples. For *P. vitticeps* and *A. mississippiensis*, the differential intron retention analysis was performed with DESeq2 (1.26.0) [459] in R version R 3.6.1 as outlined in the IRFinder manual. For *T. scripta* an Audic and Claverie Test with pooled samples was performed according to IRFinder guidelines for samples with 2 or less replicates. For differentially retained introns the following cut-offs were applied: intron retention >= 0.1 in either group, intron retention change >= 0.25, adjusted *P*-value < 0.01 for *P. vitticeps* and a *P*-value < 0.01 for *A. mississippiensis* and *T. scripta.* Bedgraphs were created for each alignment file with bedtools genomecov (https://bedtools.readthedocs.io/en/latest/index.html) and used to extract read depth over *jarid2* (*P. vitticeps*: ENSPVIT00000008211, *T. scripta*: XM_034762361.1, *A. mississippiensis*: XM_006270617.3) and *kdm6b* (*P. vitticeps:* ENSPVIT00000021647, *T. scripta*: XM_034757088.1, *A. mississippiensis*: XM_019493797.1) transcripts with costume scripts. To determine the relative abundance of the 5' truncated *jarid2* and *kdm6b* transcript isoforms in *P. vitticeps*, the read depth of a region upstream and downstream of the putative alternative transcription start site was compared. For *P. vitticeps* the *kdm6b* upstream and downstream regions comprise 293 nucleotides (covering exons 8 and 9) and 898 nucleotides (covering exons 14 to 16), respectively. The *jarid2* upstream and downstream regions comprise 721 nucleotides (covering exons 3 to 6) and 799 nucleotides (covering exons 8 to 11), respectively. Read depth was normalised by library size and length of the region. The average +/- standard deviation of all samples per group is shown.

The relative abundance of all three *jarid2* and *kdm6b* transcript isoforms (full-length, retained intron, 5' truncated) in ZZf, ZWf and ZZm in *P. vitticeps* was inferred from integration of gene differential expression analysis [54], differential intron retention analysis and the abundance calculation for the 5' truncated isoform as explained above.
We follow the standard set for the naming of genes (e.g. *kdm6b* for reptiles, *KDM6B* mammals) by Kusumi et al. [460]. Proteins are upper case.

6.5.3 Supplementary Figures

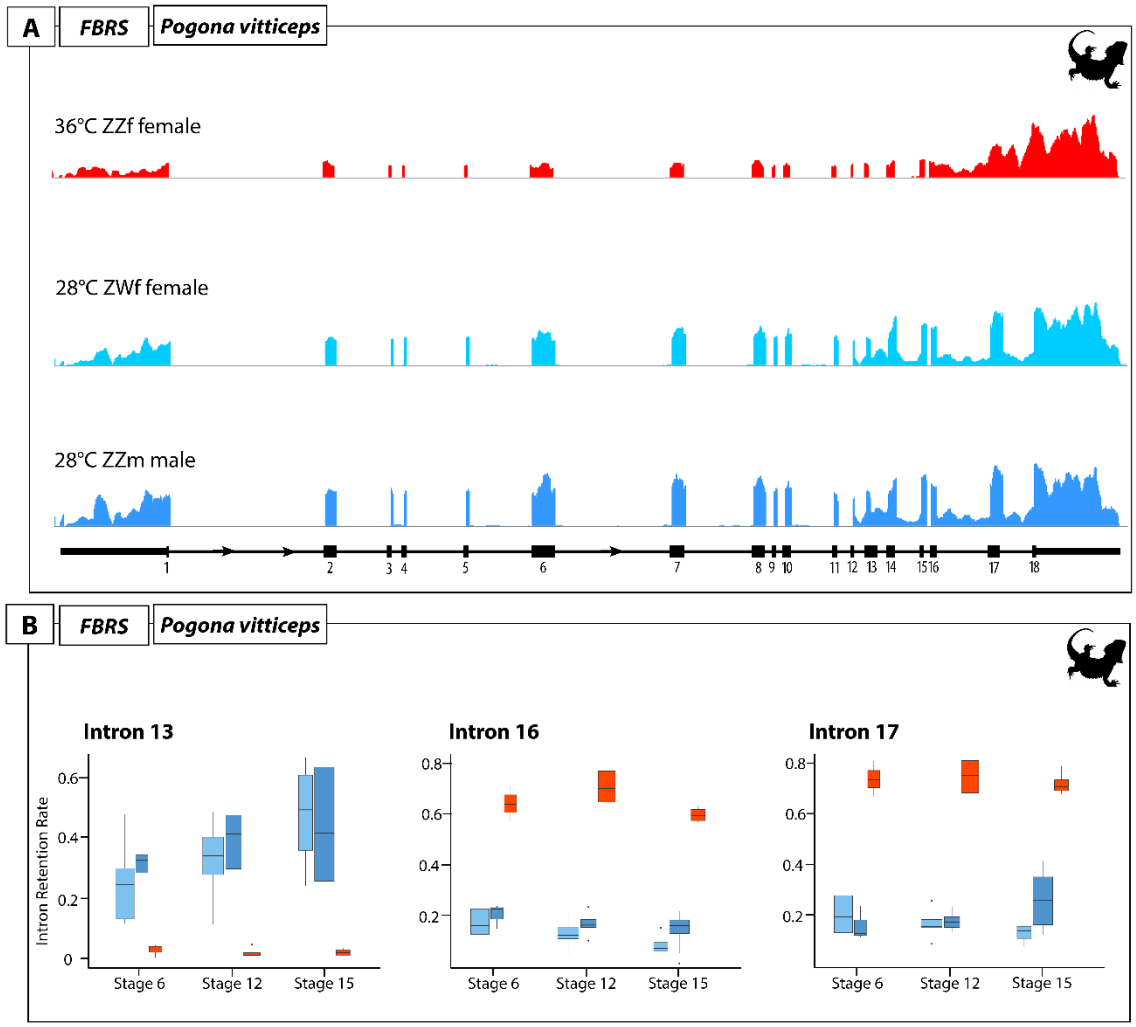

Figure 6.6: Retained introns in *fbrs* detected by IRfinder analysis in *Pogona vitticeps*. A) Read depth of *fbrs* in sex reversed (red) and concordant (light blue) females, and males (dark blue). B) Intron retention rates of the three retained introns in *fbrs* detected at the three developmental stages assessed. Intron 13 is retained in association with normal incubation temperatures in both concordant females and males. Retention of intron 16 is markedly increased in sex reversed females at high incubation temperatures.

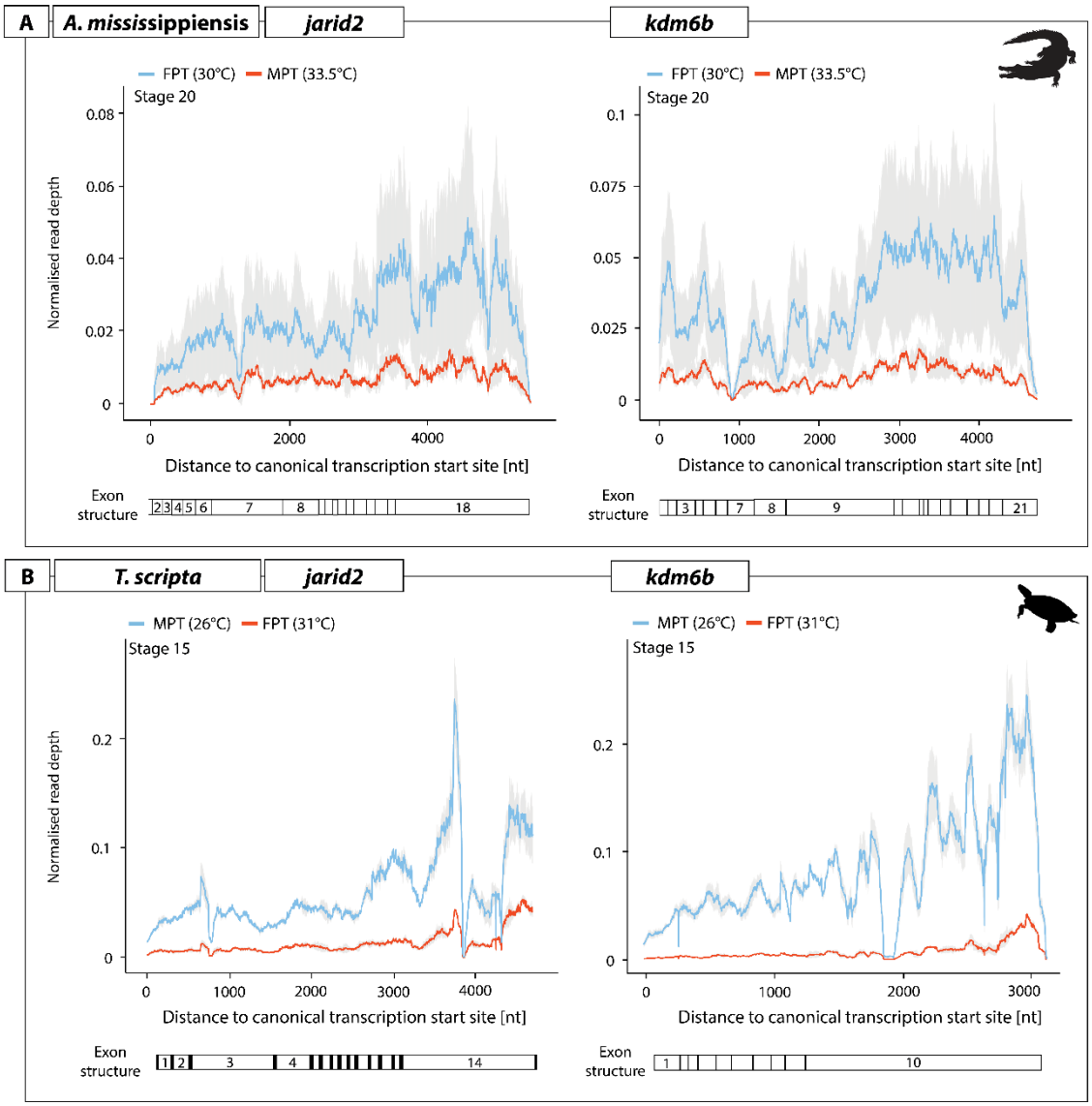

Figure 6.7: Normalised read depth for *jarid2* and *kdm6b* in *Alligator mississippiensis* at stage 20 and *Trachemys scripta* at stage 15. Data depicted for *A. mississippiensis* was obtained from [93] and shows read depth for embryos incubated at the male producing temperature in red (MPT; 33.5°C) and the female producing temperature in blue (FPT; 30°C). The data for *T. scripta* was obtained from [94] and shows read depth for embryos incubated at the male producing temperature in blue (MPT; 26°C) and the female producing temperature in red (FPT; 31°C).

6.5.4 Supplementary Files

Supplementary Data 6.1: Outputs from IRfinder analysis [450] for the three species used in this study; *Pogona vitticeps, Alligator mississippiensis*, and *Trachemys scripta.* Developmental stages for *A. mississippiensis* is from original data source [93] following the staging system developed for this species [284]. In the "comparison" column for *P. vitticeps*, 28ZW refers to ZW offspring incubated at 28°C with a ZW genotype, 28ZZ

refers to ZW offspring incubated at 28℃ with a ZZ genotype, and 36ZZ refers to ZZ offspring incubated at 36℃.

Files for each species are available for download from https://datadryad.org/stash/share/LmIJOwQvMXrmi2f1r-knaBtOB15CR7vdir9JZwkv5Yg.

Chapter 7 Developmental dynamics of sex reprogramming by high incubation temperatures in a dragon lizard

In Review: BMC Biology

Whiteley, S. L., Holleley, C. E., Georges, A. (*in review*). Developmental dynamics of sex reprogramming by high incubation temperatures in a dragon lizard

7.1 Abstract

In some vertebrate species, gene-environment interactions can determine sex, driving bipotential gonads to differentiate into either ovaries or testes. In the central bearded dragon (*Pogona vitticeps*), the genetic influence of sex chromosomes (ZZ/ZW) can be overridden by high incubation temperatures, causing ZZ male to female sex reversal. Previous research showed ovotestes, a rare gonadal phenotype with traits of both sexes, develop during sex reversal, leading to the hypothesis that sex reversal relies on high temperature feminisation to outcompete the male genetic cue. To test this, we conducted temperature switching experiments at key developmental stages, and analysed the effect on gonadal phenotypes using histology and transcriptomics. We found sexual fate is more strongly influenced by the ZZ genotype than temperature. Any exposure to low temperatures (28^{o}C) caused testes differentiation, whereas sex reversal required longer exposure to high temperatures. We revealed ovotestes exist along a spectrum of female-ness to male-ness at the transcriptional level. We found inter-individual variation in gene expression changes following temperature switches, suggesting both genetic sensitivity to, and the timing and duration of the temperature cue influences sex reversal. These findings bring new insights to the mechanisms underlying sex reversal, improving our understanding of thermosensitive sex systems in vertebrates.

7.2 Introduction

Sex determination in vertebrates exists on a continuum spanning from genetic sex determination (GSD) to temperature dependent sex determination (TSD) [5]. Some species possess sex chromosomes with a thermal override that can cause sex reversal. In the case of the Australian central bearded dragon *Pogona vitticeps*, the most well studied reptile with sex reversal, genetic males (ZZ sex chromosomes) incubated at high temperatures (>32°C) undergo sex reversal so the animal develops as a female despite being genetically male [3,38]. As these sex reversed females (ZZf) are reproductively viable, mating of ZZf and ZZm individuals yields offspring whose sex is determined solely by temperature in the absence of the W chromosome [3,38]. Despite this being akin to that observed in TSD species, where sex is determined in the absence of sex chromosomes, sex reversal in *P. vitticeps* differs in several important ways. The offspring of sex reversed mothers inherit ZZ chromosomes, and reversal of their offspring may be more sensitive to temperature than ZZ offspring of ZW mothers [3]. Some individuals do not sex reverse at high temperatures, suggesting interindividual propensity for sex reversal. Variability in rates of sex reversal also exists at the population level [78]. Both thermally-induced sex reversal and TSD require influential cells of the bipotential gonad to sense and transduce temperature to epigenetic changes that ultimately govern sex determination and differentiation [53].

Understanding the mechanisms of TSD has remained elusive despite decades of attention following the discovery of TSD in the African dragon *Agama agama* [6]. The most recent proposition for how an environmental cue can cause cellular changes that ultimately determine sexual fate invokes calcium and redox signalling at the head of the regulatory cascade [53]. This CaRe model predicts involvement of genes that govern the capacity of the cell to sense and respond to environmental changes and to subsequently modulate expression of genes in ubiquitous signalling pathways. The modulation of these signalling pathways leads to epigenetic processes (e.g. action of chromatin modifier genes) that influence the expression of sex genes [24]. CaRe mechanisms have been implicated in the TSD cascades of several species [53], and most recently in the gene expression patterns associated with sex reversal in embryonic *P. vitticeps* [54]. Four genes are consistently associated with sex reversal and TSD systems namely, *JARID2*, *KDM6B*, *CIRBP* and *CLK4* [22,24,54,55,90,402]. Chromatin remodelling genes *JARID2* and *KDM6B* regulate gene expression through modulation of methylation marks on lysine 27

on histone 3 (H3K27) [437,461]. In *Trachemys scripta KDM6B* demethylation of the *DMRT1* promoter is necessary for male development [24]. *CIRBP* is an environmentally sensitive gene that is activated by temperature, and splicing of this gene has been shown to be controlled by *CLK4*, which is itself temperature sensitive [90,402]. *CLK4* has also been shown to regulate the splicing of *JARID2* in two TSD turtles [402].

In TSD species, the epigenetic mechanisms responsible for sensing temperature and affecting gene expression can only influence sex during a window of embryonic development within which gonadal fate is responsive to temperature, known as the thermosensitive period (TSP). After the TSP, gonadal fate has been irreversibly determined [462]. The boundaries of the TSP are typically identified using temperature switching experiments, whereby eggs are switched between male and female producing temperatures at different embryonic stages during development [462]. A less common approach is to apply hormone inhibitors at different developmental stages to determine when the embryo becomes insensitive to its affects [310]. However, the timing of the TSP is not necessarily precise. For example, in *Alligator mississippiensis* the TSP occurs from embryonic stages 21 to 24 (ca 30-45 d post lay at 29-31^{o}C) [456]. Subsequent experiments showed that much earlier incubation conditions experienced around stage 15 can also influence sex [463]. Incubation at temperatures intermediate to the male and female producing temperatures (at the pivotal temperature) typically yield a mixture of the two sexes, presumably because temperature is equivocal in its influence allowing subtle genetic predisposition to prevail [225]. In TSD systems the presence of such underlying genetic predisposition is obscured by the dominant effect of temperature at all but a very narrow thermal range. In systems that display sex reversal, as in *P. vitticeps*, the complexity of gene-environment interactions involving temperature is further compounded by the presence of sex chromosomes [45].

The development of ovotestes is one effect of temperature on gonad differentiation. Ovotestes are a gonadal phenotype with both male and female traits [8]. In TSD species, ovotestes are rarely observed in embryos, and when they occur are likely a result of hormone balances at intermediate incubation temperatures [304,464]. In contrast, temperature induced sex reversal in *P. vitticeps* is observed as the temporary presence of ovotestes at stage 9 in approximately 40% of reversing embryos [8]. Ovotestes in ZZ/ZW species are thought to be caused during sex reversal by the competing influences of male sex chromosomes and feminizing incubation temperatures

[8]. As such, sex reversal is hypothesised to be a process by which the feminizing influence of temperature must override that of the masculinizing influence of the sex chromosomes [8].

To test the hypothesis that sex reversal involves over-riding the male sex determining signal, we switched incubation temperatures between 28°C where sexual phenotype and genotype are concordant and 36°C where sex reversal of ZZ individuals to a female gonadal phenotype is predominant. Switches were conducted at three developmental stages (Figure 7.1) ranging from bipotential to differentiated [7,8], and the gonadal phenotypes were analysed with histology and RNA-sequencing. With both morphological and gene expression data, the complex effects of temperature switching on sex determination and differentiation in *P. vitticeps* were revealed. We showed the timing and duration of the feminising high temperature cue that was required to override the male signal and initiate sex reversal. We profiled the gene expression characteristics of ovotestes, and temperature response genes, many of which have been implicated in the CaRe model [53] or in TSD [24,90,402]. This research provides new insights to the mechanisms of sex reversal in *P. vitticeps*, but also to vertebrate thermolabile sex determination more broadly.

7.3 Results

7.3.1 Temperature switching and gonadal phenotype

7.3.1.1 Control Experiments

Incubation at 28^{o}C without a switch resulted all individuals developing testis at all developmental stages, as would be expected from ZZ individuals (Figure 7.1a, d) [3]. Incubation at 36^{o}C yielded gonads with testis-like gonads at Stage 6, ovotestes and ovaries at stage 9, and ovaries at stages 12 and 15 (Figure 7.1a, d). Testis-like gonads were characterised by rudimentary seminiferous tubules akin to those observed in ovotestes, but without a thickened cortex (Figure 7.2). These results suggest that testes are the default developmental outcome for ZZ individuals, influenced by high temperature to become ovaries.

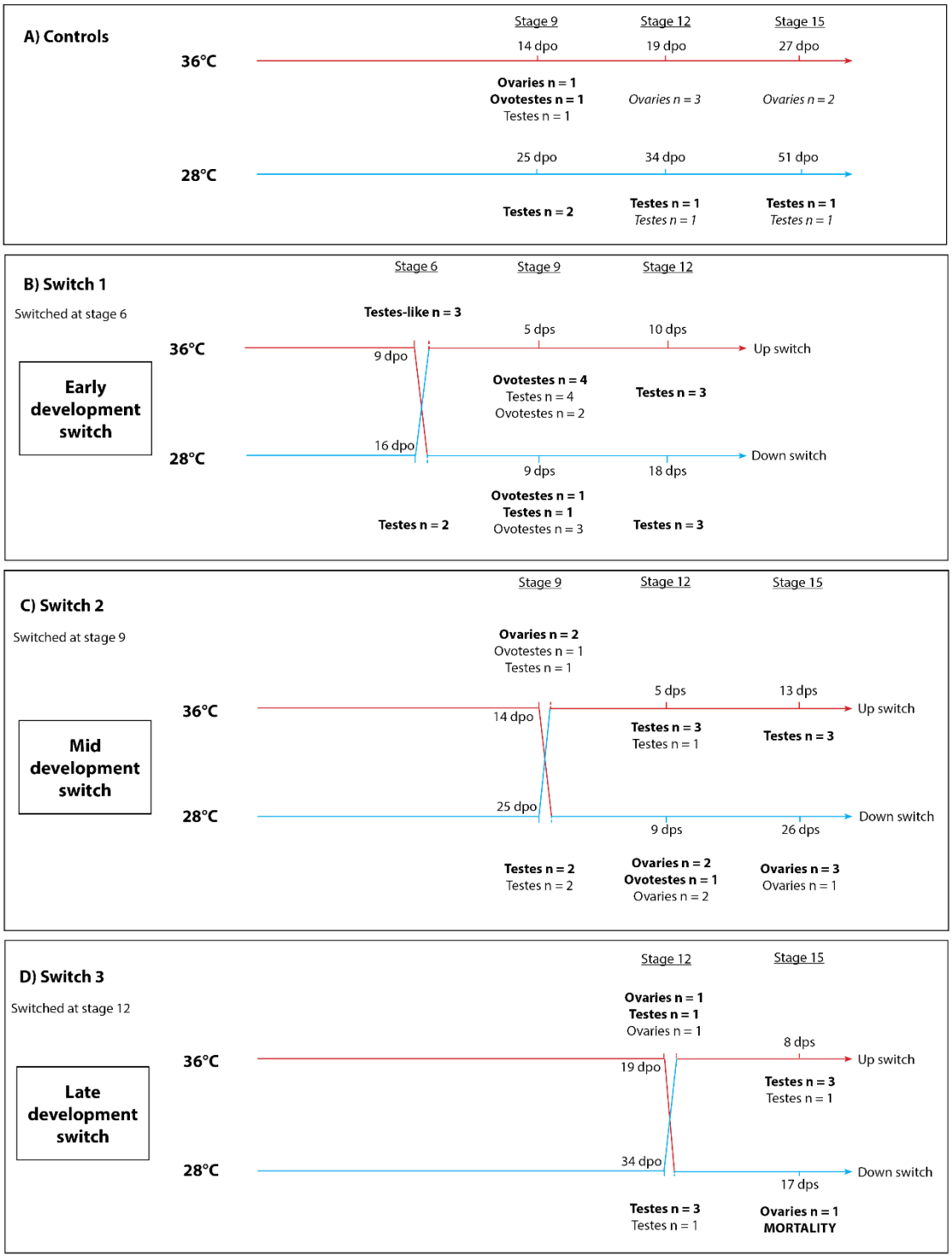

Figure 7.1: Experimental design showing the control treatment (A) and the three temperature switch treatments (B-D). Gonadal phenotypes were determined using RNA-seq and histology (bold), histology only (normal text) and for a subset of the control samples, RNA-seq only (italic text). Abbreviations: dpo, days post oviposition; dps, days post switch. A mortality rate of 80% occurred in the late development switch following a down switch at stage 12 to 36°C to 28°.

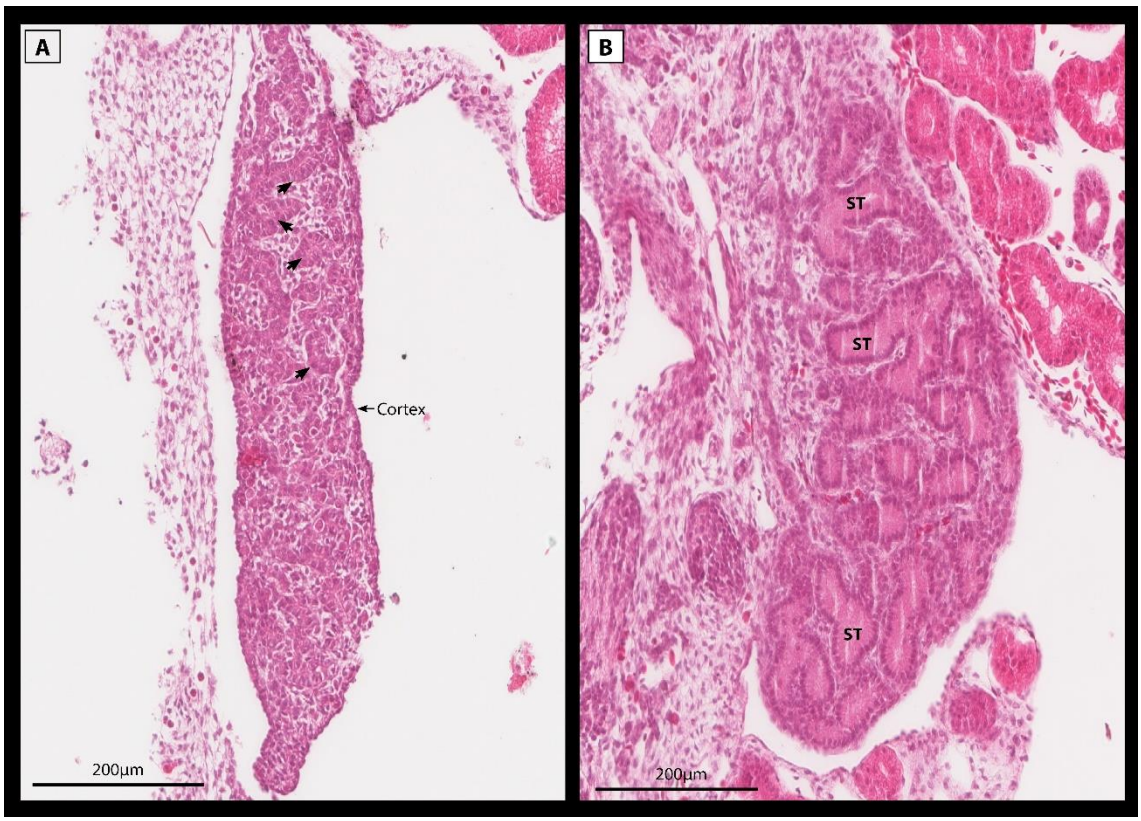

Figure 7.2: Sections of two stage 6 embryonic gonads from the same clutch with a testes-like phenotype (A) and normal testes (B). The testes-like phenotype was produced at 36°C, and is characterised by having an elongated shape typical of a bipotential gonad, with rudimentary seminiferous tubules typical of ovotestes (arrows), but having only a thin cortex layer. For comparison, a typical testes is displayed showing no cortex layer and well developed seminiferous tubules (ST).

7.3.1.2 Switch 1 (Stage 6)

The gonadal condition at stage 6, immediately before the switches from 28ºC to 36ºC (hereafter up-switched) and 36ºC to 28ºC (hereafter down-switched), was described under the control experiments. Embryos up-switched at stage 6 had ovotestes or testes by stage 9, and testes by stage 12. Thus, exposure to 28ºC for the period leading up to stage 6 was sufficient to irreversibly determine a male sexual fate, one that could not be reprogrammed by subsequent exposure to the sex reversing temperature of 36ºC.

Embryos down-switched at stage 6 had ovotestes or testes by stage 9 and testes by stage 12 (Figure 7.1b). This suggests that exposure to sex reversing temperature of 36ºC in the period leading up to stage 6 was not sufficient to irreversibly overcome the reprogramming of male sexual fate by subsequent exposure to 28ºC.

7.3.1.3 Switch 2 (Stage 9)

Embryos up-switched at stage 9 had ovotestes or testes by stage 12, maintained as testes to stage 15. Thus, exposure to 28^{o}C for the period leading up to stage 9 was, as expected from the results of Switch 1 experiments, sufficient to determine irreversible male sexual fate.

Embryos down-switched at stage 9 had ovotestes or ovaries by stage 12 and ovaries by stage 15 (Figure 7.1b). This suggests that exposure to sex reversing temperature of 36^{o}C in the period leading up to stage 9 was sufficient to irreversibly determine female fate, and overcome the programming of male sexual fate despite subsequent exposure to 28^{o}C.

7.3.1.4 Switch 3 (Stage 12)

In the context of the results of the above experiments, the results of the third switch experiment were expected (Figure 7.1c). The embryos up-switched at stage 12 had testes by stage 15, and those down-switched at stage 12 had ovaries by stage 15, though mortality was high in this latter experiment.

The broad interpretation of these results is that the default developmental program of sexual fate in ZZ individuals is male, as one would expect, and that sexual fate is more strongly influenced by the ZZ genotype than temperature. Indeed, early exposure to 28^{o}C in any of our experiments led to a male gonadal phenotype. Reprogramming of sexual fate under the influence of temperature was not observed until eggs were incubated at 36^{o}C to stage 9. The thermosensitive period for sex reversal thus begins after stage 6 and at or before stage 9.

7.3.2 Differential gene expression analysis

These data provide unique opportunities to compare combinations of developmental stage, temperature, and phenotype that are not normally possible. Principal component analysis (PCA) on normalised read counts detected an outliner sample (Figure 7.3a) that was removed from further analysis. As expected, based on the morphological characteristics of ovotestes, the samples with ovotestes were distributed between ovaries and testes along the PC2 (Figure 7.3b).

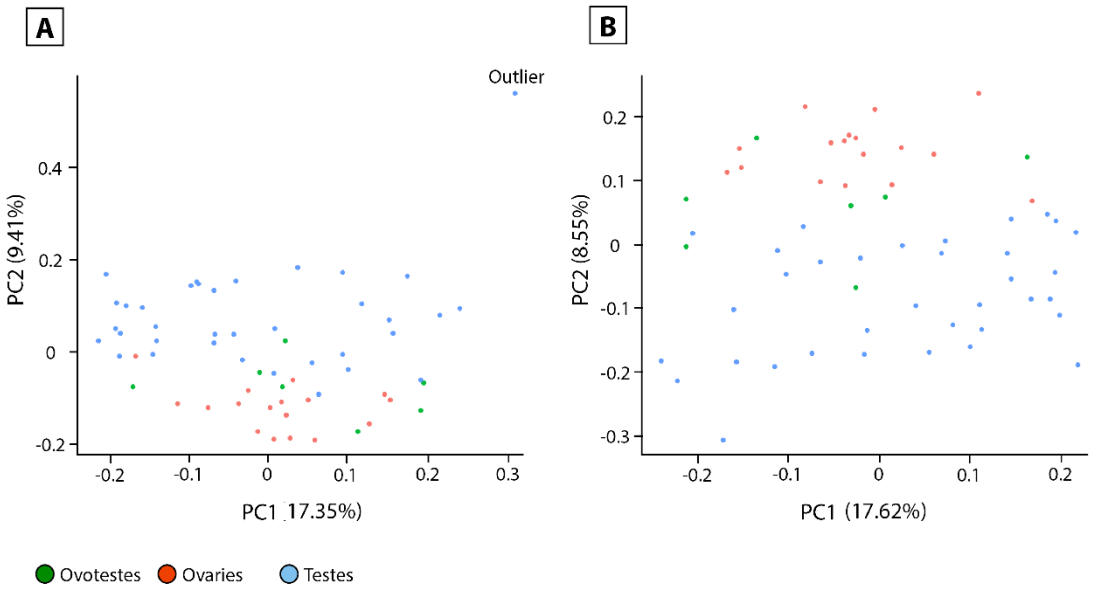

Figure 7.3: PCA plots for the complete dataset coloured by phenotype (A) and with an outlier sample (sample ID 3344zz_18_1_19) removed in panel B. The principle component analysis was conduced on normalised read counts.

7.3.2.1 Testis-like gonads vs testes (Stage 6)

In the switch 1 regime, differentially expressed genes between the testes-like gonads observed in 36°C embryos at stage 6 (control and switch experiments) compared with their 28°C incubated counterparts with normal testes, revealed genes that are associated with temperature at the same developmental stage, as well as the genes upregulated in the testes-like phenotype observed at 36°C (Supplementary File S7.1).

A variety of genes with sex-related functions are differentially expressed between the testes-like gonads and the normal testes. Gene Ontology (GO) terms enriched in testes-like gonads included RNA splicing, binding and processing, while genes upregulated in testes included regulation of developmental process and NADH dehydrogenase activity (Supplementary File S7.2). In the 28°C testes, a newly discovered testes-specific gene, *TEX33*, which is involved in spermatogenesis was upregulated [465]. *GCA* (grancalin) was also upregulated. Grancalin has previously been implicated in GSD female development in *P. vitticeps*, but the data here suggests a more generic role in reproduction that is not sex specific [54]. The testes-like gonads displayed upregulation of a mix of both male and female related genes compared to the testes. These included male associated genes *SLC26A8* (which was the most differentially expressed), *SRD5A1*,

and *SOX9*. In mammals, *SLC26A8* is required for proper sperm functioning [466]. *SRD5A1* catalyses testosterone into the more potent dihydrotestosterone, and *SOX9* is a canonical testes gene. At the same time, *WNT9a* was also upregulated, a gene in the *Wnt* signalling pathway associated with ovarian development. Also upregulated was *PIAS1*, a gene that can downregulate *SOX9* in mammals [467].

Various environmentally responsive genes were upregulated in the 36°C testes-like gonads. *CIRBP*, a gene associated with sex reversal in *P. vitticeps* and other TSD species, was upregulated. A member of the Jumonji family, *JMJD6*, which demethylates H3K4 and H3K36, was upregulated, as was *KDM4b*, which demethylates H3K9. Mitogen activated protein kinases, *MAP3K13, MAPKAPK5, MAPK1*, which mediate cell signalling pathways in response to environmental stress, were upregulated [468]. Other genes related to calcium and redox responses (CaRe) were also differentially expressed between the two groups. These included *MICU, GLRX2, TXNDC5, OXSR1, C2CD2*, and *PIDD1* [469].

7.3.2.2 Testes at 28°C vs testes at 36°C (Stage 12)

The early developmental switch regime produced testes at both 28°C and 36°C at stage 12. A suite of genes were differentially expressed between these two groups (Supplementary File S7.3). GO enrichment in 28°C testes included WNT signalling and terms relating to T cell function, while in 36°C testes GO terms involving ion channel activity were enriched (Supplementary File S7.4). In the 28°C testes, *POMC* was upregulated. This is an interesting result because in *P. vitticeps*, *POMC* upregulation has been previously associated with adult sex reversed females [55]. *CATSPER4* was highly upregulated in 28°C testes, and is associated with essential sperm functions. *RARG* a retinoic acid receptor that is normally associated with ovarian development [470] was also upregulated at 28°C, as was *GCA*, a gene previously associated with ZW female development in *P. vitticeps* [54]. Also upregulated were spliceosome genes *SNU13* and *PRPF38A* and DNA repair genes *SUMO2* and *UBE2N*. A suite of environmental stress genes was upregulated at 36°C. These included heat shock genes *DNAJB14* and *DNAJC13,* NF-kB and STAT pathway genes *RelB, IKBKE, and STAT6*, mitogen activated protein kinase *MAP3K13* and antioxidant regulator *TXNDC11* [365,471]. Well known chromatin remodelling genes *KDM6B* and *JARID2* were upregulated, as was *KATA2*, a lysine acetyltransferase . Calcium regulating genes T*RPV1, CACNB3, CADPS2* and *CABP1* were also upregulated in 36°C testes [370].

7.3.2.3 Testes at 28°C vs ovaries at 36°C (Stage 9)

In the mid development switch regime, at stage 9 ovaries (36°C) and testes (28°C) display sex specific expression (Supplementary File S7.5). In ovaries, aromatase, *CYP17A1*, *GATA2*, and *FOXL2* were upregulated, while in testes *SOX9, WIF1*, *HSD17B3, CYP26B1* were upregulated. However, genes normally associated with the opposite sex were also upregulated. At 28°C these included *FZD3, FRZB,* and *WNT6* which are associated with the *Wnt* and *Beta catenin* pathways [472,473]. In ovaries at 36°C, *SRD5A2*, a gene that converts testosterone to dihydrotestosterone[474], was upregulated. In the 36°C ovaries various CaRe related genes were upregulated, such as *CIRBP*, *TRPV1, JARID2*, *KDM6B*, *CACNA1I* and *CACNA1C*, *RALY*, *OSGIN1*, *DDIT4* and *GADD45A*. GO terms enriched in ovaries included system development, growth factor activity, and signal transduction (Supplementary file S7.6). Testes were enriched for GO terms such as calcium binding and Wnt-protein binding (Supplementary File S7.6). These results suggest that the underlying transcriptional profile can exhibit expression of genes associated with both sexes regardless of the phenotype. There are two possible explanations for this result; either some flexibility remains at the transcriptional level despite sex specific gonadal phenotypes, or gene expression may be able to change more rapidly than the cellular structures in the gonad.

7.3.3 Expression trends of temperature associated genes

The chromatin remodelling genes *JARID2* and *KDM6B,* and the temperature sensitive *CIRBP*, were highly expressed during sex reversal, and likely play an important role in initiating the female pathway [54]. Detailed analysis of the expression of these three genes showed they all exhibited similar expression patterns. *JARID2, KDM6B* and *CIRBP* all had higher expression at 36°C regardless of prior switch history, and expression decreased following up-switching. This suggests that these three genes are capable of rapid responses to environmental change. The opposite pattern occurs following up-switch, which caused an increase in expression. In all three genes there was considerable variation in expression levels between different individuals. Expression of these genes was significantly higher at 36°C compared to 28°C, but expression levels did not differ significantly between the three different phenotypes (ovaries, testes, and ovotestes).

KDM6B (Figure 7.4) exhibited the highest expression level in the switch 1 regime after the up-switching, where two ovotestes samples exhibited high expression levels at stage 9 following up-switching at stage 6. Interestingly, another two ovotestes from the same

regime had significantly lower expression, suggesting inter-individual variation in *KDM6B* expression changes in response to temperature.

KDM6B expression in switches between 28°C to 36°C for the three phenotypes (ovaries, testes, and ovotestes) was significantly higher at 36°C, but did not significantly differ between the phenotypes that were observed across the whole dataset. Taken together, these results suggests that *KDM6B* expression is sensitive to temperature and

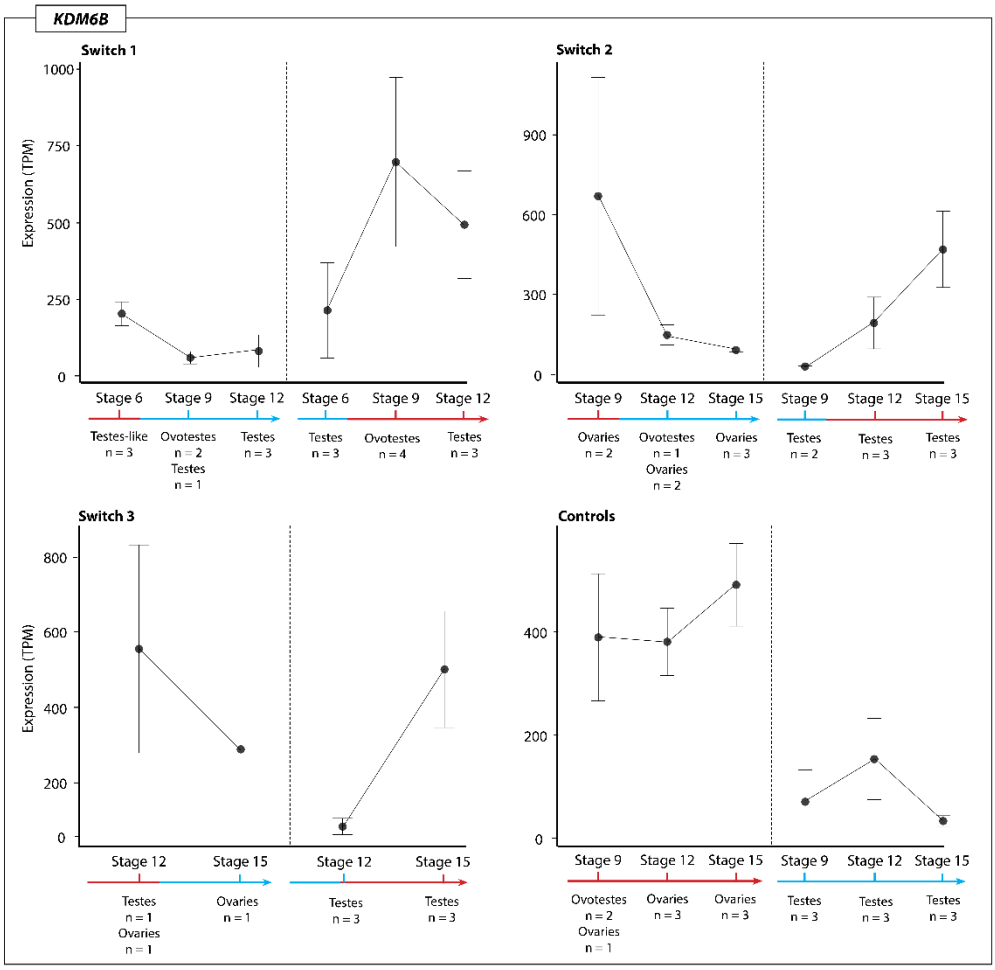

Figure 7.4: Expression (TPM, transcripts per million) of KDM6B for each temperature switch regime and controls groups at each sampling point regardless of phenotype. The variation in expression levels, mostly driven by the presence of different phenotypes, is reflected in the standard error bars.

increases expression in response to higher incubation temperatures. *JARID2* (Figure 7.5) exhibits similar patterns to *KDM6B*, though overall is more lowly expressed. Down-switching caused a decrease in *JARID2* expression, while up-switching caused increased expression. Compared to both *JARID2* and *KDM6B*, *CIRBP* was very highly expressed

under all temperature conditions, and showed the same tendency to increase following exposure to 36°C and decrease following exposure to 28°C (Figure 7.6).

7.3.4 Transcriptional Profile of Ovotestes

As expected based on previous research [8] conducted at constant incubation temperatures, ovotestes occurred at only at stage 9 in the 36°C control constant incubation temperature experiments. Temperature switching experiments did affect the frequency of

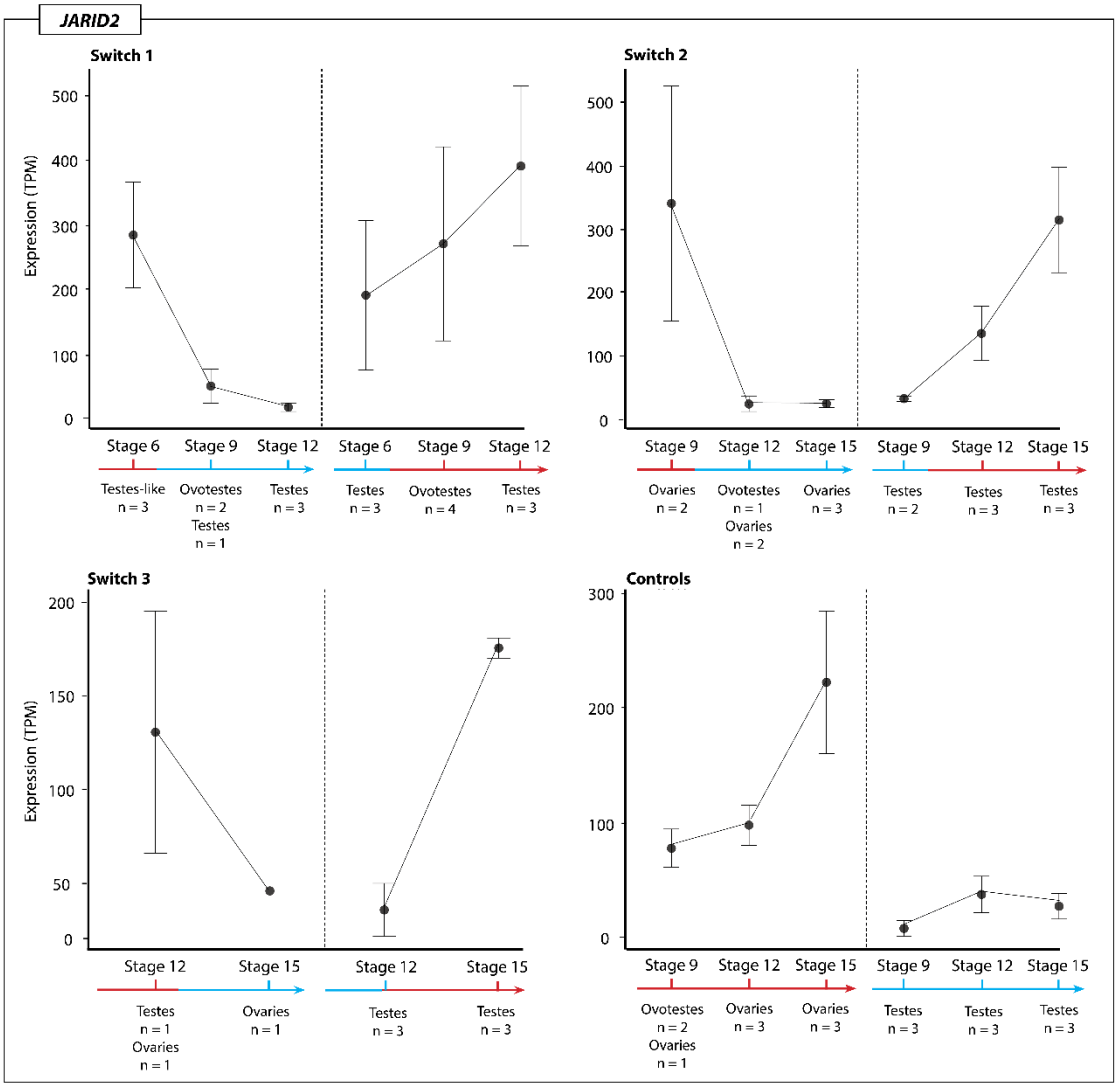

Figure 7.5: Expression (TPM, transcripts per million) of JARID2 for each temperature switch regime and controls groups at each sampling point regardless of phenotype. The variation in expression levels, mostly driven by the presence of different phenotypes, is reflected in the standard error bars.

observing ovotestes, and also affected when during development they were observed. Specifically, ovotestes were observed in stage 9 embryos immediately following early developmental switches, regardless of the direction of the change (up-switch n = 6, ovotestes, down-switch n= ovotestes; Figure 7.1b). Ovotestes were also observed in one stage 12 embryo individual subjected to a mid-development down-switch at stage 9 (Figure 7.1c).

7.3.4.1 Ovotestes at 36°C vs ovotestes at 28°C (Stage 9)

One hundred genes were upregulated in stage 9 ovotestes generated after down-switching at stage 6 compared with those produced after up-switching. Genes upregulated following down-switching included antioxidant gene *TXNDC5*, *NOVA1* and *PRPF31* associated

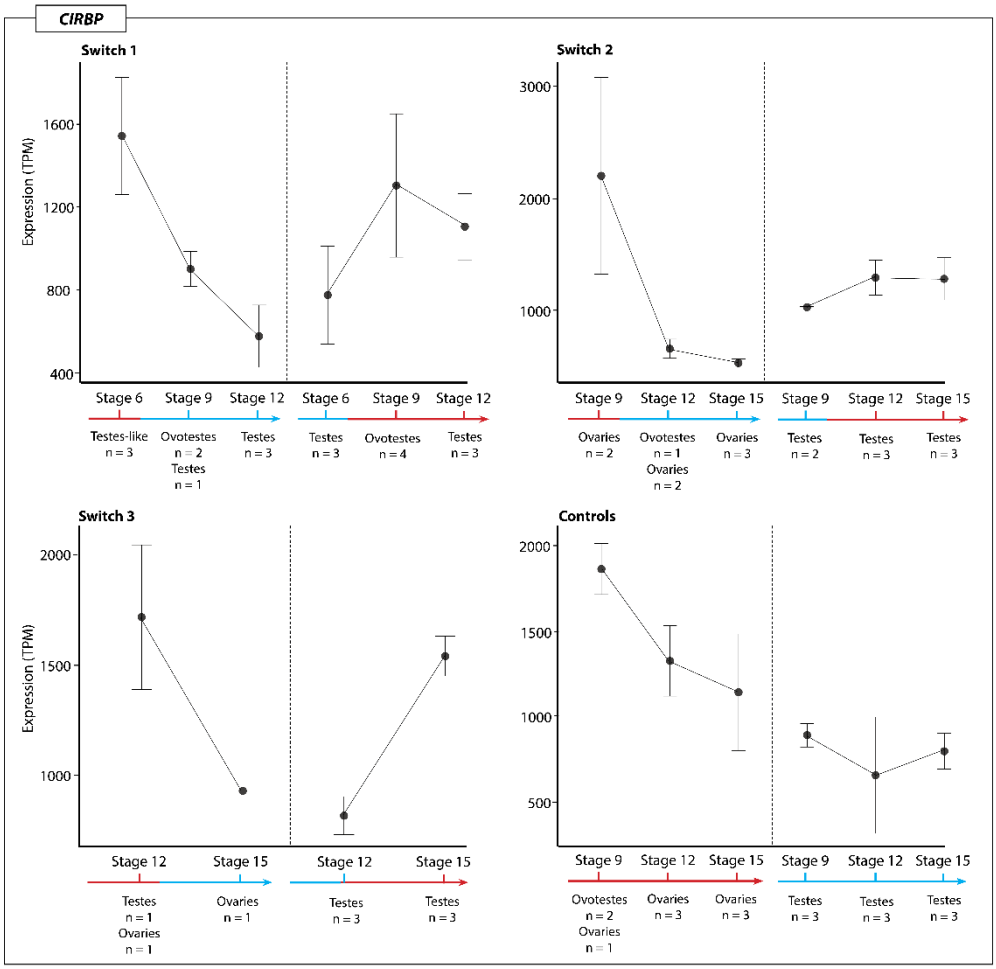

Figure 7.6: Expression (TPM, transcripts per million) of CIRBP for each temperature switch regime and controls groups at each sampling point regardless of phenotype. The variation in expression levels, mostly driven by the presence of different phenotypes, is reflected in the standard error bars.

with splicing regulation in mammalian systems, and *CTBP2* associated with sex reversal in humans. *GCA*, a gene previously associated with *Pogona* ZWf female development at 28°C [54], was also upregulated (Supplementary File S7.8). GO enrichment in the 28°C ovotestes involved terms related response to stress regulation of the immune response, and stimulus response (Supplementary File S7.9).

Fifty-two genes were upregulated in ovotestes generated after up-switching at stage 6. They included heat shock genes *DNAJB14* and *HSP90B1*, suggesting that switching to a high incubation temperature initiates the heat shock response. Also upregulated was *PDCD7*, a gene associated with splicing regulation and apoptosis, *RSF1* associated with chromatin remodelling and DNA repair, and a calcium signalling gene *CAMK2N1* (Supplementary File S7.8).

7.3.4.2 Control ovotestes vs stage 6 up-switched ovotestes (Stage 9)

The transcriptional profiles of ovotestes examined at stage 9 following up-switching at stage 6 were compared to those of ovotestes at stage 9 in the control experiments. Genes upregulated in the up-switched ovotestes included *CAMK2N1* and *ATP2A1* both associated with calcium regulation, *PAX8* associated with thyroid hormone signalling, *NOX4* which neutralises reactive oxygen species, and *PRKCZ* which regulates stress pathways in response to environmental stimuli. In the control ovotestes, the following were upregulated: (a) mitogen activated protein kinases *MAPKAP1* and *MAPK6*, (b) various circadian related genes including *RelB*, *CIPC* and *PER1*, (c) sex related genes *FZD5* (*Wnt* signalling), *CYP17A1* and *SHBG*, (d) inhibitor of the NF-κB pathway, *NFKBIE* and (e) *GADD45A*, an environmental stress response gene [360,365,475,476] (Supplemental File S10).

7.3.4.3 Stage 9 ovotestes vs stage 12 testes (36°C)

Comparison of ovotestes at stage 9 post-up-switch at stage 6 with the testes sampled later at stage 12 (switched at stage 6) can yield insights into the genes involved in resolving the gonad into testes rather than ovaries at the same incubation temperature (Supplementary File S7.11). Genes upregulated in stage 9 ovotestes included stress response genes *CRH*, *CHR2*, *STK24*, *GADD45A*, *GSTP1*, and *MSRB1*. Thermosensitive calcium channel *TRPM5* was upregulated, as was calcium signalling gene *CAMK2N1*.

Hormone related genes *CYP17A1, CYP19A1, DHRS3,* and *DHRS12* were upregulated. In the stage 12 testes produced after the temperature switch at stage 6, upregulated genes included various sex related genes including *HSD17B3, SHBG, SOX14, PAX7, FRZB,* and *WNT6*. Stress related genes were also upregulated including *DHRS7C, DNAJC11, HSPB2, PIDD1, DYRK3* and *TXNDC11*. Various calcium channels and sensors were upregulated including *CACNG1, CACNA1A, CCBE1,* and *CASQ1*.

7.3.4.4 Stage 9 ovotestes vs stage 9 ovaries (36°C)

Comparison of ovotestes at stage 9 post up-switch at stage 6 (early developmental switch regime) with ovaries at stage 9 at 36°C (mid developmental switch regime) can reveal the differences between the phenotypes at the same stage and temperature, including the influence of the temperature switch (Supplementary File S7.12). Genes upregulated in the pre-switch stage 9 ovaries included sex related genes *CYP17A1, SRD5A2, FZD1*, and *TDRP*, and stress related genes *ERO1B, OSGIN2, RRM2B*. Genes upregulated in ovotestes produced following up-switch, included *GCA,* circadian clock gene *CIART,* mitogen activated protein kinases *MAPK13* and *MAP3K9,* and thermosensitive calcium channel *TRPM3*.

7.3.4.5 Sex specific gene expression in ovotestes

When assessing the expression levels of sex specific genes (male associated genes *SOX9, AMH, NR5A1*, and female associated genes *CYP19A1, CYP17A1,* and *Beta-catenin),* considerable variation across individuals was apparent (Figure 7.8). For some genes, expression levels between individuals from the same switch regime, and even from within the same clutch, could be orders of magnitude different. For example, from the samples in the switch 1 regime, Sample B (sample ID 3603zz_18_1_7) expressed *SOX9* and *AMH* well above the mean, and well above that of its counterparts from the same clutch (Figure 7.8a). Sample B also had expression well above the mean for *SOX9,* but not for *NR5A1*. For *CYP19A1* and *CYP17A1,* expression was nearly 0, but then expression for *Beta-catenin* was above average (Figure 7.8b). This shows that an individual can radically differ in expression levels of genes compared to other individuals from the same clutch, including in expression levels of sex related genes.

The ovotestes phenotype appears to exist along a spectrum, where at one end they share more similarities with ovaries than testes, at the other they are more similar to testes

than ovaries, and in the mid-range they are a true intermediate between ovary and testis. This spectrum was evident in gene expression levels. It was also evident on histological examination in this study and previous experiments (Figure 7.7) [8].

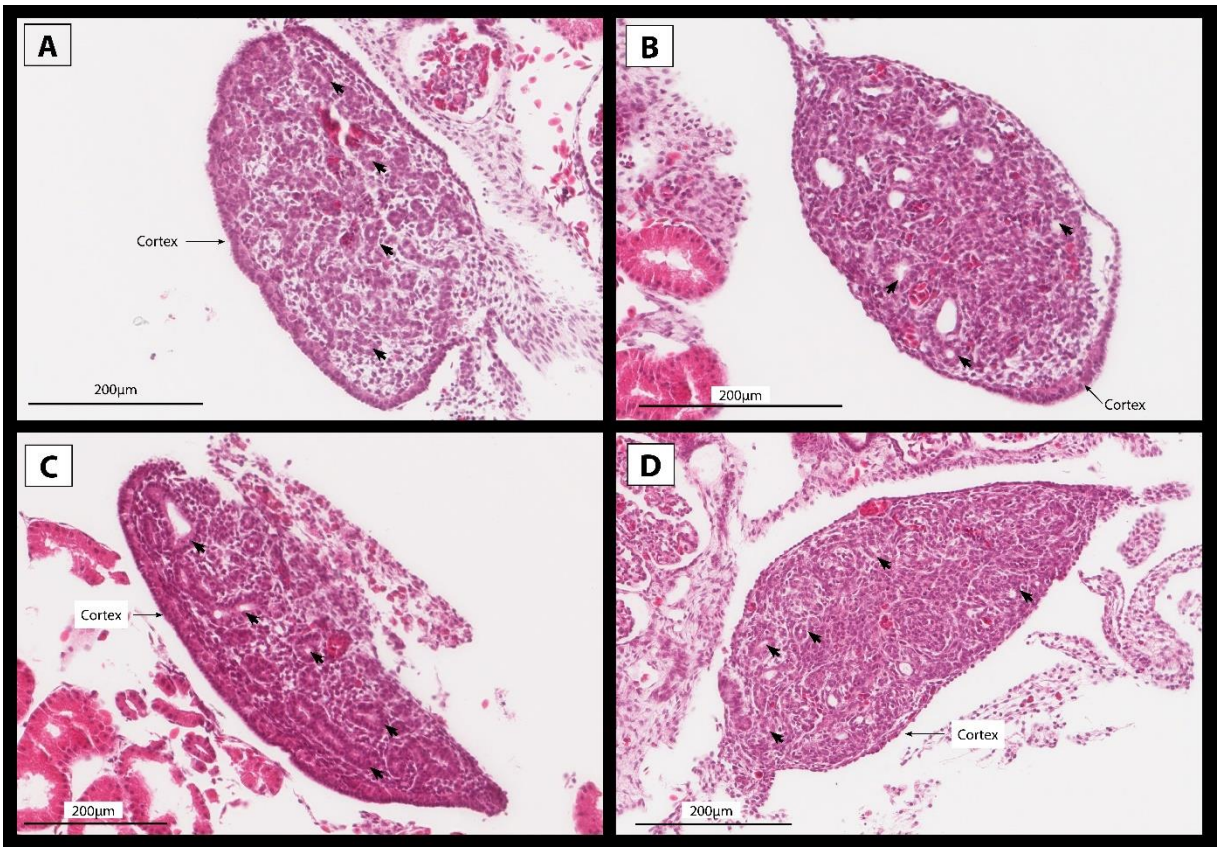

Figure 7.7: Histology sections of four individuals demonstrating the range of morphological characteristics that ovotestes can exhibit in embryonic *Pogona vitticeps*. Specimens in A and B have the most typical ovotestes phenotype where the cortex remains moderately thickened and rudimentary seminiferous tubules (indicated with arrows) dispersed throughout the medulla. The level of degeneration in the medulla varies, with specimen A showing more degradation than specimen B. Specimen C shows very pronounced characteristics of both sexes, having a thick cortex and well--formed seminiferous tubules. Specimen D possess a very thin cortex and a disorganised medulla with spare seminiferous tubules.

7.3.4.6 Temperature associated gene expression in ovotestes

Examination of the expression levels of genes associated with temperature response (*KDM6B, JARID2, CIRBP* and *CLK4*) reveal similar inter-individual variation occurred as in the expression of sex associated genes (Figure 7.9). *CIRBP* exhibited the highest expression levels, and the greatest variation in expression. For example, in the stage 9 samples up-switched at stage 6, expression of *CIRBP* was several orders of magnitude

different between individuals, ranging from 500 to over 2000 transcripts per million 9. Sample E was the only individual to have above average expression for these four genes.

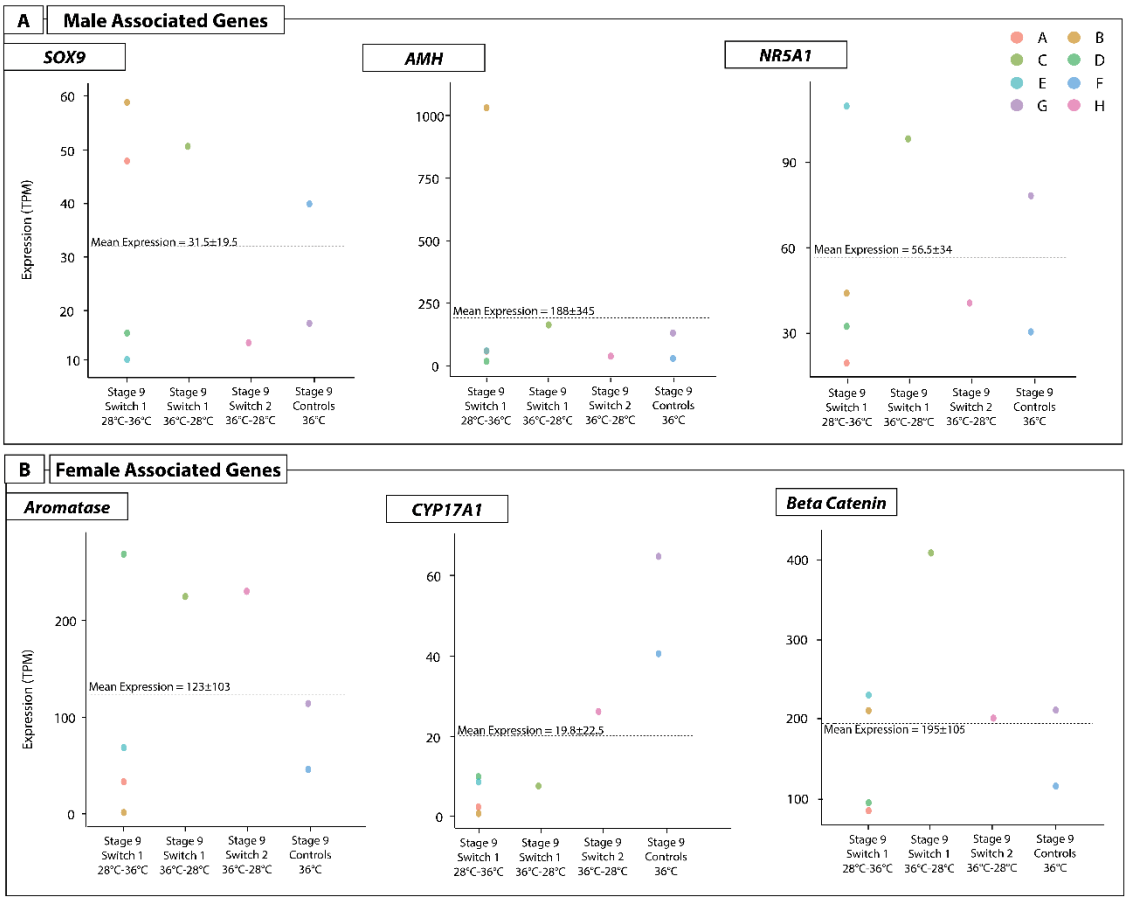

Figure 7.8: Expression (TPM, transcripts per million) of three male and three female sex-associated genes for all samples with ovotestes produced from different switching conditions (x-axis). Each point represents an individual (by colour) to depict the range of expression values different individuals can exhibit for a given gene. Sample IDs correspond to those provided in Supplementary File S7.13, and are as follows: A) 3603zz_18_1_4, B) 3603zz_18_1_7, C) 3603zz_18_1_8, D) 3603zz_18_2_4, E) 3632zz_18_2_9, F) 3632zz_18_2_19, G) 3632zz_18_2_20, H) 3232zz_18_1_19.

Inter-individual variation may be explained by differing responses to temperature switches relating to an individual's sensitivity to the environment. This certainly is likely playing a role in the patterns observed in the expression of these genes, as not all individuals respond to the treatments in the same way. These results are also likely influenced by the inter-individual variation in the cellular makeup of ovotestes.

7.3.5 Genes uniquely associated with ovotestes

In order to better understand the unique transcriptional profiles of ovotestes, differential gene expression analysis was conducted between ovotestes produced at stage 9 up-switched at stage 6 and the ovotestes from the 36°C controls, and control testes and

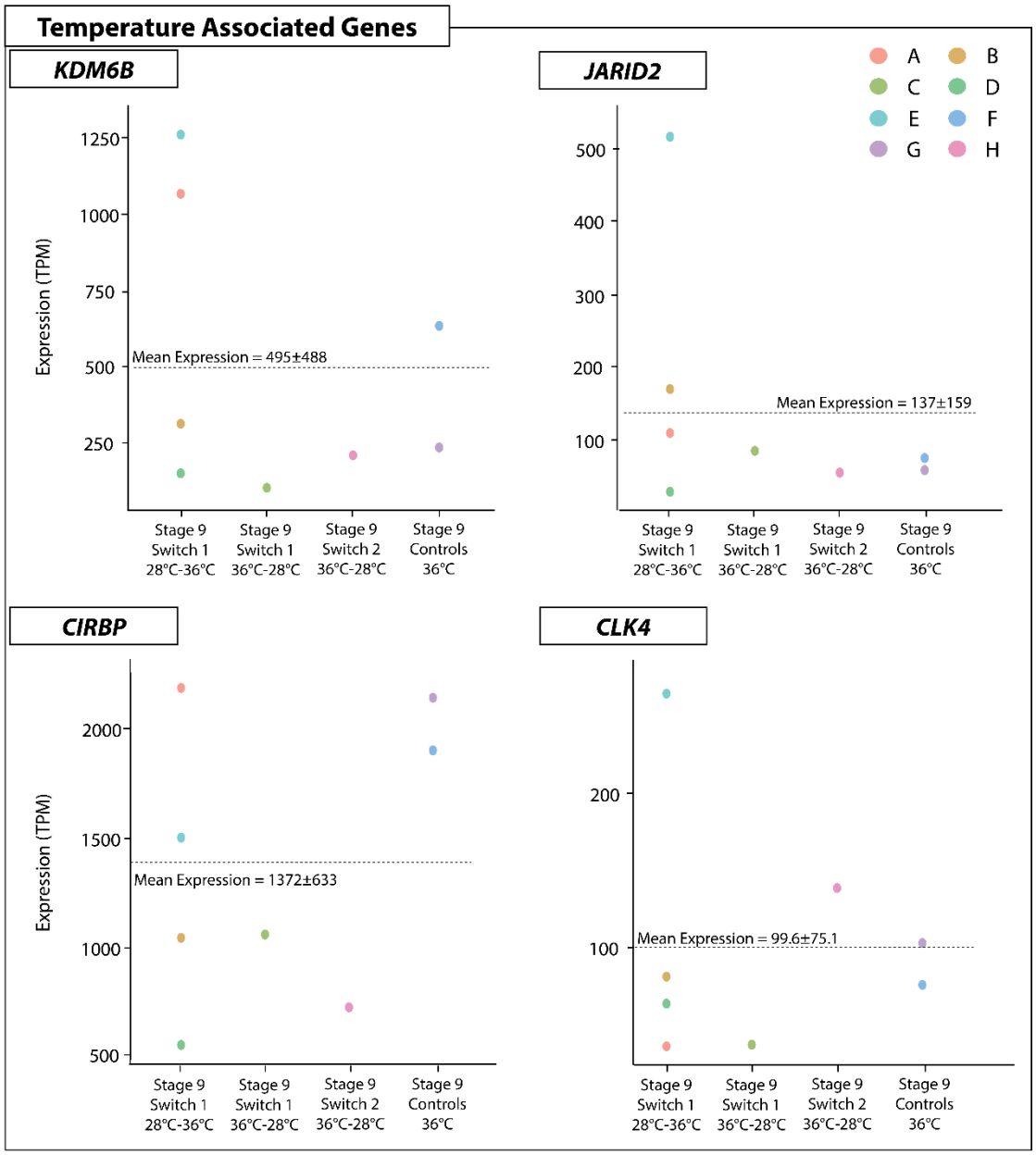

Figure 7.9: Expression (TPM, transcripts per million) of four temperature associated genes for all samples with ovotestes produced from different switching conditions (x-axis). Each point represents an individual (by colour) to depict the range of expression values different individuals can exhibit for a given gene. Sample IDs correspond to those provided in Supplementary File S7.13, and are as follows: A) 3603zz_18_1_4, B) 3603zz_18_1_7, C)

3603zz_18_1_8, D) 3603zz_18_2_4, E) 3632zz_18_2_9, F) 3632zz_18_2_19, G) 3632zz_18_2_20, H) 3232zz_18_1_19.

ovaries both at stage 9. Ovaries from the control incubations were grouped with pre-switch ovaries at stage 9 from the mid developmental switch regime. The differentially expressed genes between ovotestes and testes, and ovotestes and ovaries can reveal the differences between the phenotypes, and provide clues to which phenotype the ovotestes more closely resemble, and where on the spectrum they lie. Then by taking the genes upregulated in ovotestes from both datasets it is possible to determine genes that are uniquely associated with ovotestes, and not with either testes or ovaries.

7.3.5.1 Differential gene expression between ovotestes, and ovaries and testes

There were many more genes differentially expressed between testes and ovotestes (not including testis like ovotestes) than there were between ovaries and ovotestes, suggesting that the expression profiles of ovotestes are typically more similar to ovaries than they are to testes. A total of 579 genes were upregulated in testes compared with ovotestes, and 557 in ovotestes compared with testes (Supplementary File S7.13). GO terms enriched for testes included calcium ion binding and response to endoplasmic reticulum stress, while GO enrichment in ovotestes included regulation of hormone levels, signal transduction and the STAT cascade (Supplementary File S7.14). Whereas 132 genes were upregulated in ovaries compared with ovotestes, and 97 were upregulated in ovotestes compared with ovaries (Supplementary File S7.15).

A large number of genes were differentially expressed between ovotestes and testes. Various male specific genes were upregulated in testes compared with ovotestes, including *GHRH, AMH, DMRT1, HSD17B3, WIF1, SFRP2, WNT6, FZD6, FRZB, DLK2,* and *WLS.* In ovotestes, female related genes *CYP17A1 and CYP19A1* were upregulated, as was *STAR, FZD4, PGR, DHRS3, SOX4, SOX12, and GATA2.* Two TRP channels were differentially expressed between testes and ovotestes. *TRPV4* was upregulated in testes, whereas *TRPV1* was upregulated in ovotestes. These two genes have high sequence similarity and are highly sensitive to temperature [120]. A variety of stress response genes were differentially expressed between testes and ovotestes. Genes upregulated in testes included heat shock genes *HSPB2, DNAJB11, DNAJC15* and *DNAJB9,* antioxidant genes

TXNDC5, *PRDX4*, and *SOD2*. In ovotestes, *CLK4*, a temperature sensitive splicing regulator, was upregulated alongside *STAT2* and *JAK3*, components of the *JAK-STAT* pathway, *RELA* and *IKBKE* which are part of the NF-kB pathway, as well as *JARID2* and *KDM6B*, chromatin remodelling genes associated with sex reversal and TSD. *CRH*, a gene involved in the hormonal stress response, and previously associated with sex reversal in adults [55], was also upregulated.

Far fewer genes were differentially expressed between ovaries and ovotestes than testes and ovotestes. Genes of note upregulated in ovaries cf ovotestes included antioxidant gene *TXNDC5*, which was also upregulated in testes cf ovotestes, oxidative stress gene *OSGIN1*, and splicing regulator *NOVA1*. In ovotestes, another member of the same lysine demethylase family as *KDM6B*, *KDM5C*, was upregulated in comparison with ovaries, as was a different TRP channel, *TRPM3*. Oxidative stress genes *SQOR* and *GADD45G* were also upregulated cf ovaries. Unlike what was observed in the differential expression analysis between ovotestes and testes, no sex related genes were differentially expressed between ovaries and ovotestes. This implies that the transcriptional profiles of ovotestes are more similar to ovaries than to testes, despite the propensity for these gonads to differentiate as testes later in development following exposure to the same temperature regimes that produced these ovotestes.

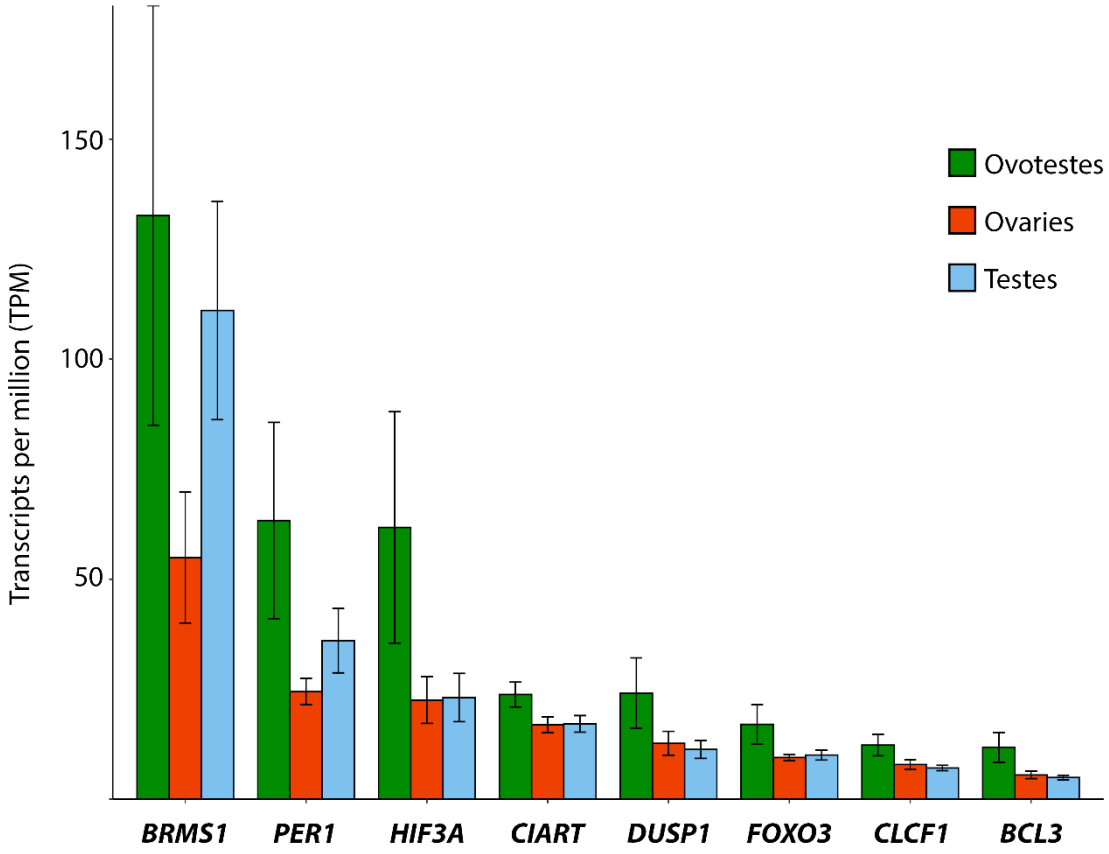

Figure 7.10: Expression (transcripts per million, TPM) for a subset of genes uniquely upregulated in ovotestes mentioned in the text. For the full list of genes see supplementary file S7.10.

7.3.5.2 Genes uniquely upregulated in ovotestes compared with ovaries and testes

Of the 689 genes upregulated in ovotestes across both datasets, 36 genes were uniquely upregulated in ovotestes when compared with both ovaries and testes (Supplementary File S7.16). Within the 36 genes uniquely upregulated in ovotestes cf both testes and ovaries (Figure 7.10), are two circadian rhythm genes, *PER1* and *CIART*. Both genes are circadian pacemakers in the mammalian brain, and are transcribed in a cyclical pattern in the suprachiasmatic nucleus [477–479]. Other organs in the body have peripheral circadian clocks, including mammalian ovaries, where *PER1* expression cycles during a 24h period in the steroidogenic cells [475]. However, mammalian testes do not appear to possess a peripheral clock, and *PER1* expression appears to be developmental only [475,480]. *CIART* has no described role in the gonads. It has previously been shown to be upregulated in the brains adult sex reversed female *P. vitticeps* [55]. An experiment assessing thermal adaptation in three Anole species found that both *PER1* and *CIART* were upregulated in brain in response to temperature [188]. The role these genes may play, or the influence circadian oscillations may have more broadly, in *P. vitticeps* ovotestes is unknown and requires further investigation.

Various genes associated with environmental stress pathways were uniquely upregulated in ovotestes. These included NF-kB pathway regulators *BCL3* and *BRMS1*, *JAK-STAT* pathway activator *CLCF1*, and *DUPS1* which regulates a MAP/ERK pathway. Also upregulated were the environmental stress genes *FOXO3* and *HIF3A.* Upregulation of these types of genes is to be expected at high incubation temperatures, however they were not differentially expressed in ovaries from the same temperature, suggesting they play a unique role in ovotestes.

7.4 Discussion

Taken together, these findings reveal the complex effects of temperature on both gonadal morphology and gene expression in *P. vitticeps* during embryonic development. This

study presents a novel approach that provides data revealing new insights into temperature responses in *P. vitticeps*, but that also has implications for vertebrates more broadly. By combining gonad histology with matched transcriptomes, this is the first study to our knowledge to sequence reptile ovotestes, and to be able to analyse gene expression profiles with validated morphology. These findings also provide new evidence supporting the role of CaRe mechanisms in sensing and transducing temperature cues in sex determination cascades.

The gonadal phenotypes produced by temperature switches at different developmental stages revealed that the gonads are responsive to temperature at stage 6, but are insensitive to temperature shifts by stage 9. The results from the early developmental switches suggest that a thermal signal of considerable strength is required to override male development and cause sex reversal. The testes-like phenotypes observed in the stage 6 samples at 36°C also suggests a propensity for male-ness even in the absence of exposure to 28°C. These results suggest, as has previously been hypothesised, that male development can be considered as the developmental default for *P. vitticeps* [8]. Thus understanding sex reversal as a process by which the male pathway must be actively repressed or overridden by the female pathway can help explain why even short exposure to the male producing temperature can be sufficient to cause testes differentiation. This may also explain instances where sex reversal does not occur at high temperatures ("resistance" to reversal). In these individuals there may be differences in temperature sensitivity and/or the threshold of expression required to initiate sex reversal, be that repression of male genes, activation of female genes, or both (Figure 7.11).

Interesting parallels can be drawn between sex reversal in embryonic *P. vitticeps*, and female to male sex change in adult bluehead wrasse (*Thalassoma bifasciatum*). In this species, it has been shown that epigenetic reprogramming driven by environmental stress involves repression of female gene aromatase and upregulation of male genes like *amh, cp11c1* and *hsd11b2* [149]. Ultimately the female gene networks are completely repressed, and via upregulation of male genes the gonads transform from ovaries to testes. Although sex reversal in reptiles is unlikely to be mediated by stress hormones as it is in fish [53,481], there are clear similarities in the transcriptional changes that underpin the transition from one sex to the other.

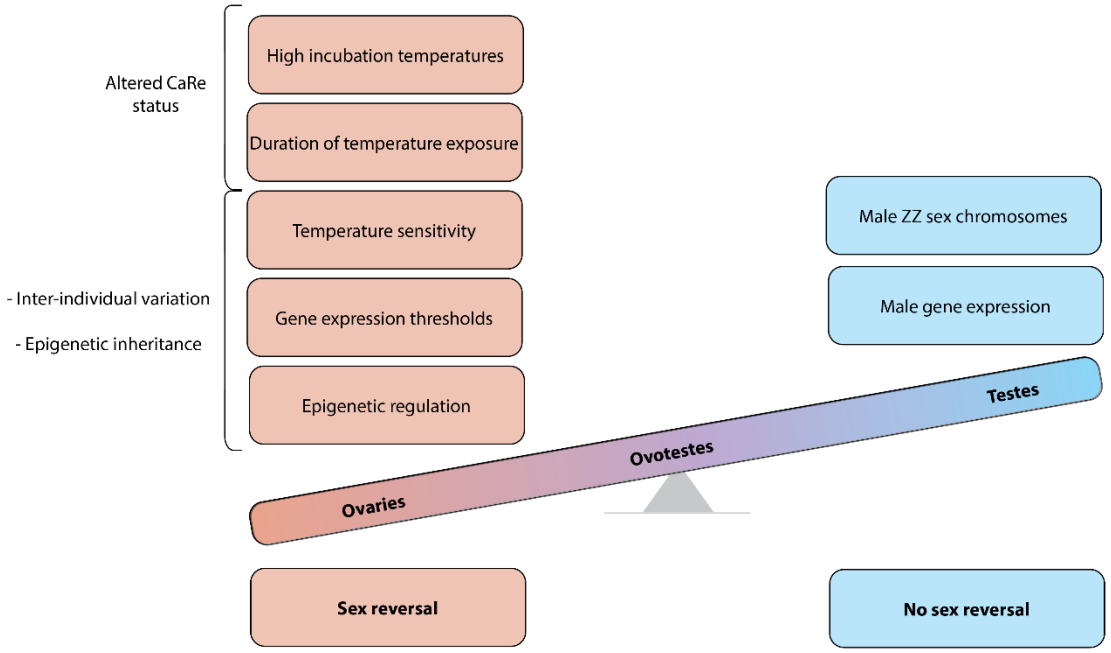

Figure 7.11: Schematic representation of the "threshold model" of sex reversal illustrating the many factors involved in initiating and maintaining sex reversal compared with male development. While male development readily progresses due to the presence of male sex chromosomes and the expression of male specific genes, the initiation of sex reversal relies on the compounding influence of many factors. Ovotestes are produced as an intermediate phenotype due to the competing influences of male and female sex determination pathways.

The transcriptomes of ovotestes show that like what is observed morphologically, ovotestes do indeed exhibit a mixed expression profile of both male and female specific genes. We further showed that there is considerable inter-individual variation in the expression profiles of ovotestes, such that they exist along a spectrum of male-ness to female-ness. This is also reflected in the phenotypes; some individuals may possess more obviously differentiated seminiferous tubules than others, or a thicker cortex with less well formed tubules. The transcriptional profile of ovotestes was found to have 36 unique genes with a variety of functions. Most are not normally associated with gonadal development or function, so require further study to understand the role the may play in sex reversal. None of these 36 genes have previously been associated with TSD in reptiles, or other ESD systems in different vertebrate groups. Due to a lack of research in this area, it is currently unclear whether this is because these genes are unique to the ovotestes phenotype, or if they may be more commonly associated with ESD systems in different species that have not yet been studied. This provides an important foundation for future research, as new species with sex reversal will likely be uncovered [482].

Analysis of gene expression changes following temperature switches showed in many cases there was expression of genes associated with the sex opposite to that seen morphologically in the same individual. This implies there may be delayed upregulation of genes from the opposite sex following a temperature switch to the opposite temperature, which is not reflected in the phenotype. This adds further weight to the hypothesis that various thresholds (temperature exposure, duration of exposure to that temperature, sensitivity to these changes, sufficiently high levels of female gene expression and/or sufficiently low levels of male gene expression) need to be surpassed for sex reversal to occur. The understanding provided by the CaRe model implies that an additional threshold may be the number of environmentally sensitive pathways that are activated by high incubation temperatures [53].

A threshold-based understanding can explain some of the observed characteristics of sex reversal. This includes how rates of sex reversal increase as temperature increases: the more extreme the temperature, the more likely it is for everything to be pushed above these thresholds. Epigenetic inheritance, or genetic variants influencing these thresholds can also explain how the offspring of sex reversed mothers reverse more readily that those produced from normal mothers. It is likely that heritable epigenetic elements of sex reversal causes increased sensitivity to temperature and/or a lowering of the various thresholds required for sex reversal.

This threshold hypothesis also implies that sex reversal is inherently difficult to produce, as a variety of molecular hurdles need to be cleared in order for sex reversal to be initiated and maintained (Figure 7.11). If this is indeed the case, why then does sex reversal occur at all? Current understanding of ESD systems, and in particular TSD, states that there must be fitness differences between the sexes under different environmental conditions to drive the evolution of these systems. In the case of *P. vitticeps*, additional complexity is introduced by the presence of sex chromosomes, as well as interaction with incubation temperature via epigenetic mechanisms and/or genetic variants influencing sex determination. Studies on wild populations of *P. vitticeps* have shown that sex reversal is not widespread, occurring in specific areas which do not experience the hottest temperatures [78]. As has been hypothesised, this implies that local adaptation can occur, limiting the rates of sex reversal, perhaps conferring a selective benefit by ensuring the W chromosome is maintained in the population [52].

The data provided by our study has given new understanding to the influences of temperature on sex determination and differentiation in *P. vitticeps*, and also lays an important foundation upon which future work can be built. The unique combination of temperature switching with gonad morphology and gene expression analysis, has provided new insights into not only the complex effects of temperature on sex determination and differentiation in *P. vitticeps*. The results from this study also have implications for understanding environmentally sensitive sex determination systems in other vertebrate species more broadly. Ultimately, the more research that is conducted into ESD systems, more questions and curiosities are uncovered, but we continue to move closer to a more complete understanding of the interactions between sex and temperature in environmentally sensitive species.

7.5 Materials and Methods

7.5.1 Egg incubation and experimental design

Eggs were obtained from the University of Canberra breeding colony during the 2018-19 breeding season in accordance with approved animal ethics procedures (Project 270). Breeding groups comprised of three sex reversed ZZf females to one male, providing some control over the effects of male genotype. Sex reversal was validated using standard genotyping procedures [3], and phenotype and reproductive output. Females were allowed to lay naturally, and eggs were collected at lay or within two hours of lay. Following inspection for egg viability (presence of vasculature inside the eggshell), eggs were incubated in temperature-controlled incubator (±1°C) on damp vermiculite (four parts water to five parts water by weight).

Eggs from clutches of ZZf mothers were randomly split between 36°C and 28°C incubation temperatures, and then assigned randomly to one of four experimental regimes. For the offspring of sex reversed ZZf females, 36°C produces 100% females, and 28°C produces 100% males [3]. For Switch 1, a subset of eggs were sampled at stage 6 from both incubation temperatures, and the remaining eggs were switched to the opposite incubation temperature, and sampled post-switch at stage 9 and 12. For Switch 2, a subset of eggs were sampled at stage 9 from both incubation temperatures, the remaining eggs switched to the opposite incubation temperature, and sampled post-switch at stage 12 and 15. For Switch 3, a subset of eggs were sampled at stage 12 from both

incubation temperatures, the remaining eggs were switched to the opposite incubation temperature, and sampled post-switch at stage 15. Additional controls were incubated at constant temperatures (either 36°C or 28°C) and sampled at each of stage 9, 12, and 15 (Figure 7.1). All embryos were staged according to the system developed for *P. vitticeps* in order to target particular developmental stages of interest [7,8]. These developmental stages were selected based on previous research characterising gonadal development during sex reversal in *P. vitticeps* [8]. At stage 6 the gonads are bipotential, and stage 9 is a period of developmental antagonism frequently characterised by the presence of ovotestes. Gonad differentiation occurs during stage 12, and by stage 15 the gonads have completely differentiated. Final sample sizes are given in Figure 7.1 and Supplementary File S7.17.

Embryos were sampled at the targeted developmental stages, taking into account differing developmental rates at the two incubation temperatures. Embryos were euthanised via intracranial injection of sodium pentobarbitone (60mg/ml in isotonic saline). For each embryo, one whole gonad was dissected from the surrounding mesonephros and snap frozen in liquid nitrogen for sequencing. The other whole gonad and mesonephros was dissected and preserved in neutral buffered formalin for histological processing. This design matches the phenotypic and genotypic data for each individual. This was also used to validate which samples possessed ovotestes prior to sequencing at stage 9, as ovotestes frequency is not 100%.

7.5.2 Histology

Samples were processed for histology following procedures previously used in *P. vitticeps* described in [8]. Briefly, samples were preserved in neutral buffered formalin before being transferred to 70% ethanol to improve tissue stability. All tissue processing was conducted at the University of Queensland's School of Biomedical Sciences Histology facility. Samples were dehydrated, embedded in wax, and sectioned 6µm thick. Slides were stained using hematoxylin and eosin. The slides were scanned at 20x using the Aperio slide scanning system, and visualised using the Leica ImageScope program. Gonadal phenotypes were characterised using standard characteristics previously used for the species, and that are common to vertebrate gonads [8]. For samples collected at stage 9, ovotestes phenotype was confirmed prior to sequencing.

7.5.3 RNA extraction and sequencing

RNA from the isolated gonadal tissues was extracted in randomised batches using the Qiagen RNeasy Micro Kit (cat. No. 74004) according to manufacturer protocols. RNA was eluted in 14µl of RNAase free water and frozen at -80°C prior to sequencing. All samples were prepared for sequencing at the Australian Genome Research Facility (Melbourne, Australia). Sequencing libraries were prepared in randomised batch, and sequenced using the Novaseq 6000 platform (Illumina).

7.5.4 Expression profiling and differential gene expression analysis

Paired-end RNA-seq libraries (.fastq format) were prepared using the sample pipeline that was established previously for *P. vitticeps* [54]. Briefly, libraries were trimmed using trim_galore with default setting, and then aligned with the *P. vitticeps* reference NCBI genome using STAR. PCR duplicates and non-unique alignments were removed using samtools. Gene expression counts and normalised gene expression (transcripts per million, TPM) were determined using RSEM. Raw count and TPM files are provided (Supplementary File S7.18 and S7.19 respectively). Sample metadata is provided in Supplementary File S7.17.

Differential gene expression analysis was conducted on raw count data using EdgeR. One sample identified as an outlier following PCA analysis was removed from the dataset (Figure 7.3). Genes with fewer than 10 counts across three samples were removed as lowly expressed. Samples were grouped according to their position in the experimental design (samples from the first switch regime at 36°C sampled at stage 6 was the first group, and so on. See Figure 7.1). Samples were also grouped according to temperature and phenotype. Full details of the EdgeR parameters used are described in [54]. A p-value cut-off of ≤ 0.01 and a $\log_2$ fold-change threshold of 1 or -1 was applied to all contrasts. To determine genes uniquely expressed in ovotestes, samples from different groups at stage 9 were combined to increase sample sizes. The ovotestes samples included those produced from the control incubations at 36°C and from the switch 1 regime (switched from 28°C to 36°C at stage 6, sampled at stage 9). Stage 9 ovaries were combined from the control incubations, and from the pre-switch stage 9 sampling at 36°C

in the second switch regime. Stage 9 testes were combined between the control 28°C and pre-switch stage 9 samples from the second switch regime.

Gene ontology (GO) analysis was conducted for sets of differentially expressed genes, where enough genes were differentially expressed between the two groups to return significantly enriched terms [432,433]. The filtered count data file (17,075 genes) was used as the background gene set, and a P-value threshold of 10^{-3} was used.

7.5.5 Supplementary Figures

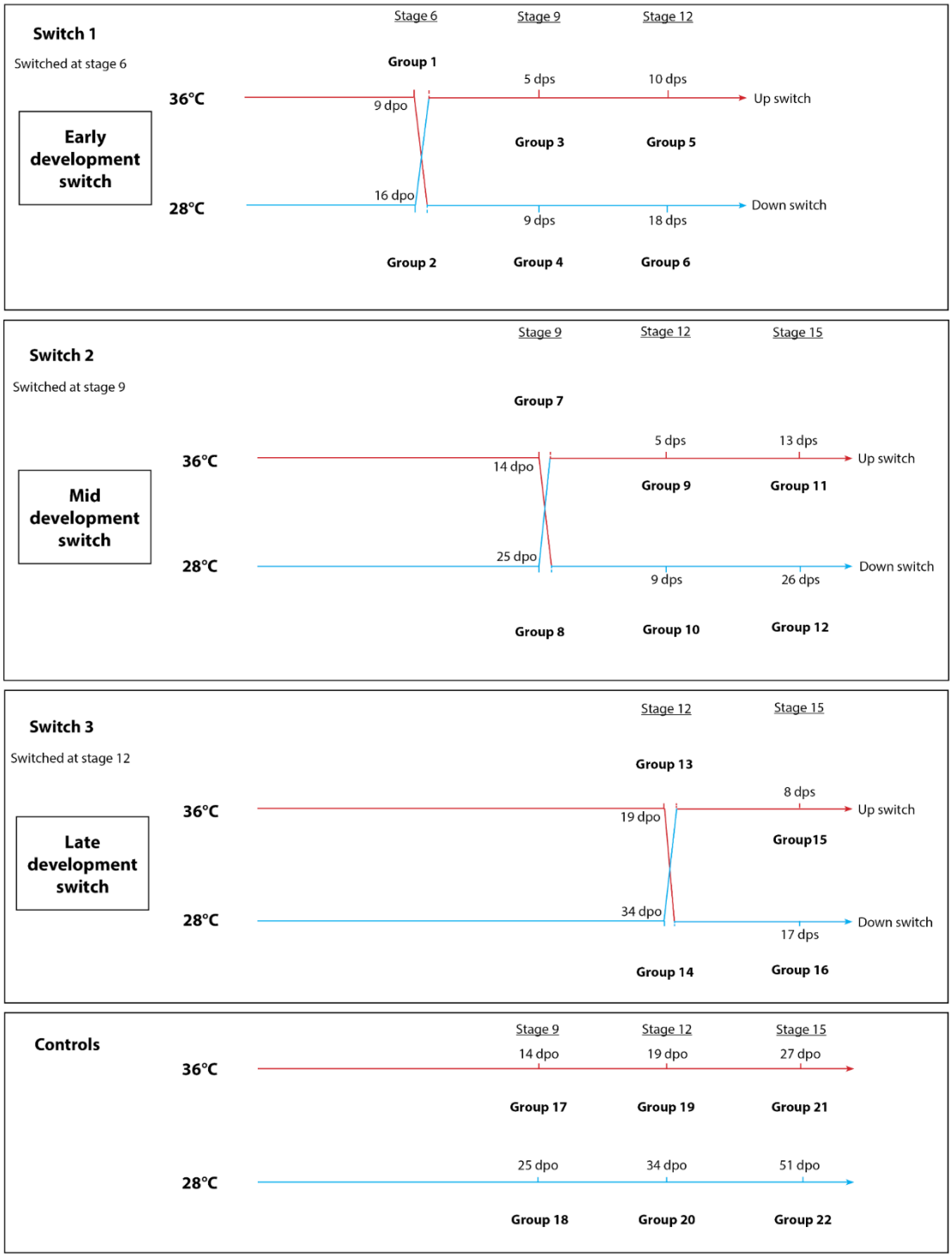

Figure 7.12: Experimental design with numbered groups denoted that match with data provided in Supplementary File S7.17.

7.5.6 Supplementary Materials

Supplementary files are available for download from https://datadryad.org/stash/share/tbDhOU4_FTKWfb75TMXLXOqlPTuomzQSVQoMdIZekvg.

Supplementary File S7.1: Genes differentially expressed between testes-like gonads at 36°C and testes at 28°C from the early developmental switch regime sampled at stage 6. A log-fold change cut-off of -1 to 1 and P-value cut-off of 0.01 was applied. The "direction" column indicates genes that were upregulated in the testes-like gonads compared with testes (negative log-fold changes), and those that were upregulated in the testes compared with testes-like gonads (positive log-fold changes).

Supplementary File S7.2: Gene ontology (GO) enrichment for process and function (denoted in GO Type column) for genes differentially expressed between testes and testes-like gonads (denoted in Phenotype column). Outputs were generated by GOrilla at a significance threshold of $P \leq 0.05$.

Supplementary File S7.3: Genes differentially expressed between the testes at 36°C and testes at 28°C from the early developmental switch regime sampled at stage 12. A log-fold change cut-off of -1 to 1 and P-value cut-off of 0.01 was applied. The "direction" column indicates genes that were upregulated in the 28°C testes compared with 36°C testes (negative log-fold changes), and those that were upregulated in the 36°C testes compared with 28°C testes (positive log-fold changes).

Supplementary File S7.4: Gene ontology (GO) enrichment for process and function (denoted in GO Type column) for genes differentially expressed between 36°C testes and 28°C testes (denoted in Phenotype column). Outputs were generated by GOrilla at a significance threshold of $P \leq 0.05$.

Supplementary File S7.5: Genes differentially expressed between the testes at 28°C and ovaries at 36°C from the mid developmental switch regime sampled at stage 9. A log-fold change cut-off of -1 to 1 and P-value cut-off of 0.01 was applied. The "direction" column indicates genes that were upregulated in the 28°C testes compared with 36°C

ovaries (negative log-fold changes), and those that were upregulated in the 36°C ovaries compared with 28°C testes (positive log-fold changes).

Supplementary File S7.6: Gene ontology (GO) enrichment for process and function (denoted in GO Type column) for genes differentially expressed between testes and ovaries (denoted in Phenotype column). Outputs were generated by GOrilla at a significance threshold of $P \leq 0.05$.

Supplementary File S7.7: Genes differentially expressed between stage 9 up-switched ovotestes (early developmental switch regime) and stage 9 pre-switch ovaries at 36°C (mid developmental switch regime). A log-fold change cut-off of -1 to 1 and P-value cut-off of 0.01 was applied. The "direction" column indicates genes that were upregulated in the ovaries compared with ovotestes (negative log-fold changes), and those that were upregulated in ovotestes compared with ovaries (positive log-fold changes).

Supplementary File S7.8: Genes differentially expressed between ovotestes at 28°C and ovotestes at 36°C from the early developmental switch regime sampled at stage 9. A log-fold change cut-off of -1 to 1 and P-value cut-off of 0.01 was applied. The "direction" column indicates genes that were upregulated in the 36°C ovotestes compared with 28°C ovotestes (negative log-fold changes), and those that were upregulated in the 28°C ovotestes compared with 36°C ovotestes (positive log-fold changes).

Supplementary File S7.9: Gene ontology (GO) enrichment for process and function (denoted in GO Type column) for genes upregulated in 28°C ovotestes. Outputs were generated by GOrilla at a significance threshold of $P \leq 0.05$.

Supplementary File S7.10: Genes differentially expressed between control ovotestes at 36°C and ovotestes from the early developmental switch regime up-switched from 28°C to 36°C sampled at stage 9. A log-fold change cut-off of -1 to 1 and P-value cut-off of 0.01 was applied. The "direction" column indicates genes that were upregulated in the up-switched ovotestes compared with control ovotestes (negative log-fold changes), and those that were upregulated in the control ovotestes compared with up-switched ovotestes (positive log-fold changes).

Supplementary File S7.11: Genes differentially expressed between stage 9 ovotestes and stage 12 testes at 36°C from the early developmental switch regime. A log-fold change cut-off of -1 to 1 and P-value cut-off of 0.01 was applied. The "direction" column indicates genes that were upregulated in the testes compared with ovotestes (negative log-fold changes), and those that were upregulated in ovotestes compared with testes (positive log-fold changes).

Supplementary File S7.12: Genes differentially expressed between stage 9 up-switched ovotestes (early developmental switch regime) and stage 9 pre-switch ovaries at 36°C (mid developmental switch regime). A log-fold change cut-off of -1 to 1 and P-value cut-off of 0.01 was applied. The "direction" column indicates genes that were upregulated in the ovaries compared with ovotestes (negative log-fold changes), and those that were upregulated in ovotestes compared with ovaries (positive log-fold changes).

Supplementary File S7.13: Genes differentially expressed between stage 9 ovotestes and stage 9 control testes. Ovotestes produced at stage 9 up-switched at stage 6 and the ovotestes from the 36°C controls were grouped. A log-fold change cut-off of -1 to 1 and P-value cut-off of 0.01 was applied. The "direction" column indicates genes that were upregulated in the testes compared with ovotestes (negative log-fold changes), and those that were upregulated in ovotestes compared with testes (positive log-fold changes).

Supplementary File S7.14: Gene ontology (GO) enrichment for process and function (denoted in GO Type column) for genes differentially expressed between testes and ovotestes (denoted in Phenotype column). Outputs were generated by GOrilla at a significance threshold of $P \leq 0.05$.

Supplementary File S7.15: Genes differentially expressed between stage 9 ovotestes and stage 9 ovaries (controls and pre-switch stage 9 36°C from the mid-development switch regime samples were grouped). Ovotestes produced at stage 9 up-switched at stage 6 and the ovotestes from the 36°C controls were grouped. A log-fold change cut-off of -1 to 1 and P-value cut-off of 0.01 was applied. The "direction" column indicates genes that were upregulated in the ovaries compared with ovotestes (negative log-fold changes), and those that were upregulated in ovotestes compared with ovaries (positive log-fold changes).

Supplementary File S7.16: Genes uniquely upregulated in stage 9 ovotestes compared with both ovaries and testes (also at stage 9). Ovotestes produced at stage 9 up-switched at stage 6 and the ovotestes from the 36°C controls were grouped. Stage 9 ovaries (controls and pre-switch stage 9 36°C from the mid-development switch regime) were grouped. Genes that were differentially between both comparisons (ovotestes vs ovaries, and ovotestes vs testes) were determined to be uniquely upregulated in ovotestes. A log-fold change cut-off of -1 to 1 and P-value cut-off of 0.01 was applied.

Supplementary File S7.17: Metadata for all samples in this study. The original sample ID is matched to the Data ID, which appears in the raw count (Supplementary File S7.11) and raw expression (Supplementary File S7.12) files. The parent IDs are provided, and the switch regime that each sample was used in is noted. The group column corresponds to the data ID, and where these groups are in the experiment design is provided in Figure 7.12. This re-naming is to facilitate data analysis. The gonadal phenotype, and how the phenotype was validated (either via histology or expression profiles) is also provided.

Supplementary File S7.18: Raw counts for all samples (n = 58) for all genes (n = 19,284) prior to any filtering or outlier sample removal. Sample metadata is provided in Supplementary File S7.17.

Supplementary File S7.19: Raw expression values (TPM, transcripts per million) for all samples (n = 58) for all genes (n = 19,284) prior to any filtering or outlier sample removal. Sample metadata is provided in Supplementary File S7.17.

Chapter 8 Dynamics of epigenetic modifiers and environmentally sensitive proteins in a reptile with temperature induced sex reversal

Published: Biology of Reproduction, 2022

Whiteley, S. L., McCuaig, R. D., Holleley, C. E., Rao, S., Georges, A. Dynamics of epigenetic modifiers and environmentally sensitive proteins in a reptile with temperature induced sex reversal. Biology of Reproduction. doi.org/10.1093/biolre/ioab217

8.1 Abstract

The mechanisms by which sex is determined, and how a sexual phenotype is stably maintained during adulthood, has been the focus of vigorous scientific inquiry. Resources common to the biomedical field (automated staining and imaging platforms) were leveraged to provide the first immunofluorescent data for a reptile species with temperature induced sex reversal. Two four-plex immunofluorescent panels were explored across three sex classes (sex reversed ZZf females, normal ZWf females, and normal ZZm males). One panel was stained for chromatin remodelling genes JARID2 and KDM6B, and methylation marks H3K27me3, and H3K4me3. The other CaRe panel stained for environmental response genes CIRBP and RelA, and H3K27me3 and H3K4me3. Our study characterised tissue specific expression and cellular localisation patterns of these proteins and histone marks, providing new insights to the molecular characteristics of adult gonads in a dragon lizard *Pogona vitticeps*. The confirmation that mammalian antibodies cross react in P. vitticeps paves the way for experiments that can take advantage of this new immunohistochemical resource to gain a new understanding of the role of these proteins during embryonic development, and most importantly for P. vitticeps, the molecular underpinnings of sex reversal.

8.2 Introduction

The phenotypic sex of an animal governs many aspects of their life history and their reproductive success. The mechanisms by which sex is determined, and how a sexual phenotype is stably maintained during adulthood, has been the focus of vigorous scientific inquiry. Across vertebrates, sex is determined by a variety of mechanisms that exist on a spectrum between genetic sex determination (GSD) and environmental sex determination (ESD). In GSD systems, sex is controlled by genes on sex chromosomes, whereas ESD systems sex determination is flexible and sensitive to a wide variety of environmental stimuli. While species typically possess one system or the other, but discovery of species with sex governed by gene-environment interactions is increasing [272]. Examples of such species are few and poorly characterised [482]. An exception is the emerging model organism, the central bearded dragon (*Pogona vitticeps*). *P. vitticeps* has sex microchromosomes (female heterogamety, ZZ/ZW) (Ezaz et al., 2005), however their influence can be overridden by high incubation temperatures (>32°C) in ZZ males [38]. This triggers sex reversal, so that ZZ males develop as phenotypic females. As such, this species possesses a sex determination system ideally suited to studying the influences of both sex chromosomes and the environment on sex. Sex reversed ZZf females differ from concordant ZWf females in several biological aspects, including karyotype, behaviour, morphology, reproduction, and gene expression [3,54,76], though the two female sex classes do not differ in bite force [77].

Molecular resources supporting the study of sex differences in *P. vitticeps* are increasing [54,418,483,484], but much remains to be characterised. For example, little is known about the adult gonadal phenotypes in *P. vitticeps*, and nothing is known about protein expression or localisation (see Maurizii et al. 2009; Machado-Santos et al. 2015; Tezak, Guthrie, and Wyneken 2017; Sarı and Kaska 2016 for protein expression in other reptile species). To better understand protein dynamics of adult gonads of *P. vitticeps*, we selected for immunofluorescence analysis, a series of chromatin modifiers, their target methylation marks and environmentally sensitive regulators, all of which have been implicated in sex determination and sex reversal in *P. vitticeps* and reptiles more broadly [24,54,55,90]. These include chromatin remodelling genes JARID2 (Jumonji and AT-rich domain containing 2) and KDM6B (lysine demethylase 6B, also known as JMJD3) both of which regulate the methylation status of lysine 27 on histone 3 (H3K27). JARID2 is part of PRC2 (polycomb remodelling complex 2), which methylates H3K27 to

H3K27me3, while KDM6B has an opposing function that activates gene expression by demethylating H3K27me3 [240,435]. Other members of the Jumonji gene family, such as JMJD1C, have roles in germ cell regulation in mammalian gonads [489,490]. The co-occurrence of H3K27me3 repressive marks with active H3K4me3 marks is characteristic of bivalent chromatin. This pattern of epigenetic modification is commonly present during germ cell proliferation in mammalian gonads [491,492]. However, the dynamics of bivalent chromatin in reptiles is completely unknown.

Genes with environmental sensitivity are of particular interest for many reptile species, including *P. vitticeps*, because they might play a role in regulating environmentally triggered sex determination. CIRBP (cold inducible RNA binding protein) is of particular interest as a regulator of temperature sex reversal in *P. vitticeps* and in temperature sex determination in turtles [54,92,402]. It is not known if the expression of CIRPB in TSD species directs sexual phenotypes only during development, if it is also required to maintain adult gonadal cellular identity, or if it performs some other function. For example, in mammalian gonads CIRBP is involved in cell protection against environmental stressors [493,494]. Thus, to further explore the importance of cell protection in the context of CIRPB expression, we selected a member of the NF-κB cell signalling pathway that mediates inflammatory and immune responses for further study. Specifically, RelA/p65 has well established roles in initiating cell protective responses in the gonad in response to the environment [246,364,495,496]. Currently nothing is known about the role of RelA in reptile gonads, and little is known about its role in mammalian gonads [496].

While protein expression and localisation in mammalian gonads is extensively studied, research in non-mammalian species, particularly reptiles, is lacking by comparison. To determine the protein profiles of adult gonads in *P. vitticeps*, antibodies raised in mammals against mammalian targets were used in *P. vitticeps* for the first time to determine if they cross-react in a reptile. Resources common to the biomedical field (automated staining and imaging platforms) were leveraged to provide the first immunofluorescent data for this species. Two four-plex immunofluorescent panels were explored across the three sex classes (sex reversed ZZf and concordant ZWf females, and ZZm males). The first panel termed the Jumonji panel stained for JARID2, KDM6B, H3K27me3, and H3K4me3. The second, called the CaRe panel after a model that implicates two of the targets in this panel in sex reversal [53], stained for CIRBP, RelA,

H3K27me3, and H3K4me3. Our study characterises tissue specific expression and cellular localisation patterns of these proteins and histone marks, providing new insights to the molecular characteristics of adult gonads in *P. vitticeps*.

8.3 Results

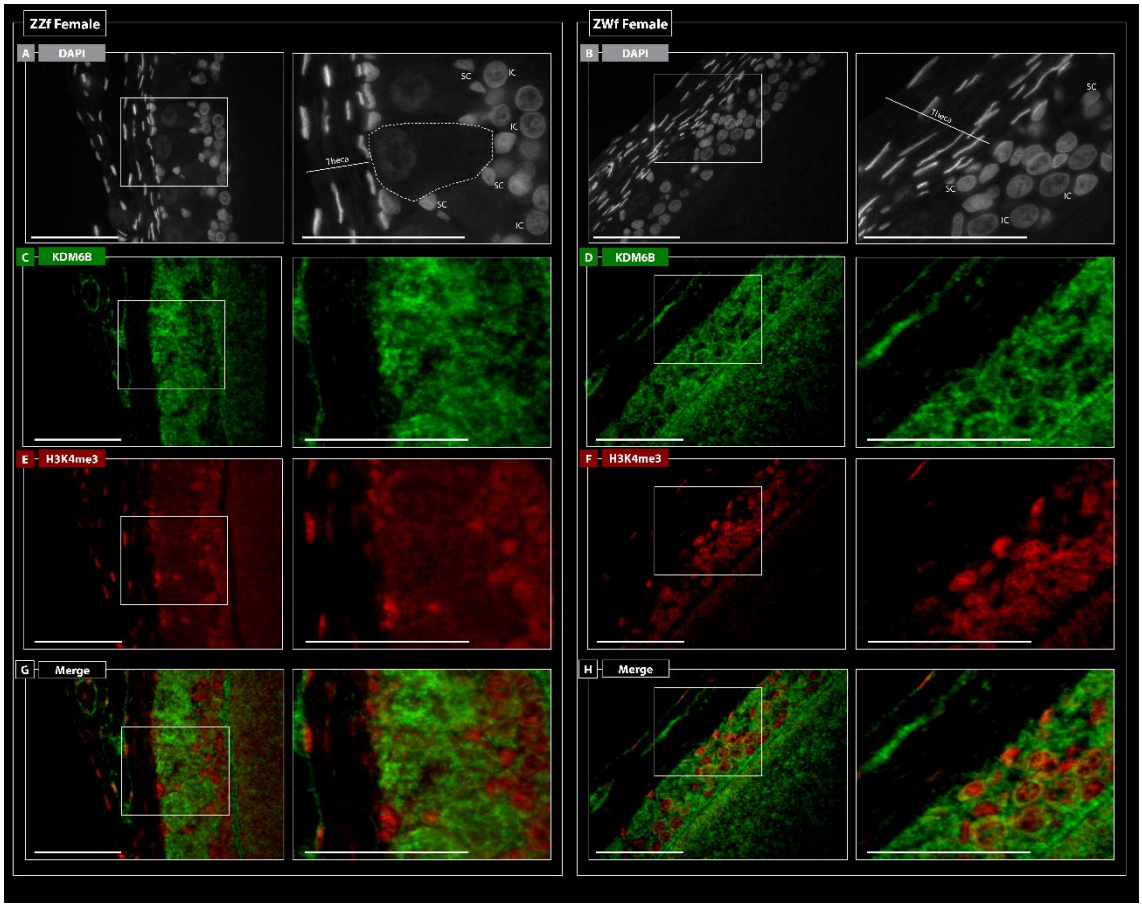

Figure 8.1: Immunofluorescence of KDM6B (green) and H4K4me3 (red) in adult ZZf sex reversed ovaries (panels A, C, E, G) and ZWf concordant (panels B, D, F, H) ovaries at 100x magnification. Panels G and H show a merged image of KDM6B and H3K4me3 staining. A pyriform cell in the ZZf female in panel A is demarcated by a dotted white outline. The white boxes indicate the portion of the image that has been zoomed in. SC = small cells, IC = intermediate cells. Scale bar = 10µm.

8.3.1 Ovarian morphology

The morphological characteristics of P. vitticeps ovarian follicles in both ZZf discordant sex reversed adult females and ZWf concordant females during the previtellogenesis phase are aligned with what has been previously published in reptiles [497–500]. In ZZf females the granulosa layer has become stratified and contains small, intermediate and

pyriform cell types [498]. The zona pellucida is present as a single layer between the granulosa and the developing ooplasm. Small cells are spherical with round nuclei that are closest to the theca and interspersed among the pyriform cells. The intermediate cells are oval with a round nucleus and are prevalent in the contact region with the ooplasm. The pyriform cells have large nuclei and a vacuolated cytoplasm. Long cytoplasmic prolongations that join the zona pellucida are also present (Figure 8.1a) (see also Uribe et al. 1995).

In the Jumonji 4-plex panels for ZZf females, the pyriform cells are extensively stained with KDM6B, weakly stained with JARID2 (Figure 8.2a). In the CaRe 4-plex panel the pyriform cells are extensively stained with CIRBP, with some weak staining for RelA and H3K4me3 in the nucleus (Figure 8.2b). In ZZf and ZWf females in both panels, the small and intermediate cells are stained almost exclusively with H3K4me3 (Figures 2 and 3). JARID2 (Figures 2a and 3a) and RelA (Figures 2b and 3b) show similar staining patterns in both ZWf and ZZf females; both are weakly dispersed throughout the theca and granulosa layers. H3K27me3 staining is very minimal and restricted to the theca in both females in each panel (Figure 8.2 and Figure 8.3).

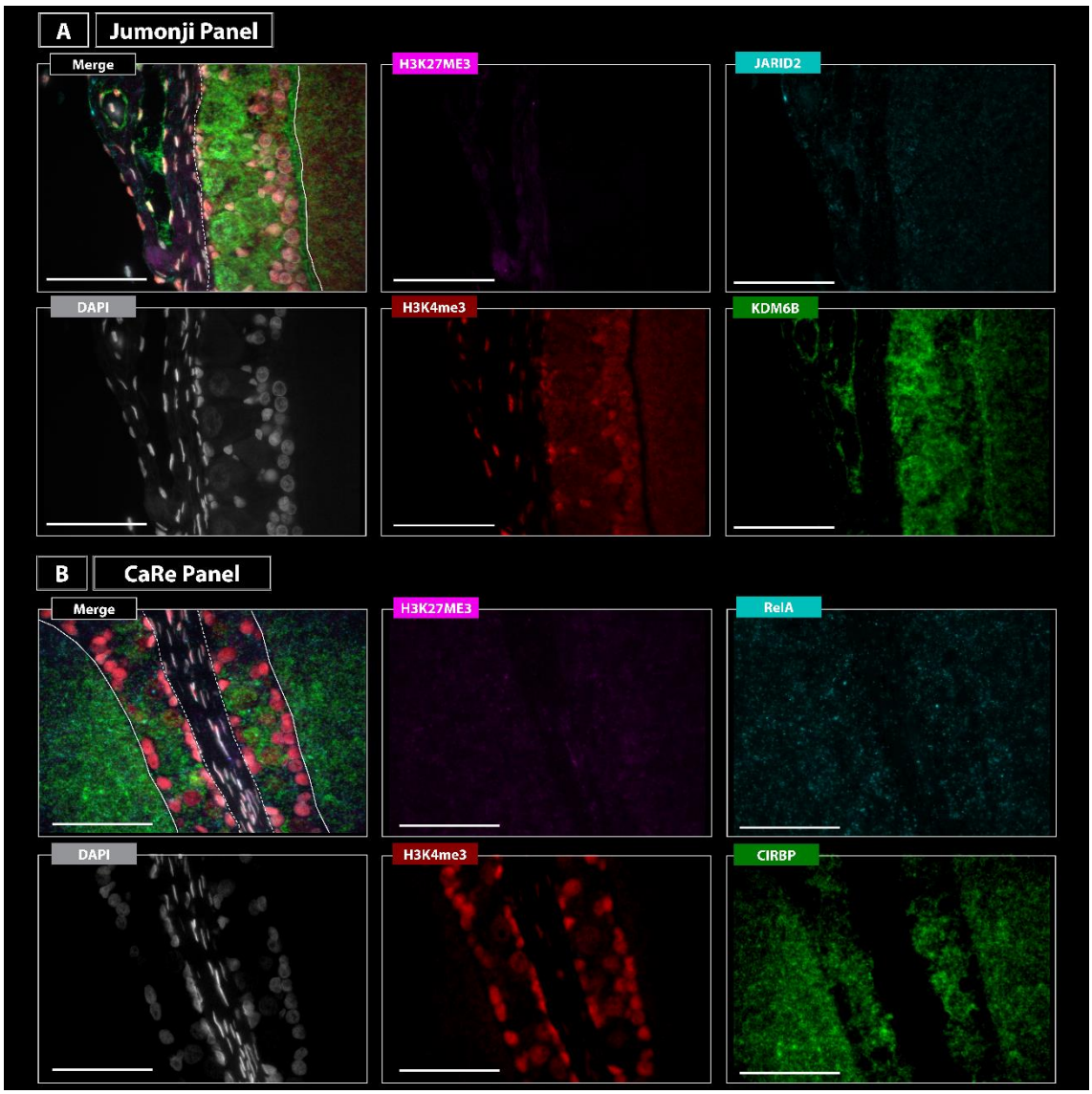

Figure 8.2: Immunofluorescence from two staining panels (Jumonji and CaRe panels) at 100x magnification in a ZZf sex reversed Pogona vitticeps female oocyte. The Jumonji panel shows staining of H3K27me3 (magenta), JARID2 (cyan), H4K4me3 (red), and KDM6B (green). H3K27me3 and JARID2 are weakly stained, while H3K4me3 and KDM6B are strongly stained in the theca and granulosa layer. The Care panel shows staining of H3K27me3 (magenta), RelA (cyan), H4K4me3 (red), and CIRBP (green). H3K27me3 and RelA are weakly stained, while H3K4me3 and CIRBP are strongly stained in the theca and granulosa layer. The dashed white line indicates the boundary between the theca (outermost layer) with the granulosa layer, and the solid white line demarcates the granulosa layer and the inside of the oocyte. Scale bar = 10µm.

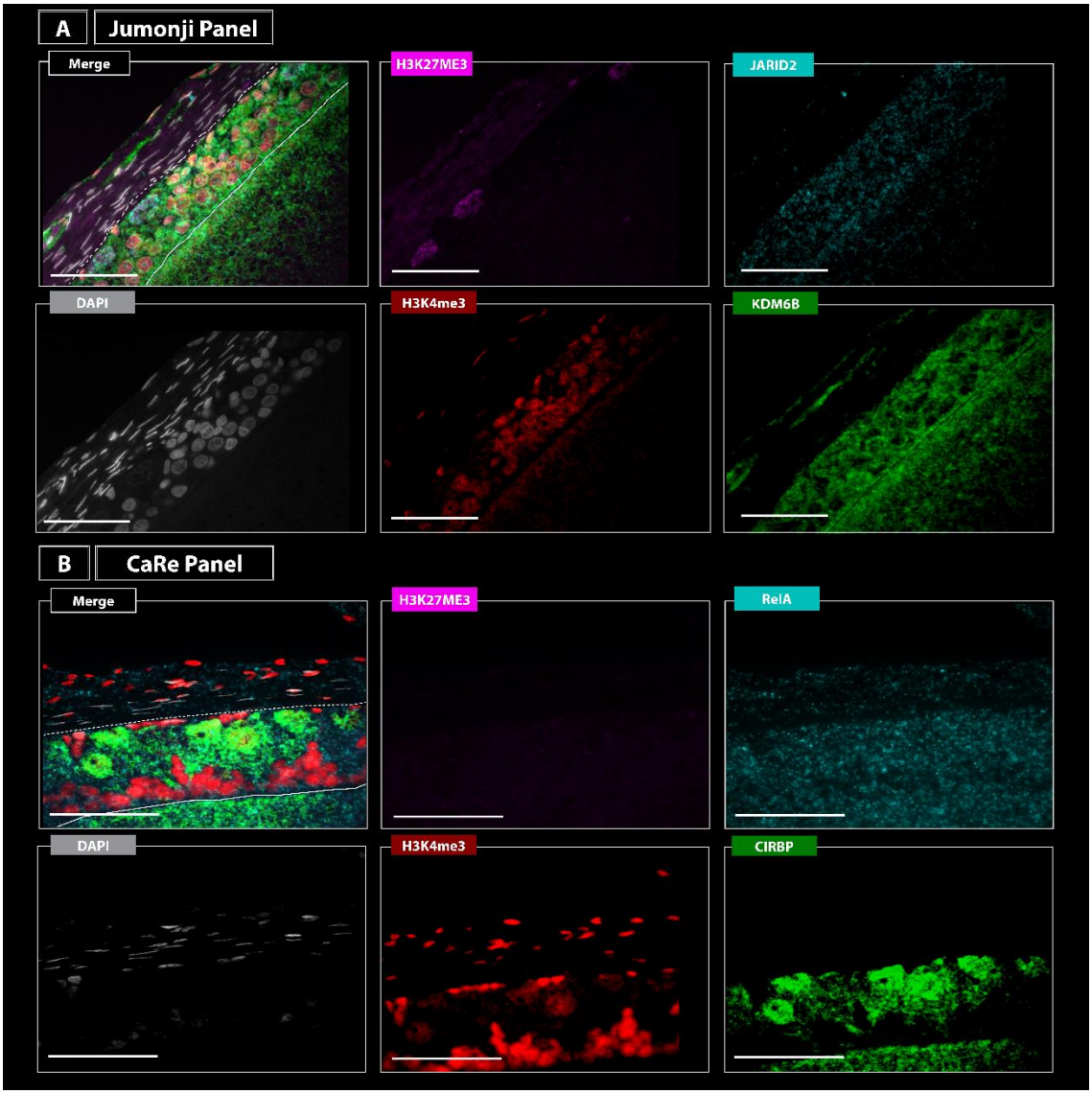

Figure 8.3: Immunofluorescence from two staining panels (Jumonji and CaRe panels) at 100x magnification in a ZWf concordant Pogona vitticeps female oocyte. The Jumonji panel shows staining of H3K27me3 (magenta), JARID2 (cyan), H4K4me3 (red), and KDM6B (green). H3K27me3 and JARID2 are weakly stained, while H3K4me3 and KDM6B are strongly stained in the theca and granulosa layer. The Care panel shows staining of H3K27me3 (magenta), RelA (cyan), H4K4me3 (red), and CIRBP (green). H3K27me3 and RelA are weakly stained, while H3K4me3 and CIRBP are strongly stained in the theca and granulosa layer. The dashed white line indicates the boundary between the theca (outermost layer) with the granulosa layer, and the solid white line demarcates the granulosa layer and the inside of the oocyte. Scale bar = 10µm.

8.3.2 Testicular morphology

In the ZZm males of *P. vitticeps*, no mature sperm are present given the samples were collected following the breeding season. Some elongating spermatids are present, as are some spermatocytes and Sertoli cells. In both panels, H3K4me3 was extensively stained in the Sertoli cells and spermatocytes, while H3K27me3 was minimally stained (Figure 8.4). In the Jumonji 4-plex panel, KDM6B was abundantly expressed within the cell

junctions that form near the basement membrane of the seminiferous tubules (Figure 8.4a). CIRBP staining was also abundant within the cell junctions, and also within the interstitial space (Figure 8.4b). JARID2 staining was weakly dispersed throughout the seminiferous tubules, a similar pattern to what was observed for RelA staining in the CaRe 4-plex panel (Figure 8.4).

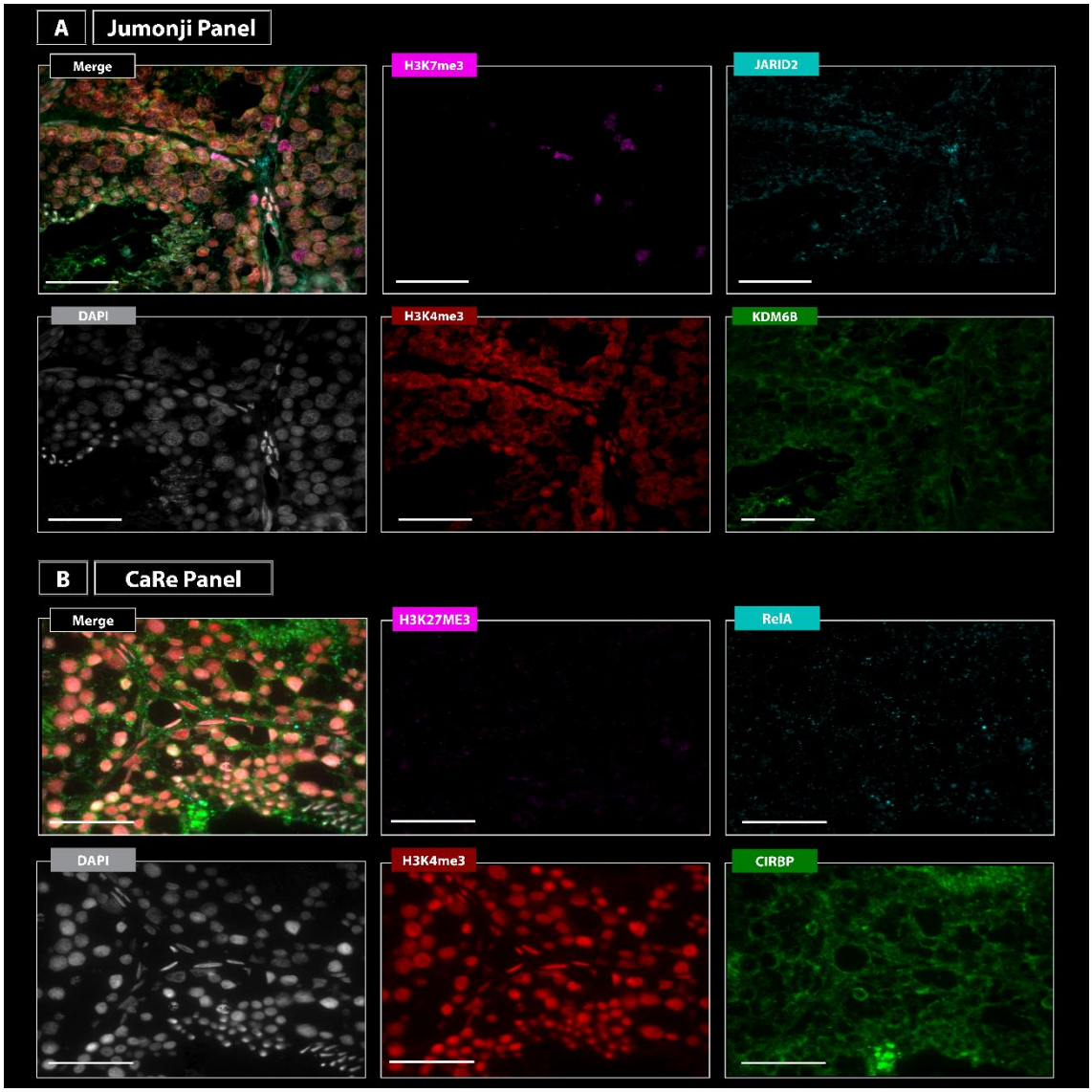

Figure 8.4: Immunofluorescence from two staining panels (Jumonji and CaRe panels) at 100x magnification in a ZZm male Pogona vitticeps testis. The Jumonji panel shows staining of H3K27me3 (magenta), JARID2 (cyan), H3K4me3 (red), and KDM6B (green). H3K27me3 and JARID2 are weakly stained, while H3K4me3 and KDM6B are strongly stained in the seminiferous tubules. The Care panel shows staining of H3K27me3 (magenta), RelA (cyan), H4K4me3 (red), and CIRBP (green). H3K27me3 and RelA are weakly stained, while H3K4me3 and CIRBP are strongly stained in the seminiferous tubules. Scale bar = 10µm.

8.3.3 Protein Expression

The level of protein expression was determined by calculating the mean integrated fluorescent intensity values for each antibody within a tissue at 100x magnification using an automated imaging system. See Methods for full details on how this analysis was conducted. As JARID2 staining was low in all tissues, it was not included in the protein expression analysis.

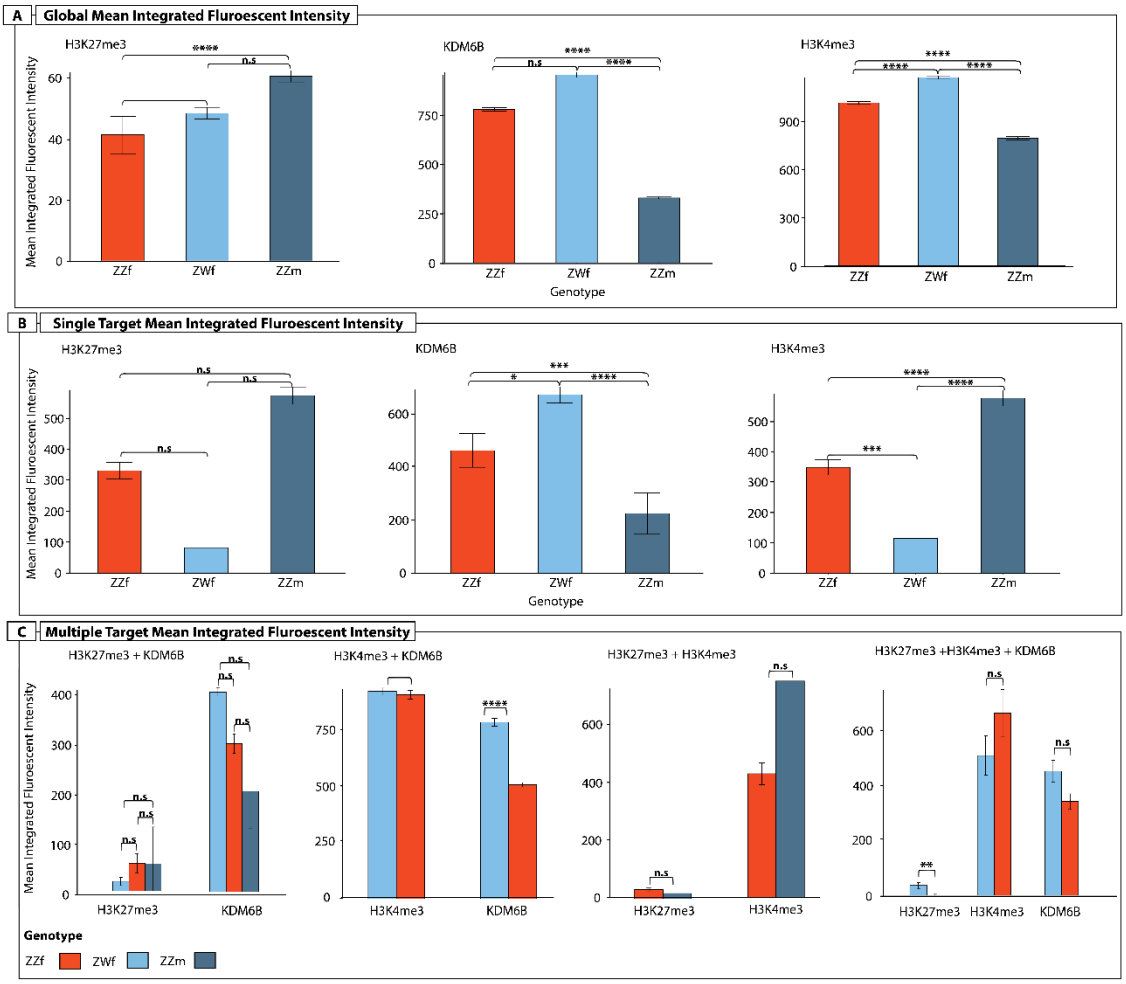

Figure 8.5: Mean integrated fluorescent intensity for the 3-plex Jumonji panel for (A) global, (B) single, and (C) grouped expression of H3K27me3, KDM6B, and H3K4me3 for each sex class in Pogona vitticeps: ZZf sex reversed females (red), ZWf concordant females (light blue), and ZZm males (dark blue). JARID2 was not included in this analysis due to low levels of staining. Analysis was conducted using a linear model, and significance (P value) is denoted with asterisks (* < 0.05, ** < 0.01, *** < 0.001, **** < 0.0001, n.s = not significant, α = 0.05).

In the Jumonji 3-plex panel (H3K27me3, H3K4me3, and KDM6B), global expression levels for H3K27me3 was significantly higher in ZZm males compared with ZZf females ($P < 0.0001$) but not with ZWf females ($P = 0.27$). H3K27me3 levels were significantly higher in ZWf females compared with ZZf females ($P < 0.005$). For cells

positive only for H3K27me3, levels did not significantly differ between the three sex classes (Figure 8.5).

Global staining of KDM6B did not differ between ZZf and ZWf females (P = 0.106), but was significantly lower in males compared with both females ($P < 0.0001$ for both pairwise comparisons). Cells positive only for KDM6B differed only marginally between the two female groups ($P < 0.02$), whereas expression was significantly lower in

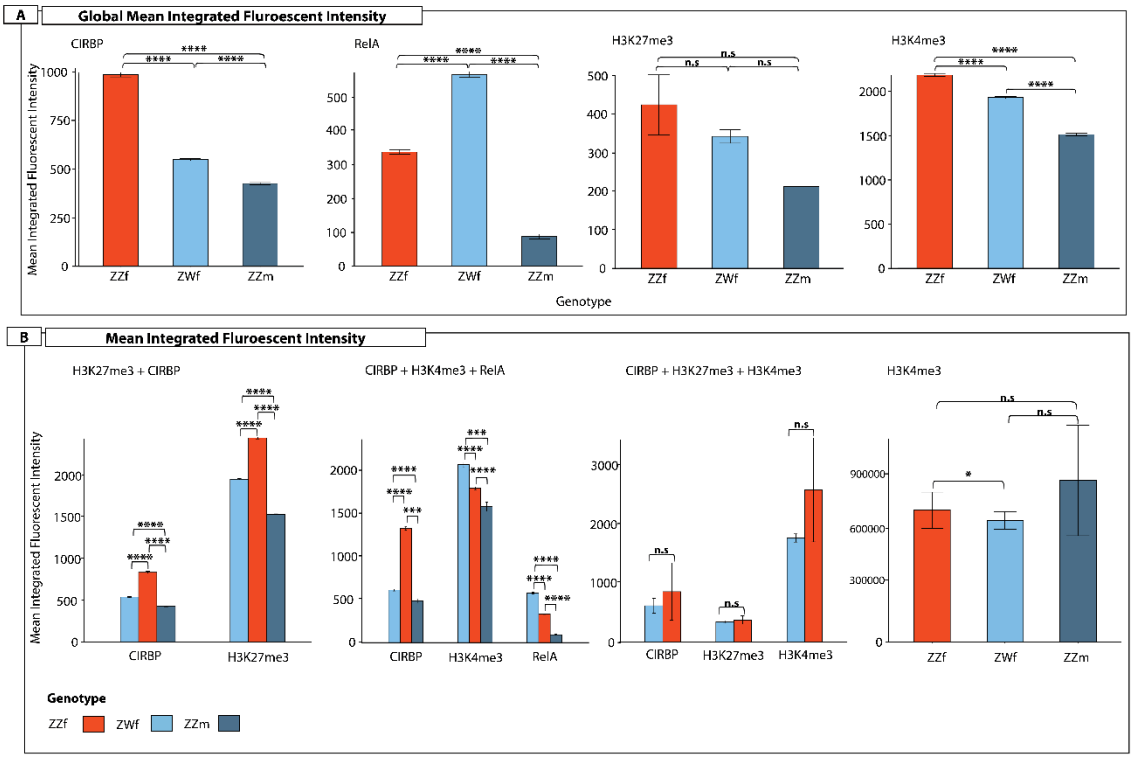

Figure 8.6: Mean integrated fluorescent intensity for (A) global or (B) grouped target expression for combinations of CIRBP, H3K27me3, RelA, and H3K4me3 for each sex class in Pogona vitticeps: ZZf sex reversed females (red), ZWf concordant females (light blue), and ZZm males (dark blue). Cells double positive for H3K4me3 and JARID2 were only detected in ZZm males. Analysis was conducted using a linear model, and significance (P value) is denoted with asterisks (* < 0.05, ** < 0.01, *** < 0.001, **** < 0.0001, n.s = not significant, α = 0.05).

ZZm males compared with both ZZf and ZWf females (P < 0.0005 and P < 0.0001 respectively).

Global expression of H3K4me3 was significantly different between all groups, as was expression in single positive cells. ZWf females had the highest global expression of H3K4me3, they had they lowest expression in single positive cells for this mark, while the opposite was true for ZZm males.

Expression of KDM6B globally and in single positive cells was consistently lower in ZZm males compared with both ZZf and ZWf females. KDM6B was consistently higher in ZWf females compared to ZZf females. By contrast, expression patterns for the histone marks were not consistent between the sex classes and between global and single cell expression levels.

Four classes of cells positive for different combinations of the four targets were identified. Cells positive for H3K27me3 and KDM6B did not differ in expression

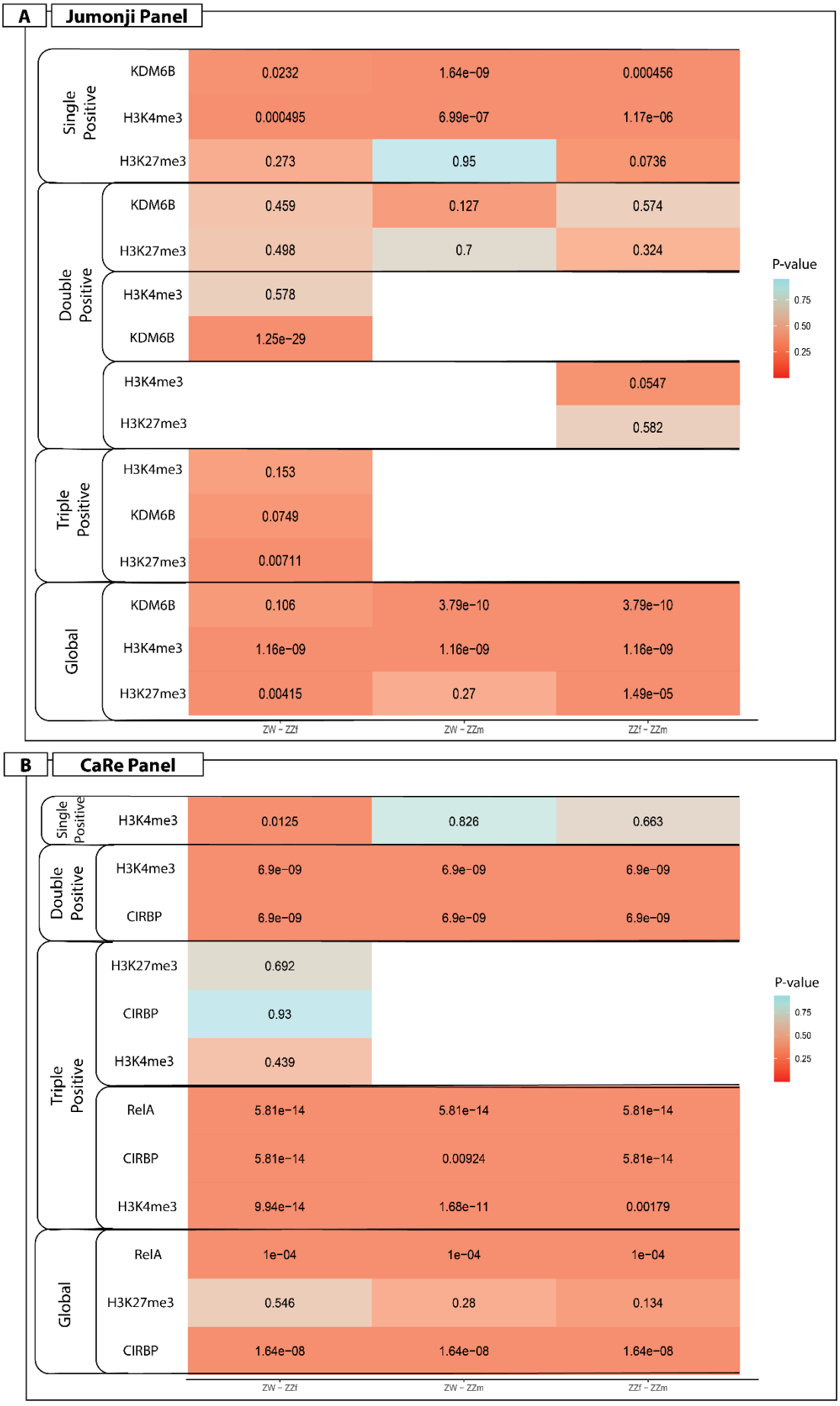

Figure 8.7: Heatmap showing a summary of all linear models conducted on mean integrate intensity values from the Jumonji (H3K27me3, H3K4me3, and KDM6B) and CaRe (H3K27me3, H3K4me3, CIRBP, and RelA) panels. P-values for each pairwise comparison for the staining classes are reported, and coloured by significance.

between the three sex classes. The H3K27me3 and H3K4me3 class was not detected in ZWf females, but did not differ between ZZf females and ZZm males. Cells double positive for H3K4me3 and KDM6B were detected in the female classes, and not in males. While the expression of H3K4me3 did not differ, expression of KDM6B was significantly higher in ZWf females compared to ZZf females. Cells triple positive for H3K27me3, H3K4me3, and KDM6B were only detected in females. Expression of H3K4me3 and KDM6B did not differ, however H3K27me3 was more highly expressed in ZWf females.

In the CaRe 4-plex panel global levels of CIRBP, RelA and H3K4me3 expression were significantly different between the three sex classes. CIRBP and H3K4me3 was highest in ZZf females, while RelA was highest in ZWf females. ZZm males exhibited the lowest expression of all targets. In all three sex classes, the only single positive cell class detected was for H3K4me3, which differed slightly between ZWf and ZZf females, but not between either female class and males. The only double positive class detected was H3K27me3 and CIRBP, which significantly differed between all sex classes, and both targets were highest in ZZf females. The only triple positive class was CIRBP, H3K4me3 and RelA, which differed significantly between the three sex classes. H3K4me3 and RelA were highest in ZZm males, while CIRBP was highest in ZZf females. Cells positive for all four targets were only detected in females, but levels did not differ between them (Figure 8.6).

It is important to note that while mean fluorescent intensity values for the protein targets can be assessed, the actual staining characteristics between the targets also needs to be considered visually. In all three sex classes in both the Jumonji and CaRe panels, H3K27me3 was very weakly stained, and in the CaRe panel RelA was weakly stained. This suggests that although differences in expression level was detected, the biological relevance of this is likely minimal.

8.4 Discussion

These data give insights to the protein dynamics in adult gonads of a squamate for the first time, and provides new understanding for reptiles more broadly, a vertebrate group for which there are few immunohistochemistry data. The data for KDM6B, JARID2, RelA, and CIRBP are also novel for vertebrates more broadly, as these four proteins have been minimally studied in adult gonads even in mammalian model species. Taking both protein localisation and expression information together, H3K4me3, KDM6B, and

CIRBP emerge as particularly important proteins with roles in the functioning of both ovaries and testes.

KDM6B was consistently more highly expressed in ZWf females compared with ZZf females, however KDM6B was localised in the same regions of the granulosa layer between both females. High expression of KDM6B in ZWf females is not consistent with previously published RNA-seq data for *P. vitticeps*, which found KDM6B to be more highly expressed in ZZf females [55]. The reason for this discrepancy is unclear, though suggests that additional post-transcriptional regulation may occur in KDM6B. In both ZWf and ZZf females, KDM6B expression was strongest in the small and intermediate cells in the granulosa, with some staining in the pyriform cells of ZZf females. These cell types were also double positive for KDM6B and H3K4me3, a double mark that was not present in male cell types. Previous research on *P. vitticeps* has shown that KDM6B is highly expressed during sex reversal in embryonic development [54], a pattern that was also observed sex reversed adult females [55].

H3K27me3 was weakly stained in both panels in all three sex classes. A possible explanation for the low levels of H3K27me3 is the prevalence of KDM6B, which demethylates H3K27me3 [435]. These results suggest low levels of H3K27me3 and high levels of KDM6B are characteristic of adult *P. vitticeps* regardless of sex, however as fundamentally different organs, the localisation of KDM6B differs between males and females. Previous work on adult gene expression in *P. vitticeps* found that KDM6B is more highly expressed in ZZf females than both ZWf females and ZZm males. An intron retention event in KDM6B genes was also observed in ZZf females, leading to the suggestion that the IR containing isoforms would not be translated into proteins [55]. The abundance of KDM6B staining observed in this study suggests the protein is translated, however future experiments are required to confirm whether or not the intron containing KDM6B isoform translated or not, and to determine the function of the resulting protein.

In the reptile granulosa, small cells are stem cells from which intermediate cells differentiate. Pyriform cells, which are a unique cell type to squamates, then differentiate from the intermediate cells [497,502]. Both intermediate cells and pyriform cells have functions similar to gonadal nurse cells found in insect ovaries [503] as they support the growth of the oocyte by transferring organelles such as vesicles, Golgi, ribosomal bodies, mitochondria, and messenger and ribosomal RNAs into the ooplasm via intracellular bridges [504]. Given this function, it is unsurprising that a lysine demethylase like

KDM6B and an active mark like H3K4me3 dominates in these cell types as opposed to those with repressive functions such as JARID2 and KDM6B.

Recent studies in mouse ovaries have shown that androgens target the catalytic subunit of the PRC2 complex, EZH2, which ultimately leads to reduced H3K27me3 methylation. At the same time, androgens also induce expression of KDM6B, which further serves to reduce levels of H3K27me3 in the ovaries [505]. Notably, cells in the *P. vitticeps* granulosa layer show an absence of H3K27me3, and an abundance of KDM6B, suggesting that this mechanism of ovarian gene regulation may be shared in P. vitticeps, and perhaps reptiles more broadly.

KDM6B is also abundantly expressed in the cell junctions within the seminiferous tubules in ZZm males, a localisation pattern that was also shared with CIRBP. In two turtle species (*Pelodiscus sinensis* and *Pelodiscus maackii*), junction proteins CLDN11 and CX43, which have established functions in mammalian testes, showed highly similar localisation patterns to those of KDM6B and CIRBP observed in *P. vitticeps* [506,507]. While further work is required, this suggests that KDM6B and CIRBP may have undescribed functions in the gap junctions of testes in *P. vitticeps*, and perhaps reptiles more broadly.

The functions of CIRBP in the ovarian granulosa under normal conditions are not well understood even in mammalian models. Its expression was associated with hypothermia in granulosa cell lines [493], and is more generally involved in the mammalian cold-shock response in other organs [170]. Its abundance in the granulosa of adult females and cell junctions in adult males of *P. vitticeps*, suggest an additional role for CIRBP that is not triggered by an environmental stressor, and relates more to normal functioning of the gonads. Immunostaining conducted on hatchlings of two turtle species (*Caretta caretta* and *Dermochelys coriacea*) showed high levels of CIRBP protein expression in female gonads rather than male gonads [487]. In this case, it was suggested that CIRBP expression may be influenced by incubation temperature, as is often the case for this gene in many reptile species (reviewed in [53]). In adult *P. vitticeps* this explanation seems unlikely, so further experimentation is required to determine the role of CIRBP in adult gonads, and roles it may have in reptiles more broadly.

Methylation dynamics during germ cell development have been extensively characterised in mammals. H3K27me3 and H3K4me3 are associated with bivalent chromatin, and are commonly observed during spermatogenesis and oogenesis [508–

510]. In *P. vitticeps,* all three sex classes exhibited abundant expression of H3K4me3 and minimal expression of H3K27me3, suggesting a lack of bivalent chromatin in both ovaries and testes. Given the samples were collected following the breeding season, these data likely capture a more latent reproductive stage, and during a more active reproductive period the dynamics of these methylation marks would likely be different.

These data give not only important new insights into the protein dynamics of these targets, but also provides a crucial foundation for future research. Confirmation that mammalian antibodies cross react in *P. vitticeps* paves the way for experiments that can take advantage of this new immunohistochemical resource to gain a new understanding of the role of these proteins during embryonic development, and most importantly for *P. vitticeps*, the molecular underpinnings of sex reversal.

8.5 Materials and Methods

8.5.1 Sample collection and histology

All adult animals (Table 8.1) were obtained from the breeding colony at the University of Canberra, Australia. All animals were humanely euthanised at the end of the 2017-18 breeding season (September to March) via an intravenous injection of sodium pentobarbitone (60mg/ml in isotonic saline) in accordance with approved animal ethics procedures at the University of Canberra. Animals were selected on the basis of their genotypic sex [3], and the gonadal phenotype was confirmed upon dissection. Sex reversed females were obtained by laboratory incubations at 36°C. Gonads were dissected immediately following euthanasia and preserved in 4% PFA-PBS. All initial tissue processing stages (tissue dehydration, wax embedding, and serial sectioning) was conducted at the University of Queensland's School of Biomedical Sciences Histology facility. Samples were processed according to standard protocols, sectioned 3µm thick, and placed on positively charged microscope slides.

Table 8.1**:** Specimen identification numbers and genotypic and phenotypic sex of all adult Pogona vitticeps used in this study.

Specimen ID	Sex Class	Genotypic Sex	Phenotypic sex
005005003424	Concordant Female	ZW	Ovaries
111880109533	Concordant Female	ZW	Ovaries
005005003551	Concordant Female	ZW	Ovaries
005005003596	Sex reversed female	ZZ	Ovaries
111880108006	Sex reversed female	ZZ	Ovaries
005005003388	Sex reversed female	ZZ	Ovaries
111880108027	Concordant Male	ZZ	Testes
111880109557	Concordant Male	ZZ	Testes
111880108009	Concordant Male	ZZ	Testes

8.5.2 Immunohistochemistry

For immunofluorescent staining, antibodies for the targets of interest (Table 8.2) were selected based on high homology with the region against which the antibody was raised. Antibodies with sequence homology to *Pogona vitticeps* greater than 85% were considered for subsequent testing and optimisation.

Table 8.2: Details of antibody targets used in this study, including their origin species and clonality, the company and catalogue number, serial and final dilutions used for each antibody, and the biological function of each target.

Target Name	Type (origin species, clonality)	Company (Catalogue number)	Serial Dilutions	Final Dilution	Function
H3K27me3 (tri-methyl lysine 27)	Mouse monoclonal	Abcam (ab6002)	1/100, 1/200, 1/400, 1/800	1/200	Methylation marks associated with transcriptional silencing deposited by the PRC2 complex
H3K4me3 (tri-methyl lysine 4)	Rabbit polyclonal	Abcam (ab8580)	1/100, 1/200, 1/400, 1/800	1/200	Methylation marks associated with active gene expression
JARID2	Rabbit polyclonal	Abcam (ab213679)	1/50, 1/100,	1/100	Component of the PRC2 complex.

			1/200, 1/400		Intron retention event in sex reversed females
JMJD3/KDM6B	Rabbit polyclonal	Genetex (GTX124222)	1/50, 1/100, 1/200, 1/400	1/100	Demethylase for H3K27me3 (antagonist to PRC2)
***RelA* (p65)**	Mouse monoclonal	Santa Cruz Biotechnology (sc-68008)	1/50, 1/100, 1/200, 1/400	1/100	Component of the NF-kB pathway
***CIRBP* (cold-inducible binding protein)**	Mouse monoclonal	Santa Cruz Biotechnology (sc-293325)	1/50, 1/100, 1/200, 1/400	1/100	Induced by environmental cues, identified as key gene in TSD pathways

Each antibody was first optimised via serial dilutions, and then each multiplex panel was optimised for staining intensity and specificity (12). All staining procedures were conducted using the Opal Polaris 4 colour Automation Kit (Perkin Elmer, cat no. NEL810001KT) optimised for use on the Leica Bond RX Automated IHC Research Stainer (Leica Biosystems). To ensure staining was specific for primary antibodies all appropriate negative controls for staining were employed for each antibody panel. This included primary antibody only controls (with no secondary detection), secondary detection controls (with no primary antibodies) and blank controls with no staining protocol (see Figure 8.8).

8.5.3 Image analysis and quantification

FFPE sections (3mM thick) from *Pogona vitticeps* of gonadal tissue sections of three individuals from each sex class in *P. vitticeps* (sex reversed ZZf and concordant ZWf females, and ZZm males) were stained with multiplex immunohistochemistry (IHC) panel of four targets (H3K27me3, H3K4me3, JARID2, and KDM6B) following single stain optimisation. A subset of samples (two from each sex class) were stained with the second multiplex panel (H3K27me3, H3K4me3, CIRBP, and RelA).

The slides were imaged using the ASI Digital Pathology System. Touching cells were automatically segmented, signal expression was quantitatively measured, and results per cell and over the entire scanned region displayed. For high-throughput

microscopy, protein targets were localized by confocal laser scanning microscopy. Single 0.5 μm sections were obtained using an Olympus-ASI automated microscope with a 100x oil immersion lens running ASI software. The final image was obtained by employing a high-throughput automated stage with ASI spectral capture software [511,512]. Digital images were analysed using automated ASI software (Applied Spectral Imaging, Carlsbad, CA) to automatically determine the distribution and immunofluorescent intensities with automatic thresholding and background correction of the mean integrated fluorescent intensity (*MIFI*, described below). Images were prepared for representative purposes using ImageJ Fiji imaging software [513].

Mean integrated fluorescent intensity (MIFI) values detected by the ASI automated software platform were obtained by normalising the fluorescent signal from each target for the area of each cell. Cells were classified into different classes depending on whether they expressed a single target, or multiple targets, yielding 10 classes of cells in which one or more target was present. A minimum of three cells within a given sex class needed to have the cell class detected to be used for the analysis. Global levels of expression for each of the four targets was determined by combining the MIFI of all classes that had positive staining for each target.

The *MIFI* values for each class were normalised via log transformation, and statistical differences of these values between the three sex classes was assessed using a linear model (lm function) in R (version 1.2.1335). Global expression of each target was obtained by summing the values for the given target in each class in which it was detected. All graphs were prepared in R using the ggplot2 package [514].

8.5.4 Supplementary Figures

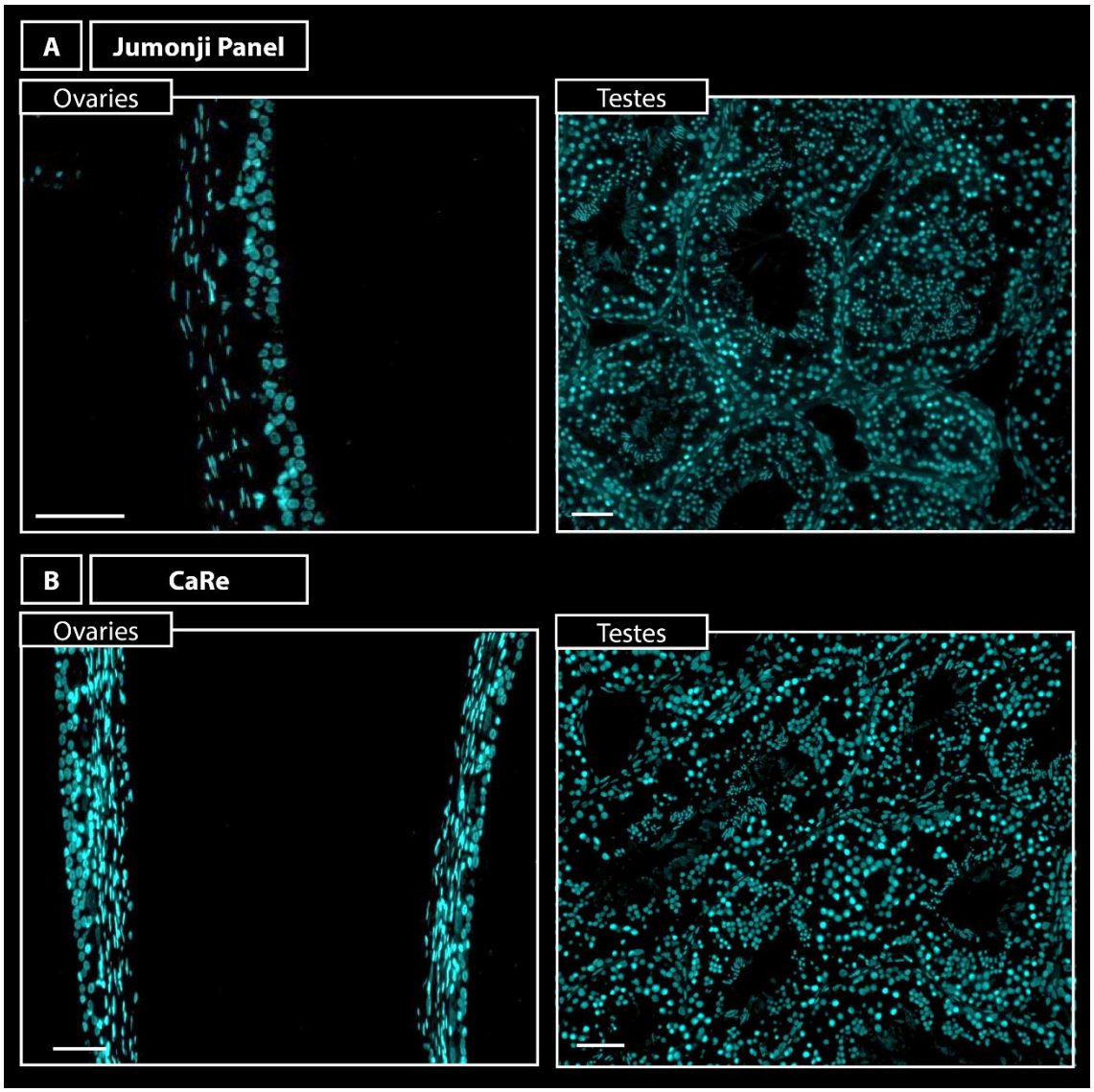

Figure 8.8: Immunofluorescence negative control staining for the secondary antibody only from two staining panels (A) Jumonji and (B) CaRe panels at 100x magnification. Images from a representative sample for ovaries and testes from each panel are shown. Scale bar = 10µm.

Chapter 9 Synopsis

For almost every eukaryote, life begins the same way: a zygote is formed by two gametes from which an entire organism will develop. This fascinating process is at the heart of developmental biology, a research field that lies at the intersection between genetics and evolutionary biology. By studying how multicellular organisms can develop from a single cell, profound insights about the fundamental processes governing the growth of all eukaryotic life can be gained. During embryonic development, complex genetic cascades drive the proliferation and differentiation of every cell, ultimately giving rise to the diverse physiological systems required for multicellular life. Of these systems, those governing sex and reproduction are critically important as they will influence many traits of the developing organism. In vertebrates, the development of sexual phenotypes is highly conserved; the bipotential gonads form and then differentiate into either ovaries or testes. These organs secrete hormones that drive the development of secondary sexual phenotypes, such as the genitalia. In vertebrates, a wide variety of sex determination modes are responsible for determining sexual fate, including those involving an interaction between genes the environment [1]. The central question of this thesis asks how temperature can determine sex during embryonic development. This is a deceptively complex question that immediately leads to many more questions, to which there are currently almost no definitive answers. How is temperature sensed by the developing embryo? How is this environmental signal transduced at the molecular level to cause gene expression changes? What are the cellular mechanisms responsible for causing these gene expression changes? Are these mechanisms shared across the vertebrate phylogeny? What are the environmentally sensitive sex determination pathways in specific species?

I present this thesis as a cohesive body of work that provides new insights into the environmentally sensitive sex determination systems of emerging model species, the Jacky dragon (*Amphibolurus muricatus*) and the central bearded dragon (*Pogona vitticeps*). This research brings improved understanding of not only fundamental biology in these species, but also has broader implications for the evolution of sex determination modes in reptiles, and other environmentally sensitive lineages. While a complete understanding of how temperature determines sex, and how the evolutionary flexibility of these systems occurs at a mechanistic level is likely still years away, this thesis provides new direction to answering these questions.

9.1 A new paradigm for ESD systems

Chapter 2 and Chapter 3 provide new directions for understanding the evolution of sex determination systems. In Chapter 2, the current understanding of the influence of temperature on reptile sex determination is reviewed, and most importantly, a practical guide to discovering sex reversal in new species is given. Chapter 3 provides a framework to understand the evolution of sex determination, and a new theoretical model that reconciles the diversity seen in ESD systems with highly conserved cellular processes required for environmental sensing. The CaRe model proposes that the biochemical processes at the interface of the environment and the cell are calcium signalling (Ca) and redox regulation (Re). This work presents a cohesive model for a universal environmentally sensitive cellular mechanism that can govern sex determination. Many vertebrate species display environmentally sensitive sex determination, particularly temperature that determines sex in many reptile species (temperature dependent sex determination, TSD). Even between closely related species, the patterns of TSD can differ, and so too can patterns of gene expression and other genetic mechanisms. How this diversity can be reconciled has been a fundamental challenge to ESD research. The role of calcium and redox regulation in sensing environmental change and provoking changes in gene expression exists in all eukaryotes, so provides a conserved mechanism by which ESD systems can be regulated.

The CaRe model provided a framework for my embryonic transcriptome studies, to interpret gene regulatory processes observed during sex reversal in *Pogona vitticeps* (presented in Chapter 5, Chapter 6, and Chapter 7, see section 9.1.1). The CaRe model also opens up many new and exciting avenues for future research, particularly in identifying genes with a functional role in ESD systems, which is also discussed in detail below (see sections 9.1.1 and 9.3). The universality of CaRe regulation extends its impacts to epigenetics and evolutionary biology research more broadly, as many organisms utilise calcium and redox to sense and respond to the environment. The many experimental possibilities that arise from the CaRe model are discussed in detail in Section 9.4 below.

9.1.1 Molecular mechanisms underpinning sex reversal

In my experimental work on *Pogona vitticeps*, which has the best characterised sex reversal system of any reptile, I began to unravel the complex genetic interactions

between genes and temperature in this species. As an emerging model species, *P. vitticeps* sex determination traits present unique opportunities to test predictions made by the CaRe hypothesis (Chapter 3). The work presented in 4.6.3 takes advantage of unique characteristics of *P. vitticeps* sex determination to assess differences in gene expression between gene and temperature driven female development. The results from this study not only provide new insights into the gene expression changes underlying sex reversal for the first time, but also provides a critical foundation for future research. The genes identified in this study were a mix of those that have been implicated in other TSD species, and novel genes not previously implicated in thermosensitive sex determination systems. Two of these genes, *KDM6B* and *JARID2* were particularly interesting as they are chromatin remodelling genes previously shown to have intron retention events in adult sex reversed *P. vitticeps* [55]. *KDM6B* plays a critical regulatory role in the male sex determination pathway in *T. scripta* [24]. Taken together, the data from this chapter shows that while sex reversal is a process distinct from TSD, certain genes are commonly co-opted in thermosensitive sex determination pathways, suggesting that despite the diversity of these systems, there is a level of evolutionary conservation.

The data presented in Chapter 6 analysed the splicing patterns of *JARID2* and *KDM6B* during sex reversal in *P. vitticeps*. Despite the common involvement of these genes in thermosensitive sex determination cascades, the data presented in this chapter clearly shows differences in the splicing of these genes between different species. Sex reversal in *P. vitticeps* is characterised by unique N-terminally truncated *JARID2* and *KDM6B* isoforms that were not present in the other two TSD species assessed, *T. scripta* and *A. mississippiensis.* The precise roles of these isoforms are currently unknown, though it is highly likely they are required to mediate the sex reversal cascade in *P. vitticeps* given their absence in the TSD species.

The temperature switch experiment presented in Chapter 7 illuminates novel aspects of sex reversal that were not previously understood. Perhaps the most important finding from this work is that sex reversal is a process that relies on numerous thresholds being surpassed in order for sex reversal to be initiated. This differs from TSD systems where a given incubation temperature will initiate the pathway of one sex but not the other. Instead, sex reversal relies on exposure to the temperature cue for a fairly long period during embryonic development (approximately 14 days, or 30% of development at 36°C), during particular developmental stages (prior to stage 9). The initiation of sex reversal is further influenced by inter-individual variation in thermosensitivity of gene

expression changes and/or the magnitude of gene expression changes. Taken together, these findings suggest that sex reversal can be understood as difficult to achieve at a molecular level, requiring a variety of factors to all coalesce in order for sex reversal to be initiated and maintained.

These three chapters together provide the most complete picture of the genetic underpinnings of sex reversal in *P. vitticeps* to date. I present a working model for sex reversal in Figure 9.1 that combines the results from Chapter 5, Chapter 6, and Chapter 7. Though many of these proposed pathways and mechanisms are yet to be experimentally demonstrated, this model presents logical and testable hypotheses based on my findings in *P. vitticeps*. This working model provides a basis for numerous future experiments to begin to functionally demonstrate elements of the sex reversal pathway. I hypothesise that the activation of all of these pathways in concert with each other may be another threshold required for the initiation of sex reversal. Activation of only one may not be sufficient to initiate or maintain sex reversal.

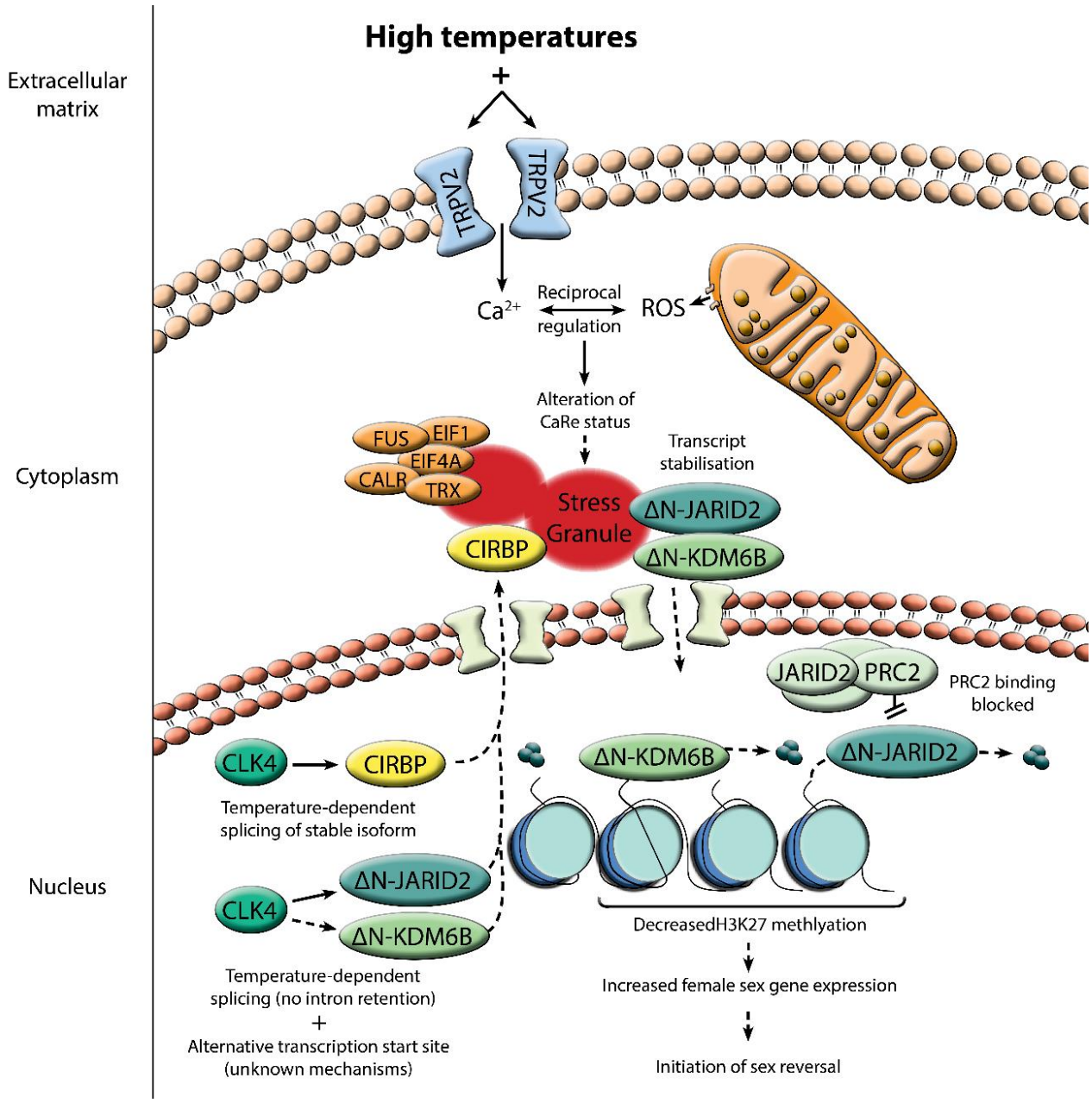

Figure 9.1: Hypothesised genetic pathways driving temperature induced sex reversal in *Pogona vitticeps*. Exposure to high temperatures causes perturbation in the CaRe status of the cell via calcium influx via thermosensitive channel TRPV2, and the release of ROS from the mitochondria due to increased metabolic rate. At the same time CLK4 respond to the high incubation temperatures and regulates the splicing of *JARID2*, *KDM6B* and *CIRBP*. The altered CaRe status triggers stress granules to which CIRBP localises, and the *JARID2* and *KDM6B* isoforms are sequestered and protected from degradation. They can then be translated into proteins and return to the nucleus where together they can decrease the levels of H3K27me3 methylation on key genes involved in female development, to ultimately initiate sex reversal.

9.2 Prevalence of transitional sex determination modes

The first investigation of thermal influence on embryonic development in *A. muricatus* revealed new evidence suggesting that although this species has been long considered to have TSD, it may in fact have a cryptic genetic influence underlying sex determination (Chapter 4). By implementing an approach proposed in Chapter 2 that used histology of the developing gonads, I showed that development at extreme incubation temperatures, which produce predominantly females, is characterised by approximately 50% of embryos developing ovotestes. This supports a hypothesis proposed by Quinn et al. [27] that species with a FMF pattern of TSD are likely to exhibit an underlying ZZ/ZW GSD system, with extreme temperatures inducing sex reversal. This can explain both how balanced sex ratios can be produced at intermediate temperatures and how a female bias occurs at both high and low temperatures in species with Type II TSD.

The Tree of Sex Consortium [271] identified 66 reptile species that have a Type II FMF pattern of TSD, including *Amphibolurus muricatus*. Within these 66 species, two have been identified as having both TSD and sex chromosomes. *Gekko japonicus* was the first squamate where both modes was observed, though additional experimentation is needed to confirm sex reversal in this species [21]. Intriguingly, this species has male heterogamety (XY/XX), which is the opposite of predictions made by Quinn et al. [27]. Subject to final experimental confirmation, sex reversal in *G. japonicus* would result in the reversal of XX females to males (XXm). This was predicted for species with a MFM pattern of TSD [27], which has only been described in fish and not reptiles [515]. The only reptile species currently identified with sex reversal in a male heterogametic system is *Bassiana duperreyi*, but it sex reverses only at low temperatures [4]. Similarly to *G. japonicus, Crotaphytus collaris* also exhibits a MFM sex ratio pattern [516], and analysis of gene dosage has suggested the presence of sex chromosomes [40]. Demonstration of sex reversal in *G. japonicus* and *C. collaris* would represent a unique condition of sex reversal not previously observed in reptiles.

Eremias multiocellata is another species requiring closer investigation as it has female heterogamety (ZZ/ZW) and Type II TSD [43,517]. This species is particularly interesting as it is viviparous, a reproductive mode typically considered to be at odds with a thermal influence on sex determination. This is because the behavioural thermoregulation of the mother would result in stable temperatures, causing consistent skewing of offspring sex ratios and an evolutionary disadvantage [518]. *E. multiocellata*

is not the only viviparous species that has sex chromosome and thermal influence on offspring sex. *Niveoscincus ocellatus* also has sex chromosomes, and although they are homomorphic, populations across an altitudinal gradient show an influence of maternal temperature during gestation on offspring sex [519,520]. This raises the possibility that other viviparous species may possess both genetic and thermal influence on sex determination. Care needs to be taken when assessing sex determination in reptiles as early work incorrectly identified *Eulamprus tympanum* has being the first viviparous species with thermal influence on sex determination [42,521].

The remaining 63 species identified with Type II TSD are obvious candidates for future investigations seeking to uncover novel interactions between genes and the environment in sex determination. Such investigations will be important for revealing whether or not sex reversal is common across reptiles, or if it occurs only rarely. Given the current phylogenetic distribution of species with known gene-environment interactions, the latter scenario seems improbable. Rather, sex determination modes in ectothermic lineages with environmental sensitivity likely provide evolutionary advantages beyond what is conferred by GSD or TSD alone. Ultimately, the influence of temperature on sex determination and differentiation in reptiles is highly complex and can vary considerably between lineages. This highlights the importance of investigating interactions between genes and the environment across the reptile phylogeny in order to understand the evolutionary dynamism of sex determination in this highly diverse order.

9.3 Establishing reptile models in the molecular era of developmental biology

To finally understand the mechanisms by which temperature determines sex, functional experimentation is required to definitively demonstrate the roles various genes and pathways might play. However, functional experiments in non-model species presents numerous logistical difficulties that have hindered research, prolonging the search for the genetic basis of environmentally sensitive sex determination systems.

For example, though now commonplace in biomedical research, CRISPR-Cas9 has only been demonstrated once in a reptile in 2019 [522]. Commonplace use of gene editing techniques remains in the distant future. RNA-interference techniques have been used in *T. scripta* [24], however this approach comes at a cost that makes it difficult to implement in other species. One major hurdle is the sample sizes required to conduct these types of

experiments. In the first paper on *T. scripta* using sh-RNA introduced via a lentivirus vector, between 300-500 eggs were used per treatment group, with only 20-50% of those eggs surviving to the latest developmental stage assessed [24]. Similarly, for the CRISPR-Cas9 gene editing in *Anolis sangrei*, surgery on gravid females was required, and timing of injection into unfertilised oocytes was extremely challenging due to internal fertilisation and sperm storage. In total 146 oocytes from 21 different females were injected, from which only 9 animals in the F0 generation carried the target mutation, a success rate of 16% [522].

While there are obvious difficulties involved in gene editing techniques, functional experiments undertaken in cell and organ culture systems are a viable alternative. Both culture systems have been successfully implemented in various reptile species, and importantly for research on sex determination, the bipotential gonad will differentiate in culture [24,224,523,524]. In cases where the interference of a target in the whole embryo would prove fatal, these culture techniques are the only viable option.

More classic developmental biology approaches also provide suitable alternatives and may be more feasible for many species compared with more sophisticated molecular approaches. As demonstrated in Chapter 3, it is possible to identify candidate species with gene-environment interactions using simple staging systems and gonadal histology [39]. Reptiles have been studied since the establishment of developmental biology as a scientific field in the mid-1800s [525]. Characterisation of reptile development began with pioneer Martin Rathke, who first described reptile embryos in 1825, a foundational work that was followed by the characterisations of embryonic development of many European lizards through the late 1800s to early 1900s. During this time, the practice of creating staging tables to characterise development become established, with the first reptile staging tables developed in 1904 in a legless lizard (*Anguis fragilis*) and the sand lizard (*Lacerta agilis*; [525–527]). Despite some limitations of this approach, staging tables remain a foundational aspect of developmental biology [528].

Despite this long history, reptile embryonic development remains poorly understood, particularly when compared to birds and mammals. The order Reptilia contains over 11,000 species, making it the largest vertebrate group after fish and birds, and considerably larger than mammals. Despite this, staging systems exist for only 56 reptile species, representing a mere 0.5% of the order (Table 9.1). Many of these staging tables are classic descriptions of embryonic development, while others take advantage of

diverse reptilian morphologies to unveil in great detail a variety of processes ranging from lamellae development to comparative analysis of skull growth (for examples see 449,450).

Table 9.1: All published developmental staging systems for reptiles, including the common and species name, and the source publication

Species	Common Name	Source
Agama impalearis	Bibron's agama	[531]
Alligator mississippiensis	American alligator	[284]
Alligator sinensis	Chinese alligator	
Amphisbaena darwini heterozonata	Darwin's ringed worm lizard	[532]
Anguis fragilis	Deaf adder	[526,533,534]
Anolis carolinensis	Carolina anole	
Anolis sagrei	Brown anole	[535]
Apalone spinifera	Spiny softshell turtle	[287]
Boaedon fuliginosus	Brown house snake	[536]
Caretta caretta	Loggerhead sea turtle	[537]
Caiman latirostris	Broad-snouted caiman	[538]
Calotes versicolor	Oriental garden lizard	[288]
Calyptommatus sinebrachiatus	Lesser microteiid	[539]
Carettochelys insculpta	Pig-nosed turtle	[540]
Chamaeleo bitaeniatus	Two-lined chameleon	[541,542]
Chamaeleo lateralis	Carpet chameleon	[543]
Chelonia mydas	Green sea turtle	[544]
Chelydra serpentina	Common snapping turtle	[286]
Chrysemys picta	Painted turtle	[545]
Chrysemys picta bellii	Western painted turtle	[546]
Crocodylus johnsoni	Freshwater crocodile	[284]
Crocodylus porosus	Saltwater crocodile	[284]
Dermochelys coriacea	Leatherback sea turtle	[547]
Emys orbicularis	European pond turtle	[292]
Eublepharis macularis	Leopard gecko	[293]
Hemidactylus turcicus	Mediterranean house gecko	[548]
Hemiergis spp.	Earless skinks	[549]
Lacerta viridis	European green lizard	[550]
Lepidochelys olivacea	Olive Ridley sea turtle	[551]
Lepidodactylus lugubris	Mourning gecko	[552]
Liolaemus gravenhorstii	Gravenhorst's tree iguana	[553]
Liolaemus t. tenuis	Jewel lizard	[554,555]
Mabuya megalura	Grass-top skink	[541]
Malayemys macrocephala	Malayan snail-eating turtle	[294]
Naja haje	Egyptian cobra	[556]
Naja kaouthia	Monocled cobra	[557]
Natrix natrix	Cyprus grass snake	[558,559]
Natrix tesselata	Dice snake	[560]
Nothobachia ablephara	NA	[539]
Paroedura pictus	Ocelot gecko	[561]
Pelodiscus sinensis	Chinese softshell turtle	[562]
Podarcis (Lacerta) vivipara	European common lizard	[314]
Podarcis (Lacerta) agilis	Sand lizard	[527,563]

Podarcis (Lacerta) muralis	Common wall lizard	[550]
Pogona vitticeps	Central bearded dragon	[7]
Psammophis sibilans	Striped sand snake	[564]
Ptyodactylus h. guttatus	Sinai fan-fingered gecko	[548]
Python reticulatus	Reticulated python	[565]
Python regius	Ball python	
Pyton sebae	African rock python	[566]
Salvator merianae	Argentine black and white tegu	[567]
Sceloporus aeneus	Southern bunchgrass lizard	[74]
Sceloporus undulatus	Eastern fence lizard	[568]
Sphaerodactylus argus	Ocellated gecko	[548]
Sphenodon punctatus	Tuatara	[569]
Tarentola annularis	White-spotted wall gecko	[529]
Testudo hermanni	Hermann's tortoise	[570]
Thamnophis s. sirtalis	Common garter snake	[571]
Trachemys scripta	Red eared slider turtle	[295]
Tropidurus torquatus	Amazon lava lizard	[572]
Varanus indicus	Mangrove monitor	[573]
Vipera aspis	Asp viper	[574]

To improve the utility of staging systems, particularly for understanding sexual evolution, some changes to the standard approaches would be required. In particular, there is a tendency to overlook the development of sexual phenotypes entirely, or to focus on male development only (Table **9**.**1**). In species with TSD, this often means that only one incubation temperature is assessed. Future work on embryonic development in reptiles would greatly benefit from including descriptions of development at different incubation temperatures, and at a minimum include descriptions of genital development, though ideally gonadal development would also be described.

Yet despite these many hurdles, many exciting advances are still being made using non-model reptile species, which are discussed in detail below (see section 9.4). Much of the work presented in this thesis provides new resources for reptiles, such as demonstrating the feasibility of sequencing isolated embryonic gonadal tissue for the first time. In particular, the data presented in Chapter 8 provides an essential new resource for *P. vitticeps* in demonstrating the efficacy of mammalian antibody staining in a reptile. The implications of this are also discussed in more detail below (see section 9.4).

Ultimately, the resources and techniques available for use in non-model species can only continue to grow, allowing research to expand in new directions to bring novel insights into environmentally sensitive sex determination systems.

9.4 Future Research Directions

As much as the research presented in this thesis brings new understanding to thermosensitive sex determination systems, it equally opens up many new questions and avenues for ongoing research. Despite the many challenges facing work on non-model species discussed above (see section 9.3) many approaches are still possible, and many more will become feasible in the future.

One of the most compelling aspects of the CaRe model is that it provides testable predictions and new experimental directions. In the context of sex reversal, the ultimate experimental goal is to inhibit sex reversal at high temperatures, and also induce sex reversal in the absence of the temperature cue. In *Pogona vitticeps*, the current model for sex reversal in reptiles, several possibilities present themselves. The CaRe model posits a central role for calcium signalling and redox regulation, and genes related to these processes were uniquely upregulated in sex reversing ZZf embryos compared to ZWf embryos (4.6.3). It follows that inhibition of these processes may stop sex reversal from occurring at high temperatures, and induction of them may cause sex reversal in the absence of the temperature cue. Such experiments may involve similar approaches to those used by the Capel team on *T. scripta*, where calcium chelators and ionophores were used in cell culture to determine the influence of calcium on the phosphorylation of STAT3 in the female sex determination pathway [22].

The development of new molecular resources is critical to all future research efforts. The sex determination characteristics of *P. vitticeps* present many interesting opportunities for future experiments. The demonstration of successful antibody staining in Chapter 8 represents an important advance for understanding protein dynamics during sex reversal. For example, though *CIRBP* has been implicated in TSD and sex reversal before, its function in this context is unknown [90,402]. Antibody staining for CIRBP during sex reversal may show a change in cellular localisation in response to temperature (Figure 9.1). Co-localisation of CIRBP in the cytoplasm with JARID2 and/or KDM6B would provide experimental support for CIRBP's role in stabilising these key transcripts, as hypothesised in Figure 9.1. The development of custom antibodies for the novel ΔN JARID2 and KDM6B variants (5.6.8) would also provide an indication of the role these isoforms play in sex reversal by showing their cellular localisation patterns, and their association with other proteins of interest. Antibodies can also be used for chromatin immunoprecipitation assays (ChIP-seq) to reveal the DNA binding sites of key proteins

such as JARID2 and KDM6B, and also can be used to analyse the methylation status of specific lysine resides like H3K27me3 and H3K4me3. Such work would prove invaluable for understanding the function of these proteins and their role in regulating changes in gene expression.

While much insight has been gained from bulk transcriptome sequencing, single cell sequencing techniques would be a powerful tool in gaining improved resolution of gene expression changes during development. In particular, single cell techniques can be used to distinguish the characteristics of specific cell types, and could be used to disaggregate the male and female cell types in ovotestes. It may also reveal that certain cell populations are more sensitive to temperature, and may be responsible for driving the initiation and maintenance of sex reversal.

Another intriguing element of the CaRe model is its predictions around the evolutionary conservation of thermosensitive sex determination mechanisms. Ongoing development of new model species, particularly those that may have sex reversal such as *A. muricatus* (Chapter 4), will improve understanding of the level of conservation in ESD mechanisms. Already we know that in species from the same genus, the thermosensitive TRP channels responsible for influx of calcium in response to temperature are not shared [25,26]. Without research investigating these mechanisms across the vertebrate phylogeny, the complex evolutionary dynamics of ESD systems will remain a mystery.

Even within *P. vitticeps*, which currently has been best studied sex reversal system of any reptile, much remains to be understood. Particularly compelling are the research avenues opened by the findings presented in Chapter 7, which showed that sex reversal relies on overcoming a variety of thresholds, and that these thresholds differ between individuals even from within the same clutch. The heritable elements of this, whether they be via transgenerational epigenetic inheritance or inheritance of allelic variation in crucial genes, warrants further investigation. There are several approaches that could be used to understand the mechanisms underlying temperature sensitivity and the propensity to sex reverse. This includes leveraging resources being developed at the University of Canberra's Animal House facility where breeding of males incubated at high temperatures but did not sex reverse can be used to create lines of animals that are insensitive to high temperature and thus do not undergo sex reversal. The genetic responses to temperature in these animals can then be compared to animals that do sex reverse to identify the genes responsible for conferring thermosensitivity and initiating

sex reversal. Previous research has also identified that in wild populations, animals living in the hottest part of the species range don't seem to sex reverse, suggesting local adaptation has changed the level of thermosensitivity [3,78]. Targeted sampling of animals in these areas and breeding of them under controlled conditions in the laboratory, would also be a viable approach to determine the genetic mechanisms underlying thermosensitivity and sex reversal.

Given that the timing of gonad differentiation in *P. vitticeps* is well understood, the potential to conduct experiments during embryonic development becomes almost limitless. In particular, developing organ culture techniques, such as those now commonly employed in in *T. scripta* [22,24], would open up many possibilities to chemically interfere with gonad differentiation, particularly as most targets of interest would be fatal to a whole embryo. This approach is crucial to demonstrate gene function in sex reversal pathways. For example, in the most recent work to employ this approach, a commercially available drug inhibitor for CLK4 was used in organ culture to demonstrate it is responsible for mediating splicing of *CIRBP* and *JARID2* in two turtle species [402]. This experiment could be used in a *P. vitticeps* organ culture system to determine the role of CLK4 in splicing, particularly as we now know that *JARID2* intron retention does not occur in sex reversed embryos (Chapter 6) its function likely differs.

The evidence for sex reversal occurring in *A. muricatus* (presented in Chapter 4) also provides new impetus to more closely explore the sex determination system of this species. As outlined in Chapter 2, there are several approaches to determine if a species has sex reversal. In the case of *A. muricatus*, future research can leverage existing resources available for the species, including a genome (prepared in collaboration with Dr Inge Seim at Nanjing Normal University), and DNA samples from across the species range, and different incubation temperatures. These resources would allow for an approach such as that used for *Bassiana duperreyi*, where a genome subtraction technique was used to identify sex linked markers, which were then applied across the species range to determine the prevalence of sex reversal in wild populations [50,79]. Sex linked markers may also be isolated used DArTSeq [64], a reduced genome representation technique [41,575], or gene dosage of sex related genes [40,576]. Given the broad distribution of *A. muricatus*, is it also possible that sex reversal or thermosensitivity may differ across the species range, perhaps in association with elevational gradients, which has been shown for *B. duperreyi* and *Niveoscincus ocellatus* [79,520].

9.5 Conclusions

The research presented in this thesis represents important advances towards finally answering the fundamental question in the field that has eluded explanation for decades: how does temperature determine sex? By using two emerging model organisms with environmentally sensitive sex determination systems, new insights have been gained in understanding the complex interplay between temperature and the epigenetic regulation of sex.

The theoretical elements of this thesis provide practical approaches for identifying sex reversal in new species (Chapter 2) and a novel framework for the proximal mechanisms by which environmental cues can be sensed by the cell and transduced to determine sex (Chapter 3). The experimental work presented in this thesis together reveals new insights into the sex determination system of *A. muricatus* (Chapter 4) and the genetic underpinnings of sex reversal in *P. vitticeps* (Chapter 5, Chapter 6, and Chapter 7). These findings do not exist in a vacuum; instead they build upon a robust foundation of research in the area of sex determination and differentiation in reptiles that began with the discovery of TSD in the 1960s [6].

While we still do not know precisely how temperature determines sex, we are closer than ever before to answering this question. We are on the cusp of critical discoveries, and this thesis is part of the body of knowledge that is driving this field towards these new horizons.

References

1. Bachtrog D *et al.* 2014 Sex Determination: Why So Many Ways of Doing It? *PLOS Biol.* **12**, e1001899. (doi:10.1371/journal.pbio.1001899)

2. Pokorná MJ, Kratochvíl L, Johnson Pokorna M, Kratochvil L. 2016 What was the ancestral sex-determining mechanism in amniote vertebrates? *Biol. Rev.* **91**, 1–12. (doi:10.1111/brv.12156)

3. Holleley CE, O'Meally D, Sarre SD, Marshall Graves JA, Ezaz T, Matsubara K, Azad B, Zhang X, Georges A. 2015 Sex reversal triggers the rapid transition from genetic to temperature-dependent sex. *Nature* **523**, 79–82. (doi:10.1038/nature14574)

4. Radder RS, Quinn AE, Georges A, Sarre SD, Shine R, Quinn AE, Georges A. 2008 Genetic evidence for co-occurrence of chromosomal and thermal sex-determining systems in a lizard. *Biol. Lett.* **4**, 176–178. (doi:10.1098/rsbl.2007.0583)

5. Sarre SD, Georges A, Quinn A. 2004 The ends of a continuum: Genetic and temperature-dependent sex determination in reptiles. *BioEssays* **26**, 639–645. (doi:10.1002/bies.20050)

6. Charnier M. 1966 Action of temperature on the sex ratio in the *Agama agama* (Agamidae, Lacertilia) embryo. *C R Seances Soc Biol Fil* **160**, 620–622.

7. Whiteley SL, Holleley CE, Ruscoe WA, Castelli M, Whitehead DL, Lei J, Georges A, Weisbecker V. 2017 Sex determination mode does not affect body or genital development of the central bearded dragon (*Pogona vitticeps*). *Evodevo* **8**. (doi:10.1186/s13227-017-0087-5)

8. Whiteley SL, Weisbecker V, Georges A, Gauthier ARG, Whitehead DL, Holleley CE. 2018 Developmental asynchrony and antagonism of sex determination pathways in a lizard with temperature-induced sex reversal. *Sci. Rep.* **8**, 1–9. (doi:10.1038/s41598-018-33170-y)

9. Irisarri I *et al.* 2017 Phylotranscriptomic consolidation of the jawed vertebrate timetree. *Nat. Ecol. Evol.* **1**, 1370–1378. (doi:10.1038/s41559-017-0240-5)

10. Alam SMI, Sarre SD, Gleeson D, Georges A, Ezaz T. 2018 Did lizards follow unique pathways in sex chromosome evolution? *Genes (Basel).* **9**. (doi:10.3390/genes9050239)

11. Eggers S, Ohnesorg T, Sinclair A. 2014 Genetic regulation of mammalian gonad

development. *Nat. Rev. Endocrinol.* **10**, 673–683. (doi:10.1038/nrendo.2014.163)

12. Smith CA, Sinclair AH. 2004 Sex determination: Insights from the chicken. *BioEssays* **26**, 120–132. (doi:10.1002/bies.10400)

13. Vining B, Ming Z, Fam SB, Harley V. 2021 Diverse Regulation but Conserved Function : SOX9 in Vertebrate Sex Determination. *Genes (Basel).* **12**. (doi:doi.org/10.3390/genes12040486)

14. Ortega-Recalde O, Goikoetxea A, Hore TA, Todd E V., Gemmell NJ. 2020 The Genetics and Epigenetics of Sex Change in Fish. *Annu. Rev. Anim. Biosci.* **8**, 47–69. (doi:10.1146/annurev-animal-021419-083634)

15. Valenzuela N. 2008 Sexual development and the evolution of sex determination. *Sex. Dev.* **2**, 64–72. (doi:10.1159/000129691)

16. Capel B. 2017 Vertebrate sex determination: evolutionary plasticity of a fundamental switch. *Nat. Rev. Genet.* **18**, 675–689. (doi:10.1038/nrg.2017.60)

17. Morrish BC, Sinclair AH. 2002 Vertebrate sex determination: Many means to an end. *Reproduction* **124**, 447–457. (doi:10.1530/rep.0.1240447)

18. DeFalco T, Capel B. 2009 Gonad morphogenesis in vertebrates: divergent means to a convergent end. *Annu. Rev. Cell Dev. Biol.* **25**, 457–482. (doi:doi:10.1146/annurev.cellbio.042308.13350)

19. Budd A, Banh Q, Domingos J, Jerry D. 2015 Sex control in fish: Approaches, challenges and opportunities for aquaculture. *J. Mar. Sci. Eng.* **3**, 329–355. (doi:10.3390/jmse3020329)

20. Todd E V, Liu H, Muncaster S, Gemmell NJ. 2016 Bending genders: The biology of natural sex change in fish. *Sex. Dev.* **10**, 223–241. (doi:10.1159/000449297)

21. Holleley CE, Sarre SD, O'Meally D, Georges A. 2016 Sex reversal in reptiles: Reproductive oddity or powerful driver of evolutionary change? *Sex. Dev.* **10**, 279–287. (doi:10.1159/000450972)

22. Weber C, Zhou Y, Lee J, Looger L, Qian G, Ge C, Capel B. 2020 Temperature-dependent sex determination is mediated by pSTAT3 repression of Kdm6b. *Science (80-.).* **3**, 303–306.

23. Ge C, Ye J, Zhang H, Zhang Y, Sun W, Sang Y, Capel B, Qian G. 2017 Dmrt1 induces the male pathway in a turtle species with temperature-dependent sex determination.

Development **144**, 2222–2233. (doi:10.1242/dev.152033)

24. Ge C, Ye J, Weber C, Sun W, Zhang H, Zhou Y, Cai C, Qian G, Capel B. 2018 The histone demethylase KDM6B regulates temperature-dependent sex determination in a turtle species. *Science (80-.).* **360**, 645–648. (doi:10.1126/science.aap8328)

25. Yatsu R *et al.* 2015 TRPV4 associates environmental temperature and sex determination in the American alligator. *Sci. Rep.* **5**, 1–10. (doi:10.1038/srep18581)

26. Lin JQ, Zhou Q, Yang HQ, Fang LM, Tang KY, Sun L, Wan QH, Fang SG. 2018 Molecular mechanism of temperature-dependent sex determination and differentiation in Chinese alligator revealed by developmental transcriptome profiling. *Sci. Bull.* **63**, 209–212. (doi:10.1016/j.scib.2018.01.004)

27. Quinn AE, Sarre SD, Ezaz T, Marshall Graves JA, Georges A. 2011 Evolutionary transitions between mechanisms of sex determination in vertebrates. *Biol. Lett.* **7**, 443–448. (doi:10.1098/rsbl.2010.1126)

28. Valenzuela N, Adams DC, Janzen FJ. 2003 Pattern Does Not Equal Process: Exactly When Is Sex Environmentally Determined? *Am. Nat.* **161**, 676–683. (doi:10.1086/368292)

29. Weber C, Capel B. 2018 Sex reversal. *Curr. Biol.* **28**, R1234–R1236. (doi:10.1016/j.cub.2018.09.043)

30. Dupoué A *et al.* 2019 Some like it dry: Water restriction overrides heterogametic sex determination in two reptiles. *Ecol. Evol.* **9**, 6524–6533. (doi:10.1002/ece3.5229)

31. Wang Q *et al.* 2019 Gonad transcriptome analysis of high temperature induced sex reversal in Chinese Tongue Sole, *Cynoglossus semilaevis*. *Front. Genet.* **10**, 1–11. (doi:10.3389/FGENE.2019.01128)

32. Hattori RS *et al.* 2009 Cortisol-induced masculinization: Does thermal stress affect gonadal fate in pejerrey, a teleost fish with temperature-dependent sex determination? *PLoS One* **4**, e6548. (doi:10.1371/journal.pone.0006548)

33. Hattori R, Castaneda-Cortes D, Arias Padilla L, Strobl-Mazzulla P, Fernandino J. 2020 Activation of stress response axis as a key process in environment - induced sex plasticity in fish. *Cell. Mol. Life Sci.* **77**, 4223–4236. (doi:10.1007/s00018-020-03532-9)

34. Eggert C. 2004 Sex determination: The amphibian models. *Reprod. Nutr. Dev.* **44**, 539–549. (doi:10.1051/rnd:2004062)

35. Flament S. 2016 Sex reversal in amphibians. *Sex. Dev.* **10**, 267–278. (doi:10.1159/000448797)

36. Nemesházi E *et al.* 2020 Novel genetic sex markers reveal high frequency of sex reversal in wild populations of the agile frog (*Rana dalmatina*) associated with anthropogenic land use. *Mol. Ecol.* , 3607–3621. (doi:10.1111/mec.15596)

37. Shine R, Elphick MJ, Donnellan S. 2002 Co-occurrence of multiple, supposedly incompatible modes of sex determination in a lizard population. *Ecol. Lett.* **5**, 486–489. (doi:10.1046/j.1461-0248.2002.00351.x)

38. Quinn AE, Georges A, Sarre SD, Guarino F, Ezaz T, Marshall Graves JA. 2007 Temperature sex reversal implies sex gene dosage in a reptile. *Science (80-.).* **316**, 411. (doi:10.1126/science.1135925)

39. Whiteley SL, Georges A, Weisbecker V, Schwanz LE, Holleley CE. 2021 Ovotestes suggest cryptic genetic influence in a reptile model for temperature-dependent sex determination. *Proc. R. Soc. B* **288**, 20202819. (doi:doi.org/10.1098/rspb.2020.2819)

40. Wiggins JM, Santoyo-Brito E, Scales JB, Fox SF. 2020 Gene dose indicates presence of sex chromosomes in collared lizards (*Crotaphytus collaris*), a species with temperature-influenced sex determination. *Herpetologica* **76**, 27–30. (doi:10.1655/herpetologica-d-19-00036)

41. Hill PL, Burridge CP, Ezaz T, Wapstra E. 2018 Conservation of sex-linked markers among conspecific populations of a viviparous skink, *Niveoscincus ocellatus*, exhibiting genetic and temperature-dependent sex determination. *Genome Biol. Evol.* **10**, 1079–1087. (doi:10.1093/gbe/evy042)

42. Cornejo-Paramo P, Dissanayake DSB, Lira-noriega A, Martinez-pacheco M, Suastegui CR. 2020 Viviparous reptile regarded to have temperature-dependent sex determination has old XY chromosomes. *Genome Biol. Evol.* **12**, 924–930. (doi:10.1093/gbe/evaa104/5841216)

43. Wang C, Tang X, Xin Y, Yue F, Yan X, Liu B, An B, Wang X, Chen Q. 2015 Identification of sex chromosomes by means of comparative genomic hybridization in a lizard, *Eremias multiocellata*. *Zoolog. Sci.* **32**, 151–156. (doi:10.2108/zs130246)

44. Tokunaga S. 1985 Temperature-dependent sex determination in *Gekko japonicus* (Gekkonidae, Reptilia). *Dev. Growth Differ.* **27**, 117–120. (doi:10.1111/j.1440-169X.1985.00117.x)

45. Ezaz T, Quinn AE, Miura I, Sarre SD, Georges A, Marshall Graves JA. 2005 The dragon lizard *Pogona vitticeps* has ZZ/ZW micro-sex chromosomes. *Chromosom. Res.* **13**, 763–776. (doi:10.1007/s10577-005-1010-9)

46. Sankovic N, Delbridge ML, Grützner F, Ferguson-Smith MA, O'Brien PCM, Marshall Graves JA. 2006 Construction of a highly enriched marsupial Y chromosome-specific BAC sub-library using isolated Y chromosomes. *Chromosom. Res.* **14**, 657–664. (doi:10.1007/s10577-006-1076-z)

47. Chen N, Bellott DW, Page DC, Clark AG. 2012 Identification of avian W-linked contigs by short-read sequencing. *BMC Genomics* **13**, 2–9. (doi:10.1186/1471-2164-13-183)

48. Traut W, Vogel H, Glöckner G, Hartmann E, Heckel DG. 2013 High-throughput sequencing of a single chromosome: A moth W chromosome. *Chromosom. Res.* **21**, 491–505. (doi:10.1007/s10577-013-9376-6)

49. Palmer DH, Rogers TF, Dean R, Wright AE. 2019 How to identify sex chromosomes and their turnover. *Mol. Ecol.* **28**, 4709–4724. (doi:10.1111/mec.15245)

50. Dissanayake DSB, Holleley CE, Hill LK, O'Meally D, Deakin JE, Georges A. 2020 Identification of y chromosome markers in the eastern three-lined skink (*Bassiana duperreyi*) using in silico whole genome subtraction. *BMC Genomics* **21**, 1–12. (doi:10.1186/s12864-020-07071-2)

51. Bókony V, Kövér S, Nemesházi E, Liker A, Székely T. 2017 Climate-driven shifts in adult sex ratios via sex reversals: The type of sex determination matters. *Philos. Trans. R. Soc. B Biol. Sci.* **372**. (doi:10.1098/rstb.2016.0325)

52. Schwanz LE, Georges A, Holleley CE, Sarre SD. 2020 Climate change, sex reversal and lability of sex-determining systems. *J. Evol. Biol.* **33**, 270–281. (doi:10.1111/jeb.13587)

53. Castelli MA, Whiteley SL, Georges A, Holleley CE. 2020 Cellular calcium and redox regulation: The mediator of vertebrate environmental sex determination? *Biol. Rev.* **95**, 680–695. (doi:doi:10.1111/brv.12582)

54. Whiteley SL, Holleley CE, Blackburn J, Deveson IW, Wagner S, Marshall Graves JA, Georges A. 2021 Two transcriptionally disctinct pathways drive female development in a reptile with temperature induced sex reversal. *PLoS Genet.* **17**, e1009465. (doi:10.1371/journal.pgen.1009465)

55. Deveson IW, Holleley CE, Blackburn J, Marshall Graves JA, Mattick JS, Waters PD, Georges A. 2017 Differential intron retention in Jumonji chromatin modifier genes is

implicated in reptile temperature-dependent sex determination. *Sci. Adv.* **3**, e1700731. (doi:10.1126/sciadv.1700731)

56. Girondot M, Zaborski P, Servan J, Pieau C. 1994 Genetic contribution to sex determination in turtles with environmental sex determination. *Genet. Res.* **63**, 117–127. (doi:10.1017/S0016672300032225)

57. Traut W, Eickhof U, Schorch JC. 2001 Identification and analysis of sex chromosomes by comparative genomic hybridization (CGH). *Methods Cell Sci.* **23**, 155–161. (doi:10.1007/978-94-010-0330-8_16)

58. Lee B, Coutanceau J, Ozouf-Costz C, D'Cotta H, Baroiller J, Kocher T. 2011 Genetic and physical mapping for sex-link AFLP markers in Nile tilapia (*Oreochromis niloticus*). *Mar. Biotechnol.* **13**, 557–562. (doi:10.1007/s10126-010-9326-7.Genetic)

59. Ezaz T *et al.* 2013 Sequence and gene content of a large fragment of a lizard sex chromosome and evaluation of candidate sex differentiating gene R-spondin 1. *BMC Genomics* **14**, 899. (doi:10.1186/1471-2164-14-899)

60. Ayers KL, Davidson NM, Demiyah D, Roeszler KN, Grützner F, Sinclair AH, Oshlack A, Smith CA. 2013 RNA sequencing reveals sexually dimorphic gene expression before gonadal differentiation in chicken and allows comprehensive annotation of the W-chromosome. *Genome Biol.* **14**, 1–16. (doi:10.1186/gb-2013-14-3-r26)

61. Bidon T, Schreck N, Hailer F, Nilsson MA, Janke A. 2015 Genome-wide search identifies 1.9 Mb from the polar bear Y chromosome for evolutionary analyses. *Genome Biol. Evol.* **7**, 2010–2022. (doi:10.1093/gbe/evv103)

62. Gamble T, Zarkower D. 2014 Identification of sex-specific molecular markers using restriction site-associated DNA sequencing. *Mol. Ecol. Resour.* **14**, 902–913. (doi:10.1111/1755-0998.12237)

63. Gamble T. 2016 Using RAD-seq to recognize sex-specific markers and sex chromosome systems. *Mol. Ecol.* **25**, 2114–2116. (doi:10.1111/mec.13648)

64. Kilian A *et al.* 2012 Diversity Arrays Technology: A generic genome profiling technology on open platforms. In *Data Production and Analysis in Population Genomics*, pp. 67–89.

65. Lowry DB, Hoban S, Kelley JL, Lotterhos KE, Reed LK, Antolin MF, Storfer A. 2017 Breaking RAD: an evaluation of the utility of restriction site-associated DNA sequencing for genome scans of adaptation. *Mol. Ecol. Resour.* **17**, 142–152. (doi:10.1111/1755-

0998.12635)

66. Deakin JE *et al.* 2019 Chromosomics: Bridging the gap between genomes and chromosomes. *Reprod. Fertil. Dev.* **31**, 1189–1202. (doi:10.1071/RD18201)

67. Quinn AE, Radder RS, Sarre SD, Georges A, Ezaz T, Shine R. 2009 Isolation and development of a molecular sex marker for Bassiana duperrey, a lizard with XX/XY sex chromosomes and temperature-induced sex reversal. *Mol. Genet. Genomics* **281**, 665–672. (doi:10.1007/s00438-009-0437-7)

68. Sakae Y, Oikawa A, Sugiura Y, Mita M, Nakamura S, Nishimura T. 2020 Starvation causes female-to-male sex reversal through lipid metabolism in the teleost fish, medaka (*Olyzias latipes*). *Biol. Open* **9**, 1–12. (doi:10.1242/bio.050054)

69. García-Cruz EL, Yamamoto Y, Hattori RS, de Vasconcelos LM, Yokota M, Strüssmann CA. 2020 Crowding stress during the period of sex determination causes masculinization in pejerrey *Odontesthes bonariensis*, a fish with temperature-dependent sex determination. *Comp. Biochem. Physiol. -Part A Mol. Integr. Physiol.* **245**, 110701. (doi:10.1016/j.cbpa.2020.110701)

70. Warner DAA, Radder RSS, Shine R. 2009 Corticosterone Exposure during Embryonic Development Affects Offspring Growth and Sex Ratios in Opposing Directions in Two Lizard Species with Environmental Sex Determination. *Physiol. Biochem. Zool.* **82**, 363–371. (doi:10.1086/588491)

71. Ballen CJ, Shine R, Andrews RM, Olsson M. 2016 Multifactorial Sex Determination in Chameleons. *J. Herpetol.* **50**, 548–551. (doi:10.1670/15-003)

72. Trenkel VM, Boudry P, Verrez-Bagnis V, Lorance P. 2020 Methods for identifying and interpreting sex-linked SNP markers and carrying out sex assignment: application to thornback ray (*Raja clavata*). *Mol. Ecol. Resour.* **00**, 1–10. (doi:10.1111/1755-0998.13225)

73. Rovatsos M, Johnson Pokorna, M Kratochvil L. 2015 Differentiation of Sex Chromosomes and Karyotype Characterisation in the Dragonsnake *Xenodermus javanicus* (Squamata: Xenodermatidae). *Cytogenet. Genome Res.* **147**, 48–54.

74. Antonio-Rubio N, Villagrán-Santa Cruz M, Santos-Vázquez A, Moreno-Mendoza N. 2015 Gonadal morphogenesis and sex differentiation in the oviparous lizard, *Sceloporus aeneus* (Squamata: Phrynosomatidae). *Zoomorphology* **134**, 279–289. (doi:10.1007/s00435-015-0259-6)

75. Harlow PS. 1996 A Harmless Technique for Sexing Hatchling Lizards. *Herpetol. Rev.* **27**, 71–72.

76. Li H, Holleley CE, Elphick M, Georges A, Shine R. 2016 The behavioural consequences of sex reversal in dragons. *Proc. R. Soc. B Biol. Sci.* **283**, 1–7. (doi:10.1098/rspb.2016.0217)

77. Jones MEH, Pistevos JCA, Cooper N, Lappin AK, Georges A, Hutchinson MN, Holleley CE. 2020 Reproductive phenotype predicts adult bite-force performance in sex-reversed dragons (*Pogona vitticeps*). *J. Exp. Zool. Part A Ecol. Integr. Physiol.* **333**, 252–263. (doi:10.1002/jez.2353)

78. Castelli MA, Georges A, Cherryh C, Rosauer DF, Stephen D. Sarre, Isabella Contador-Kelsall, Holleley CE. 2020 Evolving thermal thresholds explain the distribution of temperature sex reversal in an Australian dragon lizard. *Divers. Distrib.* **27**, 427–438. (doi:doi.org/10.1111/ddi.13203)

79. Dissanayake DS., Holleley CE, Deakin JE, Georges A. 2021 High elevation increases the risk of Y chromosome loss in Alpine skink populations with sex reversal. *Heredity (Edinb).* **126**, 805–816. (doi:10.1038/s41437-021-00406-z)

80. Fisher R. 1930 *The genetical theory of natural selection*. Oxford: Oxford University Press.

81. Charnov EL, Bull J. 1977 When is sex environmentally determined? *Nature* **266**, 828–830.

82. McGaugh SE, Janzen FJ. 2011 Effective heritability of targets of sex-ratio selection under environmental sex determination. *J. Evol. Biol.* **24**, 784–794. (doi:10.1111/j.1420-9101.2010.02211.x)

83. Geffroy B, Wedekind C. 2020 Effects of global warming on sex ratios in fishes. *J. Fish Biol.* (doi:10.1111/jfb.14429)

84. Mitchell NJ, Janzen FJ. 2010 Temperature-Dependent sex determination and contemporary climate change. *Sex. Dev.* **4**, 129–140. (doi:10.1159/000282494)

85. Refsnider JM, Janzen FJ. 2016 Temperature-dependent sex determination under rapid anthropogenic environmental change: Evolution at a turtle's pace? *J Hered* **107**, 61–70. (doi:10.1093/jhered/esv053)

86. Breitenbach AT, Carter AW, Paitz RT, Bowden RM. 2020 Using naturalistic incubation

temperatures to demonstrate how variation in the timing and continuity of heat wave exposure influences phenotype. *Proceedings. Biol. Sci.* **287**, 20200992. (doi:10.1098/rspb.2020.0992)

87. Booth D, Dunstan A, Bell I, Reina R, Tedeschi J. 2020 Low male production at the world's largest green turtle rookery. *Mar. Ecol. Prog. Ser.* **653**, 181–190. (doi:10.3354/meps13500)

88. Mittwoch U. 2000 Three thousand years of questioning sex determination. *Cytogenet. Genome Res.* **91**, 186–191. (doi:10.1159/000056842)

89. Mittwoch U. 2013 Sex determination. *EMBO Rep.* **14**, 588–592. (doi:10.1038/embor.2013.84)

90. Schroeder AL, Metzger KJ, Miller A, Rhen T. 2016 A novel candidate gene for temperature-dependent sex determination in the Common Snapping Turtle. *Genetics* **203**, 557–571. (doi:10.1534/genetics.115.182840)

91. Cutting A, Chue J, Smith CA. 2013 Just how conserved is vertebrate sex determination? *Dev. Dyn.* **242**, 380–387. (doi:10.1002/dvdy.23944)

92. Rhen T, Schroeder A. 2010 Molecular mechanisms of sex determination in reptiles. *Sex. Dev.* **4**, 16–28. (doi:10.1159/000282495)

93. Yatsu R *et al.* 2016 RNA-seq analysis of the gonadal transcriptome during *Alligator mississippiensis* temperature-dependent sex determination and differentiation. *BMC Genomics* **17**, 17–77. (doi:10.1186/s12864-016-2396-9)

94. Czerwinski M, Natarajan A, Barske L, Looger LL, Capel B. 2016 A timecourse analysis of systemic and gonadal effects of temperature on sexual development of the red-eared slider turtle Trachemys scripta elegans. *Dev. Biol.* **420**, 166–177. (doi:10.1016/j.ydbio.2016.09.018)

95. Corona-Herrera GA *et al.* 2018 Experimental evidence of masculinization by continuous illumination in a temperature sex determination teleost (Atherinopsidae) model: is oxidative stress involved? *J. Fish Biol.* **93**, 229–237. (doi:10.1111/jfb.13651)

96. Hayasaka O, Takeuchi Y, Shiozaki K, Anraku K, Kotani T. 2019 Green light irradiation during sex differentiation induces female-to-male sex reversal in the medaka *Oryzias latipes*. *Sci. Rep.* **9**, 2383. (doi:10.1038/s41598-019-38908-w)

97. Richter C, Kass GEN. 1991 Oxidative stress in mitochondria: Its relationship to cellular

Ca^{2+} homeostasis, cell death, proliferation and differentiation. *Chem. Biol. Interact.* **77**, 1–23. (doi:10.1016/0009-2797(91)90002-O)

98. Gordeeva A V., Zvyagilskaya RA, Labas YA. 2003 Cross-talk between reactive oxygen species and calcium in living cells. *Biochem.* **68**, 1077–1080. (doi:10.1023/A:1026398310003)

99. Camello-Almaraz C, Gomez-Pinilla PJ, Pozo MJ, Camello PJ. 2006 Mitochondrial reactive oxygen species and Ca^{2+} signaling. *AJP Cell Physiol.* **291**, C1082–C1088. (doi:10.1152/ajpcell.00217.2006)

100. Görlach A, Bertram K, Hudecova S, Krizanova O. 2015 Calcium and ROS: A mutual interplay. *Redox Biol.* **6**, 260–271. (doi:10.1016/j.redox.2015.08.010)

101. Yan Y, Wei C, Zhang W, Cheng H, Liu J. 2006 Cross-talk between calcium and reactive oxygen species signaling. *Acta Pharmacol. Sin.* **27**, 821–826. (doi:10.1016/j.ceca.2017.01.007)

102. Metcalfe NB, Alonso-Alvarez C. 2010 Oxidative stress as a life-history constraint: The role of reactive oxygen species in shaping phenotypes from conception to death. *Funct. Ecol.* **24**, 984–996. (doi:10.1111/j.1365-2435.2010.01750.x)

103. Martindale JL, Holbrook NJ. 2002 Cellular response to oxidative stress: Signaling for suicide and survival. *J. Cell. Physiol.* **192**, 1–15. (doi:10.1002/jcp.10119)

104. Temple MD, Perrone GG, Dawes IW. 2005 Complex cellular responses to reactive oxygen species. *Trends Cell Biol.* **15**, 319–326. (doi:10.1016/j.tcb.2005.04.003)

105. Hamanaka RB, Chandel NS. 2010 Mitochondrial reactive oxygen species regulate cellular signaling and dictate biological outcomes. *Trends Biochem. Sci.* **35**, 505–513. (doi:10.1016/j.tibs.2010.04.002)

106. Treidel LA, Carter AW, Bowden RM. 2016 Temperature experienced during incubation affects antioxidant capacity but not oxidative damage in hatchling red-eared slider turtles (*Trachemys scripta elegans*). *J. Exp. Biol.* **219**, 561–570. (doi:10.1242/jeb.128843)

107. Covarrubias L, Hernández-García D, Schnabel D, Salas-Vidal E, Castro-Obregón S. 2008 Function of reactive oxygen species during animal development: Passive or active? *Dev. Biol.* **320**, 1–11. (doi:https://doi.org/10.1016/j.ydbio.2008.04.041)

108. Dowling DK, Simmons LW. 2009 Reactive oxygen species as universal constraints in life-history evolution. *Proc. R. Soc. B Biol. Sci.* **22**, 1737–45.

(doi:10.1098/rspb.2008.1791)

109. Sies H, Berndt C, Jones DP. 2017 Oxidative stress. *Annu. Rev. Biochem.* **86**, 715–748. (doi:10.1146/annurev-biochem-061516-045037)

110. Hammond CL, Lee TK, Ballatori N. 2001 Novel roles for glutathione in gene expression, cell death, and membrane transport of organic solutes. *J. Hepatol.* **34**, 946–954. (doi:10.1016/S0168-8278(01)00037-X)

111. Morgan MJ, Liu Z. 2011 Crosstalk of reactive oxygen species and NF-κB signaling. *Cell Res.* **21**, 103–115. (doi:10.1038/cr.2010.178)

112. Cremers CM, Jakob U. 2013 Oxidant sensing by reversible disulfide bond formation. *J. Biol. Chem.* **288**, 26489–26496. (doi:10.1074/jbc.R113.462929)

113. Sen C, Packer L. 1996 Antioxidant and redox regulation of gene transcription. *FASEB* **10**, 709–720. (doi:https://doi.org/10.1096/fasebj.10.7.8635688)

114. Antelmann H, Helmann JD. 2010 Thiol-based redox switches and gene regulation. *Antioxidants Redox Signal.* **14**, 1049–1063. (doi:10.1089/ars.2010.3400)

115. Cyr AR, Domann FE. 2011 The Redox Basis of Epigenetic Modifications: From Mechanisms to Functional Consequences. *Antioxid. Redox Signal.* **15**, 551–589. (doi:10.1089/ars.2010.3492)

116. Timme-Laragy AR, Hahn ME, Hansen JM, Rastogi A, Roy MA. 2018 Redox stress and signaling during vertebrate embryonic development: Regulation and responses. *Semin. Cell Dev. Biol.* **80**, 17–28. (doi:10.1016/j.semcdb.2017.09.019)

117. West AE, Chen WG, Dalva MB, Dolmetsch RE, Kornhauser JM, Shaywitz AJ, Takasu MA, Tao X, Greenberg ME. 2001 Calcium regulation of neuronal gene expression. *Proc. Natl. Acad. Sci.* **98**, 11024–11031. (doi:10.1073/pnas.191352298)

118. Contreras L, Drago I, Zampese E, Pozzan T. 2010 Mitochondria: The calcium connection. *Biochim. Biophys. Acta - Bioenerg.* **1797**, 607–618. (doi:10.1016/j.bbabio.2010.05.005)

119. Plattner H, Verkhratsky A. 2015 The ancient roots of calcium signalling evolutionary tree. *Cell Calcium* **57**, 123–132. (doi:10.1016/j.ceca.2014.12.004)

120. Hilton JK, Rath P, Helsell CVM, Beckstein O, Van Horn WD. 2015 Understanding thermosensitive transient receptor potential channels as versatile polymodal cellular sensors. *Biochemistry* **54**, 2401–2413. (doi:10.1021/acs.biochem.5b00071)

121. Ermak G, Davies KJA. 2002 Calcium and oxidative stress: From cell signaling to cell death. *Mol. Immunol.* **38**, 713–721. (doi:10.1016/S0161-5890(01)00108-0)

122. Rottingen, Iversen, Røttingen JA, Iversen JG. 2000 Ruled by waves? Intracellular and intercellular calcium signalling. *Acta Physiol. Scand.* **169**, 203–219. (doi:10.1046/j.1365-201x.2000.00732.x)

123. Berridge MJ, Bootman MD, Roderick HL. 2003 Calcium signalling: Dynamics, homeostasis and remodelling. *Nat. Rev. Mol. Cell Biol.* **4**, 517–529. (doi:10.1038/nrm1155)

124. Brostrom MA, Brostrom CO. 2003 Calcium dynamics and endoplasmic reticular function in the regulation of protein synthesis: Implications for cell growth and adaptability. *Cell Calcium* **34**, 345–363. (doi:10.1016/S0143-4160(03)00127-1)

125. Dupont G, Sneyd J. 2017 Recent developments in models of calcium signalling. *Curr. Opin. Syst. Biol.* **3**, 15–22. (doi:10.1016/J.COISB.2017.03.002)

126. Sharma A, Nguyen H, Geng C, Hinman MN, Luo G, Lou H. 2014 Calcium-mediated histone modifications regulate alternative splicing in cardiomyocytes. *Proc. Natl. Acad. Sci.* **111**, E4920–E4928. (doi:10.1073/pnas.1408964111)

127. Ahn S-GG, Thiele DJ. 2003 Redox regulation of mammalian heat shock factor 1 is essential for Hsp gene activation and protection from stress. *Genes Dev.* **17**, 516–528. (doi:10.1101/gad.1044503)

128. Schieven GL, Kirihara JM, Gilliland LK, Uckun FM, Ledbetter JA. 1993 Ultraviolet radiation rapidly induces tyrosine phosphorylation and calcium signaling in lymphocytes. *Mol. Biol. Cell* **4**, 523–530. (doi:10.1091/mbc.4.5.523)

129. Gniadecki R, Thorn T, Vicanova J, Petersen A, Wulf HC. 2000 Role of mitochondria in ultraviolet-induced oxidative stress. *J. Cell. Biochem.* **80**, 216–222. (doi:10.1002/1097-4644(20010201)80:2<216::aid-jcb100>3.0.co;2-h)

130. Chandel NS, Trzyna WC, McClintock DS, Schumacker PT. 2000 Role of oxidants in NF-κB activation and TNF-α gene transcription induced by hypoxia and endotoxin. *J. Immunol.* **165**, 1013–1021. (doi:10.4049/jimmunol.165.2.1013)

131. Ye YZ, Ma L, Sun BJ, Li T, Wang Y, Shine R, Du WG. 2019 The embryos of turtles can influence their own sexual destinies. *Curr. Biol.* **29**, 2597–2603. (doi:10.1016/j.cub.2019.06.038)

132. Wang Y, Huang YY, Wang Y, Lyu P, Hamblin MR. 2016 Photobiomodulation (blue and green light) encourages osteoblastic-differentiation of human adipose-derived stem cells: Role of intracellular calcium and light-gated ion channels. *Sci. Rep.* **6**, 33719. (doi:10.1038/srep33719)

133. Lavi R, Shainberg A, Friedmann H, Shneyvays V, Rickover O, Eichler M, Kaplan D, Lubart R. 2003 Low energy visible light induces reactive oxygen species generation and stimulates an increase of intracellular calcium concentration in cardiac cells. *J. Biol. Chem.* **278**, 40917–40922. (doi:10.1074/jbc.M303034200)

134. Materazzi S *et al.* 2012 TRPA1 and TRPV4 mediate paclitaxel-induced peripheral neuropathy in mice via a glutathione-sensitive mechanism. *Pflugers Arch. Eur. J. Physiol.* **463**, 561–569. (doi:10.1007/s00424-011-1071-x)

135. Kozai D, Ogawa N, Mori Y. 2013 Redox regulation of transient receptor potential channels. *Antioxid. Redox Signal.* **21**, 971–986. (doi:10.1089/ars.2013.5616)

136. Ogawa N, Kurokawa T, Mori Y. 2016 Sensing of redox status by TRP channels. *Cell Calcium* **60**, 115–122. (doi:10.1016/j.ceca.2016.02.009)

137. Kumar A, Kumari S, Majhi RK, Swain N, Yadav M, Goswami C. 2015 Regulation of TRP channels by steroids: Implications in physiology and diseases. *Gen. Comp. Endocrinol.* **220**, 23–32. (doi:10.1016/j.ygcen.2014.10.004)

138. Clarke A, Fraser KPP. 2004 Why does metabolism scale with temperature? *Funct. Ecol.* **18**, 243–251. (doi:10.1111/j.0269-8463.2004.00841.x)

139. Halliwell B, Gutteridge JMC. 2015 *Free Radicals in Biology and Medicine*. Oxford University Press.

140. Maurer LM, Yohannes E, Bondurant SS, Radmacher M, Slonczewski JL. 2005 pH regulates genes for flagellar motility, catabolism, and oxidative stress in *Escherichia coli* K-12. *J. Bacteriol.* **187**, 304–319. (doi:10.1128/JB.187.1.304-319.2005)

141. Wang WN, Zhou J, Wang P, Tian TT, Zheng Y, Liu Y, Mai W jun, Wang AL. 2009 Oxidative stress, DNA damage and antioxidant enzyme gene expression in the Pacific white shrimp, *Litopenaeus vannamei* when exposed to acute pH stress. *Comp. Biochem. Physiol. Part C - Toxicol. Pharmacol.* **150**, 428–435. (doi:10.1016/j.cbpc.2009.06.010)

142. de Jager TL, Cockrell AE, Du Plessis SS. 2017 Ultraviolet light induced generation of reactive oxygen species. *Adv. Exp. Med. Biol.* **996**, 15–23. (doi:10.1007/978-3-319-56017-5_2)

143. Hirayama J, Cho S, Sassone-Corsi P. 2007 Circadian control by the reduction/oxidation pathway: Catalase represses light-dependent clock gene expression in the zebrafish. *Proc. Natl. Acad. Sci.* **104**, 15747–15752. (doi:10.1073/pnas.0705614104)

144. Sun BJ, Li T, Gao J, Ma L, Du WG. 2015 High incubation temperatures enhance mitochondrial energy metabolism in reptile embryos. *Sci. Rep.* **5**, 8861. (doi:10.1038/srep08861)

145. Deeming DC, Pike TW. 2013 Embryonic growth and antioxidant provision in avian eggs. *Biol. Lett.* **9**, 20130757. (doi:10.1098/rsbl.2013.0757)

146. Birnie-Gauvin K, Costantini D, Cooke SJ, Willmore WG. 2017 A comparative and evolutionary approach to oxidative stress in fish: A review. *Fish Fish.* **18**, 928–942. (doi:10.1111/faf.12215)

147. Border SE, Deoliveira GM, Janeski HM, Piefke TJ, Brown TJ, Dijkstra PD. 2019 Social rank, color morph, and social network metrics predict oxidative stress in a cichlid fish. *Behav. Ecol.* **30**, 490–499. (doi:10.1093/beheco/ary189)

148. Beaulieu M, Mboumba S, Willaume E, Kappeler PM, Charpentier MJE. 2014 The oxidative cost of unstable social dominance. *J. Exp. Biol.* **217**, 2629–2632. (doi:10.1242/jeb.104851)

149. Todd E V *et al.* 2019 Stress, novel sex genes and epigenetic reprogramming orchestrate socially controlled sex change. *Sci. Adv.* **5**, eaaw7006. (doi:10.1126/sciadv.aaw7006)

150. Antonsson A, Hughes K, Edin S, Grundstrom T. 2003 Regulation of c-Rel nuclear localization by binding of Ca^{2+}/calmodulin. *Mol. Cell. Biol.* **23**, 1418–1427. (doi:10.1128/mcb.23.4.1418-1427.2003)

151. Josso N, di Clemente N. 2003 Transduction pathway of anti-Müllerian hormone, a sex-specific member of the TGF-β family. *Trends Endocrinol. Metab.* **14**, 91–97. (doi:10.1016/S1043-2760(03)00005-5)

152. Hong CY, Park JH, Seo KH, Kim J-M, Im SY, Lee JW, Choi H-S, Lee K. 2003 Expression of MIS in the testis is downregulated by tumor necrosis factor alpha through the negative regulation of SF-1 transactivation by NF-κB. *Mol. Cell. Biol.* **23**, 6000–6012. (doi:10.1128/MCB.23.17.6000-6012.2003)

153. Delfino F, Walker WH. 2014 Stage-specific nuclear expression of NF-κB in mammalian testis. *Mol. Endocrinol.* **12**, 1696–1707. (doi:10.1210/mend.12.11.0194)

154. Radhakrishnan S, Literman R, Neuwald J, Severin A, Valenzuela N. 2017 Transcriptomic responses to environmental temperature by turtles with temperature-dependent and genotypic sex determination assessed by RNAseq inform the genetic architecture of embryonic gonadal development. *PLoS One* **12**, e0172044. (doi:10.1371/journal.pone.0172044)

155. Pradhan A *et al.* 2012 Activation of NF-κB protein prevents the transition from juvenile ovary to testis and promotes ovarian development in zebrafish. *J. Biol. Chem.* **287**, 37926–37938. (doi:10.1074/jbc.M112.386284)

156. Wilson CA *et al.* 2014 Wild sex in zebrafish: Loss of the natural sex determinant in domesticated strains. *Genetics* **198**, 1291–1308. (doi:10.1534/genetics.114.169284)

157. Ribas L, Liew WC, Díaz N, Sreenivasan R, Orbán L, Piferrer F. 2017 Heat-induced masculinization in domesticated zebrafish is family-specific and yields a set of different gonadal transcriptomes. *Proc. Natl. Acad. Sci.* **114**, E941–E950. (doi:10.1073/pnas.1609411114)

158. Santos D, Luzio A, Coimbra AM. 2017 Zebrafish sex differentiation and gonad development: A review on the impact of environmental factors. *Aquat. Toxicol.* **191**, 141–163. (doi:10.1016/j.aquatox.2017.08.005)

159. Uchida D, Yamashita M, Kitano T, Iguchi T. 2004 An aromatase inhibitor or high water temperature induce oocyte apoptosis and depletion of P450 aromatase activity in the gonads of genetic female zebrafish during sex-reversal. *Comp. Biochem. Physiol. - A Mol. Integr. Physiol.* **137**, 11–20. (doi:10.1016/S1095-6433(03)00178-8)

160. Chen W, Liu L, Ge W. 2017 Expression analysis of growth differentiation factor 9 (Gdf9/,*gdf9*), anti-müllerian hormone (Amh/*amh*) and aromatase (Cyp19a1a/*cyp19a1a*) during gonadal differentiation of the zebrafish, *Danio rerio*. *Biol. Reprod.* **96**, 401–413. (doi:10.1095/biolreprod.116.144964)

161. Uchida D, Yamashita M, Kitano T, Iguchi T. 2002 Oocyte apoptosis during the transition from ovary-like tissue to testes during sex differentiation of juvenile zebrafish. *J. Exp. Biol.* **205**, 711–718. (doi:doi.org/10.1242/jeb.205.6.711)

162. He Y, Shang X, Sun J, Zhang L, Zhao W, Tian Y, Cheng H, Zhou R. 2009 Gonadal apoptosis during sex reversal of the rice field eel: Implications for an evolutionarily conserved role of the molecular chaperone heat shock protein 10. *J. Exp. Zool.* **314B**, 257–266. (doi:10.1002/jez.b.21333)

163. Yamamoto Y, Zhang Y, Sarida M, Hattori RS, Strüssmann CA. 2014 Coexistence of

genotypic and temperature-dependent sex determination in pejerrey *Odontesthes bonariensis*. *PLoS One* **9**, e102574. (doi:10.1371/journal.pone.0102574)

164. Sarida M, Hattori RS, Zhang Y, Yamamoto Y, Strüssmann CA. 2019 Spatiotemporal correlations between *amh* and *cyp19a1a* transcript expression and apoptosis during gonadal sex differentiation of pejerrey, *Odontesthes bonariensis*. *Sex. Dev.* **13**, 99–108. (doi:10.1159/000498997)

165. DeFalco TJ, Verney G, Jenkins AB, McCaffery JM, Russell S, Van Doren M. 2003 Sex-specific apoptosis regulates sexual dimorphism in the *Drosophila* embryonic gonad. *Dev. Cell* **5**, 205–216. (doi:10.1016/S1534-5807(03)00204-1)

166. Gumienny TL, Lambie E, Hartwieg E, Horvitz HR, Hengartner MO. 1999 Genetic control of programmed cell death in the nematode *Caenorhabditis elegans* hermaphrodite germline. *Development* **126**, 1011–1022.

167. Kuwabara PE, Perry MD. 2001 It ain't over till it's ova: Germline sex determination in *C. elegans*. *BioEssays* **23**, 596–604. (doi:10.1002/bies.1085)

168. Peden E, Kimberly E, Gengyo-Ando K, Mitani S, Xue D. 2007 Control of sex-specific apoptosis in *C. elegans* by the BarH homeodomain protein CEH-30 and the transcriptional repressor UNC-37/Groucho. *Genes Dev.* **21**, 3195–3207. (doi:10.1101/gad.1607807)

169. De Leeuw F, Zhang T, Wauquier C, Huez G, Kruys V, Gueydan C. 2007 The cold-inducible RNA-binding protein migrates from the nucleus to cytoplasmic stress granules by a methylation-dependent mechanism and acts as a translational repressor. *Exp. Cell Res.* **313**, 4130–4144. (doi:10.1016/j.yexcr.2007.09.017)

170. Zhong P, Huang H. 2017 Recent progress in the research of cold-inducible RNA-binding protein. *Furture Sci. OA* **3**, FSO246. (doi:10.4155/fsoa-2017-0077)

171. Harry JL, Williams KL, Briscoe DA. 1990 Sex determination in loggerhead turtles: differential expression of two hnRNP proteins. *Development* **109**, 305–312.

172. Harry JL, Briscoe DA, Williams KL. 1992 Putting the heat on sex determination. *Genetica* **87**, 1–6. (doi:10.1007/BF00128767)

173. Huelga SCC *et al.* 2012 Integrative Genome-wide Analysis Reveals Cooperative Regulation of Alternative Splicing by hnRNP Proteins. *Cell Rep.* **1**, 167–178. (doi:10.1016/j.celrep.2012.02.001)

174. Kim HJ, Lee JJ, Cho JH, Jeong J, Park AY, Kang W, Lee KJ. 2017 Heterogeneous nuclear ribonucleoprotein K inhibits heat shock-induced transcriptional activity of heat shock factor 1. *J. Biol. Chem.* **292**, 12801–12812. (doi:10.1074/jbc.M117.774992)

175. Loboda A, Damulewicz M, Pyza E, Jozkowicz A, Dulak J. 2016 Role of Nrf2/HO-1 system in development, oxidative stress response and diseases: An evolutionarily conserved mechanism. *Cell. Mol. Life Sci.* **73**, 3221–3247. (doi:10.1007/s00018-016-2223-0)

176. Kohno S, Katsu Y, Urushitani H, Ohta Y, Iguchi T, Guillette JLJ, Guillette LJ. 2010 Potential contributions of heat shock proteins to temperature-dependent sex determination in the American Alligator. *Sex. Dev.* **4**, 73–87. (doi:10.1159/000260374)

177. Tedeschi JN, Kennington WJ, Berry O, Whiting S, Meekan M, Mitchell NJ. 2015 Increased expression of *Hsp70* and *Hsp90* mRNA as biomarkers of thermal stress in loggerhead turtle embryos (*Caretta caretta*). *J. Therm. Biol.* **47**, 42–50. (doi:10.1016/j.jtherbio.2014.11.006)

178. Bentley BP, Haas BJ, Tedeschi JN, Berry O. 2017 Loggerhead sea turtle embryos (*Caretta caretta*) regulate expression of stress-response and developmental genes when exposed to a biologically realistic heat stress. *Mol. Ecol.* **26**, 2978–2992. (doi:10.1111/ijlh.12426)

179. Furukawa F *et al.* 2019 Heat shock factor 1 protects germ cell proliferation during early ovarian differentiation in medaka. *Sci. Rep.* **9**, 6927. (doi:10.1038/s41598-019-43472-4)

180. Wang J *et al.* 2019 Transcriptomic and epigenomic alterations of Nile tilapia gonads sexually reversed by high temperature. *Aquaculture* **508**, 167–177. (doi:10.1016/j.aquaculture.2019.04.073)

181. Tao W, Chen J, Tan D, Yang J, Sun L, Wei J, Conte MA, Kocher TD, Wang D. 2018 Transcriptome display during tilapia sex determination and differentiation as revealed by RNA-Seq analysis. *BMC Genomics* **19**, 363. (doi:10.1186/s12864-018-4756-0)

182. Tedeschi JN, Kennington WJ, Tomkins JL, Berry O, Whiting S, Meekan MG, Mitchell NJ. 2016 Heritable variation in heat shock gene expression: A potential mechanism for adaptation to thermal stress in embryos of sea turtles. *Proc. R. Soc. B Biol. Sci.* **283**, 20152320. (doi:10.1098/rspb.2015.2320)

183. Casas L, Saborido-Rey F, Ryu T, Michell C, Ravasi T, Irigoien X. 2016 Sex change in clownfish: Molecular insights from transcriptome analysis. *Sci. Rep.* **6**, 35461. (doi:10.1038/srep35461)

184. Tsakogiannis A, Manousaki T, Lagnel J, Sterioti A, Pavlidis M, Papandroulakis N, Mylonas CC, Tsigenopoulos CS. 2018 The transcriptomic signature of different sexes in two protogynous hermaphrodites: Insights into the molecular network underlying sex phenotype in fish. *Sci. Rep.* **8**, 3564. (doi:10.1038/s41598-018-21992-9)

185. Simon AR, Rai U, Fanburg BL, Cochran BH. 1998 Activation of the JAK-STAT pathway by reactive oxygen species. *Am. J. Physiol. Physiol.* **275**, C1640–C1652. (doi:10.1152/ajpcell.1998.275.6.C1640)

186. Ravi P, Jiang J, Liew WC, Orbán L. 2014 Small-scale transcriptomics reveals differences among gonadal stages in Asian seabass (*Lates calcarifer*). *Reprod. Biol. Endocrinol.* **12**, 5. (doi:10.1186/1477-7827-12-5)

187. Díaz N, Piferrer F. 2015 Lasting effects of early exposure to temperature on the gonadal transcriptome at the time of sex differentiation in the European sea bass, a fish with mixed genetic and environmental sex determination. *BMC Genomics* **16**, 2–16. (doi:10.1186/s12864-015-1862-0)

188. Akashi HD, Cádiz Díaz A, Shigenobu S, Makino T, Kawata M. 2016 Differentially expressed genes associated with adaptation to different thermal environments in three sympatric Cuban Anolis lizards. *Mol. Ecol.* **25**, 2273–2285. (doi:10.1111/mec.13625)

189. Yin Z, Machius M, Nestler EJ, Rudenko G. 2017 Activator Protein-1: redox switch controlling structure and DNA-binding. *Nucleic Acids Res.* **45**, 11425–11436. (doi:10.1093/nar/gkx795)

190. Liu H, Lamm MS, Rutherford K, Black MA, Godwin JR, Gemmell NJ. 2015 Large-scale transcriptome sequencing reveals novel expression patterns for key sex-related genes in a sex-changing fish. *Biol. Sex Differ.* **6**, 26. (doi:10.1186/s13293-015-0044-8)

191. van der Wijst MGP, Venkiteswaran M, Chen H, Xu GL, Plösch T, Rots MG. 2015 Local chromatin microenvironment determines DNMT activity: From DNA methyltransferase to DNA demethylase or DNA dehydroxymethylase. *Epigenetics* **10**, 671–676. (doi:10.1080/15592294.2015.1062204)

192. Gupta SC, Sundaram C, Reuter S, Aggarwal BB. In press. Inhibiting NF-κB activation by small molecules as a therapeutic strategy. **1799**, 775–787.

193. Danishuddin, Subbarao N, Faheem M, Khan SN. 2019 Polycomb repressive complex 2 inhibitors: Emerging epigenetic modulators. *Drug Discov. Today* **24**, 179–188. (doi:10.1016/j.drudis.2018.07.002)

194. Haslbeck M, Vierling E. 2015 A first line of stress defense: Small heat shock proteins and their function in protein homeostasis. *J. Mol. Biol.* **427**, 1537–1548. (doi:10.1016/j.jmb.2015.02.002)

195. Ikwegbue P, Masamba P, Oyinloye B, Kappo A. 2017 Roles of Heat Shock Proteins in Apoptosis, Oxidative Stress, Human Inflammatory Diseases, and Cancer. *Pharmaceuticals* **11**, 2. (doi:10.3390/ph11010002)

196. Soncin F, Asea A, Zhang X, Stevenson MA, Calderwood SK. 2000 Role of calcium activated kinases and phosphatases in heat shock factor-1 activation. *Int. J. Mol. Med.* **6**, 705–710. (doi:10.3892/ijmm.6.6.705)

197. Kobayashi M *et al.* 2009 The antioxidant defense system Keap1-Nrf2 comprises a multiple sensing mechanism for responding to a wide range of chemical compounds. *Mol. Cell. Biol.* **29**, 493–502. (doi:10.1128/mcb.01080-08)

198. Brigelius-Flohé R, Flohé L. 2011 Basic principles and emerging concepts in the redox control of transcription factors. *Antioxidants Redox Signal.* **15**, 2335–81. (doi:10.1089/ars.2010.3534)

199. Nguyen T, Nioi P, Pickett CB. 2009 The Nrf2-antioxidant response element signaling pathway and its activation by oxidative stress. *J. Biol. Chem.* **284**, 13291–13295. (doi:10.1074/jbc.R900010200)

200. Storey KB. 1996 Oxidative stress: Animal adaptations in nature. *Brazilian J. Med. Biol. Res.* **29**, 1715–1733.

201. Robert KA, Brunet-Rossinni A, Bronikowski AM. 2007 Testing the 'free radical theory of aging' hypothesis: Physiological differences in long-lived and short-lived colubrid snakes. *Aging Cell* **6**, 395–404. (doi:10.1111/j.1474-9726.2007.00287.x)

202. Olaso G *et al.* 2013 Histone H3 glutathionylation in proliferating mammalian cells destabilizes nucleosomal structure. *Antioxidants Redox Signal.* **19**, 1305–1320. (doi:10.1089/ars.2012.5021)

203. Reyes R, Rosado A, Hernández O, Delgado NM. 1989 Heparin and glutathione: Physiological decondensing agents of human sperm nuclei. *Gamete Res.* **23**, 39–47. (doi:10.1002/mrd.1120230105)

204. Sutovsky P, Schatten G. 2005 Depletion of glutathione during bovine oocyte maturation reversibly blocks the decondensation of the male pronucleus and pronuclear apposition during fertilization. *Biol. Reprod.* **56**, 1503–1512. (doi:10.1095/biolreprod56.6.1503)

205. Sánchez-Vázquez ML, Rosado A, Merchant-larios H, Ramírez G, Reyes R, Delgado NM. 2007 DNA unpacking in guinea pig sperm chromatin by heparin and reduced glutathione. *Arch. Androl.* **40**, 15–28. (doi:10.3109/01485019808987924)

206. Georges A, Holleley CECE. 2018 How does temperature determine sex? *Science (80-.).* **360**, 601–602. (doi:10.1126/science.aat5993)

207. Goikoetxea A, Todd E V, Gemmell NJ. 2017 Stress and sex: Soes cortisol mediate sex change in fish? *Reproduction* **154**, 149–160. (doi:10.1530/REP-17-0408)

208. Geffroy B, Douhard M. 2019 The Adaptive Sex in Stressful Environments. *Trends Ecol. Evol.* **34**, 628–640. (doi:10.1016/j.tree.2019.02.012)

209. Hayashi Y, Kobira H, Yamaguchi T, Shiraishi E, Yazawa T, Hirai T, Kamei Y, Kitano T. 2010 High temperature causes masculinization of genetically female medaka by elevation of cortisol. *Mol. Reprod. Dev.* **77**, 679–686. (doi:10.1002/mrd.21203)

210. Castañeda Cortés DC, Padilla LFA, Langlois VS, Somoza GM, Fernandino JI. 2019 The central nervous system acts as a transducer of stress-induced masculinization through corticotropin-releasing hormone B. *Development* **146**, dev172866. (doi:10.1242/dev.172866)

211. Honeycutt JL *et al.* 2019 Warmer waters masculinize wild populations of a fish with temperature-dependent sex determination. *Sci. Rep.* **9**, 6527. (doi:10.1038/s41598-019-42944-x)

212. Fernandino JI, Hattori RS, Moreno Acosta OD, Strüssmann CA, Somoza GM. 2013 Environmental stress-induced testis differentiation: Androgen as a by-product of cortisol inactivation. *Gen. Comp. Endocrinol.* **192**, 36–44. (doi:10.1016/j.ygcen.2013.05.024)

213. Solomon-Lane TK, Crespi EJ, Grober MS. 2013 Stress and serial adult metamorphosis: Multiple roles for the stress axis in socially regulated sex change. *Front. Neurosci.* **7**, 1–12. (doi:10.3389/fnins.2013.00210)

214. Spiers JG, Chen HJC, Sernia C, Lavidis NA. 2015 Activation of the hypothalamic-pituitary-adrenal stress axis induces cellular oxidative stress. *Front. Neurosci.* **8**, 456. (doi:10.3389/fnins.2014.00456)

215. Persson P, Sundell K, Björnsson BT, Lundqvist H. 1998 Calcium metabolism and osmoregulation during sexual maturation of river running Atlantic salmon. *J. Fish Biol.* **52**, 334–349. (doi:10.1006/jfbi.1997.0582)

216. Johnson JD, Chang JP. 2002 Agonist-Specific and Sexual Stage-Dependent Inhibition of Gonadotropin-Releasing Hormone-Stimulated Gonadotropin and Growth Hormone Release by Ryanodine: Relationship to Sexual Stage-Dependent Caffeine-Sensitive Hormone Release. *J. Neuroendocrinol.* **14**, 144–155. (doi:10.1046/j.0007-1331.2001.00756.x)

217. Norberg B, Brown CL, Halldorsson O, Stensland K, Björnsson BT. 2004 Photoperiod regulates the timing of sexual maturation, spawning, sex steroid and thyroid hormone profiles in the Atlantic cod (*Gadus morhua*). *Aquaculture* **229**, 451–467. (doi:10.1016/S0044-8486(03)00393-4)

218. Adolfi MC, Fischer P, Herpin A, Regensburger M, Kikuchi M, Tanaka M, Schartl M. 2019 Increase of cortisol levels after temperature stress activates *dmrt1a* causing female-to-male sex reversal and reduced germ cell number in medaka. *Mol. Reprod. Dev.* **86**, 1405–1417. (doi:10.1002/mrd.23177)

219. Bekhbat M, Rowson SA, Neigh GN. 2017 Checks and balances: The glucocorticoid receptor and NFκB in good times and bad. *Front. Neuroendocrinol.* **46**, 15–31. (doi:10.1016/j.yfrne.2017.05.001)

220. Uller T, Hollander J, Astheimer L, Olsson M. 2009 Sex-specific developmental plasticity in response to yolk corticosterone in an oviparous lizard. *J. Exp. Biol.* **212**, 1087–1091. (doi:10.1242/jeb.024257)

221. Iungman JL, Somoza GM, Piña CI. 2015 Are stress-related hormones involved in the temperature-dependent sex determination of the broad-snouted caiman? *South Am. J. Herpetol.* **10**, 41–49. (doi:10.2994/SAJH-D-14-00027.1)

222. Marcó MVP, Piña CI, Somoza GM, Jahn GA, Pietrobon EO, Iungman JL. 2015 Corticosterone plasma levels of embryo and hatchling broad-snouted caimans (*Caiman latirostris*) incubated at different temperatures. *South Am. J. Herpetol.* **10**, 50–57. (doi:10.2994/SAJH-D-14-00026.1)

223. Moreno-Mendoza N, Harley VR, Merchant-Larios H. 2001 Temperature regulates SOX9 expression in cultured gonads of *Lepidochelys olivacea*, a species with temperature sex determination. *Dev. Biol.* **229**, 319–326. (doi:10.1006/dbio.2000.9952)

224. Shoemaker-Daly CM *et al.* 2010 Genetic network underlying temperature-dependent sex determination is endogenously regulated by temperature in isolated cultured *Trachemys scripta* gonads. *Dev. Dyn.* **239**, 1061–1075. (doi:10.1002/dvdy.22266)

225. Mork L, Czerwinski M, Capel B. 2014 Predetermination of sexual fate in a turtle with

temperature-dependent sex determination. *Dev. Biol.* **386**, 264–271. (doi:https://doi.org/10.1016/j.ydbio.2013.11.026)

226. Awad EM, Khan SY, Sokolikova B, Brunner PM, Olcaydu D, Wojta J, Breuss JM, Uhrin P. 2013 Cold induces reactive oxygen species production and activation of the NF-kappa B response in endothelial cells and inflammation in vivo. *J. Thromb. Haemost.* **11**, 1716–1726. (doi:10.1111/jth.12357)

227. Nelson DE *et al.* 2004 Oscillations in NF-κB signaling control the dynamics of gene expression. *Science (80-.).* **306**, 704–708. (doi:10.1126/science.1099962)

228. Chen Y, Yu H, Pask AJ, Shaw G, Renfree MB. 2017 Prostaglandin D2 regulates SOX9 nuclear translocation during gonadal sex determination in tammar wallaby, *Macropus eugenii*. *Sex. Dev.* **11**, 143–150. (doi:10.1159/000473782)

229. Malki S, Berta P, Poulat F, Boizet-Bonhoure B. 2005 Cytoplasmic retention of the sex-determining factor SOX9 via the microtubule network. *Exp. Cell Res.* **309**, 468–475. (doi:10.1016/j.yexcr.2005.07.005)

230. Malki S, Nef S, Notarnicola C, Thevenet L, Gasca S, Méjean C, Berta P, Poulat F, Boizet-Bonhoure B. 2005 Prostaglandin D2 induces nuclear import of the sex-determining factor SOX9 via its cAMP-PKA phosphorylation. *EMBO J.* **24**, 1798–1809. (doi:10.1038/sj.emboj.7600660)

231. Hanover JA, Love DC, Prinz WA. 2009 Calmodulin-driven nuclear entry: trigger for sex determination and terminal differentiation. *J. Biol. Chem.* **284**, 12593–7. (doi:10.1074/jbc.R800076200)

232. Jeyasuria P, Place AR. 1998 Embryonic brain-gonadal axis in temperature-dependent sex determination of reptiles: A role for P450 aromatase (CYP19). *J. Exp. Zool.* **281**, 428–449. (doi:10.1002/(SICI)1097-010X(19980801)281:5<428::AID-JEZ8>3.0.CO;2-Q)

233. Matthew Michael W, Choi M, Dreyfuss G. 1995 A nuclear export signal in hnRNP A1: A signal-mediated, temperature-dependent nuclear protein export pathway. *Cell* **83**, 415–422. (doi:10.1016/0092-8674(95)90119-1)

234. van der Houven van Oordt W *et al.* 2000 Signaling Cascade Alters the Subcellular Distribution of Hnrnp A1 and Modulates Alternative Splicing Regulation. *J. Cell Biol.* **149**, 307. (doi:10.1083/jcb.149.2.307)

235. Chojnowski JL, Braun EL. 2012 An unbiased approach to identify genes involved in

development in a turtle with temperature-dependent sex determination. *BMC Genomics* **13**, 308. (doi:10.1186/1471-2164-13-308)

236. Peng Y, Yang PH, Tanner JA, Huang JD, Li M, Lee HF, Xu RH, Kung HF, Lin MCM. 2006 Cold-inducible RNA binding protein is required for the expression of adhesion molecules and embryonic cell movement in *Xenopus laevis*. *Biochem. Biophys. Res. Commun.* **344**, 416–424. (doi:10.1016/j.bbrc.2006.03.086)

237. Zhang Y *et al.* 2016 Cold-inducible RNA-binding protein CIRP/hnRNP A18 regulates telomerase activity in a temperature-dependent manner. *Nucleic Acids Res.* **44**, 761–775. (doi:10.1093/nar/gkv1465)

238. Zhao Y, Mei Y, Chen HJ, Zhang LT, Wang H, Ji XS. 2019 Profiling expression changes of genes associated with temperature and sex during high temperature-induced masculinization in the Nile tilapia brain. *Physiol. Genomics* **51**, 159–168. (doi:10.1152/physiolgenomics.00117.2018)

239. Garcia-Moreno SA, Plebanek MP, Capel B. 2018 Epigenetic regulation of male fate commitment from an initially bipotential system. *Mol. Cell. Endocrinol.* **468**, 19–30. (doi:10.1016/j.mce.2018.01.009)

240. Sanulli S *et al.* 2015 Jarid2 Methylation via the PRC2 Complex Regulates H3K27me3 Deposition during Cell Differentiation. *Mol Cell* **57**, 769–783. (doi:10.1016/j.molcel.2014.12.020)

241. Holoch D, Margueron R. 2017 Mechanisms Regulating PRC2 Recruitment and Enzymatic Activity. *Trends Biochem. Sci.* **42**, 531–542. (doi:https://doi.org/10.1016/j.tibs.2017.04.003)

242. Ying Z *et al.* 2018 Short-term mitochondrial permeability transition pore opening modulates histone lysine methylation at the early phase of somatic cell reprogramming. *Cell Metab.* **28**, 935–945. (doi:10.1016/j.cmet.2018.08.001)

243. Niu Y, DesMarais TL, Tong Z, Yao Y, Costa M, Hospital BC, Medical C, Hospital BC, Gastroenterol CO. 2015 Oxidative stress alters global histone modification and DNA methylation. *Free Radic. Biol. Med.* **82**, 22–28. (doi:https://doi.org/10.1016/j.freeradbiomed.2015.01.028)

244. He C, Larson-Casey JL, Gu L, Ryan AJ, Murthy S, Carter AB. 2016 Cu,Zn-superoxide dismutase-mediated redox regulation of Jumonji domain containing 3 modulates macrophage polarization and pulmonary fibrosis. *Am. J. Respir. Cell Mol. Biol.* **55**, 58–71. (doi:10.1165/rcmb.2015-0183OC)

245. Marasca F, Bodega B, Orlando V. 2018 How polycomb-mediated cell memory deals with a changing environment: Variations in PcG complexes and proteins assortment convey plasticity to epigenetic regulation as a response to environment. *Bioessays* **40**, 1–13. (doi:10.1002/bies.201700137)

246. Nakshatri H *et al.* 2015 Nf-kB-dependent and -independent epigenetic modulation using the novel anti-cancer agent DMAPT. *Cell Death Dis.* **6**, e1608. (doi:10.1038/cddis.2014.569)

247. Inouye S, Fujimoto M, Nakamura T, Takaki E, Hayashida N, Hai T, Nakai A. 2007 Heat shock transcription factor 1 opens chromatin structure of interleukin-6 promoter to facilitate binding of an activator or a repressor. *J. Biol. Chem.* **282**, 33210–33217. (doi:10.1074/jbc.M704471200)

248. Maynard Case R, Eisner D, Gurney A, Jones O, Muallem S, Verkhratsky A. 2007 Evolution of calcium homeostasis: From birth of the first cell to an omnipresent signalling system. *Cell Calcium* **42**, 345–350. (doi:10.1016/j.ceca.2007.05.001)

249. Aguirre J, Ríos-Momberg M, Hewitt D, Hansberg W, Rios-Momberg M, Hewitt D, Hansberg W. 2005 Reactive oxygen species and development in microbial eukaryotes. *Trends Microbiol* **13**, 111–118. (doi:10.1016/j.tim.2005.01.007)

250. Nedelcu AM, Michod RE. 2003 Sex as a response to oxidative stress: the effect of antioxidants on sexual induction in a facultatively sexual lineage. *Proc. R. Soc. B Biol. Sci.* **270**, S136–S139. (doi:10.1098/rsbl.2003.0062)

251. Hörandl E, Speijer D. 2018 How oxygen gave rise to eukaryotic sex. *Proc. R. Soc. B Biol. Sci.* **285**, 20172706. (doi:10.1098/rspb.2017.2706)

252. Nedelcu AM, Marcu O, Michod RE. 2004 Sex as a response to oxidative stress: a twofold increase in cellular reactive oxygen species activates sex genes. *Proc. R. Soc. B Biol. Sci.* **271**, 1591–1596. (doi:10.1098/rspb.2004.2747)

253. Gapper C, Dolan L. 2006 Control of plant development by reactive oxygen species. *Plant Physiol.* **141**, 341–345. (doi:10.1104/pp.106.079079.vated)

254. Lara-Ortíz T, Riveros-Rosas H, Aguirre J. 2003 Reactive oxygen species generated by microbial NADPH oxidase NoxA regulate sexual development in *Aspergillus nidulans*. *Mol. Microbiol.* **50**, 1241–1255. (doi:10.1046/j.1365-2958.2003.03800.x)

255. Chailakhyan MK, Khrianin VN. 1987 *Sexuality in plants and its hormonal regulation*. 1st edn. Moscow: Springer-Verlag New York.

256. Traverso JA, Pulido A, Rodríguez-García MI, Alché JD. 2013 Thiol-based redox regulation in sexual plant reproduction: New insights and perspectives. *Front. Plant Sci.* **4**, 1–14. (doi:10.3389/fpls.2013.00465)

257. Shibata Y, Branicky R, Oviedo Landaverde I, Hekimi S. 2003 Redox regulation of germline and vulval development in *Caenorhabditis elegans*. *Science (80-.).* **302**, 1779–1782. (doi:10.1126/science.1087167)

258. Georges A, Ezaz T, Quinn AE, Sarre SD. 2010 Are reptiles predisposed to temperature-dependent sex determination? *Sex Dev* **4**, 7–15. (doi:10.1159/000279441)

259. Pennell MW, Mank JE, Peichel CL. 2018 Transitions in sex determination and sex chromosomes across vertebrate species. *Mol. Ecol.* **27**, 3950–3963. (doi:10.1111/mec.14540)

260. Pokorná M, Kratochvíl L. 2009 Phylogeny of sex-determining mechanisms in squamate reptiles: are sex chromosomes an evolutionary trap? *Zool. J. Linn. Soc.* **156**, 168–183. (doi:10.1111/j.1096-3642.2008.00481.x)

261. Janes DE, Organ CL, Edwards S V. 2010 Variability in sex-determining mechanisms influences genome complexity in reptilia. *Cytogenet. Genome Res.* **127**, 242–248. (doi:10.1159/000293283)

262. Kim DH, Doyle MR, Sung S, Amasino RM. 2009 Vernalization: Winter and the timing of flowering in plants. *Annu. Rev. Cell Dev. Biol.* **25**, 277–299. (doi:10.1146/annurev.cellbio.042308.113411)

263. Cong L, Zhang F. 2014 Genome engineering using CRISPR-Cas9 system. In *Chromosomal Mutagenesis Methods in Molecular Biology (Methods and Protocols), vol 1239* (ed S Pruett-Miller), pp. 197–217. New York, NY: Humana Press. (doi:https://doi.org/10.1007/978-1-4939-1862-1_10)

264. Parmesan C, Yohe G. 2003 A globally coherent fingerprint of climate change impacts across natural systems. *Nature* **421**, 37–42. (doi:10.1038/nature01286)

265. Umina PA, Weeks AR, Kearney MR, McKechnie SW, Hoffmann AA. 2005 Evolution: A rapid shift in a classic clinal pattern in Drosophila reflecting climate change. *Science (80-.).* **308**, 691–693. (doi:10.1126/science.1109523)

266. Etterson JR *et al.* 2007 Forecasting the Effects of Global Warming on Biodiversity. *Bioscience* **57**, 227–236. (doi:10.1641/b570306)

267. Sinervo B. 2010 Erosion of lizard diversity by climate change and altered thermal niches. *Science (80-.).* **894**, 26–28. (doi:10.1126/science.1184695)

268. IPCC. 2013 Climate Change 2013: The Physical Science Basis. Working Group I Contribution to the Fifth Assessment Report of the Intergovernmental Panel on Climate Change. *Cambridge Univ. Press. Cambridge, United Kingdom New York, NY, USA*. (doi:10.1029/2001JD001516)

269. Hays GC, Mazaris AD, Schofield G, Laloë JO. 2017 Population viability at extreme sex-ratio skews produced by temperaturedependent sex determination. *Proc. R. Soc. B Biol. Sci.* **284**. (doi:10.1098/rspb.2016.2576)

270. Singh SK, Das D, Rhen T. 2020 Embryonic temperature programs phenotype in reptiles. *Front. Physiol.* **11**, 10.3389/fphys.2020.00035. (doi:10.3389/fphys.2020.00035)

271. Ashman T-LL *et al.* 2014 Tree of Sex: A database of sexual systems. *Sci. Data* **1**, 140015. (doi:10.1038/sdata.2014.15)

272. Sarre SD, Georges A, Quinn A. 2004 The ends of a continuum: Genetic and temperature-dependent sex determination in reptiles. *BioEssays* **26**, 639–645. (doi:10.1002/bies.20050)

273. Pieau C. 1996 Temperature variation and sex determination in reptiles. *BioEssays* **18**, 19–26. (doi:10.1002/bies.950180107)

274. Forbes TR. 1964 Intersexuality in Reptiles. In *Intersexuality in vertebrates including man* (ed CN Armstrong), pp. 273–281. London: Academic Press.

275. Pieau C, Dorizzi M, Richard-Mercier N. 1999 Temperature-dependent sex determination and gonadal differentiation in reptiles. *Cell. Mol. Life Sci.* **55**, 887–900. (doi:doi:10.1007/s000180050342)

276. Crews D, Bergeron JM, Bull JJ, Flores D, Tousignant A, Skipper JK, Wibbels T. 1994 Temperature-dependent sex determination in reptiles: proximate mechanisms, ultimate outcomes, and practical applications. *Dev Genet* **15**, 297–312. (doi:10.1002/dvg.1020150310)

277. Pieau C. 1975 *Temperature and Sex Differentiation in Embryos of Two Chelonians, Emys orbicularis L. and Testudo graeca L.* 1st edn. Berlin: Springer-Verlag. (doi:10.1007/978-3-642-66069-6_31)

278. Warner DA, Shine R. 2005 The adaptive significance of temperature-dependent sex

determination: experimental tests with a short-lived lizard. *Evolution (N. Y).* **59**, 2209–2221. (doi:10.1038/nature06519)

279. Warner DA, Shine R. 2007 Fitness of juvenile lizards depends on seasonal timing of hatching, not offspring body size. *Oecologia* **154**, 65–73. (doi:10.1007/s00442-007-0809-9)

280. Warner DA, Uller T, Shine R. 2013 Transgenerational sex determination: The embryonic environment experienced by a male affects offspring sex ratio. *Sci. Rep.* **3**, 1–4. (doi:10.1038/srep02709)

281. Schwanz LE. 2016 Parental thermal environment alters offspring sex ratio and fitness in an oviparous lizard. *J. Exp. Biol.* **219**, 2349. (doi:10.1242/jeb.139972)

282. Warner DA, Shine R. 2008 The adaptive significance of temperature-dependent sex determination in a reptile. *Nature* **451**, 566–569. (doi:10.1038/nature06519)

283. Harlow PS, Taylor JE. 2000 Reproductive ecology of the jacky dragon (*Amphibolurus muricatus*): An agamid lizard with temperature-dependent sex determination. *Austral Ecol.* **25**, 640–652. (doi:10.1111/j.1442-9993.2000.tb00070.x)

284. Ferguson MWJ. 1985 *Reproductive biology and embryology of the crocodilians*. 14th edn. New York: Wiley and Sons.

285. Western PS, Harry JL, Marshall Graves JA, Sinclair AH, Graves JAM, Sinclair AH. 2000 Temperature-dependent sex determination in the American alligator: expression of SF1, WT1 and DAX1 during gonadogenesis. *Gene* **241**, 223–232. (doi:https://doi.org/10.1016/S0378-1119(99)00466-7)

286. Yntema CL. 1968 A series of stages in the embryonic development of *Chelydra serpentina*. *J. Morphol.* **125**, 219–251. (doi:10.1002/jmor.1051250207)

287. Greenbaum E, Carr JL. 2001 Sexual differentiation in the spiny softshell turtle (*Apalone spinifera*), a species with genetic sex determination. *J. Exp. Zool.* **290**, 190–200. (doi:10.1002/jez.1049)

288. Muthukkaruppan V, Kanakambika P, Manickavel V, Veeraraghavan K. 1970 Analysis of the development of the lizard, *Calotes versicolor*. I. A series of normal stages in the embryonic development. *J. Morphol.* **130**, 479–489. (doi:10.1002/jmor.1051300407)

289. Doddamani LS. 2006 Differentiation and development of testis in the oviparous lizard, *Calotes versicolor* (Daud.). *J. Exp. Zool.* **305A**, 299–308. (doi:10.1002/jez.a.265)

290. Yntema CL. 1979 Temperature levels and periods of sex determination during incubation of eggs of *Chelydra serpentina*. *J. Morphol.* **159**, 17–27. (doi:10.1002/jmor.1051590103)

291. Anand A, Patel M, Lalremruata A, Singh AP, Agrawal R, Singh L, Aggarwal RK. 2008 Multiple alternative splicing of Dmrt1 during gonadogenesis in Indian mugger, a species exhibiting temperature-dependent sex determination. *Gene* **425**, 56–63. (doi:https://doi.org/10.1016/j.gene.2008.08.005)

292. Pieau C, Dorizzi M. 1981 Determination of temperature sensitive stages for sexual differentiation of the gonads in embryos of the turtle, *Emys orbicularis*. *J. Morphol.* **170**, 373–382. (doi:10.1002/jmor.1051700308)

293. Wise PAD, Vickaryous MK, Russell AP. 2009 An embryonic staging table for in ovo development of *Eublepharis macularius*, the Leopard Gecko. *Anat. Rec. Adv. Integr. Anat. Evol. Biol.* **292**, 1198–1212. (doi:10.1002/ar.20945)

294. Pewphong R, Kitana J, Kitana N. 2020 Chronology of Gonadal Development in the Malayan Snail-eating Turtle *Malayemys macrocephala*. *Zool. Stud.* **59**. (doi:10.6620/ZS.2020.59-20)

295. Greenbaum E. 2002 A standardized series of embryonic stages for the emydid turtle *Trachemys scripta*. *Can. J. Zool.* **80**, 1350–1370. (doi:10.1139/Z02-111)

296. Barske LA, Capel B. 2010 Estrogen represses SOX9 during sex determination in the red-eared slider turtle *Trachemys scripta*. *Dev. Biol.* **341**, 305–314. (doi:https://doi.org/10.1016/j.ydbio.2010.02.010)

297. Muralidhar P, Veller C. 2018 Sexual antagonism and the instability of environmental sex determination. *Nat. Ecol. Evol.* **2**, 343–351. (doi:10.1038/s41559-017-0427-9)

298. Carter AL, Bodensteiner BL, Iverson JB, Milne-Zelman CL, Mitchell TS, Refsnider JM, Warner DA, Janzen FJ. 2019 Breadth of the thermal response captures individual and geographic variation in temperature-dependent sex determination. *Funct. Ecol.* **33**, 1928–1939. (doi:10.1111/1365-2435.13410)

299. Rhen T, Lang JW. 1998 Among-Family Variation for Environmental Sex Determination in Reptiles. *Evolution (N. Y).* **52**, 1514–1520. (doi:10.2307/2411322)

300. Rhen T, Schroeder A, Sakata JT, Huang V, Crews D. 2011 Segregating variation for temperature-dependent sex determination in a lizard. *Heredity (Edinb).* **106**, 649–660. (doi:10.1038/hdy.2010.102)

301. Zaborski P, Dorizzi M, Pieau C. 1982 H-Y Antigen Expression in Temperature Sex-Reversed Turtles (*Emys orbicularis*). *Differentiation* **22**, 73–78. (doi:10.1111/j.1432-0436.1982.tb01228.x)

302. Dournon C, Houillon C, Pieau C. 1990 Temperature sex-reversal in amphibians and reptiles. *Int. J. Dev. Biol.* **34**, 81–92. (doi:10.1387/ijdb.2393628)

303. Girondot M, Fouillet H, Pieau C. 1998 Feminizing turtle embryos as a conservation tool. *Conserv. Biol.* **12**, 353–362. (doi:10.1046/j.1523-1739.1998.96382.x)

304. Pieau C, Dorizzi M, Richard-Mercier N, Desvages G. 1998 Sexual differentiation of gonads as a function of temperature in the turtle *Emys orbicularis*: Endocrine function, intersexuality and growth. *J. Exp. Zool. Part A Comp. Exp. Biol.* **281**, 400–408. (doi:10.1002/(sici)1097-010x(19980801)281:5<400::aid-jez5>3.0.co;2-s)

305. Dorizzi M, Richard-Mercier N, Pieau C. 1996 The ovary retains male potential after the thermosensitive period for sex determination in the turtle *Emys orbicularis*. *Differentiation* **60**, 193–201. (doi:10.1007/s002580050149)

306. Liu JF, Guiguen Y, Liu SJ. 2009 Aromatase (P450arom) and 11β-hydroxylase (P45011β) genes are differentially expressed during the sex change process of the protogynous rice field eel, *Monopterus albus*. *Fish Physiol. Biochem.* **35**, 511–518. (doi:10.1007/s10695-008-9255-9)

307. Shin HS, An KW, Park MS, Jeong MH, Choi CY. 2009 Quantitative mRNA expression of sox3 and DMRT1 during sex reversal, and expression profiles after GnRHa administration in black porgy, *Acanthopagrus schlegeli*. *Comp. Biochem. Physiol. - B Biochem. Mol. Biol.* **154**, 150–156. (doi:https://doi.org/10.1016/j.cbpb.2009.05.013)

308. Wu GC, Chiu PC, Lin CJ, Lyu YS, Lan DS, Chang CF. 2012 Testicular dmrt1 is involved in the sexual fate of the ovotestis in the protandrous black porgy. *Biol. Reprod.* **86**, 1–11. (doi:10.1095/biolreprod.111.095695)

309. M Real F *et al.* 2020 The mole genome reveals regulatory rearrangements associated with adaptive intersexuality. *Science* **370**, 208–214. (doi:10.1126/science.aaz2582)

310. Shine R, Warner DA, Radder R. 2007 Windows of embryonic sexual lability in two lizard species with environmental sex determination. *Ecology* **88**, 1781–1788. (doi:10.1890/06-2024.1)

311. Chapple DG. 2005 Life history and reproductive ecology of White's skink, *Egernia whitii*. *Aust. J. Zool.* **53**, 353–360. (doi:10.1071/ZO05030)

312. Martínez-Torres M *et al.* 2015 Hemipenes in females of the mexican viviparous lizard *Barisia imbricata* (Squamata: Anguidae): An example of heterochrony in sexual development. *Evol. Dev.* **17**, 270–277. (doi:10.1111/ede.12134)

313. Neaves L, Wapstra E, Birch D, Girling JE, Joss JM. 2006 Embryonic gonadal and sexual organ development in a small viviparous skink, *Niveoscincus ocellatus*. *J. Exp. Zool. Part A Comp. Exp. Biol.* **305**, 74–82. (doi:10.1002/jez.a.249)

314. Dufaure JP, Hubert J. 1961 Table de developpement du lezard vivipare: *Lacerta (Zootoca) vivipara*. *Arch. d'anatomie Microsc. Morphol. Exp.* **50**, 309–327.

315. Esquerré D, Keogh JS, Schwanz LE. 2014 Direct effects of incubation temperature on morphology, thermoregulatory behaviour and locomotor performance in jacky dragons (*Amphibolurus muricatus*). *J. Therm. Biol.* **43**, 33–39. (doi:10.1016/j.jtherbio.2014.04.007)

316. Georges A. 1989 Female turtles from hot nests: is it duration of incubation or proportion of development at high temperatures that matters? *Oecologia* **81**, 323–328. (doi:10.1007/BF00377078)

317. Koopman P, Gubbay J, Vivian N, Goodfellow P, Lovell-Badge R. 1991 Male development of chromosomally female mice transgenic for Sry. *Nature* **351**, 117–21. (doi:10.1038/351117a0)

318. Sinclair AH *et al.* 1990 A gene from the human sex-determining region encodes a protein with homology to a conserved DNA-binding motif. *Nature* **346**, 240–244. (doi:10.1038/346240a0)

319. Smith CA, Roeszler KN, Ohnesorg T, Cummins DM, Farlie PG, Doran TJ, Sinclair AH. 2009 The avian Z-linked gene DMRT1 is required for male sex determination in the chicken. *Nature* **461**, 267–271. (doi:10.1038/nature08298)

320. Barske LA, Capel B. 2008 Blurring the edges in vertebrate sex determination. *Curr. Opin. Genet. Dev.* **18**, 499–505. (doi:10.1016/j.gde.2008.11.004)

321. Herpin A, Schartl M. 2015 Plasticity of gene-regulatory networks controlling sex determination: Of masters, slaves, usual suspects, newcomers, and usurpators. *EMBO Rep.* **16**, 1260–1274. (doi:10.15252/embr.201540667)

322. Ross A, Munger S, Capel B. 2007 *Bmp7* regulates germ cell proliferation in mouse fetal gonads. *Sex. Dev.* **1**, 127–137. (doi:10.1159/000100034)

323. Windley SP, Wilhelm D. 2016 Signaling pathways involved in mammalian sex determination and gonad development. *Sex. Dev.* **9**, 297–315. (doi:10.1159/000444065)

324. Tang H, Brennan J, Karl J, Hamada Y, Raetzman L, Capel B. 2008 Notch signaling maintains Leydig progenitor cells in the mouse testis. *Development* **135**, 3745–3753. (doi:10.1242/dev.024786)

325. Krone N, Hanley NA, Arlt W. 2007 Age-specific changes in sex steroid biosynthesis and sex development. *Best Pract. Res. Clin. Endocrinol. Metab.* **21**, 393–401. (doi:10.1016/j.beem.2007.06.001)

326. Russell DW, Wilson JD. 1994 Steroid 5a-Rreducatse : Two genes/two enzymes. *Annu. Rev. Biochem.* **63**, 25–61.

327. Eid W, Opitz L, Biason-Lauber A. 2015 Genome-wide identification of CBX2 targets: Insights in the human sex development network. *Mol. Endocrinol.* **29**, 247–257. (doi:10.1210/me.2014-1339)

328. Gnessi L, Basciani S, Mariani S, Arizzi M, Spera G, Wang C, Bondjers C, Karlsson L, Betsholtz C. 2000 Leydig cell loss and spermatogenic arrest in platelet-derived growth factor (PDGF)-A-deficient mice. *J. Cell Biol.* **149**, 1019–1025. (doi:10.1083/jcb.149.5.1019)

329. Schmahl J, Rizzolo K, Soriano P. 2008 The PDGF signaling pathway controls multiple steroid-producing lineages. *Genes Dev.* **22**, 3255–3267. (doi:10.1101/gad.1723908)

330. Chawengsaksophak K, Svingen T, Ng ET, Epp T, Spiller CM, Clark C, Cooper H, Koopman P. 2011 Loss of *Wnt5a* disrupts primordial germ cell migration and male sexual development in mice. *Biol. Reprod.* **86**, 1–12. (doi:10.1095/biolreprod.111.095232)

331. Warr N *et al.* 2009 Sfrp1 and Sfrp2 are required for normal male sexual development in mice. *Dev. Biol.* **326**, 273–284. (doi:10.1016/j.ydbio.2008.11.023)

332. Kollara A, Brown TJ. 2010 Variable expression of nuclear receptor coactivator 4 (NcoA4) during mouse embryonic development. *J. Histochem. Cytochem.* **58**, 595–609. (doi:10.1369/jhc.2010.955294)

333. Padua MB, Jiang T, Morse DA, Fox SC, Hatch HM, Tevosian SG. 2015 Combined loss of the GATA4 and GATA6 transcription factors in male mice disrupts testicular development and confers adrenal-like function in the testes. *Endocrinology* **156**, 1873–1886. (doi:10.1210/en.2014-1907)

334. Sarraj M, Chua HK, Umbers A, Loveland K, Findlay J, Stenvers KL. 2007 Differential expression of TGFBR3 (betaglycan) in mouse ovary and testis during gonadogenesis. *Growth Factors* **25**, 334–345. (doi:10.1080/08977190701833619)

335. Carré GA, Couty I, Hennequet-Antier C, Govoroun MS. 2011 Gene expression profiling reveals new potential players of gonad differentiation in the chicken embryo. *PLoS One* **6**, 1–12. (doi:10.1371/journal.pone.0023959)

336. Zhao L, Arsenault M, Ng ET, Longmuss E, Chau TCY, Hartwig S, Koopman P. 2017 SOX4 regulates gonad morphogenesis and promotes male germ cell differentiation in mice. *Dev. Biol.* **423**, 46–56. (doi:10.1016/j.ydbio.2017.01.013)

337. Adolfi MC, Nakajima RT, N RH, Schartl M. 2019 Intersex, hermaphroditism, and gonadal plasticity in vertebrates: Evolution of the Mullerian duct and Amh/Amhr2 signaling. *Annu. Rev. Anim. Biosci.* **7**, 149–172. (doi:10.1146/annurev-animal-020518-114955)

338. Sekido R, Lovell-Badge R. 2008 Sex determination involves synergistic action of SRY and SF1 on a specific Sox9 enhancer. *Nature* **453**, 930–934. (doi:10.1038/nature06944)

339. Good SR, Thieu VT, Mathur AN, Yu Q, Stritesky GL, Yeh N, O'Malley JT, Perumal NB, Kaplan MH. 2009 Temporal induction pattern of STAT4 target genes defines potential for Th1 lineage-specific programming. *J. Immunol.* **183**, 3839–3847. (doi:10.4049/jimmunol.0901411)

340. Rawlings JS, Rosler KM, Harrison DA. 2004 The JAK/STAT signaling pathway. *J. Cell Sci.* **117**, 1281–1283. (doi:10.1242/jcs.00963)

341. Wang DS, Kobayashi T, Zhou LY, Paul-Prasanth B, Ijiri S, Sakai F, Okubo K, Morohashi KI, Nagahama Y. 2007 Foxl2 up-regulates aromatase gene transcription in a female-specific manner by binding to the promoter as well as interacting with Ad4 binding protein/steroidogenic factor. *Mol. Endocrinol.* **21**, 712–725. (doi:10.1210/me.2006-0248)

342. Park M, Shin E, Won M, Kim JH, Go H, Kim HL, Ko JJ, Lee K, Bae J. 2010 FOXL2 interacts with steroidogenic factor-1 (SF-1) and represses SF-1-induced *CYP17* transcription in granulosa cells. *Mol. Endocrinol.* **24**, 1024–1036. (doi:10.1210/me.2009-0375)

343. Lei N, Heckert LL. 2002 Sp1 and Egr1 Regulate Transcription of the *Dmrt1* Gene in Sertoli Cells. *Biol. Reprod.* **66**, 675–684. (doi:10.1095/biolreprod66.3.675)

344. Topilko P, Schneider-Maunoury S, Levi G, Trembleau A, Gourdji D, Driancourt MA, Rao C V., Charnay P. 1998 Multiple pituitary and ovarian defects in Krox-24 (NGFI-A, Egr-1)- targeted mice. *Mol. Endocrinol.* **12**, 107–122. (doi:10.1210/me.12.1.107)

345. Lee SL, Sadovsky Y, Swirnoff AH, Polish JA. 1996 Luteinizing hormone deficiency and female infertility in mice lacking the transcription factor NGF1-A (Egr-1). *Science (80-.).* **273**, 1219–1221. (doi:10.1126/science.273.5279.1219)

346. Lydon JP, DeMayo FJ, Funk CR, Mani SK, Hughes AR, Montgomery CA, Shyamala G, Conneely OM, O'Malley BW. 1995 Mice lacking progesterone receptor exhibit pleiotropic reproductive abnormalities. *Genes Dev.* **9**, 2266–2278. (doi:10.1101/gad.9.18.2266)

347. Birk OS *et al.* 2000 The LIM homeobox gene *Lhx9* is essential for mouse gonad formation. *Nature* **403**, 909–913. (doi:10.1038/35002622)

348. Oréal E, Mazaud S, Picard JY, Magre S, Carré-Eusébe D. 2002 Different patterns of anti-Müllerian hormone expression, as related to DMRT1, SF-1, WT1, GATA-4, Wnt-4, and Lhx9 expression, in the chick differentiating gonads. *Dev. Dyn.* **225**, 221–232. (doi:10.1002/dvdy.10153)

349. Wilhelm D, Englert C. 2002 The Wilms tumor suppressor WT1 regulates early gonad development by activation of Sf1. *Genes Dev.* **16**, 1839–1851. (doi:10.1101/gad.220102)

350. Duester G. 2000 Families of retinoid dehydrogenases regulating vitamin A function: Production of visual pigment and retinoic acid. *Eur. J. Biochem.* **267**, 4315–4324. (doi:10.1046/j.1432-1327.2000.01497.x)

351. Bowles J *et al.* 2006 Retinoid signaling determines germ cell fate in mice. *Science (80-.).* **312**, 596–599. (doi:10.1126/science.1125691)

352. Koubova J, Menke DB, Zhou Q, Cape B, Griswold MD, Page DC. 2006 Retinoic acid regulates sex-specific timing of meiotic initiation in mice. *Proc. Natl. Acad. Sci. U. S. A.* **103**, 2474–2479. (doi:10.1073/pnas.0510813103)

353. Roes J, Choi BK, Power D, Xu P, Segal AW. 2003 Granulocyte function in grancalcin-deficient mice. *Mol. Cell. Biol.* **23**, 826–30. (doi:10.1128/mcb.23.3.826-830.2003)

354. Maki M, Kitaura Y, Satoh H, Ohkouchi S, Shibata H. 2002 Structures, functions and molecular evolution of the penta-EF-hand Ca^{2+}-binding proteins. *Biochim. Biophys. Acta - Proteins Proteomics* **1600**, 51–60. (doi:10.1016/S1570-9639(02)00444-2)

355. Lloyd S. 1982 Least squares quantization in PCM. *IEEE Trans. Inf. Theory* **28**, 129–137. (doi:10.1109/TIT.1982.1056489)

356. Nef S *et al.* 2005 Gene expression during sex determination reveals a robust female genetic program at the onset of ovarian development. *Dev. Biol.* **287**, 361–377. (doi:10.1016/j.ydbio.2005.09.008)

357. Greenlee AR *et al.* 2012 Deregulated sex chromosome gene expression with male germ cell-specific loss of Dicer1. *PLoS One* **7**, 1–13. (doi:10.1371/journal.pone.0046359)

358. Koenig PA, Nicholls PK, Schmidt FI, Hagiwara M, Maruyama T, Frydman GH, Watson N, Page DC, Ploegh HL. 2014 The E2 ubiquitin-conjugating enzyme UBE2J1 is required for spermiogenesis in mice. *J. Biol. Chem.* **289**, 34490–34502. (doi:10.1074/jbc.M114.604132)

359. La Fortezza M, Schenk M, Cosolo A, Kolybaba A, Grass I, Classen AK. 2016 JAK/STAT signalling mediates cell survival in response to tissue stress. *Dev.* **143**, 2907–2919. (doi:10.1242/dev.132340)

360. Paul A, Wilson S, Belham CM, Robinson CJM, Scott PH, Gould GW, Plevin R. 1997 Stress-activated protein kinases: Activation, regulation and function. *Cell. Signal.* **9**, 403–410. (doi:10.1016/S0898-6568(97)00042-9)

361. Davis RJ. 2000 Signal transduction by the JNK group of MAP kinases. *Cell* **103**, 239–252. (doi:10.1016/S0092-8674(00)00116-1)

362. Wang X, Martindale JL, Liu Y, Holbrook NJ. 1998 The cellular response to oxidative stress: influences of mitogen-activated protein kinase signalling pathways on cell survival. *Biochem. J.* **333**, 291–300. (doi:10.1091/mbc.11.3.1103)

363. Martinez P *et al.* 2010 Mammalian Rap1 controls telomere function and gene expression through binding to telomeric and extratelomeric sites. *Nat. Cell Biol.* **12**, 768–780. (doi:10.1038/ncb2081)

364. Teo H *et al.* 2010 Telomere-independent Rap1 is an IKK adaptor and regulates NF-κB-dependent gene expression. *Nat. Cell Biol.* **12**, 758–767. (doi:10.1038/ncb2080)

365. Gilmore TD. 2006 Introduction to NF-κB: players, pathways, perspectives. *Oncogene* **25**, 6680. (doi:10.1038/sj.onc.1209954)

366. Oeckinghaus A, Hayden MS, Ghosh S. 2011 Crosstalk in NF-κB signaling pathways. *Nat. Immunol.* **12**, 695–708. (doi:10.1038/ni.2065)

367. McGuire NL, Bentley GE. 2010 Neuropeptides in the gonads: From evolution to pharmacology. *Front. Pharmacol.* **1**, 1–13. (doi:10.3389/fphar.2010.00114)

368. Ulrich-Lai YM, Herman JP. 2009 Neural regulation of endocrine and autonomic stress responses. *Nat Rev Neurosci* **10**, 397–409. (doi:10.1038/nrn2647.Neural)

369. Liu J, Liu X, Jin C, Du X, He Y, Zhang Q. 2019 Transcriptome profiling insights the feature of sex reversal induced by high temperature in tongue sole *Cynoglossus semilaevis*. *Front. Genet.* **10**, 1–15. (doi:10.3389/fgene.2019.00522)

370. Benham CD, Gunthorpe MJ, Davis JB. 2003 TRPV channels as temperature sensors. *Cell Calcium* **33**, 479–487. (doi:10.1016/S0143-4160(03)00063-0)

371. Carafoli E. 2003 The calcium-signalling saga: Tap water and protein crystals. *Nat. Rev. Mol. Cell Biol.* **4**, 326–332. (doi:10.1038/nrm1073)

372. Penna E, Espino J, De Stefani D, Rizzuto R. 2018 The MCU complex in cell death. *Cell Calcium* **69**, 73–80. (doi:10.1016/j.ceca.2017.08.008)

373. Hoffman NE *et al.* 2015 Ca^{2+} signals regulate mitochondrial metabolism by stimulating CREB-mediated expression of the mitochondrial Ca^{2+} uniporter gene *MCU*. *Sci. Signal.* **8**, ra23–ra23. (doi:10.1126/scisignal.2005673)

374. Strehler E, Caride A, Filoteo A, Xiong Y, Penniston J, Enyedi A. 2013 Plasma membrane Ca2+-ATPases as dynamic regulators of cellular calcium handling. *Ann. N. Y. Acad. Sci.* **1099**, 1–10. (doi:10.1196/annals.1387.023.Plasma)

375. Stocker M. 2004 Ca^{2+}-activated K^+ channels: Molecular determinants and function of the SK family. *Nat. Rev. Neurosci.* **5**, 758–770. (doi:10.1038/nrn1516)

376. Faber ESL, Sah P. 2007 Functions of SK channels in central neurons. *Clin. Exp. Pharmacol. Physiol.* **34**, 1077–1083. (doi:10.1111/j.1440-1681.2007.04725.x)

377. Catterall W. 2004 Structure and regulation of voltage-gated Ca^{2+} channels. *Annu. Rev. Immunol.* **22**, 485–501. (doi:10.1146/annurev.immunol.22.012703.104707)

378. Campiglio M, Flucher BE. 2015 The role of auxiliary subunits for the functional diversity of voltage-gated calcium channels. *J. Cell. Physiol.* **230**, 2019–2031. (doi:10.1002/jcp.24998)

379. Miehe S, Crause P, Schmidt T, Löhn M, Kleemann HW, Licher T, Dittrich W, Rütten H, Strübing C. 2012 Inhibition of diacylglycerol-sensitive TRPC channels by synthetic and natural steroids. *PLoS One* **7**, e35393. (doi:10.1371/journal.pone.0035393)

380. Ramsey IS, Delling M, Clapham DE. 2006 An introduction to TRP channels. *Annu. Rev. Physiol.* **68**, 619–647. (doi:10.1146/annurev.physiol.68.040204.100431)

381. Schaefer M, Plant TD, Obukhov AG, Hofmann T, Gudermann T, Schultz G. 2000 Receptor-mediated regulation of the nonselective cation channels TRPC4 and TRPC5. *J. Biol. Chem.* **275**, 17517–17526. (doi:10.1074/jbc.275.23.17517)

382. Michalak M, Corbett EF, Mesaeli N, Nakamura K, Opas M. 1999 Calreticulin: One protein, one gene, many functions. *Biochem. J.* **344**, 281–292. (doi:10.1042/0264-6021:3440281)

383. Dedhar S. 1994 Novel functions for calreticulin: interaction with integrins and modulation of gene expression? *Trends Biochem. Sci.* **19**, 269–271. (doi:10.1016/0968-0004(94)90001-9)

384. Echevarria W, Leite MF, Guerra MT, Zipfel WR, Nathanson MH. 2003 Regulation of calcium signals in the nucleus by a nucleoplasmic reticulum. *Nat. Cell Biol.* **5**, 440–446. (doi:10.1038/ncb980)

385. Burns K, Duggan B, Atkinson EA, Famulski KS, Nemer M, Bleackley RC, Michalak M. 1994 Modulation of gene expression by calreticulin binding to the glucocorticoid receptor. *Nature* **367**, 476–480. (doi:10.1038/367476a0)

386. Michalak M, Burns K, Andrin C, Mesaeli N, Jass GH, Busaan JL, Opas M. 1996 Endoplasmic reticulum form of calreticulin modulates glucocorticoid- sensitive gene expression. *J. Biol. Chem.* **271**, 29436–29445. (doi:10.1074/jbc.271.46.29436)

387. Wang X *et al.* 2019 Structural basis for activity of TRIC counter-ion channels in calcium release. *Proc. Natl. Acad. Sci.* **116**, 4238–4243. (doi:10.1073/pnas.1817271116)

388. Santamaria-Kisiel L, Rintala-Dempsey A, Shaw G. 2006 Calcium-dependent and -independent interactions of the S100 protein family. *Biochem. J.* **396**, 201–214. (doi:10.1042/bj20060195)

389. Heizmann C. 2008 S-100 proteins. In *Encyclopedia of Molecular Pharmacology* (eds S Offermanns, W Rosenthal), pp. 123–145. Berlin: Springer. (doi:10.1016/0143-4160(86)90017-5)

390. Heizmann CW. 2002 S100 proteins: structure, functions and pathology. *Front. Biosci.* **7**, d1356. (doi:10.2741/heizmann)

391. Rebecchi MJ, Pentyala SN. 2000 Structure, function, and control of phosphoinositide-

specific phospholipase C. *Physiol. Rev.* **80**, 1291–1335. (doi:10.1152/physrev.2000.80.4.1291)

392. Thannickal V, Fanburg B. 2000 Reactive oxygen species in cell signaling. *Am. J. Physiol. - Lung Cell. Mol. Physiol.* **279**, 1005–1028.

393. Schenk H, Klein M, Erdbrügger W, Dröge W, Schulze-Osthoff K. 1994 Distinct effects of thioredoxin and antioxidants on the activation of transcription factors NF-kappa B and AP-1. *Proc. Natl. Acad. Sci. U. S. A.* **91**, 1672–1676. (doi:10.1073/pnas.91.5.1672)

394. Matsuzawa A. 2017 Thioredoxin and redox signaling: Roles of the thioredoxin system in control of cell fate. *Arch. Biochem. Biophys.* **617**, 101–105. (doi:https://doi.org/10.1016/j.abb.2016.09.011)

395. Van Der Vos KE, Coffer PJ. 2008 FOXO-binding partners: It takes two to tango. *Oncogene* **27**, 2289–2299. (doi:10.1038/onc.2008.22)

396. Tao GZ, Lehwald N, Jang KY, Baek J, Xu B, Omary MB, Sylvester KG. 2013 Wnt/β-catenin signaling protects mouse liver against oxidative stress-induced apoptosis through the inhibition of forkhead transcription factor FoxO3. *J. Biol. Chem.* **288**, 17214–17224. (doi:10.1074/jbc.M112.445965)

397. Xiong Y, Uys JD, Tew KD, Townsend DM. 2011 S-Glutathionylation: From molecular mechanisms to health outcomes. *Antioxid. Redox Signal.* **15**, 233–270. (doi:10.1089/ars.2010.3540)

398. Yankovskaya V, Horsefield R, Törnroth S, Luna-Chavez C, Miyoshi H, Léger C, Byrne B, Cecchini G, Iwata S. 2003 Architecture of succinate dehydrogenase and reactive oxygen species generation. *Science (80-.).* **299**, 700–704. (doi:10.1126/science.1079605)

399. Mikhed Y, Görlach A, Knaus UG, Daiber A. 2015 Redox regulation of genome stability by effects on gene expression, epigenetic pathways and DNA damage/repair. *Redox Biol.* **5**, 275–289. (doi:https://doi.org/10.1016/j.redox.2015.05.008)

400. Cho SS, Kim KM, Yang JH, Kim JY, Park SJ, Kim SJ, Kim JK, Cho IJ, Ki SH. 2018 Induction of REDD1 via AP-1 prevents oxidative stress-mediated injury in hepatocytes. *Free Radic. Biol. Med.* **124**, 221–231. (doi:10.1016/j.freeradbiomed.2018.06.014)

401. Tonelli C, Chio I, Tuveson D. 2018 Transcriptional Regulation by Nrf2. *Antioxidants Redox Signal.* **29**, 1727–1745. (doi:10.1089/ars.2017.7342)

402. Haltenhof T *et al.* 2020 A conserved kinase-based body temperature sensor globally controls alternative splicing and gene expression. *Mol. Cell* **78**, 1–13. (doi:10.2139/ssrn.3486026)

403. Wang YT, Lim Y, McCall MN, Huang K-T, Haynes CM, Nehrke K, Brookes PS. 2019 Cardioprotection by the mitochondrial unfolded protein response requires ATF5. *Am. J. Physiol. Circ. Physiol.* **317**, H472–H478. (doi:10.1152/ajpheart.00244.2019)

404. Zhou D, Palam LR, Jiang L, Narasimhan J, Staschke KA, Wek RC. 2008 Phosphorylation of eIF2 directs ATF5 translational control in response to diverse stress conditions. *J. Biol. Chem.* **283**, 7064–7073. (doi:10.1074/jbc.M708530200)

405. Metchat A, Akerfelt M, Bierkamp C, Delsinne V, Sistonen L, Alexandre H, Christians ES. 2009 Mammalian heat shock factor 1 is essential for oocyte meiosis and directly regulates Hsp90α expression. *J. Biol. Chem.* **284**, 9521–9528. (doi:10.1074/jbc.M808819200)

406. Aloia L, Di Stefano B, Di Croce L. 2013 Polycomb complexes in stem cells and embryonic development. *Development* **140**, 2525–2534. (doi:10.1242/dev.091553)

407. Endoh M *et al.* 2017 PCGF6-PRC1 suppresses premature differentiation of mouse embryonic stem cells by regulating germ cell-related genes. *Elife* **6**, 1–26. (doi:10.7554/eLife.21064)

408. Cohen I, Bar C, Ezhkova E. 2020 Activity of PRC1 and histone H2AK119 monoubiquitination : Revising popular misconceptions. *Bioessays* **1900192**, 1–8. (doi:10.1002/bies.201900192)

409. Yang CS, Chang KY, Dang J, Rana TM. 2016 Polycomb group protein Pcgf6 acts as a master regulator to maintain embryonic stem cell identity. *Sci. Rep.* **6**, 1–12. (doi:10.1038/srep26899)

410. Yan Y, Zhao W, Huang Y, Tong H, Xia Y, Jiang Q, Qin J. 2017 Loss of polycomb group protein Pcgf1 severely compromises proper differentiation of embryonic stem cells. *Sci. Rep.* **7**, 1–11. (doi:10.1038/srep46276)

411. Fursova NA, Blackledge NP, Nakayama M, Ito S, Koseki Y, Farcas AM, King HW, Koseki H, Klose RJ. 2019 Synergy between variant PRC1 complexes defines polycomb-mediated gene repression. *Mol. Cell* **74**, 1020-1036.e8. (doi:10.1016/j.molcel.2019.03.024)

412. Blackledge NP *et al.* 2014 Variant PRC1 complex-dependent H2A ubiquitylation drives

PRC2 recruitment and polycomb domain formation. *Cell* **157**, 1445–1459. (doi:10.1016/j.cell.2014.05.004)

413. Yokobayashi S, Liang CY, Kohler H, Nestorov P, Liu Z, Vidal M, Van Lohuizen M, Roloff TC, Peters AHFM. 2013 PRC1 coordinates timing of sexual differentiation of female primordial germ cells. *Nature* **495**, 236–240. (doi:10.1038/nature11918)

414. Shen H, Xu W, Lan F. 2017 Histone lysine demethylases in mammalian embryonic development. *Exp. Mol. Med.* **49**, e325-7. (doi:10.1038/emm.2017.57)

415. Stauffer DR, Howard TL, Nyun T, Hollenberg SM. 2001 CHMP1 is a novel nuclear matrix protein affecting chromatin structure and cell-cycle progression. *J. Cell Sci.* **114**, 2383–2393.

416. Todd E V *et al.* 2019 Stress, novel sex genes and epigenetic reprogramming orchestrate socially-controlled sex change. *Sci. Adv.* **5**, eaaw7006. (doi:10.1101/481143)

417. Ribas L, Crespo B, Xavier D, Kuhl H, Rodríguez JM, Díaz N, Boltañá S. 2019 Characterization of the European Sea Bass (Dicentrarchus labrax) gonadal transcriptome during sexual development. *Mar. Biotechnol.* **21**, 359–373. (doi:10.1007/s10126-019-09886-x)

418. Georges A *et al.* 2015 High-coverage sequencing and annotated assembly of the genome of the Australian dragon lizard *Pogona vitticeps*. *Gigascience* **4**, 45. (doi:10.1186/s13742-015-0085-2)

419. Dobin A, Davis CA, Schlesinger F, Drenkow J, Zaleski C, Jha S, Batut P, Chaisson M, Gingeras TR. 2013 STAR: Ultrafast universal RNA-seq aligner. *Bioinformatics* **29**, 15–21. (doi:10.1093/bioinformatics/bts635)

420. Li H, Handsaker B, Wysoker A, Fennell T, Ruan J, Homer N, Marth G, Abecasis G, Durbin R. 2009 The Sequence Alignment/Map format and SAMtools. *Bioinformatics* **25**, 2078–2079. (doi:10.1093/bioinformatics/btp352)

421. Li B, Dewey CN. 2011 RSEM: accurate transcript quantification from RNA-Seq data with or without a reference genome. *BMC Bioinformatics* **12**, 21–40. (doi:10.1201/b16589)

422. Robinson MD, McCarthy DJ, Smyth GK. 2009 edgeR: A Bioconductor package for differential expression analysis of digital gene expression data. *Bioinformatics* **26**, 139–140. (doi:10.1093/bioinformatics/btp616)

423. 2015 RStudio: Integrated development for R.

424. McCarthy DJ, Chen Y, Smyth GK. 2012 Differential expression analysis of multifactor RNA-Seq experiments with respect to biological variation. *Nucleic Acids Res.* **40**, 4288–4297. (doi:10.1093/nar/gks042)

425. Anders S, Huber W. 2010 Differential expression analysis for sequence count data. *Genome Biol.* **11**, R106. (doi:10.1016/j.jcf.2018.05.006)

426. Cox DR, Reid N. 1987 Parameter orthogonality and approximate conditional inference. *J. R. Stat. Soc. B* **49**, 1–39.

427. Chen Y, Lun ATL, Smyth GK. 2016 From reads to genes to pathways: Differential expression analysis of RNA-Seq experiments using Rsubread and the edgeR quasi-likelihood pipeline. *F1000Research* **5**, 1–49. (doi:10.12688/F1000RESEARCH.8987.2)

428. Lun A, Chen Y, Smyth G. 2016 It's DE-licious: A recipe for differential expression analyses of RNA-seq experiments using quasi-likelihood methods in edgeR. In *Statistical Genomics* (eds E Mathe, S Davis), pp. 391–416. New York: Humana Press. (doi:10.1007/978-1-4939-3578-9)

429. Lund SP, Nettleton D, McCarthy DJ, Smyth GK. 2012 Detecting differential expression in RNA-sequence data using quasi-likelihood with shrunken dispersion estimates. *Stat. Appl. Genet. Mol. Biol.* **11**, 1–42. (doi:10.1515/1544-6115.1826)

430. Lun ATL, Smyth GK. 2017 No counts, no variance: allowing for loss of degrees of freedom when assessing biological variability from RNA-seq data. *Stat. Appl. Genet. Mol. Biol.* **16**, 83–93. (doi:10.1515/sagmb-2017-0010)

431. Phipson B, Lee S, Majewski IJ, Alexander WS, Smyth GK. 2016 Robust hyperparameter estimation protects against hypervariable genes and improves power to detect differential expression. *Ann. Appl. Stat.* **10**, 946–963. (doi:10.1214/16-AOAS920)

432. Eden E, Navon R, Steinfeld I, Lipson D, Yakhini Z. 2009 GOrilla: a tool for discovery and visualization of enriched GO terms in ranked gene lists. *BMC Bioinformatics* **10**, 48. (doi:10.1186/1471-2105-10-48)

433. Eden E, Lipson D, Yogev S, Yakhini Z. 2007 Discovering motifs in ranked lists of DNA sequences. *PLoS Comput. Biol.* **3**, 0508–0522. (doi:10.1371/journal.pcbi.0030039)

434. Ezaz T, Quinn A, Sarre S, O'Meally D, Georges A, Marshall Graves J. 2009 Molecular marker suggests rapid changes of sex-determining mechanisms in Australian dragon

lizards. *Chromosom. Res.* **17**, 91–98. (doi:10.1007/s10577-008-9019-5)

435. Xiang Y, Zhu Z, Han G, Lin H, Xu L, Chen CD. 2007 JMJD3 is a histone H3K27 demethylase. *Cell Res* **17**, 850–857. (doi:10.1038/cr.2007.83)

436. Chen S *et al.* 2012 The histone H3 Lys 27 demethylase JMJD3 regulates gene expression by impacting transcriptional elongation. *Genes Dev.* **26**, 1364–1375. (doi:doi/10.1101/gad.186056.111)

437. Burchfield JS, Li Q, Wang HY, Wang R-FF. 2015 JMJD3 as an epigenetic regulator in development and disease. *Int. J. Biochem. Cell Biol.* **67**, 148–157. (doi:10.1016/j.biocel.2015.07.006)

438. Peng JC, Valouev A, Swigut T, Zhang J, Zhao Y, Sidow A, Wysocka J. 2009 Jarid2/Jumonji Coordinates Control of PRC2 Enzymatic Activity and Target Gene Occupancy in Pluripotent Cells. *Cell* **139**, 1290–1302. (doi:10.1016/j.cell.2009.12.002)

439. Kaneko S *et al.* 2014 Interactions between JARID2 and noncoding RNAs regulate PRC2 recruitment to chromatin. *Mol Cell* **53**, 290–300. (doi:10.1016/j.molcel.2013.11.012)

440. Landeira D, Fisher AG. 2011 Inactive yet indispensable: the tale of Jarid2. *Trends Cell Biol* **21**, 74–80. (doi:10.1016/j.tcb.2010.10.004)

441. Revil T, Gaffney D, Dias C, Majewski J, Jerome-Majewska LA. 2010 Alternative splicing is frequent during early embryonic development in mouse. *BMC Genomics* **11**. (doi:10.1186/1471-2164-11-399)

442. Pasqualini C, Guivarc'h D, Boxberg Y V., Nothias F, Vincent JD, Vernier P. 1999 Stage- and region-specific expression of estrogen receptor α isoforms during ontogeny of the pituitary gland. *Endocrinology* **140**, 2781–2789. (doi:10.1210/endo.140.6.6752)

443. Dillman AA, Hauser DN, Gibbs JR, Nalls MA, McCoy MK, Rudenko IN, Galter D, Cookson MR. 2013 MRNA expression, splicing and editing in the embryonic and adult mouse cerebral cortex. *Nat. Neurosci.* **16**, 499–506. (doi:10.1038/nn.3332)

444. Warner AD, Gevirtzman L, Hillier LDW, Ewing B, Waterston RH. 2019 The C. elegans embryonic transcriptome with tissue, time, and alternative splicing resolution. *Genome Res.* **29**, 1036–1045. (doi:10.1101/gr.243394.118)

445. Gehring NH, Roignant JY. 2020 Anything but Ordinary – Emerging Splicing Mechanisms in Eukaryotic Gene Regulation. *Trends Genet.* **37**, 355–372. (doi:10.1016/j.tig.2020.10.008)

446. Kohno S, Parrott BB, Yatsu R, Miyagawa S, Moore BC, Iguchi T, Guillette Jr L, Guillette LJ. 2014 Gonadal differentiation in reptiles exhibiting environmental sex determination. *Sex. Dev.* **8**, 208–226. (doi:10.1159/000358892)

447. Agrawal R, Wessely O, Anand A, Singh L, Aggarwal Ramesh K. 2009 Male-specific expression of Sox9 during gonad development of crocodile and mouse is mediated by alternative splicing of its proline-glutamine-alanine rich domain. *FEBS J.* **276**, 4184–4196. (doi:10.1111/j.1742-4658.2009.07127.x)

448. Mizoguchi B, Valenzuela N. 2020 Alternative splicing and thermosensitive expression of Dmrt1 during urogenital development in the painted turtle, *Chrysemys picta*. *PeerJ* , 1–25. (doi:10.7717/peerj.8639)

449. Marroquín-flores RA, Bowden RM, Paitz RT. 2021 Brief exposure to warm temperatures reduces intron retention in Kdm6b in a species with temperature-dependent sex determination. *Biol. Lett.* **17**, 20210167. (doi:10.1098/rsbl.2021.0167)

450. Middleton R *et al.* 2017 IRFinder: Assessing the impact of intron retention on mammalian gene expression. *Genome Biol.* **18**, 1–11. (doi:10.1186/s13059-017-1184-4)

451. Kundu S, Ji F, Sunwoo H, Jain G, Lee JT, Sadreyev RI, Dekker J, Kingston RE. 2017 Polycomb Repressive Complex 1 Generates Discrete Compacted Domains that Change during Differentiation. *Mol. Cell* **65**, 432-446.e5. (doi:10.1016/j.molcel.2017.01.009)

452. Bourgeois CF, Mortreux F, Auboeuf D. 2016 The multiple functions of RNA helicases as drivers and regulators of gene expression. *Nat. Rev. Mol. Cell Biol.* **17**, 426–438. (doi:10.1038/nrm.2016.50)

453. Cooper C, Vincett D, Yan Y, Hamedani MK, Myal Y, Leygue E. 2011 Steroid receptor RNA activator bi-faceted genetic system: Heads or Tails? *Biochimie* **93**, 1973–1980. (doi:10.1016/j.biochi.2011.07.002)

454. Al-Raawi D, Jones R, Wijesinghe S, Halsall J, Petric M, Roberts S, Hotchin NA, Kanhere A. 2019 A novel form of JARID2 is required for differentiation in lineage-committed cells. *EMBO J.* **38**. (doi:10.15252/embj.201798449)

455. Kamikawa YF, Donohoe ME. 2014 The localization of histone H3K27me3 demethylase Jmjd3 is dynamically regulated. *Epigenetics* **9**, 834–841. (doi:10.4161/epi.28524)

456. Lang JW, Andrews H V. 1994 Temperature-dependent sex determination in crocodilians. *J. Exp. Zool.* **270**, 28–44. (doi:10.1002/jez.1402700105)

457. Ninomiya K, Kataoka N, Hagiwara M. 2011 Stress-responsive maturation of Clk1/4 pre-mRNAs promotes phosphorylation of SR splicing factor. *J. Cell Biol.* **195**, 27–40. (doi:10.1083/jcb.201107093)

458. Martin M. 2011 Cutadapt removes adapter sequences from high-throughput sequencing reads. *EMBnet J* **17**, 10–12. (doi:10.14806/ej.17.1.200)

459. Love MI, Huber W, Anders S. 2014 Moderated estimation of fold change and dispersion for RNA-seq data with DESeq2. *Genome Biol.* **15**, 1–21. (doi:10.1186/s13059-014-0550-8)

460. Kusumi K *et al.* 2011 Developing a community-based genetic nomenclature for anole lizards. *BMC Genomics* **12**. (doi:10.1186/1471-2164-12-554)

461. Li G, Margueron R, Ku M, Chambon P, Bernstein BE, Reinberg D. 2010 Jarid2 and PRC2, partners in regulating gene expression. *Genes Dev* **24**, 368–380. (doi:10.1101/gad.1886410)

462. Deeming DC, Ferguson MWJ. 1991 Physiological effects of incubation temperature on embryonic development in reptiles and birds. In *Egg Incubation* (eds DC Deeming, MWJ Ferguson), pp. 147–172. Cambridge: Cambridge University Press. (doi:10.1017/CBO9780511585739.011)

463. McCoy JA, Parrott BB, Rainwater TR, Wilkinson PM, Guillette LJ. 2015 Incubation history prior to the canonical thermosensitive period determines sex in the American alligator. *Reproduction* **150**, 279–287. (doi:10.1530/REP-15-0155)

464. Fox H. 1977 The urogenital system of reptiles. In *Biology of the Reptilia* (eds C Gans, T Parsons), pp. 1–157. London: Academic Press.

465. Kwon JT, Ham S, Jeon S, Kim Y, Oh S, Cho C. 2017 Expression of uncharacterized male germ cell-specific genes and discovery of novel sperm-tail proteins in mice. *PLoS One* **12**, 1–20. (doi:10.1371/journal.pone.0182038)

466. Touré A, Lhuillier P, Gossen JA, Kuil CW, Lhôte D, Jégou B, Escalier D, Gacon G. 2007 The Testis Anion Transporter 1 (Slc26a8) is required for sperm terminal differentiation and male fertility in the mouse. *Hum. Mol. Genet.* **16**, 1783–1793. (doi:10.1093/hmg/ddm117)

467. Oh H, Kido T, Lau Y. 2007 PIAS1 interacts with and represses SOX9 transactivation activity. *Mol. rep* **74**, 1446–1445. (doi:10.1002/mrd)

468. Whitmarsh AJ. 2007 Regulation of gene transcription by mitogen-activated protein kinase signaling pathways. *Biochim. Biophys. Acta - Mol. Cell Res.* **1773**, 1285–1298. (doi:10.1016/j.bbamcr.2006.11.011)

469. Sladky V, Schuler F, Fava LL, Villunger A. 2017 The resurrection of the PIDDosome - Emerging roles in the DNA-damage response and centrosome surveillance. *J. Cell Sci.* **130**, 3779–3787. (doi:10.1242/jcs.203448)

470. Minkina A, Lindeman RE, Gearhart MD, Chassot AA, Chaboissier MC, Ghyselinck NB, Bardwell VJ, Zarkower D. 2017 Retinoic acid signaling is dispensable for somatic development and function in the mammalian ovary. *Dev. Biol.* **424**, 208–220. (doi:10.1016/j.ydbio.2017.02.015)

471. Qiu XB, Shao YM, Miao S, Wang L. 2006 The diversity of the DnaJ/Hsp40 family, the crucial partners for Hsp70 chaperones. *Cell. Mol. Life Sci.* **63**, 2560–2570. (doi:10.1007/s00018-006-6192-6)

472. Liu CF, Bingham N, Parker K, Yao HHC. 2009 Sex-specific roles of β-catenin in mouse gonadal development. *Hum. Mol. Genet.* **18**, 405–417. (doi:10.1093/hmg/ddn362)

473. Kimura T, Nakamura T, Murayama K, Umehara H, Yamano N, Watanabe S, Taketo MM, Nakano T. 2006 The stabilization of β-catenin leads to impaired primordial germ cell development via aberrant cell cycle progression. *Dev. Biol.* **300**, 545–553. (doi:10.1016/j.ydbio.2006.06.038)

474. Fukami M, Homma K, Hasegawa T, Ogata T. 2013 Backdoor pathway for dihydrotestosterone biosynthesis: Implications for normal and abnormal human sex development. *Dev. Dyn.* **242**, 320–329. (doi:10.1002/dvdy.23892)

475. Fahrenkrug J, Georg B, Hannibal J, Hindersson P, Gräs S. 2006 Diurnal rhythmicity of the clock genes Per1 and Per2 in the rat ovary. *Endocrinology* **147**, 3769–3776. (doi:10.1210/en.2006-0305)

476. Rhen T, Even Z, Brenner A, Lodewyk A, Das D. 2021 Evolutionary Turnover in Wnt Gene Expression but Conservation of Wnt Signaling during Ovary Determination in a TSD Reptile. (doi:10.1159/000516973)

477. Gerhart-Hines Z, Lazar MA. 2015 Circadian metabolism in the light of evolution. *Endocr. Rev.* **36**, 289–304. (doi:10.1210/er.2015-1007)

478. Okamura H. 2004 Clock genes in cell clocks: Roles, actions, and mysteries. *J. Biol. Rhythms* **19**, 388–399. (doi:10.1177/0748730404269169)

479. Goriki A *et al.* 2014 A Novel Protein, CHRONO, Functions as a Core Component of the Mammalian Circadian Clock. *PLoS Biol.* **12**, e1001839. (doi:10.1371/journal.pbio.1001839)

480. Morse D, Cermakian N, Brancorsini S, Parvinen M, Sassone-Corsi P. 2003 No circadian rhythms in testis: Period1 expression is Clock independent and developmentally regulated in the mouse. *Mol. Endocrinol.* **17**, 141–151. (doi:10.1210/me.2002-0184)

481. Castelli M, Georges A, Holleley CE. 2021 Corticosterone does not have a role in temperature sex reversal in the central bearded dragon (*Pogona vitticeps*). *J. Exp. Zool.* **335**, 301–310. (doi:10.1002/jez.2441)

482. Whiteley SL, Castelli MA, Dissanayake DS, Holleley CE, Georges A. 2021 Temperature-induced sex reversal in reptiles: Prevalence, discovery, and evolutionary implications. *Sex. Dev.* **15**, 148–156. (doi:10.1159/000515687)

483. Amer SAM, Kumazawa Y. 2005 Mitochondrial genome of *Pogona vitticepes* (Reptilia; Agamidae): Control region duplication and the origin of Australasian agamids. *Gene* **346**, 249–256. (doi:10.1016/j.gene.2004.11.014)

484. Deakin JE *et al.* 2016 Anchoring genome sequence to chromosomes of the central bearded dragon (*Pogona vitticeps*) enables reconstruction of ancestral squamate macrochromosomes and identifies sequence content of the Z chromosome. *BMC Genomics* **17**, 447. (doi:10.1186/s12864-016-2774-3)

485. Maurizii MG, Cavaliere V, Gamberi C, Lasko P, Gargiulo G, Taddei C. 2009 Vasa protein is localized in the germ cells and in the oocyte-associated pyriform follicle cells during early oogenesis in the lizard *Podarcis sicula*. *Dev. Genes Evol.* **219**, 361–367. (doi:10.1007/s00427-009-0295-7)

486. Machado-Santos C, Santana LN de S, Vargas RF, Abidu-Figueiredo M, Brito-Gitirana L de, Chagas MA. 2015 Histological and immunohistochemical study of the ovaries and oviducts of the juvenile female of *Caiman latirostris* (Crocodilia: Alligatoridae). *Zool.* **32**, 395–402. (doi:10.1590/S1984-46702015000500008)

487. Tezak BM, Guthrie K, Wyneken J. 2017 An Immunohistochemical Approach to Identify the Sex of Young Marine Turtles. *Anat. Rec.* **300**, 1512–1518. (doi:10.1002/ar.23589)

488. Sarı F, Kaska Y. 2016 Histochemical and immunohistochemical studies of the gonads and paramesonephric ducts of male and female hatchlings of loggerhead sea turtles (*Caretta caretta*). *Biotech. Histochem.* **91**, 428–437. (doi:10.1080/10520295.2016.1201143)

489. Nakajima R, Okano H, Noce T. 2016 JMJD1C exhibits multiple functions in epigenetic regulation during spermatogenesis. *PLoS One* **11**, 1–22. (doi:10.1371/journal.pone.0163466)

490. Kuroki S, Akiyoshi M, Tokura M, Miyachi H, Nakai Y, Kimura H, Shinkai Y, Tachibana M. 2013 JMJD1C, a jmjc domain-containing protein, is required for long-term maintenance of male germ cells in mice. *Biol. Reprod.* **89**, 1–9. (doi:10.1095/biolreprod.113.108597)

491. Godmann M, Auger V, Ferraroni-Aguiar V, Di Sauro A, Sette C, Behr R, Kimmins S. 2007 Dynamic regulation of histone H3 methylation at lysine 4 in mammalian spermatogenesis. *Biol. Reprod.* **77**, 754–764. (doi:10.1095/biolreprod.107.062265)

492. Lesch BJ, Page DC. 2014 Poised chromatin in the mammalian germ line. *Dev.* **141**, 3619–3626. (doi:10.1242/dev.113027)

493. Kun Y, Qian Z, GuYue L, YangYang P, SiJiu Y, JunFeng H, Yan C. 2015 Effects of mild cold shock followed by warming up at 37°C on the ovarian granulosa cellular stress response of the yak. *Acta Vet. Zootech. Sin.* **46**, 738–745.

494. Rao M *et al.* 2019 The regulation of CIRBP by transforming growth factor beta during heat shock-induced testicular injury. *Andrology* **7**, 244–250. (doi:10.1111/andr.12566)

495. Yeung F, Hoberg JE, Ramsey CS, Keller MD, Jones DR, Frye RA, Mayo MW. 2004 Modulation of NF-κB-dependent transcription and cell survival by the SIRT1 deacetylase. *EMBO J.* **23**, 2369 LP – 2380.

496. Pavlová S, Klucska K, Vašíček D, Ryban L, Harrath AH, Alwasel SH, Sirotkin A V. 2013 The involvement of SIRT1 and transcription factor NF-κB (p50/p65) in regulation of porcine ovarian cell function. *Anim. Reprod. Sci.* **140**, 180–188. (doi:10.1016/j.anireprosci.2013.06.013)

497. Vieira S, de Pérez GR, Ramírez-Pinilla MP. 2010 Ultrastructure of the ovarian follicles in the placentotrophic Andean lizard of the genus Mabuya (Squamata: Scincidae). *J. Morphol.* **271**, 738–749. (doi:10.1002/jmor.10830)

498. Silva D Da, Cassel M, Mehanna M, Ferreira A, Dolder MAH. 2018 Follicular Development and Reproductive Characteristics in Four Species of Brazilian Tropidurus Lizards. *Zoolog. Sci.* **35**, 553–563. (doi:10.2108/zs180030)

499. Prisco M, Valiante S, Romano M, Ricchiari L, Liguoro A, Laforgia V, Limatola E, Andreuccetti P. 2004 Ovarian Follicle Cells in *Torpedo marmorata* Synthesize

Vitellogenin. *Mol. Reprod. Dev.* **67**, 424–429. (doi:10.1002/mrd.20036)

500. Raucci F, Di Fiore MM. 2010 The maturation of oocyte follicular epithelium of *Podarcis s. sicula* is promoted by D-aspartic acid. *J. Histochem. Cytochem.* **58**, 157–171. (doi:10.1369/jhc.2009.954636)

501. Uribe MDCA, Omana MEM, Quintero JG, Guillette LJ. 1995 Seasonal variation in ovarian histology of the viviparous lizard *Sceloporus torquatus torquatus*. *J. Morphol.* **226**, 103–119. (doi:10.1002/jmor.1052260107)

502. Lozano A, Ramírez-Bautista A, Uribe MC. 2014 Oogenesis and ovarian histology in two populations of the viviparous lizard *Sceloporus grammicus* (Squamata: Phrynosomatidae) from the central Mexican Plateau. *J. Morphol.* **275**, 949–960. (doi:10.1002/jmor.20275)

503. Tammaro S, Simoniello P, Filosa S, Motta CM. 2007 Block of mitochondrial apoptotic pathways in lizard ovarian follicle cells as an adaptation to their nurse function. *Cell Tissue Res.* **327**, 625–635. (doi:10.1007/s00441-006-0256-7)

504. Motta CM, Scanderbeg MC, Filosa S, Andreuccetti P. 1995 Role of pyriform cells during the growth of oocytes in the lizard *Podarcis sicula*. *J. Exp. Zool.* **273**, 247–256. (doi:10.1002/jez.1402730310)

505. Roy S, Huang B, Sinha N, Wang J, Sen A. 2021 Androgens regulate ovarian gene expression by balancing Ezh2-Jmjd3 mediated H3K27me3 dynamics. *PLoS Genet.* **17**, 1–21. (doi:10.1371/journal.pgen.1009483)

506. Ahmed N *et al.* 2018 Characterization of inter-Sertoli cell tight and gap junctions in the testis of turtle: Protect the developing germ cells from an immune response. *Microb. Pathog.* **123**, 60–67. (doi:10.1016/j.micpath.2018.06.037)

507. Park CJ, Ha CM, Lee JE, Gye MC. 2015 Claudin 11 inter-sertoli tight junctions in the testis of the Korean soft-shelled turtle (*Pelodiscus maackii*). *Biol. Reprod.* **92**, 1–13. (doi:10.1095/biolreprod.114.117804)

508. Bonnet-Garnier A, Feuerstein P, Chebrout M, Fleurot R, Jan HU, Debey P, Beaujean N. 2012 Genome organization and epigenetic marks in mouse germinal vesicle oocytes. *Int. J. Dev. Biol.* **56**, 877–887. (doi:10.1387/ijdb.120149ab)

509. Zhang L, Wang J, Pan Y, Jin J, Sang J, Huang P, Shao G. 2014 Expression of histone H3 lysine 4 methylation and its demethylases in the developing mouse testis. *Cell Tissue Res.* **358**, 875–883. (doi:10.1007/s00441-014-1991-9)

510. An J, Qin J, Wan Y, Zhang Y, Hu Y, Zhang C, Zeng W. 2015 Histone lysine methylation exhibits a distinct distribution during spermatogenesis in pigs. *Theriogenology* **84**, 1455–1462. (doi:10.1016/j.theriogenology.2015.07.013)

511. Tu WJ *et al.* 2021 Targeting novel LSD1-dependent ACE2 demethylation domains inhibits SARS-CoV-2 replication. *Cell Discov.* **7**. (doi:10.1038/s41421-021-00279-w)

512. Tu WJ *et al.* 2020 Targeting Nuclear LSD1 to Reprogram Cancer Cells and Reinvigorate Exhausted T Cells via a Novel LSD1-EOMES Switch. *Front. Immunol.* **11**, 1–23. (doi:10.3389/fimmu.2020.01228)

513. Schindelin J *et al.* 2012 Fiji: An open-source platform for biological-image analysis. *Nat. Methods* **9**, 676–682. (doi:10.1038/nmeth.2019)

514. Wickham H. 2016 ggplot2: Elegant Graphics for Data Analysis.

515. Edmands S. 2021 Sex ratios in a warming world: thermal effects of sex-biased survival, sex determination, and sex reversal. *J. Hered.* **112**, 155–164. (doi:10.1093/jhered/esab006)

516. Santoyo-Brito E, Anderson M, Fox S. 2017 Incubation Temperature Modifies Sex Ratio of Hatchlings in Collared Lizards, *Crotaphytus collaris*. *J. Herpetol.* **51**, 197–201. (doi:10.1670/15-167)

517. Zhang DJ, Tang XL, Yue F, Chen Z, Li R De, Chen Q. 2010 Effect of gestation temperature on sexual and morphological phenotypes of offspring in a viviparous lizard, *Eremias multiocellata*. *J. Therm. Biol.* **35**, 129–133. (doi:10.1016/j.jtherbio.2010.01.003)

518. Bull JJ. 1980 Sex Determination in Reptiles. *Q. Rev. Biol.* **55**, 3–21. (doi:10.1086/411613)

519. Wapstra E, Olsson M, Shine R, Edwards A, Swain R, Joss JMP. 2004 Maternal basking behaviour determines offspring sex in a viviparous reptile. *Proc. R. Soc. B Biol. Sci.* **271**, 230–232. (doi:10.1098/rsbl.2003.0152)

520. Cunningham GD, While GM, Wapstra E. 2017 Climate and sex ratio variation in a viviparous lizard. *Biol. Lett.* **13**, 20170218. (doi:10.1098/rsbl.2017.0218)

521. Robert KA, Thompson MB. 2006 Sex determination: viviparous lizard selects sex of embryos. *Nature* **412**, 698–699.

522. Rasys AM, Park S, Ball RE, Alcala AJ, Lauderdale JD, Menke DB. 2019 CRISPR-Cas9 Gene Editing in Lizards through Microinjection of Unfertilized Oocytes. *Cell Rep.* **28**,

2288-2292.e3. (doi:10.1016/j.celrep.2019.07.089)

523. Merchant-Larios H, Villalpando I. 1990 Effect of Temperature on Gonadal Sex-Differentiation in the Sea Turtle *Lepidochelys Olivacea*: An Organ Culture Study. *J. Exp. Zool.* **254**, 327–331. (doi:10.1002/jez.1402540312)

524. Sifuentes-Romero I, Merchant-Larios H, Milton SL, Moreno-Mendoza N, Díaz-Hernández V, García-Gasca A. 2013 RNAi-Mediated Gene Silencing in a Gonad Organ Culture to Study Sex Determination Mechanisms in Sea Turtle. *Genes (Basel).* **4**, 293–305. (doi:10.3390/genes4020293)

525. Gilbert S. 2000 *Developmental Biology*. 6th edn. Sunderland (MA): Sinauer Associates.

526. Nicholas A. 1904 Reserches sur l'embryologie des reptiles. IV. La segmentation chez l'ovet. *Arch. Biol. Paris* **20**, 611–658.

527. Peter K. 1904 Normentafeln zur entwicklungsgeschichte der zauneidechse (*Lacerta agilis*). In *Jena: Keibel's Normentafeln* (ed G Fischer), pp. 1–65.

528. Werneburg I. 2009 A standard system to study vertebrate embryos (staging vertebrate embryos). *PLoS One* **4**, e5887. (doi:10.1371/journal.pone.0005887)

529. Khannoon ER. 2015 Developmental stages of the climbing gecko *Tarentola annularis* with special reference to the claws, pad lamellae, and subdigital setae. *J. Exp. Zool. Part B Mol. Dev. Evol.* **324**, 450–464. (doi:10.1002/jez.b.22630)

530. Ollonen J, Da Silva FO, Mahlow K, Di-Poï N. 2018 Skull development, ossification pattern, and adult shape in the emerging lizard model organism *Pogona vitticeps*: A comparative analysis with other squamates. *Front. Physiol.* **9**, 1–26. (doi:10.3389/fphys.2018.00278)

531. Moudena E El, Bonsb J, Pieau C, Renousd S, Znaria M, Boumezzougha A. 2000 Developmental table of an Agamind lizard, *Agama impaleuris* Boettger, 1874. *Ann. des Sci. Nat.* **21**, 93–115.

532. Montero R, Gans C, Luisa Lions M. 1999 Embryonic development of the skeleton of *Amphisbaena darwini heterozonata* (Squamata: Amphisbaenidae). *J. Morphol.* **239**, 1–25. (doi:10.1002/(SICI)1097-4687(199901)239:1<1::AID-JMOR1>3.0.CO;2-A)

533. Ballowitz E. 1905 Die gastrulation bei der blindschleiche (*Anguis fragilis* L.). *Zeitschrift für wissenschaftliche Zool.* **83**.

534. Meyer E. 1910 Uber die Entwicklung der Blindschleiche (*Anguis fragilis* L.) vom

Auftreten des Proamnion bis zum Schlusse. *Zeitschrift für wissenschaftliche Zool.* **94**, 447–487.

535. Sanger TJ, Losos JB, Gibson-Brown JJ. 2008 A developmental staging series for the lizard genus Anolis: A new system for the integration of evolution, development, and ecology. *J. Morphol.* **269**, 129–137. (doi:10.1002/jmor.10563)

536. Boback SM, Dichter EK, Mistry HL. 2012 A developmental staging series for the African house snake, *Boaedon (Lamprophis) fuliginosus*. *Zoology* **115**, 38–46. (doi:10.1016/j.zool.2011.09.001)

537. Kaska Y, Downie R. 1999 Embryological development of sea turtles (*Chelonia mydas*, *Caretta caretta*) in the Mediterranean. *Zool. Middle East* **19**, 55–69. (doi:10.1080/09397140.1999.10637796)

538. Lungman J, Piña CI, Siroski P. 2008 Embryological development of *Caiman latirostris* (Crocodylia: Alligatoridae). *Genesis* **46**, 401–417. (doi:10.1002/dvg.20413)

539. Roscito JG, Rodrigues MT. 2012 Embryonic development of the fossorial gymnophthalmid lizards *Nothobachia ablephara* and *Calyptommatus sinebrachiatus*. *Zoology* **115**, 302–318. (doi:10.1016/j.zool.2012.03.003)

540. Beggs K, Young J, Georges A, West P. 2000 Ageing the eggs and embryos of the pig-nosed turtle, *Carettochelys insculpta* (Chelonia: Carettochelydidae), from northern Australia. *Canada J. Zool.* **78**, 373–392.

541. Pasteels J. 1956 Une table analytique du developpement des reptiles. I. Stades de gastrulation chez cheloniens et lacertiliens. *Ann. la Soc. R. Zool. Belgique* **87**, 217–241.

542. Milaire J. 1957 Contribution a la connaissance morphologique et cytologique des bourgeions de membres chez quelques reptiles. *Arch. Biol. (Liege).* **68**, 429–512.

543. Blanc F. 1974 Table de developpement de *Chamaeleo lateralis* Gray, 1831. *Ann. Embryol. Morphol.* **7**, 99–115.

544. Parker W. 1880 Report on the development of the green turtle (*Chelone viridis*, Schneid.). *Zoology* **1**, 1–57.

545. Cordero GA, Janzen FJ. 2014 An enhanced developmental staging table for the painted turtle, *Chrysemys picta* (Testudines: Emydidae). *J. Morphol.* **275**, 442–455. (doi:10.1002/jmor.20226)

546. Mahmoud IY, Klicka J, Hess GL. 1973 Normal embryonic stages of the western painted

turtle, *Chrysemys picta bellii*. *J. Morphol.* **141**, 269–279. (doi:10.1002/jmor.1051410303)

547. Renous S, Rimblot-Baly F, Fretey J, Pieau C. 1989 Charactéristique du développement embryonnaire de la tortue luth, *Dermochelys coriacea* (Vandelli, 1761). *Ann. des Sci. Nat. Zool. Paris* **10**, 197–229.

548. Werner YL. 1971 The ontogenic development of the vertebrae in some Gekkonoid lizards. *J. Morphol.* **133**, 41–91. (doi:10.1002/jmor.1051330104)

549. Shapiro MD. 2002 Developmental morphology of limb reduction in *Hemiergis* (Squamata: Scincidae): Chondrogenesis, osteogenesis, and heterochrony. *J. Morphol.* **254**, 211–231. (doi:10.1002/jmor.10027)

550. Dhouailly D, Saxod R. 1974 Les stades du developpement de *Lacerta muralis* Laurent entre la ponte et l'eclosion. *Bull. la Soc. Zool. Fr.* **99**, 489–494.

551. Crastz F. 1982 Embryological stages of the marine turtle *Lepidochelys olivacea* (Eschscholtz). *Rev. Biol. Trop. J. Trop. Biol. Conserv.* **30**, 113–120. (doi:10.15517/rbt.v30i2.25228)

552. Griffing AH, Sanger TJ, Daza JD, Nielsen S V., Pinto BJ, Stanley EL, Gamble T. 2019 Embryonic development of a parthenogenetic vertebrate, the mourning gecko (*Lepidodactylus lugubris*). *Dev. Dyn.* **248**, 1070–1090. (doi:10.1002/dvdy.72)

553. Lemus A. 1967 Contribucion al estudio de la embriologia de reptiles chilenos. II. Tabla de desarollo de la lagartija vivipara *Liolaemus gravenhorsti*. *Biologie* **40**, 39–61.

554. Lemus D, Illanes J, Fuenzalida M, De La Vega YP, Garcia M. 1981 Comparative analysis of the development of the lizard *Liolaemus tenuis tenuis*. II. A series of normal postlaying stages in embryonic development. *J. Morphol.* **169**, 337–349. (doi:10.1002/jmor.1051690307)

555. Lemus A, Duvauchelle C. 1966 Desarollo intrauiterino de *Liolaemus tenuis tenuis* (Dumeril y Bibron). Contribucion al estudio del desarollo embriologico de reptiles chilenos. *Biologie* **39**, 80–98.

556. Khannoon ER, Evans SE. 2014 The embryonic development of the Egyptian cobra *Naja h. haje* (Squamata: Serpentes: Elapidae). *Acta Zool.* **95**, 472–483. (doi:10.1111/azo.12043)

557. Jackson K. 2002 Post-ovipositional development of the monocled cobra, *Naja kaouthia*

(Serpentes: Elapidae). *Zoology* **105**, 203–214. (doi:10.1078/0944-2006-00077)

558. Krull J. 1906 Die Entwicklung der Ringelnatter (*Tropidonotus natrix* Boie) vom ersten Aufstehen des Proamnion bis zum Schlusse des amnion. *Zeitschrift für wissenschaftliche Zool.* **85**, 107–155.

559. Vielhaus T. 1907 Die entwicklung der rhingelnatter (*Tropidonotus natrix* Boie) nach ausbildung der falterform bis zur erhebung des proamnions. *Zeitschrift für wissenschaftliche Zool.* **86**, 55–99.

560. Korneva L. 1969 Embryonic development of the water snake (*Natrix tessellata*). *Zool Zhour* **98**, 100–120.

561. Noro M, Uejima A, Abe G, Manabe M, Tamura K. 2009 Normal developmental stages of the Madagascar ground gecko *Paroedura pictus* with special reference to limb morphogenesis. *Dev. Dyn.* **238**, 100–109. (doi:10.1002/dvdy.21828)

562. Tokita M, Kuratani S. 2001 Normal embryonic stages of the Chinese softshelled turtle *Pelodiscus sinensis* (Trionychidae). *Zoolog. Sci.* **18**, 705–715. (doi:10.2108/zsj.18.705)

563. Rieppel O. 1994 Studies on Skeleton Formation in Reptiles. Patterns of Ossification in the Skeleton of *Lacerta agilis exigua*. *J. Herpetol.* **28**, 145–153.

564. Khannoon ER, Zahradnicek O. 2017 Postovipositional development of the sand snake *Psammophis sibilans* (Serpentes: Lamprophiidae) in comparison with other snake species. *Acta Zool.* **98**, 144–153. (doi:10.1111/azo.12157)

565. Lourdais O, Hoffman TCM, DeNardo DF. 2007 Maternal brooding in the children's python (*Antaresia childreni*) promotes egg water balance. *J. Comp. Physiol. B Biochem. Syst. Environ. Physiol.* **177**, 569–577. (doi:10.1007/s00360-007-0155-6)

566. Boughner JC, Buchtová M, Fu K, Diewert V, Hallgrímsson B, Richman JM. 2007 Embryonic development of *Python sebae* – I: Staging criteria and macroscopic skeletal morphogenesis of the head and limbs. *Zoology* **110**, 212–230. (doi:10.1016/j.zool.2007.01.005)

567. Arrieta MB, Olea GB, Evelyn RF, Marcelo D. 2020 Ultrastructure of eggshell and embryological development of *Salvator merianae* (Squamata : Teiidae). *Anat. Rec.* (doi:10.1002/ar.24546)

568. Austin HB. 1988 Differentiation and Development of the Reproductive lguanid Lizard, *Sceloporus undulatus*. *Gen. Comp. Endocrinol.* **72**, 351–363.

569. Moffat L. 1985 Embryonic development and aspects of reproductive biology in the Tuatara, Sphenodon punctatus. In *Biology of the Reptilia* (eds C Gans, F Billet, P Maderson), pp. 495–521. New York: Academic Press.

570. Guyot G, Pieau C, Renous S. 1994 Développement embryonnaire d'une tortue terrestre, la tortue d'Hermann, *Testudo hermanni Gmelin*, 1789. *Ann. des Sci. Nat.* **15**, 115–137.

571. Zehr DR. 1962 Stages in the normal development of the common garter snake, *Thamnophis sirtalis sirtalis*. *Copeia* **1962**, 322–329. (doi:10.2307/1440898)

572. Rapp Py-Daniel T, Kennedy Soares De-Lima A, Campos Lima F, Pic-Taylor A, Rodrigues Pires Junior O, Sebben A. 2017 A staging table of post-ovipositional development for the South American Collared Lizard *Tropidurus torquatus* (Squamata: Tropiduridae). *Anat. Rec.* **300**, 277–290. (doi:10.1002/ar.23500)

573. Gregorovicova M, Zahradnicek O. 2012 Embryonic development of the monitor lizard, *Varanus indicus*. *Amphibia-Reptilia* **33**, 451–468. (doi:10.1163/15685381-00002849)

574. Hubert J, Dufaure JP. 1968 Table de developpement de la vipere aspic: *Vipera aspis*. *Bull. la Soc. Zool. Fr.* **93**, 135–148.

575. Nagahama Y, Chakraborty T, Paul-Prasanth B, Ohta K, Nakamura M. 2021 Sex Determination, Gonadal Sex Differentiation and Plasticity in Vertebrate Species. *Physiol. Rev.* **101**, 1237–1308. (doi:doi.org/10.1152/physrev.00044.2019)

576. Rupp SM, Webster TH, Olney KC, Hutchins ED, Kusumi K, Wilson Sayres MA. 2017 Evolution of Dosage Compensation in Anolis carolinensis, a Reptile with XX/XY Chromosomal Sex Determination. *Genome Biol. Evol.* **9**, 231–240. (doi:10.1093/gbe/evw263)

577. Valenzuela N, Lance V. 2004 *Temperature-dependent sex determination in vertebrates*. Washington, DC: Smithsonian Books.

578. Boutz PL, Bhutkar A, Sharp PA. 2015 Detained introns are a novel, widespread class of post-transcriptionally spliced introns. *Genes Dev.* **29**, 63–80. (doi:10.1101/gad.247361.114)